

ENGINEERING ASSESSMENT OF ICE GOUGE STATISTICS
FROM THE CANADIAN & AMERICAN ARCTIC OCEANS

JONATHAN V.M. CAINES

ENGINEERING ASSESSMENT OF ICE GOUGE STATISTICS FROM THE
CANADIAN & AMERICAN ARCTIC OCEANS

By

© Jonathan V.M. Caines

A thesis submitted to the
School of Graduate Studies
in partial fulfilment of the
requirements for the degree of
Master of Engineering

Faculty of Engineering & Applied Science
Memorial University of Newfoundland
April 2009

St. John's

Newfoundland & Labrador

Canada

ABSTRACT

An engineering assessment of seabed ice gouging has been conducted for the American Beaufort, Canadian Beaufort, and Chukchi Seas. This assessment was limited to compilation of historical public domain ice gouge data and statistics. Data bias, correlation, and regional ice gouge measurement and analysis procedures used in probabilistic assessment of ice gouge geometry and recurrence rate estimates have been evaluated through investigation of previous studies and available data sets.

The United States Geological Survey has collected a significant amount of ice gouge data through numerous seabed survey programs conducted in the American Beaufort and Chukchi Seas. The interpreted data is available in the public domain as numerous open-file report publications. Historical Canadian Beaufort Sea ice gouge data was collected through Geological Survey of Canada and the Program for Energy Research and Development research initiatives. Interpreted data was archived in the SCOURBASE and ECHOBASE databases and is updated in the NEWBASE database through ongoing studies; however, data interpretation was contracted to Canadian Seabed Research and is not publicly available. Therefore, numerous summary reports and subsets of the Canadian Beaufort Sea ice gouge databases, available through Environmental Studies Research Fund (ESRF), have been utilized in this work.

Research has indicated that seabed soil conditions limit ice gouging processes, with deeper gouge depths generally occurring in weak marine silts and clays. Dynamic ice gouge infilling processes are influenced by seabed sediment properties, general sediment

deposition rates, water depth, gouge geometry, and bathymetry, although waves and currents are the dominant infilling mechanisms. Ice gouge infilling processes, minimum gouge depth cut-offs, and class range sizes contribute to interpretation subjectivity, bias, and perceived differences between regional ice gouge data collections. These processes were reviewed in this work, but were not integrated in statistical and probabilistic analyses.

Investigated ice gouge depth statistical distributions included the gamma, Weibull, and exponential forms. In contrast with many early investigators (i.e., Lewis, 1977a; 1977b; Weeks et al., 1983; Lanan et al., 1986) who recommended the single-parameter exponential distribution as an effective and conservative probabilistic ice gouge model, this study has found the three-parameter gamma and/or Weibull distributions to more appropriately model ice gouge depth data from each region. However, both of these distributions may be reduced to the exponential form under specific conditions. Available ice gouge depth data sets were analyzed as mixed distributions during this thesis, with fixed probabilities of exceedence assigned to shallow gouge depth data and continuous distributions fit to the distribution tails. The mixed distributions were not associated with gouge depth resolution cut-offs, but due to large amounts of shallow gouge depth data in discrete bins. These discrete data bins were characteristics of the available data used for analysis and may be associated with data bias and uncertainty in the ice gouge process. Previous researchers (i.e., Nessim & Hong, 1992) have analyzed entire ice gouge depth data distributions as continuous. By analyzing available gouge depth data sets as mixed distributions, this study has removed bias and uncertainty introduced by the large

amounts of shallow gouge depth data. Goodness-of-fit assessments were based on comparison of the fitted distributions and empirical cumulative distribution functions with data histograms and cumulative distributions, respectively. Assessment using probability plots and formal goodness-of-fit tests was not conducted since the available data sets were too large to produce meaningful results.

Analysis was conducted for investigation of ice gouge parameter correlation, including ice gouge depth, width, and water depth relationships. In general, ice gouge depths exhibited positive relationships with associated water depths. Other parameters were also examined, including gouge widths and lengths, but did not show any relationship. Analysis of dominant ice gouge orientation data indicated a general northeast – southwest ice gouging direction in each analyzed region, thus suggesting that gouges are not necessarily formed orthogonal to the shoreline.

Additional work is recommended to address ice gouge modeling issues such as considerations for ice gouge infilling processes, gouge correlation with geotechnical and environmental data, and analysis of gouge depth and width correlations.

ACKNOWLEDGEMENTS

I would like to thank Dr. Shawn Kenny and Dr. Faisal Khan of Memorial University of Newfoundland's Faculty of Engineering and Applied Science, as well as Dr. Michael Paulin of IMV Projects Atlantic Inc for their guidance and supervision during the completion of this work. Moreover, I wish to thank them for their critical reviews of this thesis.

Dr. Shawn Kenny and Dr. Faisal Khan must also be thanked for valuable instruction provided during my academic career.

I am also very grateful for the financial support provided by Shell Canada Energy, and the valuable academic and professional opportunities provided by Dr. Paulin and IMV Projects Atlantic. IMV Projects Atlantic has also provided access to numerous technical reports and publications related to my field of research, which is gratefully acknowledged.

Most importantly, I wish to thank the main source of inspiration in my life; my wife, Vanessa, for her patience and support during this undertaking.

TABLE OF CONTENTS

ABSTRACT.....	II
1 INTRODUCTION & OVERVIEW.....	1
1.1 OVERVIEW OF ICE GOUGING	1
1.2 ENGINEERING MODELS	5
1.3 SIGNIFICANCE OF STUDY	17
1.4 THESIS OBJECTIVES	20
2 PHYSICAL ICE GOUGE DATA STUDIES	22
2.1 ICE GOUGE CHARACTERISTICS & MEASUREMENT PROCEDURES.....	23
2.1.1 American Beaufort & Chukchi Seas.....	29
2.1.2 Canadian Beaufort Sea.....	31
2.1.3 Gouge Measurement Accuracy & Technological Advancements	34
2.2 ICE GOUGE DATING METHODS.....	42
2.3 BACKGROUND & EARLY WORKS	44
2.4 AMERICAN BEAUFORT SEA.....	48
2.5 CANADIAN BEAUFORT SEA	55
2.6 CHUKCHI SEA	62
2.7 SUMMARY OF AVAILABLE ICE GOUGE DATA COLLECTIONS.....	67
2.8 GOUGE MEASUREMENT BIAS	72
3 PREVIOUS ENGINEERING ANALYSES.....	78
3.1 EXTRAPOLATION TO DESIGN EVENTS	78
3.2 ICE GOUGE PARAMETER CORRELATIONS.....	91
3.3 ICE GOUGE VARIATION WITH SEABED SEDIMENT TYPE.....	94
3.4 ICE GOUGE INFILLING & SEDIMENTATION STUDIES.....	101

3.4.1	Wave & Current Action	106
3.4.2	Influence of Local Seabed Soil Conditions	114
3.4.3	Influence of Local Geography	116
3.5	ICE GOUGE RECURRENCE RATE STUDIES.....	117
3.5.1	American Beaufort Sea	117
3.5.2	Canadian Beaufort Sea.....	121
3.5.3	Chukchi Sea	130
3.5.4	Historical Data	130
3.5.5	Alternate Methods.....	133
3.5.5.1	<i>Ice Feature Drift Rates</i>	133
3.5.5.2	<i>Keel Draft to Sail Height Ratios</i>	138
3.5.5.3	<i>Upward Looking Sonar</i>	141
4	EXAMINATION & INTERPRETATION OF PHYSICAL ICE GOUGE DATA COLLECTIONS.....	144
4.1	STATISTICAL METHODS & APPLICATION TO ICE GOUGE DEPTH ANALYSIS ..	144
4.1.1	Exponential Distribution.....	144
4.1.2	Gamma Distribution.....	148
4.1.3	Weibull Distribution	151
4.2	STATISTICAL DISTRIBUTION CHARACTERISTICS	154
4.2.1	Correlation Analysis	154
4.2.2	Goodness-of-fit	155
4.2.3	Distribution Tails	155
4.3	ASSESSMENT OF STATISTICAL DISTRIBUTIONS.....	156
4.3.1	American Beaufort Sea	157
4.3.2	Canadian Beaufort Sea.....	163
4.3.3	Chukchi Sea	169
4.4	COMPARISON WITH PREVIOUS RESEARCH.....	174
5	STATISTICAL ICE GOUGE CHARACTERIZATION & MODELING	178
5.1	CORRELATION OF ICE GOUGE DISTRIBUTION CHARACTERISTICS.....	178
5.1.1	Gouge Depth vs. Water Depth	178
5.1.2	Gouge Width vs. Water Depth.....	181
5.1.3	Gouge Width vs. Gouge Depth.....	184
5.1.4	Gouge Length vs. Water Depth	186
5.1.5	Ice Gouge Orientation.....	187
5.2	PROBABILISTIC GOUGE DEPTH ANALYSIS	191

6	SUMMARY & CONCLUSIONS.....	199
6.1	ICE GOUGE PARAMETER INFLUENCES	201
6.2	PIPELINE BURIAL DEPTH CONSIDERATIONS	202
6.3	RECOMMENDED ICE GOUGE MODEL	204
6.4	AREAS FOR FURTHER WORK.....	205
7	BIBLIOGRAPHY & REFERENCES.....	208
 APPENDIX A: STATISTICAL DISTRIBUTIONS & PROBABILITY PLOTS		
USING ALTERNATE MIXED DISTRIBUTION LIMITS		

LIST OF TABLES

Table 1: Comparison of Side-scan Sonar Systems (K.R. Croasdale & Associates, 2000)	41
Table 2: Comparison of Seabed Profiler Systems (K.R. Croasdale & Associates, 2000)	42
Table 3: Summary of American Beaufort Sea Ice Gouge Surveys used in this Study	54
Table 4: Summary of Canadian Beaufort Sea Ice Gouge Surveys used in this Study	60
Table 5: Summary of Chukchi Sea Ice Gouge Surveys used in this Study	67
Table 6: Summary of Available American Beaufort Sea Ice Gouge Data Collections	69
Table 7: Summary of Available Canadian Beaufort Sea Ice Gouge Data Collections	70
Table 8: Summary of Available Chukchi Sea Ice Gouge Data Collections	71
Table 9: Liberty Pipeline Project Ice Gouge Infilling Rates due to Winds, Subsea Currents & Sedimentation (MMS, 2002)	112
Table 10: Summary of USGS Open-file Report 89-151 Ice Gouge Density and Recurrence Rate Data	120
Table 11: Canadian Beaufort Sea Ice Gouge Impact Rates at Seabed Surface (Lewis, 1977b)	122
Table 12: Ice Gouge Recurrence Rates for Eastern Mackenzie Bay, Canadian Beaufort Sea (Comfort et al., 1990)	126
Table 13: Ice Gouge Recurrence Rates for Offshore Tuktoyaktuk Peninsula, Canadian Beaufort Sea (Comfort et al., 1990)	126
Table 14: 100-year Seabed Disturbance (Blasco et al., 1998)	128
Table 15: American Beaufort Sea Ice Gouge Recurrence Rate Summary Data	131
Table 16: Canadian Beaufort Sea Ice Gouge Recurrence Rate Summary Data	132
Table 17: Distribution Parameters – American Beaufort Sea Ice Gouge Depth Data	163
Table 18: Distribution Parameters – Canadian Beaufort Sea Ice Gouge Depth Data	169
Table 19: Distribution Parameters – Chukchi Sea Ice Gouge Depth Data	174
Table 20: Ice Gouge Depth vs. Water Depth Sample Populations	181
Table 21: Ice Gouge Width vs. Water Depth Sample Populations	184
Table 22: Ice Gouge Width vs. Gouge Depth Sample Populations	186
Table 23: Ice Gouge Length vs. Water Depth Sample Populations	187

Table 24: Dominant Ice Gouge Orientation Analysis Summary Data	189
Table 25: Predicted Ice Gouge Depths, 1% Probability of Exceedence per Statistical Distribution & Continuity Limit (Approximate)	195
Table 26: Gouge Depth Continuity Limit Discrete Exceedence Probability (Approximate)	195

LIST OF FIGURES

Figure 1: Illustrated Single Keeled Ice Gouge Characteristics with a Trenched & Buried Pipeline Shown below an Ice Gouge Deformation (Lanan et al., 1986)	2
Figure 2: Illustration of an Ice Gouge Event & Associated Subgouge Deformations (Kenny et al., 2007b)	3
Figure 3: Diagram of Typical USGS Single Keeled & Multiplet Ice Gouge Measurement Characteristics (Rearic et al., 1981).....	4
Figure 4: Idealized Multiyear Pressure Ridge Ice Feature Geometry (Been et al., 1990b)	10
Figure 5: Comparison of Measured and Calculated Ice Gouge Forces in Sand (Phillips et al., 2005)	13
Figure 6: Continuum Finite Element Model of an Ice Gouge (Kenny et al., 2007b)	15
Figure 7: Comparison of Computerized vs. Manual Interpretation of Echo Sounder Ice Gouge Database (Gilbert & Pedersen, 1987).....	36
Figure 8: Location Map for Ice Gouge Data Presented Within USGS Open-File Report 78-730 (Barnes et al., 1978).....	49
Figure 9: Location Map of USGS 81-950 Survey Tracklines (Rearic et al., 1981)	50
Figure 10: Location Map of USGS 82-974 Survey Tracklines (Reimnitz et al., 1982) ...	51
Figure 11: Location Map for USGS 85-463 Ice Gouge Data (Barnes & Rearic, 1985)...	54
Figure 12: Location Map Showing Physiographic Regions of the Canadian Beaufort Sea (Myers et al., 1996).....	61
Figure 13: Location of Side-Scan Sonar Tracklines as Determined by Satellite Navigation (Toimil, 1978).....	64
Figure 14: Northwest Chukchi Sea Survey Trackline Locations (Phillips et al., 1988)...	65
Figure 15: Northeast Chukchi Sea Survey Trackline Locations (Phillips et al., 1988)....	65
Figure 16: Effect of Poor Ice Gouge Depth Resolution/Wide Data Bins (Marcellus & Morrison, 1986)	76
Figure 17: Canadian Beaufort Sea Shelf Sedimentation Rates (mm/yr) (Gilbert & Pedersen, 1987).....	106

Figure 18: Simulated Ice Gouge Population as a Function of Time and Current Velocity: Sand Seabed Sediment (Weeks et al., 1985)	108
Figure 19: Simulated Ice Gouge Population as a Function of Time and Current Velocity: Silt Seabed Sediment (Weeks et al., 1985; 1986).....	109
Figure 20: Time-Dependent Infilling of the Palmer & Niedoroda (2005) Ice Gouge Profile.....	111
Figure 21: Infilling of a 2m Deep Ice Gouge as a Function of Water Depth (Palmer & Niedoroda, 2005)	111
Figure 22: Relationship between Ice Gouge Infilling Rate and Gouge Depth for Biased Hydrodynamic Effects (Palmer & Niedoroda, 2005)	114
Figure 23: Ice Gouge Infilling Rates as Functions of Grain Size & Water Depth (Weeks et al., 1985)	116
Figure 24: Canadian Beaufort Sea Ice Gouge Recurrence Rate Data from ESRF Report No. 032 (Shearer et al., 1986).....	125
Figure 25: Recommended Ice Gouge Recurrence Rates for the Canadian Beaufort Shelf (Lewis & Blasco, 1990)	127
Figure 26: Exponentially Distributed Weighted Ice Gouge Recurrence Rates for the Canadian Beaufort Sea, Analysis of 2005 Updated NEWBASE Database (CSR, 2008)	129
Figure 27: Multiyear Pressure Ridge K/S Relationship, Revised from Kovacs (1983) (Kovacs & Holladay, 1989)	140
Figure 28: Sample Exponential Distribution Shape (Devore, 2004)	146
Figure 29: Sample Gamma Distribution Shape (Devore, 2004).....	151
Figure 30: Sample Weibull Distribution Shape (Devore, 2004).....	153
Figure 31: Histogram – American Beaufort Sea Ice Gouge Depth Data.....	159
Figure 32: Histogram – American Beaufort Sea Ice Gouge Depth Data, 0 – 15m Water Depths Only	160
Figure 33: Exponential Fit – American Beaufort Sea Ice Gouge Depth Data >0.1m ...	160

Figure 34: Exponential ECDF – American Beaufort Sea Ice Gouge Depth Data >0.1m	161
Figure 35: Gamma Fit – American Beaufort Sea Ice Gouge Depth Data >0.1m	161
Figure 36: Gamma ECDF – American Beaufort Sea Ice Gouge Depth Data >0.1m	162
Figure 37: Weibull Fit – American Beaufort Sea Ice Gouge Depth Data >0.1m	162
Figure 38: Weibull ECDF – American Beaufort Sea Ice Gouge Depth Data >0.1m	163
Figure 39: Histogram – Canadian Beaufort Sea Ice Gouge Depth Data	165
Figure 40: Histogram – Canadian Beaufort Sea Ice Gouge Depth Data, 0 – 15m Water Depths Only	166
Figure 41: Exponential Fit – Canadian Beaufort Sea Ice Gouge Depth Data >0.9m	166
Figure 42: Exponential ECDF – Canadian Beaufort Sea Ice Gouge Depth Data >0.9m	167
Figure 43: Gamma Fit – Canadian Beaufort Sea Ice Gouge Depth Data >0.9m	167
Figure 44: Gamma ECDF – Canadian Beaufort Sea Ice Gouge Depth Data >0.9m	168
Figure 45: Weibull Fit – Canadian Beaufort Sea Ice Gouge Depth Data >0.9m	168
Figure 46: Weibull ECDF – Canadian Beaufort Sea Ice Gouge Depth Data >0.9m	169
Figure 47: Histogram – Chukchi Sea Ice Gouge Depth Data	171
Figure 48: Exponential Fit – Chukchi Sea Ice Gouge Depth Data	171
Figure 49: Exponential ECDF – Chukchi Sea Ice Gouge Depth Data	172
Figure 50: Gamma Fit – Chukchi Sea Ice Gouge Depth Data	172
Figure 51: Gamma ECDF – Chukchi Sea Ice Gouge Depth Data	173
Figure 52: Weibull Fit – Chukchi Sea Ice Gouge Depth Data	173
Figure 53: Weibull ECDF – Chukchi Sea Ice Gouge Depth Data	174
Figure 54: Probability Paper Plot for All Canadian Beaufort Sea New Gouge Data – Weibull Distribution (Nessim & Hong, 1992)	176
Figure 55: Probability Plot of All Available Canadian Beaufort Sea Ice Gouge Depth Data – Weibull Distribution	177
Figure 56: LOWESS Matrix Plot, Water Depth & Gouge Depth, American Beaufort Sea	179

Figure 57: LOWESS Matrix Plot, Water Depth & Gouge Depth, Canadian Beaufort Sea	180
Figure 58: LOWESS Matrix Plot, Water Depth & Gouge Depth, Chukchi Sea	180
Figure 59: LOWESS Matrix Plot, Water Depth & Gouge Width, American Beaufort Sea	182
Figure 60: LOWESS Matrix Plot, Water Depth & Gouge Width, Canadian Beaufort Sea	183
Figure 61: LOWESS Matrix Plot, Water Depth & Gouge Width, Chukchi Sea	183
Figure 62: LOWESS Matrix Plot, Gouge Depth & Width, American Beaufort Sea.....	184
Figure 63: LOWESS Matrix Plot, Gouge Depth & Width, Canadian Beaufort Sea	185
Figure 64: LOWESS Matrix Plot, Gouge Depth & Width, Chukchi Sea.....	185
Figure 65: LOWESS Matrix Plot, Water Depth & Gouge Length, American Beaufort Sea	186
Figure 66: LOWESS Matrix Plot, Water Depth & Gouge Length, Canadian Beaufort Sea	187
Figure 67: Ice Gouge Orientation Frequency – American Beaufort Sea.....	190
Figure 68: Ice Gouge Orientation Frequency – Canadian Beaufort Sea	190
Figure 69: Ice Gouge Orientation Frequency – Chukchi Sea	191
Figure 70: Ice Gouge Depth Exceedence Probability – American Beaufort Sea, 0 – 65m WD, Gouge Depths >0.1m	196
Figure 71: Ice Gouge Depth Exceedence Probability – Canadian Beaufort Sea, 0 – 55.5m WD, Gouge Depths >0.9m	197
Figure 72: Ice Gouge Depth Exceedence Probability – Chukchi Sea, 21 – 59m WD, Gouge Depths >0.45m	198

LIST OF ABBREVIATIONS & SYMBOLS

A	seabed unit area
APOA	Arctic Petroleum Operators Association
CDF	cumulative distribution function
CHC	Canadian Hydraulics Centre
COGLA	Canada Oil & Gas Lands Administration
CRREL	Cold Regions Research & Engineering Laboratory
D	water depth (m)
D	ice keel depth (m)
DOF	degrees of freedom
ESRF	Environmental Studies Revolving (Research) Funds
FEIS	final environmental impact statement
F(x)	cumulative distribution function
G	linear ice gouge recurrence rate (gouges/km/year) measured in the north – south direction
GBSC	Grand Banks Scour Catalogue

GSC	Geological Survey of Canada
IPS	Ice-profiling sonar
L	pipeline length (km)
L	distance of annual ice cover drift (km)
L [*]	mean effective ice gouge length measured perpendicular to the pipeline segment
LOWESS	locally weighted scatter plot smoothing
MMS	Minerals Management Service
N/A	not available
NGDC	National Geophysical Data Center
N	average ice gouge recurrence rate (average number of gouges/km/year)
N	number of gouges that is predicted to occur during the selected return period
N	corrected number of ice gouge observations per trackline segment length (i.e., per km)
N _D	number of ice keels passing a particular point with draft 'D' (m) per year

N_0	total number of keels passing over the seafloor area per year (spatial density)
N_{obs}	observed number of ice gouges per trackline segment
$N(>D)$	number of ice feature keels passing over a specified seafloor area each year with draft greater than D (m)
N_1	expected number of ice gouges that would be observed along a sampling line oriented normal to the dominant gouge trend
PDF	probability density function
PERD	Program of Energy Research & Development
$P(d)$	probability of an ice gouge of depth 'd' (m) occurring at a water depth of 'D' (m)
$P[X \geq x]$	probability of exceedence for an ice gouge of depth (x)
S_D	predicted ice gouge recurrence rate (gouge/km/year)
T	extreme design ice gouge average return period (years)
T_k	total number of ice feature keels passing overtop of a pipeline of length (L) with draft greater than D
U	mean iceberg keel drift velocity (m/s)

$U_{(i)}$	cumulative probability of the i -th observation
ULS	upward looking sonar
USGS	United States Geological Survey
W	width of the seabed section subjected to iceberg keel grounding (m)
X	pipeline or trackline segment length
Y	twice the slant range of the side-scan sonar
c	minimum ice gouge depth cut-off (m)
cm	centimetres
d	design maximum ice gouge depth (m)
dm	decimetres
d_{bar}	mean ice gouge depth (m)
f_g	iceberg keel grounding frequency
g	linear ice gouge recurrence rate (gouges/km/year)
h_{avg}	observed mean ice keel draft experimentally observed via ULS (m)
h_0	ice keel low value limit (m)

k	a parameter of the exponential distribution; reciprocal of the mean ice gouge depth
km	kilometers
kPa	kiloPascals
l	average length of ice gouges (km)
l	mean ice keel length for a continuous keel with draft greater than 'D' (km)
ln	natural logarithm
m	meters
n.d.	no date
n	predicted ice gouge crossing frequency
n	number of ice gouges per dm of gouge depth per km of seabed
n_g	annual ice gouge frequency per unit area
n_k^*	average number of ice keels per unit area, based on ice keel observation statistics
n_o	areal density of all icebergs observed on the water surface (icebergs/km ² /year)

n_0	number of ice gouges per dm at zero gouge depth per km of seabed
n_0	ice gouge crossing rate or linear density in area subjected to sedimentation (gouges/km)
q_b	unit-less bathymetric shielding factor
r	Pearson product-moment correlation coefficient
r^2	coefficient of determination
r_{cr}	critical r-value
r_d	proportion of total icebergs with sufficient draft to impact the seabed in a specific water depth range (1/m)
r_θ	proportion of time that an iceberg drifts in a particular direction
s	average seabed slope
u	sedimentation rate (mm/year)
v^*	net upslope (incursion) ice drift velocity
w	width or length of the ice keel (m)
x	random variable in the data (gouge depth) distribution (m)
y	linear function of the observed variant x (Gumbel distribution)

yr	year
α	statistical significance level
α	acute angle formed between the survey vessel's track and the gouge orientation (°)
α	spatial ice gouge recurrence rate (gouges/km ² /year)
α	Gamma or Weibull distribution shape parameter
β	Gamma or Weibull distribution scale parameter
β	measure of spread related to the standard deviation of the cumulative distribution
$\Delta F^*(z_1, z_2)$	increment of ice keel draft cumulative distribution over the water depth range z_1 to z_2
Φ	angle formed between the dominant ice gouge trend over the trackline segment and the trackline orientation (°)
$\Gamma(\alpha)$	gamma function
λ	exponential distribution parameter (slope of negative exponential curve) (1/m)
μ	mean number of ice keels observed per km of annual ice cover drift

μ	arithmetic mean
μ	mode of the maximum ice gouge depth frequency curve
θ	orientation between the upslope seabed and dominant iceberg keel drift direction (°)
θ	angle between the pipeline route and the trend of the ice gouges (°)
θ	orientation of ice gouges (°), referenced to the east – west direction (θ cannot equal 90°)
θ	threshold parameter
ρ_g	iceberg keel grounding frequency
ρ_k	areal (spatial) density of iceberg keels with sufficient draft to impact the seabed in a specific area (iceberg keels/km ² /year)
σ	standard deviation
%	percentage

1 INTRODUCTION & OVERVIEW

1.1 OVERVIEW OF ICE GOUGING

The steady-state process of an ice feature keel contacting and scraping along the seabed often produces many characteristic seabed deformations that may be observed and measured for further analysis through marine geophysical surveying techniques. The impact and grounding of an ice keel upon the seabed typically produces 'pock mark' indentations upon the seafloor, which become noticeable once the ice has sufficiently melted to allow the indenting ice keel to dislodge and move off of the grounding site.

If the grounded ice possesses enough momentum or driving force to facilitate further movement, the impacting ice keel may scrape along the seabed and thus create a noticeable ice gouge (American terminology) or ice scour (Canadian terminology) on the seafloor. Ice gouges/scours may also be referred to as 'ice scores'. Ice 'gouging' has been adopted in the current study in order to avoid confusion with other forms of seabed scouring (i.e., strudel scouring, hydrodynamic scouring, etc) and for standardization of terminology in this thesis.

Although dependent on regional physical, environmental and ice regime characteristics, ice gouge features are on the order of meters deep, tens of meters wide and hundreds of meters long. A study by Croasdale et al. (2005) introduced the various limits to available forces capable of creating an ice gouge, which include ice feature momentum/kinetic energy, pack ice driving forces, environmental driving forces, and global/local keel failure limits. Refer to a study by Marchenko (2005) for a detailed discussion of the ice

gouging momentum balance and the influence of semidiurnal tides, wind, and waves on the formation of seabed ice gouges.

Single-keeled ice features, associated with first-year pressure ridges, and large ice feature such as icebergs and ice islands, have a single keel projection contacting the seafloor (see Figure 1), which generally creates gouge deformations that produce a localized ridge berm and furrow seabed deformation, with associated vertical and horizontal sediment displacement and redistribution. Vertical and lateral stresses are applied to the soil at the keel base as an ice keel gouges the seabed, resulting in some distribution of vertical and lateral soil displacement with depth beneath the ice keel known as subgouge deformation, as illustrated in Figure 2. Some uncertainty exists regarding the attack angle formed between the gouging ice keel and seabed soil.

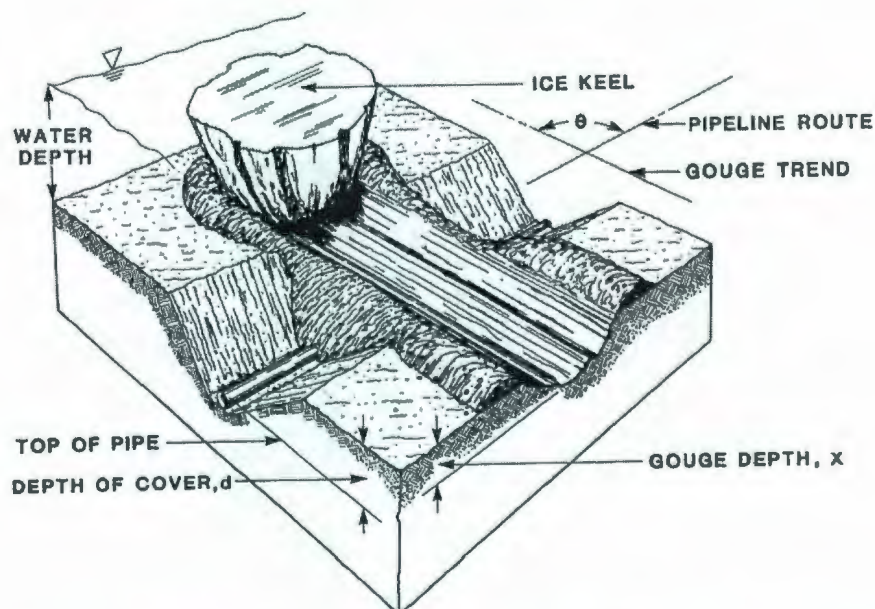


Figure 1: Illustrated Single Keeled Ice Gouge Characteristics with a Trenched & Buried Pipeline Shown below an Ice Gouge Deformation (Lanan et al., 1986)

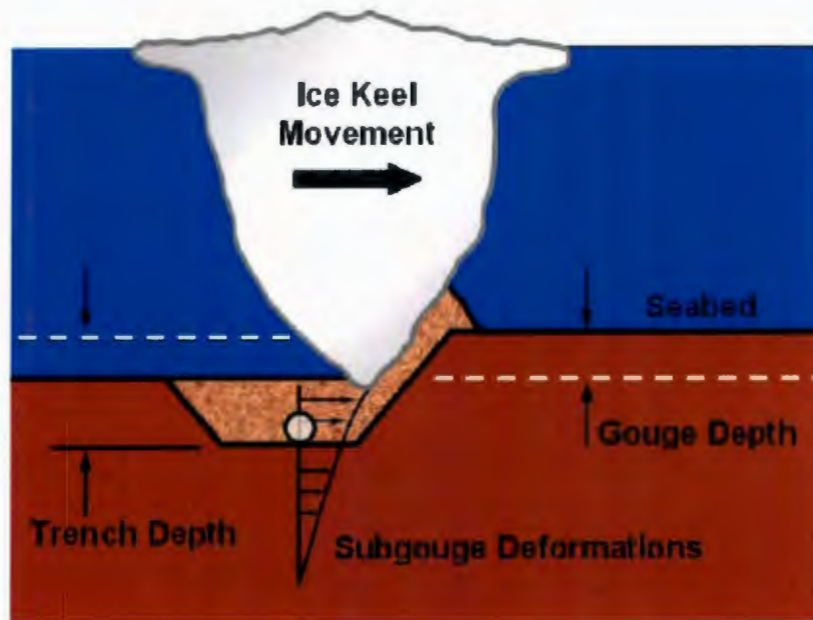


Figure 2: Illustration of an Ice Gouge Event & Associated Subgouge Deformations

(Kenny et al., 2007b)

In industry, ice gouges created by multi-keeled ice features, which are associated with extended first-year and multi-year pressure ridge features, are generally termed 'multiplet' events (see Figure 3). These keels possess multiple keel projections which contact and gouge the seafloor. Multiplet gouges typically exhibit a characteristic gouge deformation which simulates rake marks upon the localized seabed. An ice gouge may alternately be referred to as an ice 'scour' or 'score', however, the term 'gouge' has been adopted for use within the current thesis.

The seabed sedimentology, morphology, ice feature, physical location and localized bathymetry influences gouge geometry and recurrence rate statistics. Annual variations in ice feature concentrations also strongly affect the distribution of seabed gouges. The depth and extent of ice gouges in the seabed are also dependent upon the type of ice

keel/feature encountered. Arctic nearshore areas are often prone to first-year and/or multiyear ice invasions, pressure ridge formations (stamukhi), ice island drifts, and icebergs. In addition to environmental driving forces (wind, waves, and currents), key aspects to the ice gouging process include the indenting ice keel's strength, attack angle, and the seabed soil's resistance to deformation. Water depth, proximity to the shear ice zone, and seabed slope also influence the ice gouging process. Together these factors determine the resultant gouging capability of the keel, which may therefore vary, depending on its origin, age, and gouging location.

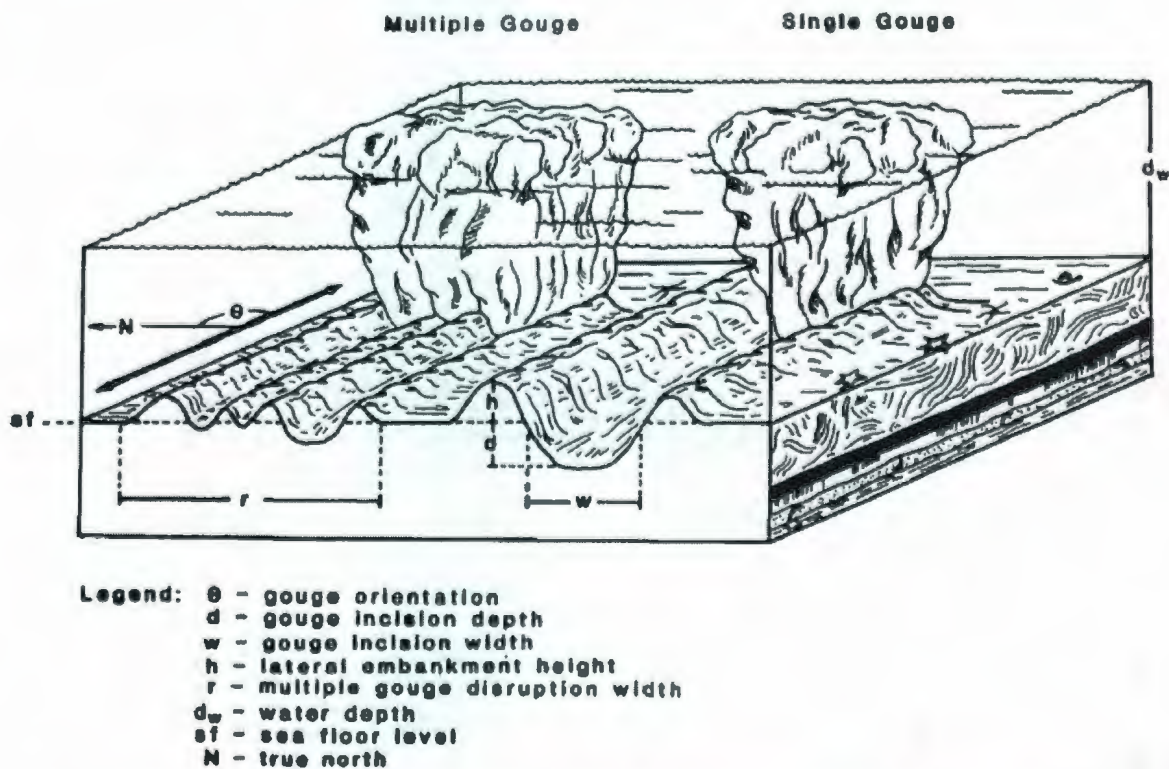


Figure 3: Diagram of Typical USGS Single Keeled & Multiplier Ice Gouge Measurement

Characteristics (Rearic et al., 1981)

Subsea pipelines have been used for offshore transmission of oil and gas in ice environments that include the U.S. Beaufort Sea, Caspian Sea, Grand Banks and Sakhalin Island. Pipelines located in these ice environments must be designed and analyzed for protection against the risk of ice gouging in order to ensure asset integrity and design operability throughout the installation's lifespan. Apart from the Grand Banks pipeline systems, which are treated as sacrificial elements, the pipeline is trenched and buried beneath the natural seabed mudline in order to protect the pipeline from a gouging ice keel and maintain pipeline integrity and safety during operation.

Design and analysis for ice gouge events has evolved from the early school of thought which simply recommended pipeline burial beneath the maximum observed and/or predicted ice gouge depth, to the suggestion for deep burial depths, and now to recommended burial somewhere between these depths (Palmer et al., 1990; Kenny et al., 2007a). This evolution is a result of increased experience in ice gouge design and analysis and paralleled decreases in uncertainties associated with the ice gouging process. Two distinct approaches are commonly utilized for assessing seabed ice gouging, however each has inherent limitations and uncertainties.

1.2 ENGINEERING MODELS

In general, ice gouge depth analysis procedures can be classified as statistical or numerical. Statistical ice gouge analysis procedures rely on historical survey data and aim to predict extreme events through probabilistic analysis of relevant ice gouge data distributions. This is the most commonly used approach, and may be applied to ice gouge

depth and/or keel draft statistics (Palmer et al., 2005). The maximum ice gouge geometry is also important for establishing the extent of subgouge deformation, in addition to hindcasting historical statistics to determine maximum ice gouge depths. Inherent limitations to statistical ice gouge analysis procedures include:

- Regional differences in ice gouge geometry and subjective gouge interpretation and enumeration practices exist between Canadian and American researchers, thus introducing uncertainty when merging or comparing regional data;
- Inconsistencies with respect to field data surveying and collection procedures (i.e., across-track versus along-track ice gouge surveying, correlation of sidescan and echosounder records, sonar towfish height, etc);
- Uncertainties in the assessment of ice gouge age and identification of recent vs. relic ice gouge records, as well as the water depth limit which separates recent ice gouge occurrences from relic;
- Older geophysical surveying technologies were limited in available seabed microrelief resolution (i.e., gouge depth resolution cut-off limits) and tended to potentially underestimate shallow water ice gouges. Older systems were also influenced by the sea state which affected sonar control and resolution;
- Measured ice gouge parameters may be biased due to immediate, preferential, or long-term ice gouge infilling, as well as overestimated ice gouge infilling rates;

- Traditionally, ice gouge survey programs mapped tracklines oriented normal to the dominant gouge trend and did not track a given gouge from start to finish, thus introducing limitations and uncertainties when recording maximum gouge parameters and length estimates (i.e., maximum parameters were recorded for the viewable survey area, as opposed to the entire gouge length);
- Detailed ice gouge recurrence rate information is desired, however there is a paucity of repetitive mapping data available for some regions; and,
- Commonly employed statistical distributions may not fit entire ice gouge depth data ranges or distribution tails (extreme events) well and therefore model extreme gouge depth data poorly, thus providing inaccurate maximum gouge depth predictions.

Where statistical ice gouge data is non-existent or of insufficient quantity, numerical models may be utilized to account for the interactions of environmental driving forces, soil reactive forces, and hydrodynamic/hydrostatic ice feature energy sinks during ice gouge processes. These mechanistic approaches suffer from model uncertainty. Stepanov (2000) suggested conventional statistical analysis procedures may not produce reliable ice gouge depth predictions, but provide valuable information for validation of theoretical deterministic models.

Driving force models developed by previous researchers have coupled statistical environmental data and ice feature geometry with mechanical models to define the ice

gouge process and associated ice gouge and seabed interactions (C-CORE, 1999). These models generally rely on (Pilkington & Marcellus, 1981; Comfort & Graham, 1986; C-CORE, 1999):

1. Work energy methods which utilize ice feature kinetic energy in dynamic analysis;
2. Force equilibrium analysis procedures which assume steady state processes governed by the laws of static equilibrium; and,
3. Hybrid work energy and force equilibrium methods.

In a comparison of deterministic versus probabilistic ice gouge analysis procedures, Comfort and Graham (1986) investigated numerical ice gouge models which included force-balance, work-energy, and the limiting gouge depth method. Deterministic ice gouge models available at the time of the study were analyzed and calibrated against baseline environmental data. Work-energy ice gouge models were generally shown to overestimate ice gouge depths by a factor of two; a hybrid dynamic force-balance model was found to be the most complete and sophisticated deterministic model available at the time, but could not be used with confidence (Comfort & Graham, 1986). In a more recent study, Chouinard (1995) suggested that hybrid statistical-deterministic ice gouge depth analysis models may be the optimal solution for ice gouge depth prediction in arctic regions.

The numerical ice gouge models discussed below are inherently limited by key assumptions which facilitate application of these models to ice gouge design and analyses procedures. Deterministic models are limited to the seabed soil conditions, ice and/or soil failure mechanisms, and environmental conditions tested, and may be greatly influenced by the geometry of the ice feature model. Many deterministic (or mechanistic) ice gouge models utilize seabed soil properties and sea ice conditions to estimate ice gouge depths. However, broad soil type classifications and/or limited sea ice data may introduce uncertainty to the models and make correlation with ice gouge parameters difficult (Chouinard, 1995). Recent advances have been made in deterministic/numerical modeling of the ice gouge process, which consider ice keel-seabed interactions, seabed soil failure and redistribution mechanisms, structural pipeline-soil behaviours, and subgouge soil deformations. Physical model tests by Paulin et al. (1993) have shown that seabed response and subgouge soil displacement can occur up to 3-½ gouge depths below the seabed.

Chari (1979; 1982; 1986) presented what is perhaps the earliest model for calculation of probable ice gouge depths (see C-CORE, 1999). The model balanced the kinetic driving force energy of a gouging ice feature, which is converted to potential energy and primarily dissipated by the seabed soil's frontal resistance to the gouging face. The assumption of extremely low seabed shear strength and comparatively large ice keel strength was a main hypothesis in this model, therefore presenting soil failure as the critical criterion for gouging (Chari, 1979; 1982). The model considered wind and current

drag forces, iceberg mass, and seabed slope, among other parameters, in predicted worst-case ice gouge depths. A similar work-energy model was developed by Wahlgren (1979).

Been et al. (1990a; 1990b) have developed an energy-force balance model which balances ice-soil interaction forces with the uplift resistance forces on a gouging ice keel. An idealized multiyear ice feature was utilized, as shown in Figure 4. Been et al. (1990b; 1990c) indicated that typical passive pressure or bearing capacity soil failure mechanisms applied to ice gouge modeling neglected the direction of motion of the indenting ice keel, therefore neglecting kinematic restrictions to rupture surface development and propagation due to motions of the applied load. The Been et al. (1990a; 1990b) model considered environmental driving forces due to wind and current, with resistance to ice feature movement due to passive pressures generated between the advancing ice keel and seabed soil, and friction. The model also considered surge and heave motions, righting moments due to buoyancy, flexural strength of the surrounding ice, and ice keel failure, among other parameters.

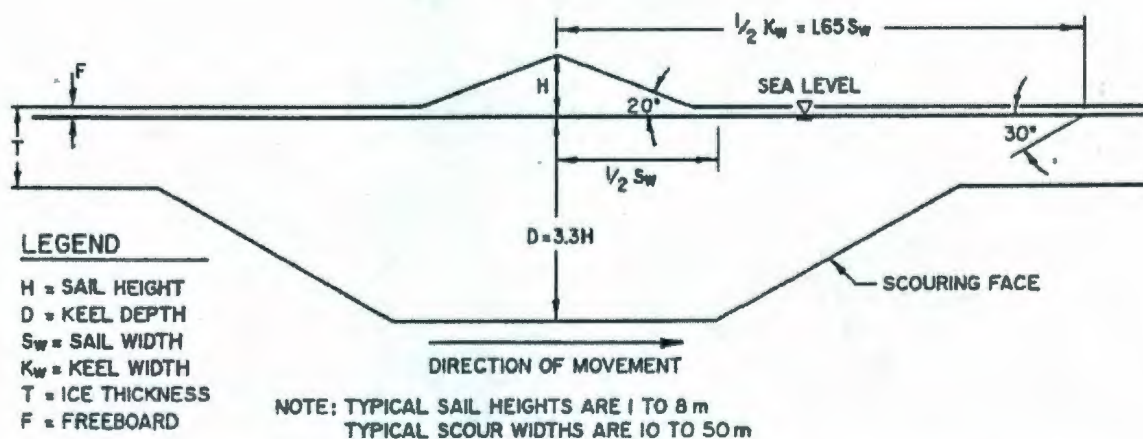


Figure 4: Idealized Multiyear Pressure Ridge Ice Feature Geometry (Been et al., 1990b)

In a more recent study, Croasdale et al. (2005) improved upon Been et al.'s (1990a; 1990b) soil model to allow calculation of vertical and horizontal seabed soil forces as functions of ice gouge parameters (gouge depth, width, and keel angle) and seabed soil strength. The updated model allowed deterministic and probabilistic analysis; deterministic analyses indicated the influence of ice keel strength, soil strength, and attack angle on maximum predicted ice gouge depths. The probabilistic method allowed simulation of ice gouge parameter statistics for regions lacking reliable ice gouge surveys (Croasdale et al., 2005).

Kioka et al. (1995; 1998) developed a simple mechanical ice gouge model which considered soil pressures on the front and sides of a model indenter, buoyancy, subgouge soil deformation, and dynamic friction between the model ice and steeply sloped soil. Ice model velocity was held constant and passive soil pressure on the ice model face was calculated using the Coulomb model. Horizontal and vertical ice model movements were considered.

Yoon et al. (1997) studied an ice gouge model developed through combination of the Chari (1979) and Kioka et al. (1995) models. The model calculated ice gouge depth and interaction forces considering environmental loading and parameters such as ice mass, velocity, and soil strength, among others. Yoon et al. (1997) assumed sufficient seabed bearing capacity to support ice gouge motions and complete soil distribution to the front and sides of the gouging ice keel. The model was idealized as a rectangular block, subjected to frontal and side passive soil pressure, vertical reaction and friction forces,

self-weight, and buoyant resistance and interaction forces. Newton-Raphson numerical analysis techniques were utilized to solve nonlinear equations developed from the model. Yoon et al. (1997) also provided comparison of their model with Chari's (1979) model in analysis of design subsea pipeline burial depths for a Sakhalin Island offshore site.

Abdelnour et al. (1981) developed physical ice gouge models to determine gouge resistance forces, horizontal and vertical ice and soil pressure distributions, soil behaviours, and gouge characteristics for various model shapes and soil types. The objective was to correlate the experimental results with published model and full-scale data. However, the Abdelnour et al. (1981) report has only provided description of the testing conditions and data analysis techniques, with no detailed presentation of the results.

As part of the Pressure Ridge Ice Scour Experiment (PRISE) joint industry program, an ice gouge model was developed which assessed the effects of soil type, soil condition, ice gouge attack angle, depth, and width on the ice gouge process (Phillips et al., 2005; Kenny et al., 2005). PRISE studies utilized a plan-view rectangular rigid-faced indenter which was constrained to translate in the horizontal direction only. The model assumed decoupled ice-soil-pipeline interaction into separate ice-soil and soil-pipeline interactions, therefore allowing consideration of ice gouge geometry, pipeline geometry, and soil conditions in determining optimal pipeline burial depths (Phillips et al., 2005). The PRISE model failure mechanism assumed a triangular dead wedge of soil located beneath an inclined ice keel (i.e., the ice gouge attack angle) with passive soil failure

occurring in front of the dead wedge, similar to the Been et al. (1990b) model. The PRISE model emphasized the development of a significant soil surcharge in front and away from the gouging indenter, as well as subgouge soil deformation caused by a basal shear component which accounts for much of the gouge force. Kenny et al. (2007a) have shown the attack angle's influence on the ice gouge mechanism.

Phillips et al. (2005) also introduced a range of previously developed analytical ice gouge models and compared measured and predicted ice gouge forces resulting from each model with the PRISE model tests (see Figure 5). As shown in the figure, the PRISE model fit the measured test data well. According to Phillips et al. (2005), the Surkov (1995) analytical ice force gouge model was reported to overestimate measured ice gouge forces, as it did not account for any surcharge clearing mechanism in front of the gouging ice keel.

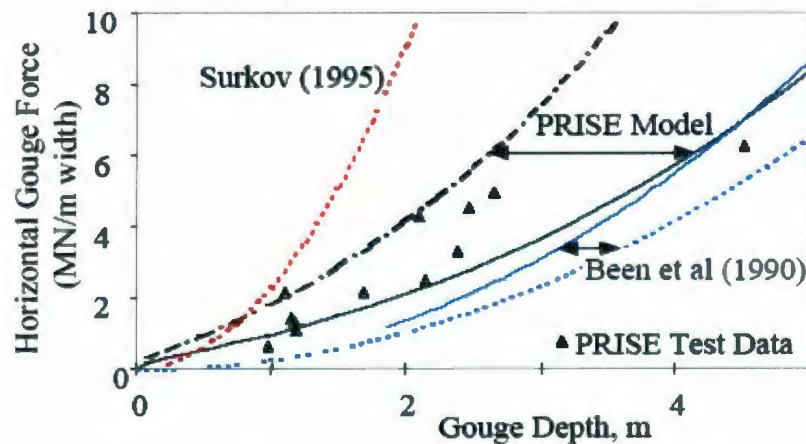


Figure 5: Comparison of Measured and Calculated Ice Gouge Forces in Sand (Phillips et al., 2005)

Preliminary methods to simulate the ice-soil-pipeline interactions were conducted by Konuk and Gracie (2004), among others. PRISE also attempted continuum ice-soil-pipeline interaction finite element analysis, but failed due to technology limitations (Phillips et al., 2005; Kenny et al., 2005).

Recent advances in ice gouge modeling procedures have incorporated finite element analysis methods for modeling of ice gouge processes, subgouge deformations, and ice-soil interaction mechanisms (see Figure 6). Konuk et al. (2004; 2005; 2007) have developed an Arbitrary Lagrangian Eulerian (ALE) finite element model for ice gouge analysis, based on continuum representation of the seabed soil and conventional soil properties. This advanced analysis method considers soil deformation and transport processes around the gouging ice keel, and investigates the effects of interaction with subsea pipeline installations. Use of advanced finite element methods allows determination of soil deformation profiles as functions of depth below seabed for specified ice gouge parameters (width and depth), and calculation of resulting pipeline material strains based on pipeline-soil interaction models. Knowledge of pipeline failure strains consequently allows determination of acceptable ice gouge scenarios for the pipeline installation conditions.

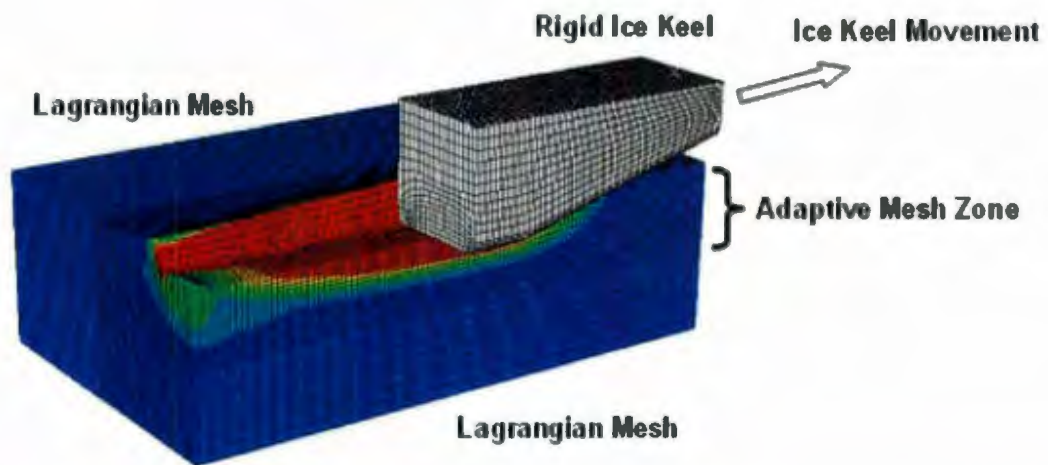


Figure 6: Continuum Finite Element Model of an Ice Gouge (Kenny et al., 2007b)

Liferov et al. (2007) developed several numerical ice ridge gouge models which incorporated finite difference (FD) and ALE solution methods in a parametric study for ice gouge depth determination. Solid ice keel failure was analyzed in two decoupled numerical models, finite element and FD ALE. Three-dimensional ice-soil-pipeline interactions were also considered using coupled and decoupled approaches. The parametric study considered soil properties and stratigraphy, seabed slope, ice ridge dimensions, velocity, attack angle, keel strength, keel-soil friction, and driving forces. Model development procedures determined that ice forces drive gouging processes, soil modeling is critical to accurate analyses, keel failure may be significant during gouging, and vertical reactionary forces must be considered during the initial transient stage only. Monte Carlo simulation was also utilized in development of a traditional probabilistic model.

Jukes et al. (2008) developed a three-dimensional coupled Eulerian Lagrange finite element model to numerically model pipeline-soil-ice keel interactions. The gouging ice

keel is modeled as a three-dimensional solid rigid shape with a 30° attack angle driven into the seabed at some predefined velocity. Younan et al. (2007) have presented a method of analysis for pipeline non-performance due to ice gouging, which considers pipeline-soil interactions and the ability of seabed soils to limit ice gouge depths. Pipeline non-performance was defined as pipeline-ice keel contact or exceedence of an acceptable pipeline strain limit.

Kenny et al. (2000; 2004) have developed a hybrid numerical pipeline response model which utilizes three coupled components; soil-pipeline interaction, ice gouge-soil relationships, and finite element formulation procedures. The model assumes soil-pipeline interactions following guidance provided by the American Society of Civil Engineers, and empirical subgouge deformation response functions derived from PRISE studies. The model considers seabed soil type, ice gouge depth and width, ice gouge overburden stress due to ice keel mass and driving forces, and soil load-displacement behaviours, among other factors.

Kenny et al. (2004) and Nobahar et al. (2007) have discussed probabilistic assessment of joint ice gouge geometry distributions using gouge depth and width distributions which are treated as independent relationships. The hybrid ice gouge design approach developed by Kenny et al. (2004) integrated deterministic ice gouge models within a probabilistic assessment framework to optimize ice gouge/pipeline design with respect to project economics and technical constraints. The analysis procedure utilizes an input matrix of joint ice gouge depth and width data determined from probabilistic assessment of

physical ice gouge survey data in a matrix of deterministic finite element analysis procedures which consider pipeline-soil interaction models. The analysis is conducted for a range of pipeline clearance depths (due to burial) and a probabilistically defined ice gouge parameter matrix to determine the mechanical pipeline stress and strain response to each gouging scenario. The analysis results in minimum pipeline clearance depth contours for joint ice gouge depth and width distributions based on allowable mechanical pipeline design criteria (i.e., factored serviceability or ultimate limit state design). The hybrid probabilistic-deterministic ice gouge analysis procedure is suggested as providing the current industry best practice for ice gouge design optimization, based on the literature reviewed as part of the present work.

Refer to papers by Kenny et al. (2000; 2004) and Nobahar et al. (2007) for further discussion of hybrid probabilistic-deterministic ice gouge analysis procedures.

As discussed below in Section 1.4, this thesis work focuses on statistical ice gouge analysis procedures. However, an overview of numerical ice gouge modeling was presented above for completeness of technical literature research and review.

1.3 SIGNIFICANCE OF STUDY

This thesis project has involved extensive research and compilation of historical ice gouge data and statistics from the Canadian and American Arctic Oceans, and is deemed to be a timely thesis project given current arctic oil and gas interests. Research and review of previous ice gouge depth analysis studies has been conducted in order to

provide the reader with a comprehensive overview of preceding ice gouge works relevant to the Canadian Beaufort, American Beaufort, and Chukchi Seas.

Nearshore arctic environments are emerging as viable locations for oil and gas exploration and production activities as conventionally 'easily recoverable' resource areas are exploited. Arctic nearshore areas are highly sensitive to environmental damage, which has led to thorough environmental risk and impact analysis of arctic oil and gas projects prior to governmental and regulatory approval. The safe and effective transport of produced reserves is of utmost interest to project approvals. Due to the remoteness of many arctic installations, the lack of local infrastructure, and harsh environmental conditions, offshore and overland pipeline transmission networks have been developed for reliable transport of oil and gas products over a wide range of distances (for example, the overland *Trans Alaska Pipeline System*, or the *Northstar* and *Oooguruk* subsea pipeline bundles). Subsea pipelines are generally recognized as the safest and most economically viable means of transporting produced offshore arctic hydrocarbons to shore (Palmer et al., 1990).

There are many environmental and operational risks associated with the construction, installation, and operation of pipelines located in arctic environments. Of particular interest is pipeline integrity in arctic offshore areas subjected to seabed ice gouging. A pipeline directly contacted by a gouging ice keel and/or subjected to subgouge deformations may rupture and impart severe environmental, economic, and/or human damage on a local, or even global, scale. The environmental and economic consequences

associated with a pipeline failure in any environment are extensive and complex, and must be prevented via thorough risk based design, analysis, and assessment procedures.

As part of comprehensive subsea pipeline design for arctic locations, design ice gouge depth analysis must be conducted in an effort to safely predict the maximum depth to which an ice keel may be expected to gouge the seabed during a specified return period. Probabilistic methods endeavour to predict design gouge depths and/or geometry based on environmental criteria, historical ice gouge depth statistics, and the accepted level of risk that may be posed to the pipeline installation. Ice gouge statistics may require adjustment for technical limitations, bias, and/or infilling effects, prior to inclusion in probabilistic or numerical ice gouge models. The maximum expected gouge depth or profile geometry estimate is then an input to the pipeline trenching and burial depth requirements for protection of the pipeline against ice keel interaction.

Ongoing arctic geophysical programs conducted in the Canadian and American Beaufort Seas have led to a better understanding of ice gouge processes and procedures, in addition to significant historical data collection. Data collections are available in both the public and private domain, with many publication dates ranging from the early 1970's and onward to the present day. In general, these works and data collections have been analyzed and presented in numerous technical reports and studies specific to the research program, geographic area of interest, and/or the technical body performing the data collection and/or analysis. Significant products of the current thesis include the consolidation of this data and analysis into one work which may be updated and revised

when additional data becomes available, as well as statistical analysis of the available data.

Ice gouge depth statistical analysis and design depth estimation is an important factor in subsea pipeline design for arctic nearshore regions subject to ice gouging. As such, various statistical methods applicable to measured ice gouge depth distributions have been researched and evaluated, with presentation of various methods for extrapolating ice gouge depth statistics to design events. As ice gouging methods and processes have become better understood, studies have been conducted with respect to the age of observed seabed gouges, associated gouge infilling rates, and methods of ice gouge recurrence rate prediction. These factors must be considered in thorough ice gouge depth analyses for subsea pipeline design, and are thus addressed in detail as part of the forthcoming thesis project.

1.4 THESIS OBJECTIVES

Iceberg gouging of the seabed was first hypothesized in published literature by Charles Darwin in 1855 but "...attracted very little attention until the discovery of substantial hydrocarbon plays in the North Sea and Canada's east and arctic coasts" (Pereira et al., 1988). Through investigation of recent studies and collection of historic public domain ice gouge data, data bias, correlation, and gouge measurement and analysis procedures have been evaluated, specific to each arctic nearshore region of interest to the current work.

Investigation of probabilistic ice gouge characterization and modeling was conducted as part of this thesis work, with the objective of evaluating the suitability of statistical distributions to observed ice gouge depth data. Discussion and analysis of data correlation observed among ice gouge distribution characteristics, recurrence, and degradation was investigated, where possible on the basis of available data. The collected ice gouge data was assessed in terms of quality and quantity, and then probabilistically analyzed for recommendation of the most appropriate statistical distribution for each region and water depth range. Evaluation of statistical distribution tails was of particular interest within this current work, as the upper tail represents the extreme ice gouge events which the subsea pipeline design engineer must consider during design gouge depth analysis and subsequent pipeline burial studies. The impacts of wave and current action, as well as local seabed soil conditions, have been investigated with respect to ice gouge infilling and degradation. The limiting effects of seabed soil properties on ice gouge processes were also researched.

2 PHYSICAL ICE GOUGE DATA STUDIES

Extensive research and review has been conducted of publicly available technical reports and studies of ice gouge occurrences on the inner shelf of the Canadian Beaufort, American Beaufort, and Chukchi Seas during the development of this thesis. Topical reports from the American Beaufort and Chukchi Seas have been obtained from the United States Geological Survey (USGS), the U.S. National Geophysical Data Center (NGDC), the Division of Geological and Geophysical Surveys of the Alaska Department of Natural Resources, and the U.S. Army Corps of Engineers Cold Regions Research and Engineering Laboratory (CRREL). Investigated documents pertinent to ice gouge occurrences in the Canadian Beaufort Sea have been obtained from the Geological Survey of Canada (GSC), Environmental Studies Research Funds (ESRF), the Canadian Hydraulics Center of the National Research Council Canada (CHC-NRC), the National Research Council Canada Program for Energy Research and Development (PERD), and Arctic Petroleum Operators Association (APOA) publications.

Industry workshops on seabed ice gouging were also researched and reviewed for use in thesis development, and have included papers and proceedings from conferences on Port and Ocean Engineering Under Arctic Conditions (POAC), International Offshore and Polar Engineering (ISOPE), Offshore Mechanics and Arctic Engineering (OMAE), Offshore Technology Conference (OTC), a Workshop on Ice Scour Research, Ice Scour and Seabed Engineering sponsored by ESRF and PERD, and the Workshop on Ice Scouring and the Design of Offshore Pipelines sponsored by the Canada Oil and Gas Lands Administration (COGLA) and the Center for Cold Ocean Resource Engineering

(C-CORE). In addition, relevant technical publications from academic and/or industry professionals known to be renowned in the fields of ice gouge research, design, and analysis have been sought out for reference within the current work. Not all of the preceding reference sources have provided documents suitable for use in this study. Sections 2.4 through 2.6 provide discussion of investigated ice gouge data studies.

2.1 ICE GOUGE CHARACTERISTICS & MEASUREMENT PROCEDURES

As an ice keel impacts and scrapes along the seabed, many characteristic seabed deformations are produced. These deformations may be observed and measured for further analysis through marine surveying techniques, as discussed in Section 2.1.3. 'Pock mark' seabed indentations are typically produced when an ice keel impacts and grounds upon the seafloor, which become noticeable once the ice has sufficiently melted to allow the indenting ice keel to dislodge and move off of the grounding site.

Single-keeled ice features have a single keel projection that may contact the seafloor. These keels generally create gouge deformations exhibiting localized ridge berms and furrowed seabed micro-topography, with associated vertical and horizontal sediment displacement and redistribution (Rearic & Ticken, 1988). Ice gouges created by multi-keeled ice features which possess multiple keel projections contacting and gouging the seafloor are commonly termed 'multiplets'. These gouge deformations typically exhibit a characteristic multiplet gouge deformation which simulates rake marks upon the seabed surface (Rearic & Ticken, 1988).

Common ice gouge deformation parameters and associated characteristics are discussed below. Figure 1 presents single-keeled ice gouge characteristics; Figure 3 provides a diagram of a single-keeled and multiplet ice gouge characteristics as defined by the USGS. The geotechnical conditions (seabed soil shear strength and resistance to ice keel penetration), morphology, and localized bathymetry of the seabed areas subject to ice gouging events influence gouge attributes. Therefore, gouge characteristics may fluctuate along the length of an ice gouge with changing seabed conditions. Annual variations in ice concentrations also strongly effect the distribution of seabed gouges.

As shown in Figure 1 and Figure 3, the ice gouge incision depth is measured as the vertical distance between the average gouge trough (or floor) and the undisturbed seabed elevation. This measurement practice allows the seafloor penetration depth of the impacting ice keel to be accurately measured and recorded, referenced to an ungouged seabed datum. Factors which influence ice gouge depths include the size and shape of the gouging ice keel, seabed geotechnical conditions, environmental driving forces, and gouge orientation, among others. The vertical distance measured between the deepest point in the ice gouge trough and the ungouged seabed datum is referred to as the maximum ice gouge depth. Not only is the maximum gouge depth important, but also the localized width over which this maximum depth occurs. Interpreted ice gouge statistics are normally reported as having a maximum depth and an overall or maximum width, with measurements referenced from the surrounding ungouged seabed level. This could lead to the interpretation of there being a deep gouge over a significant width, when, in fact, the maximum gouge depth may have been the result of the deepest part of the keel

(or a single keel in a multi-keeled event) acting over a significantly smaller width (on the order of meters).

Total ice gouge relief heights are measured as the vertical distance between the gouge trough and the maximum sidewall berm height. This is a misleading characteristic for use in ice gouge analysis as it may lead to over-estimation of the size of the gouging ice keel or maximum keel penetration depth.

The ice gouge incision width is the horizontal distance extending across the ice gouge and measured at the undisturbed, or ungouged, seabed elevation. The gouge incision width parameter thus excludes the width of the gouge sidewall berms, or ridges, and is a defining characteristic of the impacting ice keel. Berm-to-berm ice gouge widths represent the horizontal distance measured across the gouge from the uppermost center point of one sidewall berm crest to the other. The gouge berm-to-berm width is thus inclusive of the gouge incision width and is a characteristic of the impacting ice keel and resulting seabed soil displacement. Canadian ice gouge studies record gouge 'widths' as the horizontal distance measured across the gouge referenced from berm crest to berm crest (i.e., the berm-to-berm width) (Myers et al., 1996).

Multiplet ice gouge widths are termed the maximum 'disturbance' or multiple gouge 'disruption' width by US studies and the 'multi-keeled' width in Canadian studies, but each record the maximum width of the recorded ice gouge event, inclusive of all individual gouge tracks formed by the multi-keeled ice feature (Myers et al., 1996; Rearic et al., 1981; Rearic & McHendrie, 1983). Multiple gouge 'disruption' widths are

referenced from the ungouged seabed, inclusive of bounding ice gouge ridges, or berms (Rearic et al., 1981).

The ice gouge berm height is the vertical height of the ridge embankment (or berm) of sidecast seabed soil on either side of the gouge trough(s) which was created as an ice keel penetrated and gouged along the seabed. Similar to the gouge depth and width measurements, the berm height is referenced from the level of the surrounding undisturbed seabed.

The ice gouge sidewall slope represents the angle formed between the horizontal ungouged seabed reference datum and the deepest point in the gouge trough. This parameter may be measured at various points along the gouge sidewall and characteristically fluctuates along the overall gouge length.

The relative age of seafloor ice gouges is also important, as the gouge rate of recurrence can be an input to the maximum ice gouge depth prediction. Ice gouge recurrence rates are reported as the total number of ice gouges observed per linear distance of survey trackline in a given year (i.e., the number of gouges/km/year), and is thus determined by dividing the total number of observed ice gouges during a specific survey year by the overall survey trackline length. As discussed in Sections 2.1.1 and 2.1.2 below, there are distinct differences in Canadian and American ice gouge recurrence rate measurement and estimation procedures that may cause over-estimation during American ice gouge investigations. Previous ice gouge recurrence rate studies were researched and

investigated as part of this thesis work, with results and findings presented above in Section 3.5.

In general, ice gouges of unknown age are termed 'old' or 'baseline' within industry, whereas gouge formations of known maximum age are termed 'new' or 'dated'. Ice gouges known to be on the order of thousands of years old are commonly termed 'relic'. Use of old ice gouge depth statistics for design depth analysis (see Section 3.1) may potentially result in over-conservative estimates since these gouges may have formed at a time when sea levels were lower. During times of lower sea levels, ice keel features with shallower drafts could impact and gouge the seabed, perhaps giving the current-day impression of deep draft ice keels in contemporary deep water locations when these gouges were actually created in shallower water depths. Design ice gouge depth estimates based on old ice gouge statistics may therefore over-predict deepwater gouge depths beyond the limits of modern ice keel drafts.

Ice gouge linear density or crossing rate is commonly presented for base year or single-year seabed surveys, which fundamentally do not present dated new gouge occurrence data. In such cases, the linear ice gouge density (or crossing rate) is often reported as the number of gouges observed per linear survey trackline length (i.e., the number of gouges/km), whereas the spatial density is reported as the number of gouges observed per surveyed area (i.e., the number of gouges/km²). As discussed in Section 2.1.3 below, spatial survey areas and/or trackline observations widths are highly dependent upon the visible width of the seabed reconnaissance equipment and technology used.

An ice gouge generally reflects a predominant direction of ice keel movement, which is characteristically dependent upon the geographic location of the ice gouge event. The dominant gouge trend, or orientation, is oftentimes reported as the angle formed by the ice gouge deformation path, relative to true north.

The weathering, infilling, and subsequent obliteration of ice gouge deformations in the seafloor is a dynamic and time dependent process that is highly contingent upon the soil and sediment properties of the seabed, as well as immediate and/or long-term sediment reworking processes that may be present. Sediment reworking displaces material from areas of high vertical relief, such as ice gouge berms, and deposits this material into the gouge trough, with transport from wave and current action representing a significant although intermittent factor which affects ice gouge characteristics (Barnes & Reimnitz, 1979). Ice gouge infilling and estimation of obliteration rates may be observed and analyzed through repetitive surveying of dated gouges. Refer to Section 3.4 of this report for discussion and presentation of ice gouge infilling and sedimentation studies investigated as part of this thesis work.

Many historical ice gouge data sets (see Section 2) provide estimated ice gouge lengths for observed gouge deformations, where available, which represent the overall linear distance of the ice gouge path along the impacted seabed. This ice gouge characteristic is generally prone to underestimation due to the manner of ice gouge surveying typically employed. In general, ice gouge survey tracklines are oriented across seabed ice gouges as opposed to following gouges along their entire lengths. This procedure is employed for

enumeration and estimation of ice gouge densities and/or recurrence rates, but consequently necessitates estimation of the overall ice gouge length as only a potentially small portion of a particular gouge may be surveyed at each ice gouge/survey trackline crossing.

2.1.1 American Beaufort & Chukchi Seas

Ice gouge survey programs conducted in American Arctic oceans characteristically record each individual ice gouge deformation or furrow in a multi-tracked seabed deformation as an individual ice gouge, regardless of whether it was created by a single-keeled or multiplet event (Morrison & Marcellus, 1985; Marcellus & Roth, 1991). Ice gouge depth measurements are subsequently recorded for each gouge track identified. This method of recording basic ice gouge data treats each observed ice gouge track as an independent, single-keeled event, thus neglecting the possible occurrence of multiplet gouges resulting from a single ice feature with multiple keel projections contacting the seabed (a known phenomenon).

Similarly, observation of USGS ice gouge survey program data sets indicate that the USGS counts every gouge deformation present within a multiplet deformation swath as a single ice gouge and then normalizes the total gouge count to correct for the angle formed between the dominant gouge trend and the survey vessel's course (Barnes et al., 1978; Rearic et al., 1981). The following correction procedure normalizes ice gouge counts to represent the number of gouges that could be seen if all dominant ice gouge trends were

oriented perpendicular to the direction of survey vessel travel (Barnes et al., 1978; Weeks et al., 1983):

$$N_1 = N / \sin(\alpha) \quad (2.1)$$

where

N_1 = the expected number of ice gouges that would be observed along a sampling line; oriented normal to the dominant gouge trend;

N = number of ice gouges observed per kilometer of survey trackline; and,

α = acute angle formed between the survey vessel's track and the gouge orientation.

In addition, USGS ice gouge analysis procedures count each gouge deformation visible on side-scan sonar records, regardless of whether they may be correlated on echo sounder records or not (i.e., including those which do not cross the survey vessel's path) (Marcellus and Roth, 1991; Rearic et al., 1981). Canadian ice gouge analysts only record gouge data for ice gouge events that are identifiable and may be correlated on both side-scan and echo sounder records (Marcellus & Roth, 1991). Consequently, ice gouge frequencies and recurrence rates derived from survey programs conducted in the American Arctic oceans may be overestimated when compared to Canadian procedures.

In general, the USGS records maximum ice gouge depth and width data per one-kilometre survey trackline segment lengths for statistical analyses (Rearic et al., 1981; Reimnitz et al., 1982). Ice gouges observed on side-scan sonar records but which cannot

be correlated to echo sounder records (i.e., did not cross the survey trackline) are counted as observed ice gouges by the USGS. The USGS records ice gouge width measurements for these observations, although no associated ice gouge depth can be measured due to the unavailability of correlated echo sounder records.

2.1.2 Canadian Beaufort Sea

In addition to differences in nomenclature between American and Canadian ice gouge (or scour) studies, a significant difference exists in the method of ice gouge enumeration. Canadian ice gouge data is generally recorded for the entire ice gouge, for each gouge which crosses the survey trackline, as opposed to obtaining measurements per a defined ice gouge trackline segment length (i.e., one-kilometre, as utilized by the USGS; see Section 2.1.1). In general, Canadian ice gouge studies classify multi-keeled 'multiplet' ice gouge deformations and zones of multiple gouges as single ice gouge events, not as numerous single-keeled events (as classified by the USGS; see Section 2.1.1). The maximum depth observed amongst all individual gouge tracks in the multi-keeled zone is then recorded as the gouge depth for the entire event (Morrison & Marcellus, 1985; Marcellus & Roth, 1991). The overall width for the entire deformation zone is likewise recorded as the gouge width (Marcellus & Roth, 1991). As discussed above, American ice gouge studies count each individual seabed incision as a single event with an associated gouge depth measurement, regardless of whether it was created by a single-keeled or multi-keeled ice feature (Morrison & Marcellus, 1985; Marcellus & Roth, 1991). Consequently, ice gouge frequencies and recurrence rates may potentially be overestimated in American arctic waters when compared to Canadian data.

Ice gouge analysis procedures from the Canadian Beaufort Sea measure the ice gouge width as the overall incision width of a deformation, less the width of the spoil pile (or berm). In general, Canadian ice gouge width data represents the average width measured perpendicular to the gouge axis and averaged along the length of the gouge (Myers et al., 1996). Ice gouge length measurements are limited to the range of the side-scan sonar system, which thus limits accurate derivation of overall average gouge width values. Canadian ice gouge depth data is generally recorded for the entire ice gouge, for each gouge which crosses the survey trackline. Dominant orientations are measured relative to true north. Ice gouge width and orientation measurements are easily observed from side-scan sonar records, whereas measurement of ice gouge depths requires establishment of an approximated ungouged seafloor reference datum. In historical Canadian Beaufort Sea ice gouge analysis procedures, this line may be visually smoothed and approximated as the bisection of the gouge berm and associated incised seabed areas (Marcellus & Roth, 1991).

Marcellus and Roth (1991) presented the results of a study to compare Canadian analysis of USGS geophysical ice gouge data records with the interpreted results provided by the USGS. The Canadian data interpretation was conducted by C.M.E.L. Enterprises Ltd. (CMEL), acting on behalf of Gulf Canada Resources Ltd. The Marcellus and Roth (1991) study indicated that USGS analysis procedures recorded all gouge depths less than 0.2m as 'No Measurement Possible', as well as all gouges counted on side-scan sonar records but not recorded by the echo sounder (i.e., gouges which did not intersect the survey

trackline). The echo sounder equipment utilized by the USGS allowed 0.15m gouge depth resolution.

Through comparison of USGS and Canadian ice gouge analysis procedures, it was identified that the USGS consistently positioned the ungouged seabed datum higher on the echo sounder records than CMEL did in their (Canadian) analysis. This resulted in increased USGS ice gouge counts and measurement of consistently deeper gouge depths than recorded through Canadian analysis procedures (Marcellus & Roth, 1991).

Unlike the USGS, Canadian analysis of these geophysical records measured gouge depths with less than 0.2m resolution, but only counted gouges which crossed the survey trackline (i.e., gouges that could be correlated on the side-scan and echo sounder records). Again, ice gouge frequencies and recurrence rates may therefore be over-estimated by USGS analysis procedures when compared to Canadian data.

Similar ice gouge depth distributions were obtained when Canadian analysis procedures were used for interpretation of separate American and southern Canadian Beaufort Sea geophysical survey records of seabed ice gouging to 20m water depth (Marcellus & Roth, 1991). It was therefore shown that differences in American and Canadian ice gouge data are more likely a result of subjective data analysis procedures than due to the existence of different ice gouging regimes. Marcellus and Roth (1991) concluded that ice features gouging the seabed in American and Canadian Beaufort Sea regions are stochastically the same, assuming that seabed soils are the same in each region.

2.1.3 Gouge Measurement Accuracy & Technological Advancements

Historical geophysical surveying techniques used for ice gouge data collection generally employed echo sounders and dual channel, single beam side-scan sonar for analysis of seafloor bathymetry and detection of ice gouge deformations. However, recent technological advancements in subsea geophysical surveying techniques incorporate multibeam sonar for use in detailed seafloor and ice gouge profiling (see below). Multibeam profiling allows collection of significantly more data for each gouge, although the data is conducive to automated (or quasi-automated) processing and may not require manual interpretation. Therefore, more data can be collected for statistical analysis, including depths along the gouge axis at set intervals, cross-sectional profiles, etc. This data may be useful in developing a better statistical representation of ice gouges and the estimation of a design gouge event, as opposed to the use of maximum ice gouge depth and width parameters only (for an overall or predetermined ice gouge length).

Gilbert and Pedersen (1987) provided discussions of ice gouge observation and measurement from interpretation and processing of side-scan sonar and echo sounder data retrieved in the Canadian Beaufort Sea. During the Gilbert and Pedersen (1987) study, analogue side-scan sonar records were manually digitized for measurement of ice gouge characteristics from the generated sub-bottom profiles. Analogue echo sounder data was manually digitized in a similar manner for processing and manual measurement of the sub-bottom profile. Gilbert and Pedersen (1987) indicated that ice gouge depth, sediment infill, and subgouge deformation manual measurement and digitization resolution was available to 0.5m accuracy. Reworked seabed sediment thicknesses were

recorded in 5m intervals, to a maximum measurement depth of 10m. An early, computerized ice gouge data interpretation software program named *DBase II* was also introduced by Gilbert and Pedersen (1987), along with comparison of ice gouge depth measurements derived manually, as well as when using the software program. As shown in the following Figure 7, this early form of interpretive ice gouge parameter analysis software compared well with manual ice gouge measurements. The analysis software also satisfied chi-square goodness-of-fit testing at the 5% significance level (conducted by others) (Gilbert & Pedersen, 1987).

A study by Gilbert et al. (1985) also found that manual and computerized ice gouge depth interpretation compared well, based on independent analysis and data processing of analogue Canadian Beaufort Sea ice gouge data. In this comparison, manual interpretation was averaged over nine separate interpreters in an effort to account for subjectivity exhibited between interpreters.

In a study of iceberg gouging on the Canadian east coast (Newfoundland Grand Banks), King et al. (1989) addressed geophysical seabed surveying instruments commonly used for ice gouge analysis, as well as their associated accuracies, limitations, and resultant data quality.

Medium range, 70 kHz side-scan sonar systems were reported to provide medium seabed resolution over wide swaths on the order of 1.5km (750m per channel for a dual channel system) (King et al., 1989). Higher frequency (100 kHz) side-scan sonar can be utilized to provide greater seabed resolution, but are usually operated on the range of 200m

viewable seabed width per channel (King et al., 1989). Lower frequency side-scan sonar systems (on the order of 27 to 30 kHz) may be utilized in deepwater applications to obtain coverage swath widths of up to 5km, albeit it at very low seabed resolution. In general, seabed resolution accuracy increases with increasing side-scan sonar system frequency, but also results in decreased range capabilities and thus collection of narrower seabed swath widths.

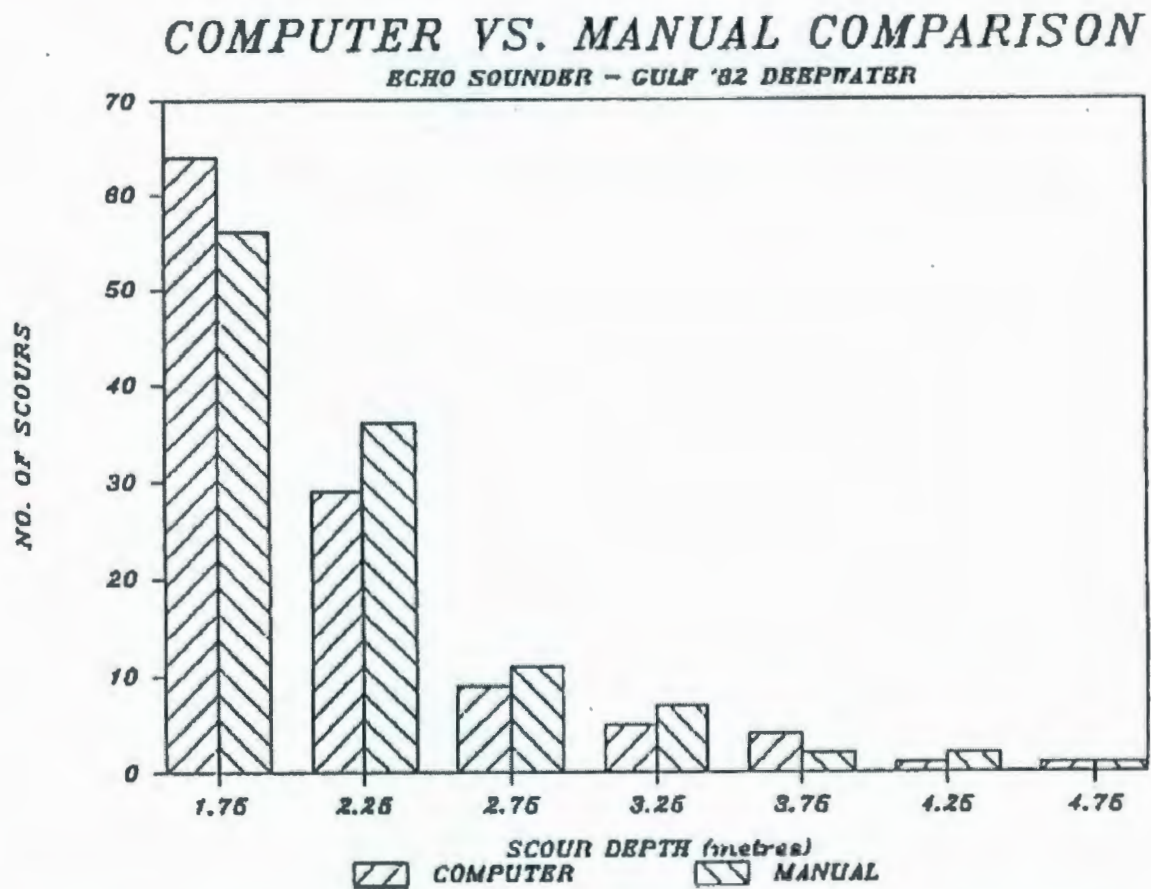


Figure 7: Comparison of Computerized vs. Manual Interpretation of Echo Sounder Ice Gouge Database (Gilbert & Pedersen, 1987)

King et al. (1989) reported that side-scan sonar data quality is highly dependent upon the sea state during operation, with rough seas producing high levels of ambient noise which reduces the brightness or darkness of the sonogram. Difficulties are subsequently encountered during identification of seabed features and microrelief. Pitch and yaw of the sonar towfish can also result in decreased data quality, and generally produces a reduction of seabed spatial resolution and a 'saw-toothed' appearance to otherwise linear seabed features (King et al., 1989). Side-scan sonar data quality can also be reduced by temperature, salinity, or suspended matter stratification in the water column. Stratification of the water column in a specific survey area may alter sonic velocity profiles and refract sonar signals, thus reducing the range of coverage and altering recovered signals (King et al., 1989). Vertical ice gouge resolution is also affected by the height of the towfish when towed above the seabed; seabed gouging records may not appear as 'crisp' or shallow gouges may not be resolved at all if the towfish is not operated at its optimum height (King et al., 1989).

In addition, King et al. (1989) reported that side-scan sonar systems might exhibit scale distortions as high as 5:1 due to differences in across-track and along-track (aspect ratio) scales. Scale distortions may result in round seabed objects appearing oblong on side-scan sonar records, as well as linear features appearing to be oriented perpendicular to the survey trackline (King et al., 1989). The orientation of seabed features relative to side-scan survey tracklines must also be considered, as acoustic pulses experience greater reflection and thus higher resolution from angled surfaces (i.e., such as ice gouges) when oriented parallel to the survey trackline than when perpendicular (King et al., 1989). This

inherent limitation to side-scan sonar systems therefore introduces a data bias when surveying ice gouge features based on their relative orientation to the survey trackline.

K.R. Croasdale and Associates (2000) also studied ice gouge detection techniques commonly employed on the Grand Banks of Newfoundland, on the Canadian East Coast. Although discussed with respect to the Canadian east coast, similar side-scan sonar systems may be utilized in any region. Towed side-scan sonar transducers emit an acoustic pulse with a narrow beam angle in the horizontal plane, generally on the order of 0.5° to 1.5° , and wider beam angles in the vertical plane (K.R. Croasdale & Associates, 2000). Survey vessels typically tow two side-looking transducers (port and starboard side) mounted in a single towfish unit. Thus, depending on the water depth, seabed swaths on the order of hundreds of meters may be scanned per transducer channel, as discussed by King et al. (1989). Successive sonar ping recordings obtained along a survey trackline allow derivation of seabed sediment types, bathymetry, and associated irregularities, based on the amount of sonar energy (backscatter) returned to the transducers. K.R. Croasdale & Associates (2000) reported that seabed ice gouges are well suited to side-scan sonar detection and interpretation, although the ability to accurately detect individual gouges is dependent upon the seabed morphology. Factors include the size and shape of ice gouges, gouge age (see Section 2.2) and amount of infilling or degradation (see Section 3.4), geological complexity of the surrounding seafloor, side-scan sonar data quality, and manual interpretation techniques or skill.

Side-scan sonar systems may be utilized to measure ice gouge lengths, widths, and orientation (two-dimensional parameters), although ice gouge depths cannot be accurately obtained from side-scan sonar records, thus necessitating the use of seabed profiler or echo sounder systems. These systems allow more accurate measurement of ice gouge depths, berm heights, and gouge profile shapes (in the vertical plane). Side-scan sonar records may also be utilized to evaluate surficial seabed sediment types, gouge morphology and plan view shapes, side berm development, and termination points or points where the gouging direction changes. Table 1 provides comparison of various side-scan sonar systems utilized in compilation of the *Grand Banks Scour Catalogue* (GBSC) and investigated by K.R. Croasdale and Associates (2000).

Echo sounders and sub-bottom seabed profilers both transmit acoustic pulses through the water column and retrieve a return echo from the seafloor (similar to side-scan sonar). The major difference between echo sounder and sub-bottom profiler technology is the frequency at which each operates; echo sounders transmit a high frequency, narrow beam pulse to the seabed on the order of 12 to 200 kHz, whereas sub-bottom profilers transmit a broad frequency spectrum on the order of 400 to 10,000 kHz (K.R. Croasdale & Associates, 2000). Echo sounder acoustic pulses cannot pass through coarse seabed sediments and therefore provide a detailed profile of the seafloor surface only; sub-bottom profiler acoustic pulses transmit sufficient low frequency energy to obtain profiles through most near surface seabed sediments and therefore provide some profile of surficial sediments to some thickness below the seabed surface (K.R. Croasdale & Associates, 2000).

In order to accurately measure ice gouge depths from echo sounder and/or sub-bottom profiles, the survey trackline must pass directly across an entire ice gouge event. In addition, ice gouges observed on side-scan sonar records must be correlated with profiler or echo sounder records in order to provide associated gouge width and depth data, among other data parameters. Ice gouge depth resolutions obtained using echo sounder systems were commonly observed on the order of 0.1m during development of this thesis work (i.e., refer to discussions of previous ice gouge studies and available data collections). Table 2 provides comparison of echo sounder and sub-bottom profiler systems utilized in compilation of the GBSC and investigated by K.R. Croasdale and Associates (2000).

Recent advances in multibeam ice gouge profiling technology allow detailed three-dimensional imaging of seafloor bathymetric profiles. Earlier multibeam profilers operated at 95 kHz frequencies and transmitted 32 individual 2° by 3° beams in a fan-shaped array. Advanced multibeam profiling systems utilize 127 separate 1.5° by 1.5° beams (K.R. Croasdale & Associates, 2000). Multibeam sonar scanning swath widths are dependent upon the angle formed between the water depth being surveyed and the outermost sounding beams (K.R. Croasdale & Associates, 2000). The number of beams utilized, beam spacing, and survey water depths determine the beam density on the seafloor. When corrected for survey vessel motions, water column velocity, and tide variations, multibeam systems may provide digital terrain modeling of seafloor morphology at resolutions of a few centimetres, although acoustic morphologies are better defined using side-scan sonar systems (K.R. Croasdale & Associates, 2000).

Multibeam sonar analysis allows measurement of ice gouge depths, widths, and sidewall parameters along the entire length of the gouge, therefore providing knowledge of gouge parameter variation. Thus, rather than having reported maximum ice gouge depth and width data for a given ice gouge event, use of multibeam sonar can provide significantly larger data sets of gouge measurements for statistical analysis during engineering design. Refer to discussions by Davis et al. (2005) for further details on advanced multibeam sonar methods and interpretation procedures for ice gouge profile analysis.

Table 1: Comparison of Side-scan Sonar Systems (K.R. Croasdale & Associates, 2000)

Sidescan System	Frequency (kHz)	Pulse Width (msec)	Beam Width (Degrees)	Range Resolution	Transverse Resolution ¹
Klein	50	0.2	1.5	0.2 m	6.5 m
Klein	100	0.1	1.0	0.1 m	4.4 m
ORE	100	0.1	1.0	0.1 m	4.4 m
BIO	70	1.0	1.5	0.8 m	6.5 m
Simrad	120	0.1	0.75	0.1 m	3.3 m
Edgetech	100	0.1	1.2	0.1 m	5.2 m
¹ Calculated at 250 meter range for all systems.					

Table 2: Comparison of Seabed Profiler Systems (K.R. Croasdale & Associates, 2000)

Profiler System	Platform Type	Frequency (kHz)	Beam Width (Degrees)	Footprint Diameter ¹	Vertical Resolution ²
Echo Sounder ³	hull-mount	3.5-200	8	7m, 28 m	0.1 m
ORE 3.5	towed body	3.5	55	26m, 104m	0.2 m
Huntec DTS	towed body	0.8-10	11	10m, 39m	0.2 m
NSRF V-Fin	towed body	1-3	N/A	N/A	0.5 m

¹For source located at 50 and 200 meters above the seafloor.

²Theoretical system resolution. GBSC sources incorporate a minimum detectable scour depth of 0.3-0.5 m (Huntec), 0.5 m (ORE 3.5 kHz), or 1.0 m (NSRF V-Fin). The detection limit for scours profiled using hull-mounted systems is variable, depending on the sea state during the survey.

³Individual echo sounder types are not identified in the GBSC (beam width and footprint based on survey grade 200 kHz system).

2.2 ICE GOUGE DATING METHODS

Numerous methods of determining ice gouge age have been reviewed during research conducted as part of this thesis. These methods are summarized as follows:

- Microfaunal and sedimentological studies of gouge sediment cores using radiocarbon (Carbon C-14) dating for recognition of probable buried ice gouge trough surfaces (see Pereira et al., 1988);
- Cross-cutting ice gouge dating techniques which analyze the relative age of gouges based on side-scan sonar observations and observed gouge cross-cutting patterns (see Pereira et al., 1988);

- Palynology with an accuracy of ± 1000 years, based on analysis of fossil pollen and spores within Pleistocene sediments and radiocarbon dating of core sample indicator species, which include spruce, fir, and birch tree pollen, birch and alder shrub pollen, herb pollen, and fern spores (refer to Mudie, 1986);
- Alternate biogenic ice gouge dating methods include isotope dating, amino acid racemization, electron spin resonance, biological growth, or foraminiferal dating (see Barrie and Woodworth-Lynas, 1984);
- Qualitative extreme ice gouge relative ages, or morphological 'freshness', may be estimated based on gouge appearances on high-resolution side-scan sonar observations and categorized according to their amount of infilling and/or weathering (as discussed by Shearer & Blasco, 1986);
- Comparison of known regional sedimentation rates and observed (ice gouge) infill thicknesses (see Blasco et al., n.d.; Pelletier & Shearer, 1972);
- Analysis of known ice gouge impact/recurrence rates and observed gouge cross-cutting patterns (see Pereira et al., 1988; Blasco et al., n.d.); and,
- Repetitive surveying techniques conducted along established survey corridors, or tracklines, within a given survey area.

All of the preceding ice gouge dating approaches are essentially unreliable, with the exception of repetitive ice gouge mapping procedures. For instance, determining ice

gouge ages using radiocarbon dating is problematic due to the lack of sufficient carbonate shell material required for accurate carbon-14 dating (Pereira et al., 1988). Similarly, Mudie (1986) postulates that (ice gouge) sediments containing less than 60% silt and clay oftentimes contain an insufficient amount of pollen for palynological analysis, and reliably dated regional palynostratigraphy must be available for comparison of onshore and offshore sediment samples. Pelletier and Shearer (1972) have discussed how ice gouge ages estimated on the basis of sediment infill thicknesses may be overestimated due to preferential ice gouge infilling.

Ice gouge dating through repetitive ice gouge mapping is suggested to be the most reliable method of determining quantifiable ice gouge ages. Repetitive surveying techniques quantifiably identify 'new' ice gouges formed during the elapsed time period between two surveys as events observed at a specific location during a re-survey procedure which were not evident during the previous year's survey. However, repetitive mapping is problematic in arctic areas with low ice gouge recurrence rates and is best suited to areas with high ice gouge frequencies, such as the Beaufort and Chukchi seas.

2.3 BACKGROUND & EARLY WORKS

A number of sources of ice gouge data and associated studies are available in the open literature from seabed surveys conducted in the American Beaufort and Chukchi Seas. In particular, the United States Geological Survey (USGS) has collected a significant amount of ice gouge data through numerous seabed survey programs conducted in the 1970s and 80s, although little, if any data has been collected since then. Ice gouge

statistics, as interpreted by the USGS, are available in the public domain in the form of numerous open-file reports for various survey locations in Beaufort and Chukchi Sea nearshore areas.

Canadian ice gouge data was collected during numerous phases of the Beaufort Sea SCOURBASE database which was established through funding provided by the Geological Survey of Canada and the Program for Energy Research and Development Offshore Geotechnics subprogram. The funding was provided through the auspices of the Environmental Studies Research Funds (Myers et al., 1996). Historical ice gouge data is archived in the SCOURBASE and ECHOBASE databases which are no longer updated (Myers et al., 1996). New ice gouge data is contained in the NEWBASE data set, which incorporates updates and new data obtained through repetitive seabed surveying. The ECHOBASE database contains 26,565 ice gouge depth and associated bathymetry data records obtained from echo sounder bathymetric and seabed relief profiling conducted from 1980 to 1986 (CSR, 2008). The SCOURBASE database contains baseline, unknown age ice gouge characteristics (depth, width, orientation, bathymetry, etc) for 66,557 records obtained using side-scan sonar surveying from 1970 to 1986 (CSR, 2008). A SCOURBASEII database containing 798 gouge records was established from ice gouge survey baseline data obtained between 2001 and 2003, and utilized for repetitive mapping conducted by Canadian Seabed Research (CSR) in 2001, 2003, 2004, and 2005 (CSR, 2008). The NEWBASE database contains only new ice gouge data and updates obtained via repetitive seabed surveying with echo sounders and side-scan sonar micro-profilers (Myers et al., 1996). As a result of the CSR (2008) NEWBASE updates in 2005, the

database now contains a total of 14,147 geographically referenced new ice gouge data records collected from repetitive mapping conducted between 1978 and 2005. However, only ice gouge records greater than or equal to 0.5m were entered in the 2005 NEWBASE updates for water depths less than or equal to 25m, whereas all gouge depths were recorded in greater than 25m water depths. This minimum gouge depth limit was imposed due to the postulation that all new ice gouges formed since previous NEWBASE updates in 1990 could not be measured due to gouge superimposition. All gouge depths were recorded for survey lines established during the NEWBASE 2005 updates, which were not available during previous surveys. Although Canadian Beaufort Sea geophysical data collection was conducted via public funding (GSC/PERD) along with industry participation, ice gouge data interpretation was contracted to Canadian Seabed Research and is not in the public domain.

Pelletier and Shearer (1972) and Brooks (1973) have summarized the early recognition of ice gouging in the Canadian and American Beaufort Seas, and represent the precursors to organized seabed surveys and geophysical data collection endeavours. Side-scan sonar records collected in 1970 from the Mackenzie Canyon area of the Canadian Beaufort Sea led to what is perhaps one of the earliest recognitions of ice gouges in the Canadian Beaufort seabed. Subsequently, the Atlantic Oceanography Laboratory of the Bedford Institute and the Geological Survey of Canada conducted investigations in the Canadian Beaufort Sea in 1970 and 1971 during APOA Projects 19 and 32 (APOA, 1980), and found significant ice gouging in water depths ranging from 10 to 50m, to a maximum of 75m. Gouge relief was observed up to 10m in Mackenzie Bay, with widths on the order

of tens of metres and lengths of up to 8 km (Pelletier & Shearer, 1972; Brooks, 1973; Kovacs & Mellor, 1974; Lewis, 1977b). Lewis and Blasco (1990) have reported maximum confirmed gouge lengths of 13km, and unconfirmed lengths ranging from 19 to 37km. In general, ice gouge orientations trended in an east-southeast direction (Pelletier & Shearer, 1972; Pelletier, 1973; CSR, 2008).

Records of ice gouge surveying from the American Beaufort Sea indicate that perhaps the earliest organized studies were conducted by the US Coast Guard Office of Marine Geology in 1970 and 1971 on the outer continental shelf offshore Prudhoe Bay (Brooks, 1973). Ice gouging was observed from the shoreline and offshore to the slope break (the edge of the outer continental shelf), with widths up to 18m and gouge depths of 3m or less. Harrison Bay was investigated in 1971 by the US Coast Guard Academy, which found significant ice gouging between 18 and 46m. Ice gouge widths were reported up to 37m, depths to 2.1m, and maximum lengths on the order of 1.6 km (Brooks, 1973). Reimnitz et al. (1972) have indicated the prevalence of ice gouging on the entire American Beaufort Sea shelf to 75m water depths, and have suggested that ice gouging may occur to water depths of 100m or more. Early ice gouge observations indicated a general east – west orientation on the American Beaufort shelf (Reimnitz et al., 1972).

The following thesis subsections present review of historic physical ice gouge data studies found for use in the present study. Refer to Section 3 for literature review of previous ice gouge engineering analyses of interest in the current work.

2.4 AMERICAN BEAUFORT SEA

Numerous sources of American Beaufort Sea ice gouge data collection have been obtained from the USGS for review and use in this thesis. Key information obtained from each data source is discussed below and assessed in its applicability to subsea pipeline and ice gouge design and analysis.

Barnes et al. (1978) collected ice gouge survey data from two repetitively mapped tracklines located seaward of the Harrison Bay barrier islands, as shown in Figure 8. The surveys were conducted in 1973 and from 1975 to 1977, and recorded water depths, gouge population, and maximum and average ice gouge parameter observations (depth, width, etc) for new and unknown age observations, among other relevant parameters. An earlier study by Barnes et al. (1977) contained a subset of the data provided by Barnes et al. (1978), whereas later work by Rearic (1986) presented a similar study of Harrison Bay ice gouging, but for a different data set which was originally collected by Barnes and Rearic (1985). Barnes and Reimnitz (1979) also studied ice gouge depths and seabed morphology within Harrison Bay, but did not indicate the source of their data.

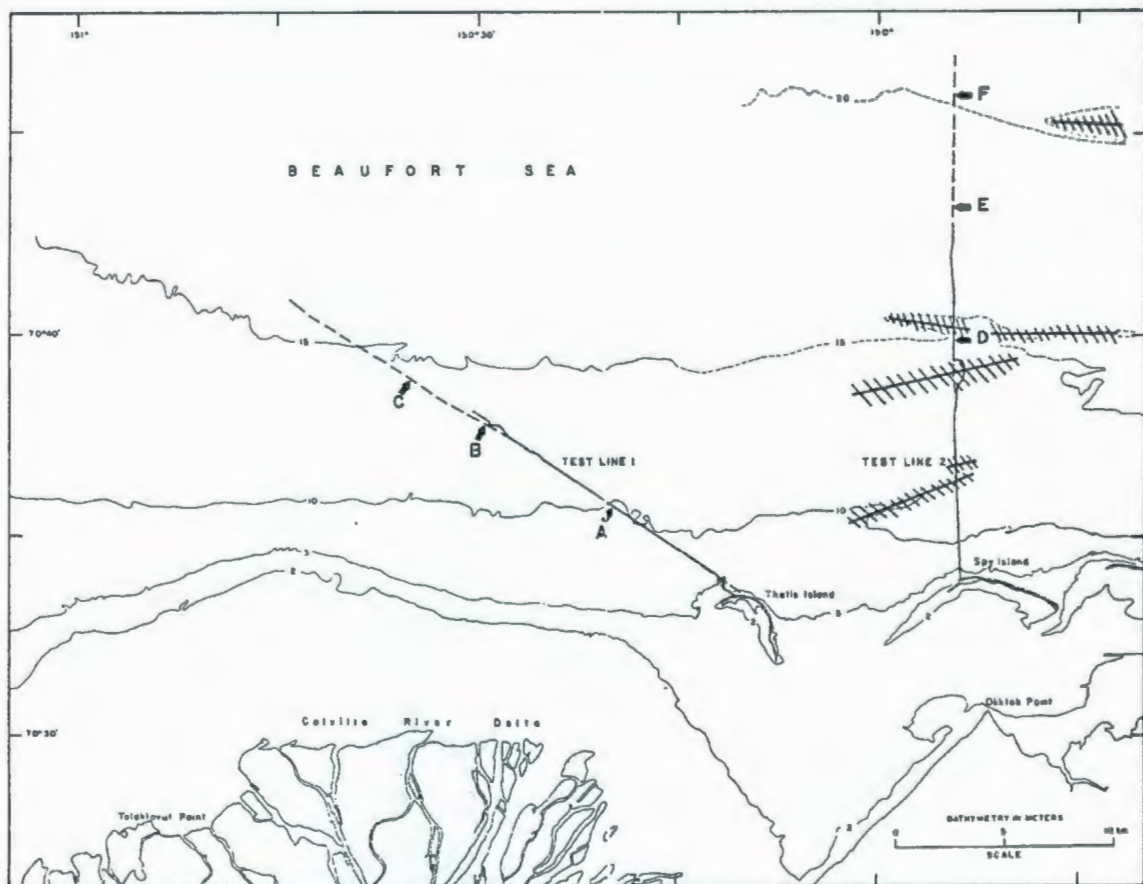


Figure 8: Location Map for Ice Gouge Data Presented Within USGS Open-File Report 78-730 (Barnes et al., 1978)

Rearic et al. (1981) collected unknown age ice gouge data ranging from Camden Bay and westward to Smith Bay, both inshore and seaward of barrier islands (see Figure 9). As shown in the figure, surveyed locations included Harrison Bay, Prudhoe Bay, Oliktok Point, and Cape Halkett, among others. The ice gouge data was collected from 1972 and 1973, and again from 1975 to 1980. Recorded ice gouge data included water depth, gouge geometry, density, dominant orientation, and multiplet gouge data, among other parameters, and represents a contributing data set to a larger collection compiled by

Rearic and McHendrie (1983). Rearic et al. (1981) also recorded ice gouge depth frequency data for gouge depth classes ranging from less than 0.4m (0.2 to 0.4m) to less than 4.0m (3.8 to 4.0m). However, the data files indicated a maximum single ice gouge incision depth of 5.5m, which is significantly greater than the upper limit of the reported ice gouge depth classes. Also, the 'number of incisions per interval' recorded in the data set oftentimes did not equal the sum of the gouge depth class range frequency data and hundreds of incisions were sometimes recorded for a single set of geodetic coordinates. Therefore, only maximum ice gouge depth records were utilized in this study due to discrepancies with the frequency data.

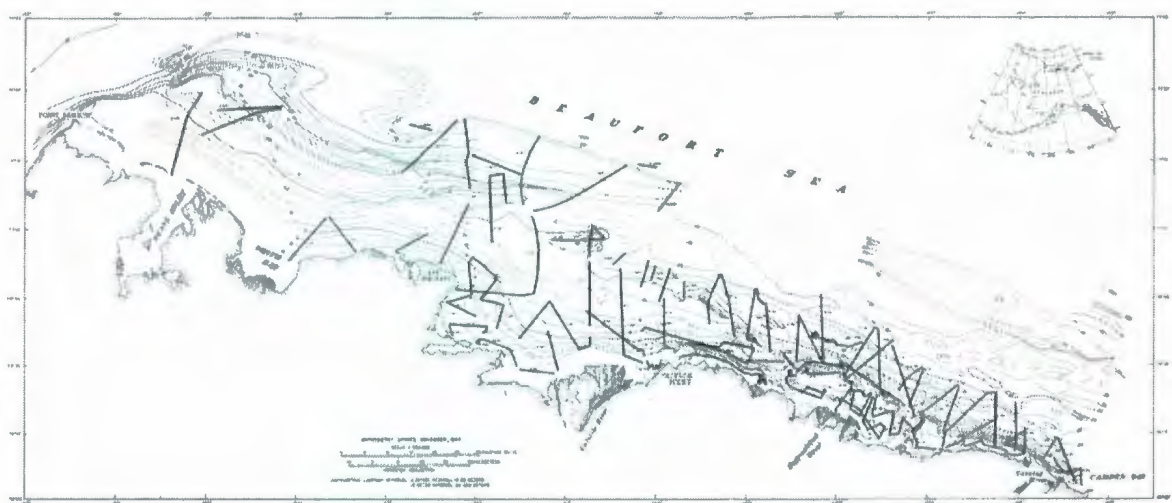


Figure 9: Location Map of USGS 81-950 Survey Tracklines (Rearic et al., 1981)

Reimnitz et al. (1982) collected unknown age ice gouge data ranging from the Colville River and eastward to the Canadian border, both inshore and seaward of the barrier islands as shown in Figure 10. The surveys were conducted in 1981 and recorded water depth, gouge geometry, density, dominant orientation, and sediment cohesion, among

other parameters. Preliminary surficial seabed sediment analysis was conducted, with sediments qualitatively classified as 'muddy, cohesive' or 'coarse, granular, non-cohesive'. Sediment types were recorded for each ice gouge observation; however, the classifications were not discussed in the accompanying report. Similar to the Rearic et al. (1981) data set, the Reimnitz et al. (1982) data was also contained in Rearic and McHendrie's (1983) data compilation.

Rearic and McHendrie (1983) presented their American Beaufort Sea ice gouge data within two electronic text files; Data File 1 corresponded to the Rearic et al. (1981) study, whereas Data File 2 corresponded to the Reimnitz et al. (1982) data. Geodetic coordinates were provided for each ice gouge observation record, in addition to the parameters discussed above.

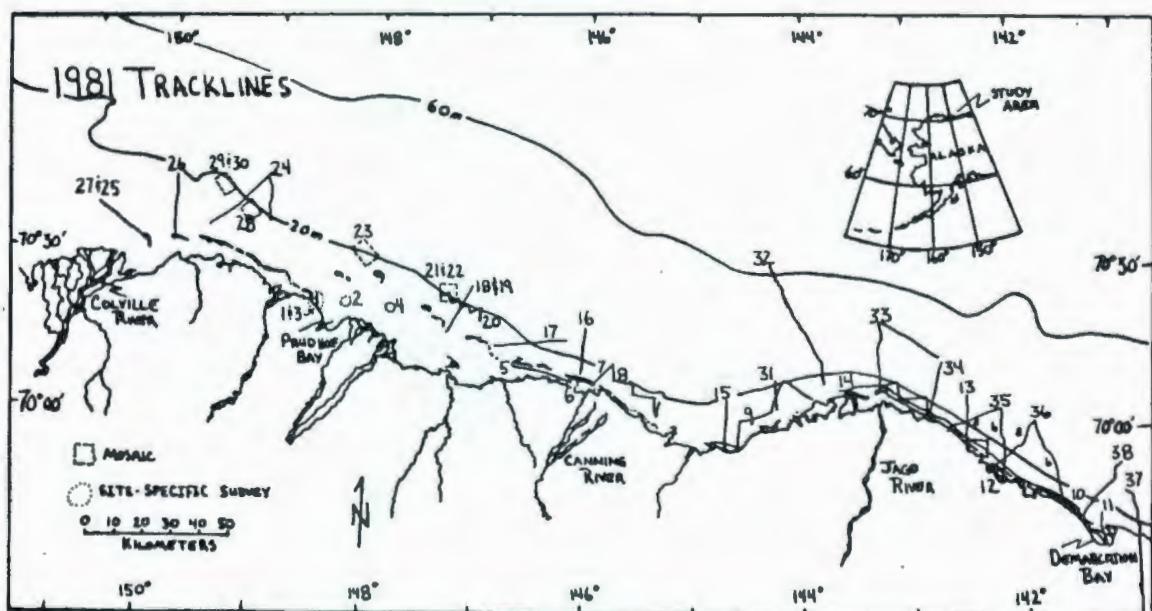


Figure 10: Location Map of USGS 82-974 Survey Tracklines (Reimnitz et al., 1982)

Barnes and Rearic (1985) collected repetitively mapped ice gouge survey data seaward of the barrier islands and within Camden Bay of the Alaskan Beaufort Sea inner shelf (see Figure 11). The known age ice gouge data was collected from 1975 to 1982 and recorded water depth, gouge geometry, and dominant orientation; in addition, ice gouge densities were graphically presented but of poor quality. Seabed sediments were qualitatively observed to be muddy sands, sandy muds, pebbly clay, and coarse granular material. The majority of Barnes and Rearic's (1985) ice gouge depth data were of poor quality, with measurements below the lower limit of the echo sounder resolution (0.2m) recorded as '<0.2m'. Unknown age ice gouge data records only provided the number of gouges observed per water depth and are thus of no use to the present study. The Barnes and Rearic (1985) survey data was subsequently reassessed by Weber et al. (1989), who reanalyzed and updated the earlier survey data and provided additional data obtained from two 1985 surveys. Ice gouge depth measurements were recorded to a lower limit of 0.1m, as opposed to the '<0.2m' classification previously reported by Barnes and Rearic (1985). However, Weber et al. (1989) did not discuss their method of obtaining greater gouge depth accuracy. As such, the validity of the shallow ice gouge depth data recorded by Weber et al. (1989) is questioned by the current author, but included in subsequent analysis nonetheless.

Additional reference sources have provided analysis and discussion of American Beaufort Sea ice gouge data collected by the USGS. Barnes et al. (1982) provided analysis of ice regime characteristics, parameter relationships, and summary statistics for data obtained by Rearic et al. (1981). Weeks et al. (1983) statistically analyzed the

unknown age ice gouge data collected by Rearic et al. (1981) and presented recurrence rate information duplicated from Barnes et al. (1978).

Weeks et al. (1983) introduced the negative exponential as a convenient and reasonable initial approximation for ice gouge depth prediction (see Section 3.1), which was later refined by Lanan et al. (1986).

Barnes and Reimnitz (1986) summarized the USGS's American Beaufort Sea ice gouge data collection programs, and provided general preliminary analysis of ice gouge parameter correlation, gouge age, and ice gouge reworking of the seabed. Proprietary American Beaufort Sea ice gouge survey programs were conducted by Harding Lawson Associates from 1983 to 1985, as summarized by Ticken and Toimil (1992). Ticken and Toimil's (1992) study paper provided a general overview of significant ice gouge parameters, processes, and field surveillance methods, with limited discussion of Harding Lawson Associates survey data and sediment property observations.

Table 3 provides a summary of the American Beaufort Sea ice gouge data records reviewed in the preceding discussions which provide data collection used in this study's analysis. As shown in the table, a small amount of ice gouge depth data was available for water depths less than 5m and greater than 25m, compared to the 5 to 25m range. Table 6 of Section 2.7 provides a summary of available American Beaufort Sea ice gouge data collections complete with maximum ice gouge depth and width parameters, associated survey resolution, maximum gouge density/recurrence rate, and dominant soil type observations.

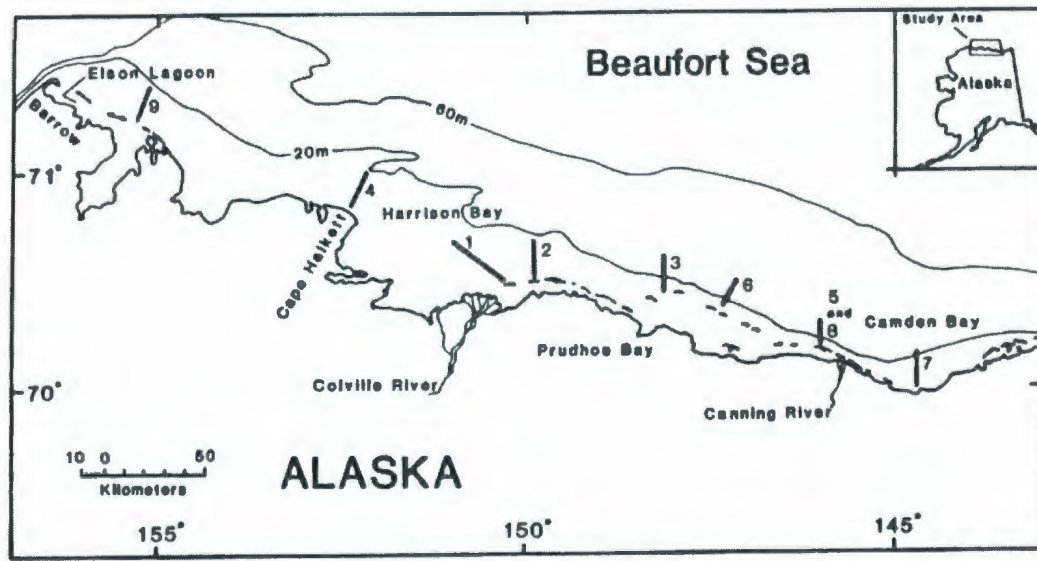


Figure 11: Location Map for USGS 85-463 Ice Gouge Data (Barnes & Rearic, 1985)

Table 3: Summary of American Beaufort Sea Ice Gouge Surveys used in this Study

Ice Gouge Data Collection	Survey Date	Age of Data	Number of Gouge Depth Records per Water Depth ^a		
			<5m	5 – 25m	>25m
USGS 78-730 (Barnes et al., 1978)	1973 & 1975 – 77	Old	0	130	0
USGS 78-730 (Barnes et al., 1978)	1973 & 1975 – 77	New	0	125	0
USGS 83-706 (Rearic & McHendrie, 1983) ^b	1972 – 73 & 1975 – 81	Old	403	1446	556
USGS 89-151 (Weber et al., 1989) ^c	1977 – 85	New	11	2356	11

^a Water depth not recorded for some ice gouge data records, therefore best approximation.

^b Compilation of ice gouge data provided in USGS Open-File Reports 81-950 and 82-974; combined data set utilized in present thesis work. The number of gouge depth records per water depth reported in this table corresponds to maximum gouge depth data only and excludes the gouge depth frequency data recorded in USGS 81-950, as well as the 'number of incisions' recorded in both USGS 81-950 and 82-974. This information was provided by Rearic & McHendrie (1983) but excluded from the present study due to observed data inconsistencies/discrepancies.

^c Contains reassessed ice gouge data originally presented in USGS Open-File Report 85-463. Updated data set (USGS 89-151) utilized in present thesis work. The number of gouge depth records per water depth reported in this table corresponds to new gouge depth data only.

2.5 CANADIAN BEAUFORT SEA

As discussed in Section 2.3, Canadian Beaufort Sea geophysical ice gouge surveying programs have been conducted through GSC and PERD funding, among other industry participants, and administered through the auspices of the ESRF. However, geophysical data interpretation was contracted to Canadian Seabed Research and is not available in the public domain.

Some of the earliest studies of ice gouging in the Canadian Beaufort Sea were conducted during APOA Projects 19 and 32 (APOA, 1980) conducted by Hunting Geology and Geophysics (1971; 1973). Numerous research efforts (Lewis, 1977b; Hnatiuk & Brown, 1977) subsequently utilized the APOA Projects 19 and/or 32 ice gouge data; Hnatiuk and Wright (1983) also studied this data, but combined it with additional data obtained up to the end of 1976. As part of APOA Project 151, Shearer (1979) analyzed ice gouge survey data collected in 1971, 1972, 1974, 1975, and 1978. It is suggested (by the current author) that this study may potentially represent an update to APOA Projects 19 and 32; however, no reference for this hypothesis was found among reviewed technical documents.

Historically, frequent ice gouging has been observed between approximately 15 and 45m water depths in the Canadian Beaufort Sea, as reported by numerous researchers (Hunting Geology and Geophysics, 1971; 1973; Hnatiuk & Brown, 1977; Lewis 1977a; 1977b; Hnatiuk & Brown, 1983). The 15m bathymetric contour coincides with the shoreward boundary of the dynamic shear ice zone (Hnatiuk & Brown, 1977) and thus

represents the nearshore boundary of frequent ice gouging, although significant ice gouge activity has been found close to shore in shallower water depths (Lewis et al., 1976; Shearer, 1979). The approximate 10 to 50m water depth range was found to be saturated by ice gouging activity (Shearer & Blasco, 1986), with the maximum new gouge occurrence frequency exhibited inshore of approximately 25m water depth (CSR, 2008). Multiple research studies (Hunting Geology & Geophysics, 1971; 1973; Lewis et al., 1976; 1977a; 1977b) have commonly reported decreasing ice gouge frequencies with increasing water depth, particularly beyond approximately 45m in the Canadian Beaufort Sea, with essentially no gouging observed beyond 80m water depth. Hnatiuk and Wright (1983) reported that the deepest ice gouges were located approximately 80km north of Herschel Island.

Due to the unavailability of entire SCOURBASE, ECHOBASE, or NEWBASE data collections, numerous summary reports were obtained for review from ESRF and COGLA (i.e., Shearer et al., 1986; Comfort et al., 1990; Myers et al., 1996; Gilbert & Pedersen, 1987; Gilbert et al., 1989). In some instances, these reports allowed extraction of a limited amount of ice gouge data from tabulated database subsets and/or data extrapolation from ice gouge data distribution histograms. A previous thesis by Wahlgren (1979) was also utilized, as it contained a small amount of data and analysis pertaining to eastern Mackenzie Bay. However, the amount of ice gouge data retrieved from these reports is small in comparison to the number of data records contained in each database (see Section 2.3 and Table 4 below).

Wahlgren (1979) studied early Canadian Beaufort Sea ice gouge data collected by the GSC in 1974 using areal seabed surveys conducted in eastern Mackenzie Bay and offshore Pullen Island; unfortunately, some of the data was of poor quality (i.e., Elf Island site). Wahlgren's (1979) report and data collection represents one of the earliest endeavours to analyze ice gouge and seabed slope relationships, although the study produced many inconclusive results.

Shearer et al. (1986) have provided results and analysis of new and unknown age ice gouge data studies, with a focus on investigation of ice gouge recurrence rates through repetitive seabed surveying. The surveys were conducted from 1974 to 1984 on behalf of numerous industry participants, as discussed by Caulfield Engineering (1979). Shearer et al. (1986) also provided discussion of ice gouge rise-up and the 'stages' of the ice gouging process, based on their observations. Repetitive ice gouge data was provided for the *Kaubvik*, *Nipterk*, *Minuk*, *Kadluk*, *west Sauvrak*, *east Mackenzie*, *south Tingmiark-Nerlerk corridor*, *Kagulik*, *Tarsiut-Nektoralik*, and *Pullen Island* survey sites, which included gouge geometry, dominant orientations, and general seabed sediment observations. This ice gouge data was later incorporated into the Canadian Beaufort Sea SCOURBASE database (see Gilbert & Pedersen, 1987; Myers et al., 1996), and also utilized in studies by Shearer and Stirbys (1986). In addition to discussion and evaluation of the SCOURBASE database by Gilbert and Pedersen (1987), Gilbert et al. (1989) provided the results of 1986 updates to the ECHOBASE and SCOURBASE Canadian Beaufort Sea ice gouge databases. Gilbert et al. (1989) indicated that ECHOBASE

originally included ice gouge depth records greater than 0.5m deep only, but the 1986 updates included gouge depths below this limit.

Comfort et al. (1990) conducted a case study for the *Kringalik* and *Amauligak* proposed pipeline routes, using unknown age ice gouge data from the ECHOBASE database. However, ice gouge depth data below 0.6m was excluded due to unspecified data inconsistencies. The data included tabulated ice gouge depth class frequencies and water depths (used in the current study), as well as preliminary seabed sediment property, gouge parameter, and recurrence rate analyses for the study areas. In a separate study, Comfort (1990) utilized SCOURBASE data obtained from Gilbert et al. (1989) to conduct similar site-specific ice gouge analysis for the *Kringalik* and *Amauligak* pipeline routes. It appears as though Lewis and Blasco (1990) have also provided summary and analysis of ice gouge data from SCOURBASE, based on recorded data population and regional study similarities, although this hypothesis is uncertain.

Myers et al. (1996) summarized new ice gouge data contained in the 1990 updated NEWBASE database. This database was developed and is intermittently updated through repetitive mapping programs conducted in the various physiographic regions of the Canadian Beaufort Sea (Figure 12). The 1990 updated NEWBASE ice gouge data was also utilized in later studies conducted by Blasco et al. (1998).

CSR (2008) discusses 2001 and 2003 through 2005 updates of the NEWBASE database. CSR (2008) added a total of 1038 new ice gouges resulting from the 2001 survey program, 988 gouges from the 2003 survey, 4225 during 2004, and 2562 were added to

NEWBASE from the 2005 survey program. It was indicated that the CSR (2008) updated NEWBASE data set contains similarly sized populations of single-keeled and multiplet ice gouge events, however, these updates were not available for review.

With respect to 1990 NEWBASE updates, Myers et al. (1990) provided histograms of available new ice gouge depth data binned in 0.5m intervals and separated into 10m bathymetric intervals; where applicable, this data was approximated using the midpoint of the appropriate ice gouge depth class (i.e., 0.25m, 0.75m, and so on) for use within the present study. It is acknowledged that this approximation introduces uncertainty to the data, but has been utilized nonetheless due to the paucity of publicly available Canadian Beaufort Sea ice gouge data. Report appendices also contained a limited amount of tabulated new and old ice gouge parameters obtained from gouge tracking studies conducted between Herschel Island and the Tuktoyaktuk Peninsula.

The NEWBASE database contains seabed sediment property data per each ice gouge record (see Myers et al., 1996), although this information was unavailable for review during this study. Alternately, Rogers (1990) provided general sedimentary analyses for the regions shown in Figure 12.

Nessim and Hong (1992) provided additional independent analysis and summary of the SCOURBASE, ECHOBASE, and NEWBASE databases, although only a limited summary of the ice gouge data was provided. Héquette et al. (1995) provided summary and analysis of ice gouges observed on the inner shelf of the southeastern Canadian Beaufort Sea, although the source of their data collection was not provided.

Table 4 provides a summary of the Canadian Beaufort Sea ice gouge data records reviewed in the preceding discussions which provide data collection used in this study's analysis. As shown in the table, no gouge depth data was available for water depths less than 5m. Table 7 of Section 2.7 provides a summary of available Canadian Beaufort Sea ice gouge data collections complete with maximum ice gouge depth and width parameters, associated survey resolution, maximum gouge density/recurrence rate, and dominant soil type observations.

Table 4: Summary of Canadian Beaufort Sea Ice Gouge Surveys used in this Study

Ice Gouge Data Collection	Survey Date	Age of Data	Number of Gouge Depth Records per Water Depth ^a		
			<5m	5 – 25m	>25m
Wahlgren (1979)	1974	Old	0	0	177
Shearer et al. (1986)	1974 – 1984	New	0	472	63
Comfort et al. (1990) ^b	Unknown	Old	0	2580	2660
Myers et al. (1996)	1989 & 1990	Old	0	45	144
Myers et al. (1996)	1978 – 1990	New	0	4686	171

^a Water depth not recorded for some ice gouge data records, therefore best approximation.

^b Water depths correspond to midpoint of recorded water depth range.

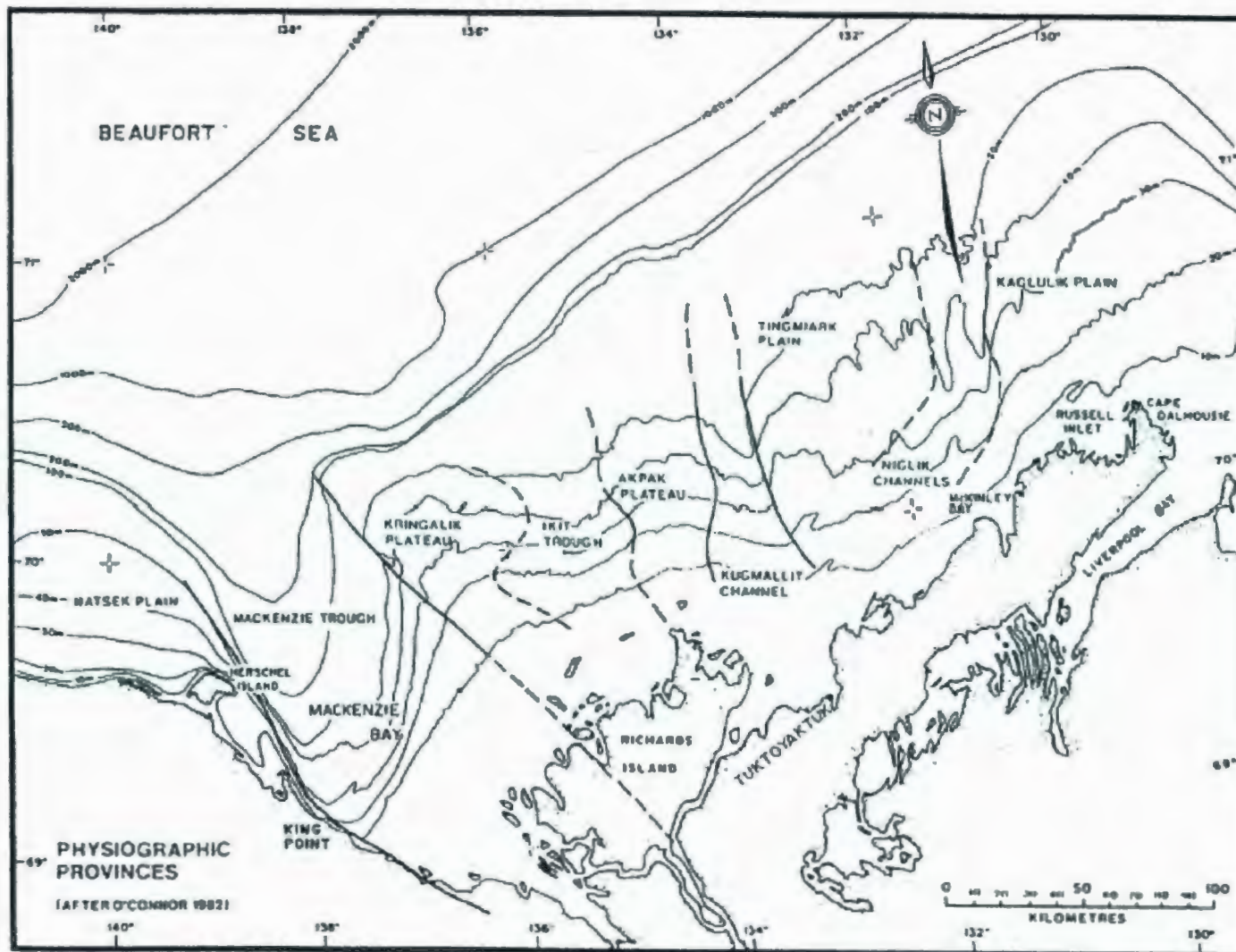


Figure 12: Location Map Showing Physiographic Regions of the Canadian Beaufort Sea (Myers et al., 1996)

2.6 CHUKCHI SEA

Only a limited amount of public domain Chukchi Sea ice gouge data collection has been found for use in this thesis. Ice gouge data collections containing usable amounts of historical survey data were limited to two USGS survey programs conducted by Toimil (1978) and Phillips et al. (1988).

Toimil (1978) recorded a significant amount of unknown age Chukchi Sea ice gouge data during surveys conducted in 1974 (see Figure 13). The recorded ice gouge data included water depths, maximum gouge geometric parameters (width, depth), density, and dominant orientation, among other observations. Toimil's (1978) ice gouge density records included all identifiable ice gouge deformations (including individual multiplet depressions) and were normalized to represent the theoretical number of gouges that would have been encountered along a survey trackline oriented perpendicular to the dominant gouge orientation. In addition to tabulated ice gouge data, Toimil (1978) provided some analysis of ice gouge densities and geometric parameter relationships observed in various regions and water depths of the Chukchi Sea (see Section 3.2).

Phillips et al. (1988) provided tabulated ice gouge depth frequency data as a function of water depth for surveys conducted in the northwest Chukchi Sea (Figure 14) and Barrow Sea Valley region (Figure 15) during 1984. The gouge frequency data was recorded in 2m water depth and 0.1m gouge depth bins. Sandy to muddy gravel seabed sediments were dominantly reported for these regions along with substantial qualitative sediment

analysis for the study areas, although quantitative surficial sediment properties were not provided.

Due to the paucity of Chukchi Sea ice gouge data collections found in the public domain, a significant effort was made to research previous ice gouge parameter studies relevant to the present work. In fact, Grantz et al. (1982b) have commented on the lack of data and referenced USGS Open-File Report 78-693 by Toimil (1978) as providing the most comprehensive ice gouge data collection available for the Chukchi Sea. This has been confirmed through literature research and review conducted as part of this thesis. Subsequent studies by multiple researchers (i.e., Toimil, 1979; Grantz, 1982b; Thurston & Theiss, 1987; INTEC 1986, 1991; among others) have been found to directly utilize the data originally presented in Toimil's (1978) study.

Rex (1955) conducted one of the earliest known Chukchi Sea ice gouge investigations, which found that the greatest extent of seabed ice gouging occurred between 6 and 24m water depths, and that gouge depths ranged from less than 1m in shallow waters located southwest of Barrow, to 3.8m in areas located west of Barrow. Alternate hypotheses were originally considered for seabed deformations observed by Rex (1955), including residual features of thawed permafrost, slump topography, current gouging, and sand wave formations.

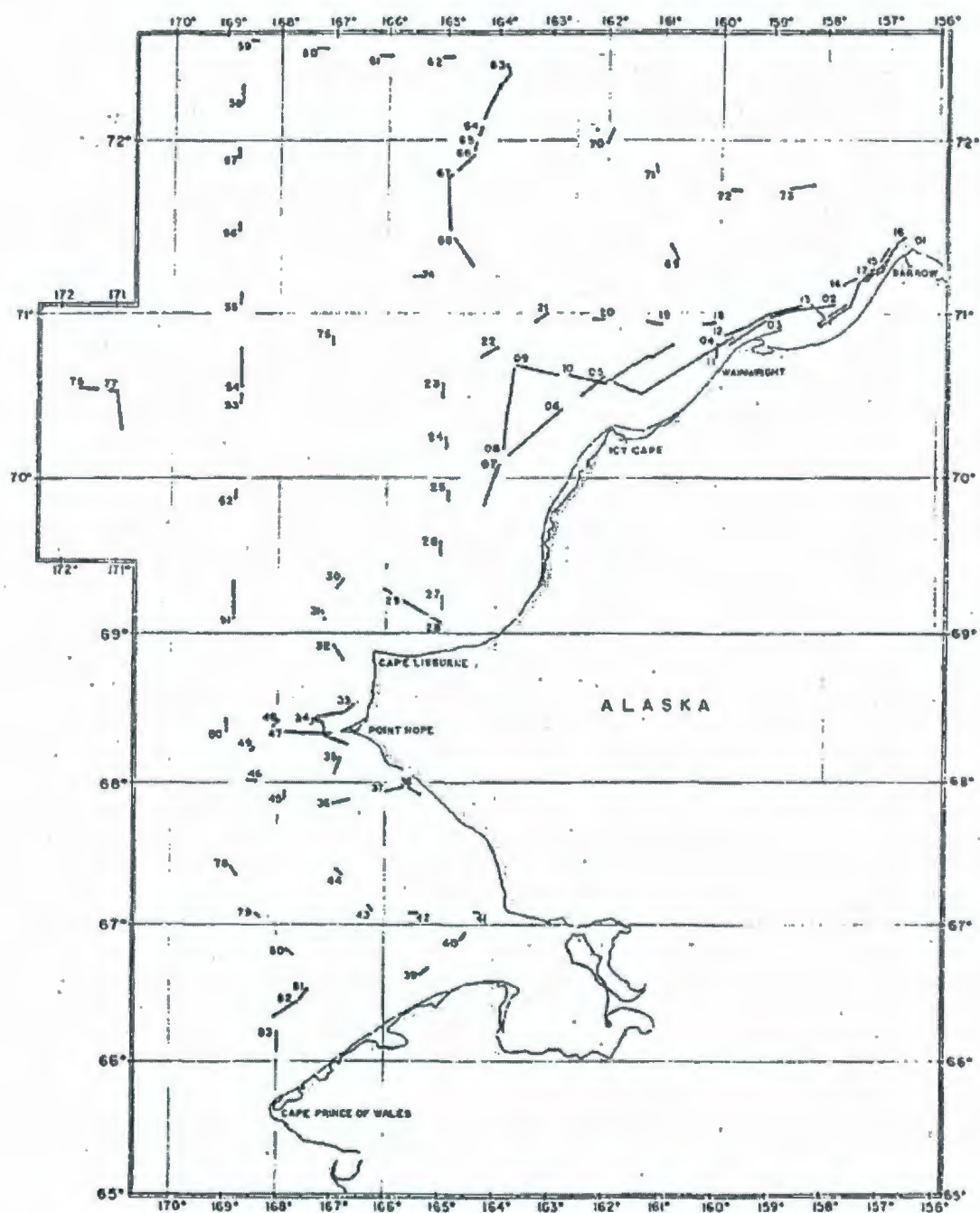


Figure 13: Location of Side-Scan Sonar Tracklines as Determined by Satellite Navigation
(Toimil, 1978)

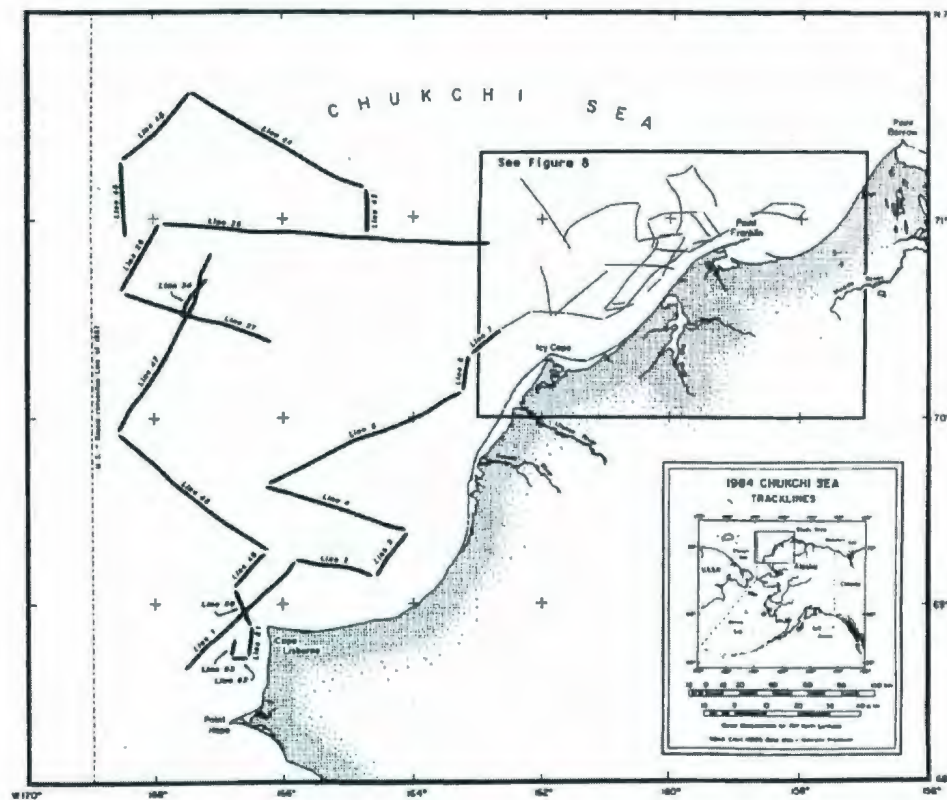


Figure 14: Northwest Chukchi Sea Survey Trackline Locations (Phillips et al., 1988)

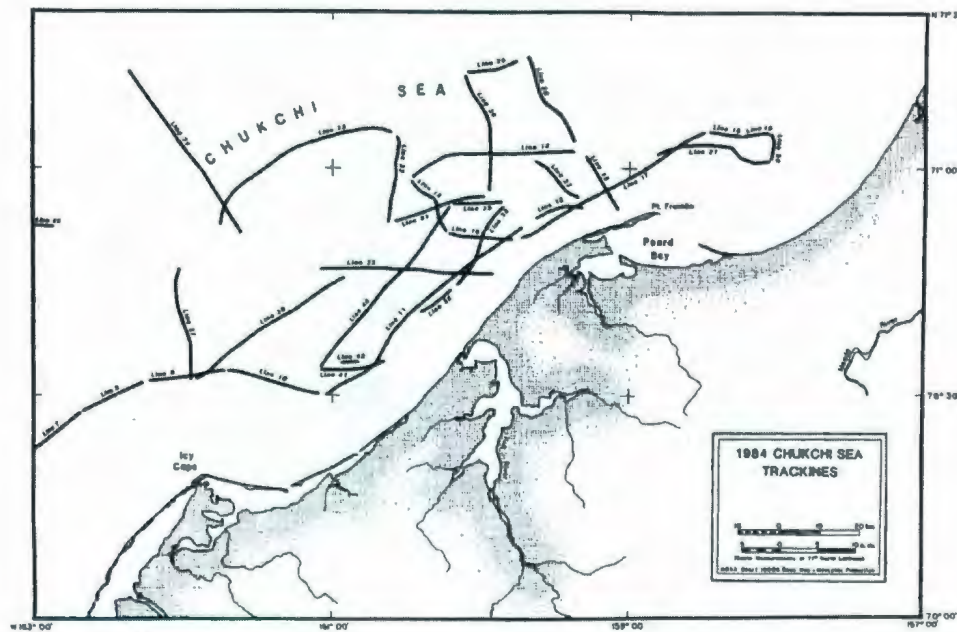


Figure 15: Northeast Chukchi Sea Survey Trackline Locations (Phillips et al., 1988)

Numerous MMS lease sale final environmental impact statements, technical reports, and USGS ice gouge studies (MMS 1987; 1990; 2007; Wilson et al., 1982; Grantz et al., 1982a) have reported frequent Chukchi Sea ice gouging inshore of approximately 60m water depth, with rare occurrences in deeper water. However, quantitative ice gouge data was commonly reported to be rare to nonexistent, with the exception of localized historical studies. Unknown age ice gouge depths were reported to a maximum of 4.5m (MMS, 1987; Wilson et al., 1982; Grantz et al., 1982a), with maximum densities occurring in the Barrow Sea Valley region of the northeast Chukchi Sea and between 10 and 20m water depths. Grantz et al. (1982b) presented a maximum ice gouge depth of 5m observed between 48 and 55m water depths in the Barrow Sea Valley, with shallower gouge depths found on the central Chukchi shelf. Maximum ice gouge width records of up to 175m (Phillips et al., 1984) were found during research for this work.

Table 3 provides a summary of the Chukchi Sea ice gouge data records reviewed in the preceding discussions which provide data collection used in this study's analysis. As shown in the table, no gouge depth data was available for water depths less than 5m and a limited amount of data was available for the 5 to 25m water depth range when compared to greater than 25m. Table 8 of Section 2.7 provides a summary of available Chukchi Sea ice gouge data collections complete with maximum ice gouge depth and width parameters, associated survey resolution, maximum gouge density/recurrence rate, and dominant soil type observations.

Table 5: Summary of Chukchi Sea Ice Gouge Surveys used in this Study

Ice Gouge Data Collection	Survey Date	Age of Data	Number of Gouge Depth Records per Water Depth ^a		
			<5m	5 – 25m	>25m
USGS 78-693 (Toimil, 1978) ^b	1974	Old	0	53 ^c	566
USGS 88-25 (Phillips et al., 1988)	1984	Old	0	252	1957

2.7 SUMMARY OF AVAILABLE ICE GOUGE DATA COLLECTIONS

The ice gouge data collections obtained for use in the current thesis work have been summarized in the following Table 6 through Table 8 for each of the investigated regions. Where possible, known and/or apparent ice gouge depth and width resolutions have been indicated, based on applicable report reviews and/or data set observations. Likewise, ice gouge parameters provided in the tables have been obtained from applicable data collection discussions and/or analysis of the associated data sets. Review and discussion of the individual ice gouge data collections are provided above in Sections 2.4 through 2.6. Where a particular parameter was not provided, the ‘not available’ (N/A) placeholder has been utilized. Detailed discussion of regional ice gouge recurrence rate data may be found in Section 3.5. Single-keeled and multiplet ice gouge width records have been combined for use in the present study; therefore, maximum gouge width

^a Water depth not recorded for some ice gouge data records, therefore best approximation.

^b The number of gouge depth records per water depth reported in this table corresponds to maximum gouge depth data only, and excludes the ‘number of gouges’ also recorded in USGS 78-693.

^c 25m water depth records only, no data available for less than 25m water depth.

records may correspond to multi-keeled gouge deformations. The ice gouge form was unknown for many data records.

As indicated in the footnotes of Table 6 and discussed above in Section 2.4, individual discussion of the USGS Open-File Report 81-950, 82-974, and 85-463 data collections have been excluded from the summary table as they have been included within or superseded by later data collections.

As part of the current thesis project, Microsoft Excel spreadsheets containing extracted ice gouge data have been created for each of the analyzed arctic regions. Three ice gouge data collection spreadsheets were developed, which correspond to each of the summary tables provided below. Each of the investigated ice gouge data collections have been included as separate tabbed worksheets within the appropriate Microsoft Excel spreadsheet.

Table 6: Summary of Available American Beaufort Sea Ice Gouge Data Collections

Ice Gouge Data Collection	Surveyed Water Depth Range (m)	Gouge Depth		Gouge Depth Resolution (m)	Gouge Width		Gouge Width Resolution (m)	Max. Gouge Density / Recurrence Rate ^a	Dominant Soil Type
		Max. (m)	Water Depth (m)		Max. (m)	Water Depth (m)			
USGS 78-730 (Old Data)	3 – 21	1.8	19	0.1	65	14	2	N/A	N/A
USGS 78-730 (New Data)	5 – 20	1.2	13.5		48	18		80 gouges/km ² /yr	N/A
USGS 83-706 ^b (Old Data)	1.2 – 125	5.5	39.1	0.1 – 0.15	67	53.5	1	4903 gouges/km ²	Muddy Cohesive (Clay) or Coarse Granular Non-Cohesive (Sand)
USGS 89-151 ^c (New Data)	3.1 – 27.9	3	12.1 & 15	0.1	265	16.5	0.1	~7.5 gouges/km/yr	Muddy Sands, Sandy Muds, Pebbly Clay & Coarse Granular Material

^a Refer to Section 3.5 for further discussion of recurrence rate data.

^b Compilation of ice gouge data provided in USGS Open-File Reports 81-950 and 82-974; combined data set utilized in present thesis work.

^c Contains reassessed ice gouge data originally presented in USGS Open-File Report 85-463. Updated data set (89-151) utilized in present thesis work.

Table 7: Summary of Available Canadian Beaufort Sea Ice Gouge Data Collections

Ice Gouge Data Collection	Surveyed Water Depth Range (m)	Gouge Depth		Gouge Depth Resolution (m)	Gouge Width		Gouge Width Resolution (m)	Max. Gouge Density / Recurrence Rate ^a	Dominant Soil Type
		Max. (m)	Water Depth (m)		Max. (m)	Water Depth (m)			
Wahlgren (1979)	~27 – 50	3.7	N/A	0.1	300	~39.35	5	N/A	Silt & Clay with Fine-Grained Mud
ESRF 032 (Old Data)	10 – 50	4.5	N/A	0.17 ^b	N/A	N/A	N/A	N/A	Soft Silty Clay, Except Sand Near Pullen Island
ESRF 032 (New Data)	10 – 40	5	15		N/A	N/A	N/A	4 gouges/km/yr	
Comfort et al. (1990) (Old Data)	<50	5.2 – 5.4	40 – 50	0.6	N/A	N/A	N/A	N/A	Silty Clays & Clayey Silts
ESRF 129 (Old Data)	16 – 55.5	8.5	42	0.1	50	45.5	5	N/A	Sand, Silt, & Clay ^c
ESRF 129 (New Data)	0 – 40	3.5 – 4	20 – 30	0.25	65	~27		12.5 gouges/km/yr	Sand, Silt, & Clay ^c

^a Refer to Section 3.5 for further discussion of recurrence rate data.

^b Minimum 0.25m ice gouge depth exhibited in ESRF Report No. 032 Appendix A for new ice gouge data records.

^c Refer to study by Rogers (1990).

Table 8: Summary of Available Chukchi Sea Ice Gouge Data Collections

Ice Gouge Data Collection	Surveyed Water Depth Range (m)	Gouge Depth		Gouge Depth Resolution (m)	Gouge Width		Gouge Width Resolution (m)	Max. Gouge Density / Recurrence Rate ^a	Dominant Soil Type
		Max. (m)	Water Depth (m)		Max. (m)	Water Depth (m)			
USGS 78-693 (Old Data)	20 – 70	4.5	38	0.5	110	36.5	2	364 gouges/km	Silt, Sand & Gravel
USGS 88-25 (Old Data)	38 – 52	2.9	45	0.2	N/A	N/A	N/A	24 gouges/km	Sandy – Muddy Gravel

^a Refer to Section 3.5 for further discussion of recurrence rate data.

2.8 GOUGE MEASUREMENT BIAS

Marcellus and Morrison (1986) have indicated that the USGS has a tendency to report echo sounder data records at a scale of 1:100 (1 cm equals 1m) in collection of geophysical ice gouge survey data. Even smaller scales, on the order of 1:500 (1 cm equals 5m) have also been reported. According to Marcellus and Morrison (1986) the use of small echo sounder record scales subsequently reduces the interpreter's ability to accurately resolve ice gouge depths and may thus lead to the use of large depth class intervals in data compilations. In addition, small scales may potentially result in exclusion of shallow gouge depths from ice gouge data sets due to an inability to resolve shallow seabed features on scaled echo sounder records. Underestimated shallow ice gouge depth populations bias data distributions towards deeper gouge depths and can potentially overestimate ice gouge infilling rates in shallow water locations.

Ice gouge detection and bias is dependent on the amount of gouge degradation, seafloor morphology, and technology, in addition to the interpreter's skill and subjectivity. The quality of the raw data and the survey speed are also important factors to accurate ice gouge detection.

Ice gouge depth data bias is also introduced by the minimum ice gouge depth resolution cut-off limit which is defined by the data interpreter, as well as geometric and beam angle considerations associated with the survey system (Gilbert, 1989). The combination of multiple ice gouge depth data sets with varying cut-off limits (i.e., one with 0.1m cut-off

and another with 0.5m) can potentially produce an ice gouge depth histogram that does not adequately represent the actual number of shallow gouges.

Ice gouge depth distributions may also be biased towards deep gouge depths by rapid infilling of ice gouges by wave and current action. Due to rapid infilling procedures, it is possible that an ice gouge may be partially or completely infilled at the time of geophysical surveying, thus leading to underestimated gouge depths or complete omission of the gouge altogether. Furthermore, as discussed below in Section 3.4.1, rapid ice gouge infilling due to wave and current action has been found by multiple researchers to be the most prominent in nearshore shallow water locations with gouge infilling rates generally decreasing with offshore position. Therefore, rapid nearshore ice gouge infilling can potentially bias ice gouge occurrences towards deepwater locations by rapidly obliterating nearshore records and preventing detection during ice gouge survey programs.

Biasing of ice gouge data distributions due to gouge infilling may be counteracted through knowledge of sediment infill thickness data derived from sub-bottom profiler surveying (see Section 2.1.3). In this manner, measured ice gouge depths may be offset by associated sediment infill thickness observations in order to provide approximation of initial gouge depths created prior to any infilling occurrences. Alternately, sediment infill thickness data could be statistically analyzed and probabilistic ice gouge depth distributions and/or associated probability of exceedence contours (see Section 4.1)

shifted by an average or most probable infill thickness in order to reflect initial gouge incision depths.

Lanan et al. (1986) have reported that analysis of repetitive ice gouge surveying records can potentially bias ice gouge depth distributions towards shallow ice gouge depths. This may result from enhanced recognition of shallow ice gouges by the interpreter as these gouges can be conspicuous on side-scan sonar records when compared with previous survey records, but not so noticeable on echo sounder data. This form of bias is subjective to the interpreter and is thus impossible to normalize or assess within available ice gouge data collections. Recent advancements in microprofilier and sub-bottom profiler technologies allow high-resolution sediment infill profiling and, subsequently, accurate determination of accurate ice gouge depths.

Marcellus and Morrison (1986) have discussed how many researchers commonly utilize large ice gouge depth class ranges (on the order of 0.5m) when reporting ice gouge data in distribution histograms, rather than attempt to correct depth resolution uncertainties. This practice may introduce data bias towards deeper gouge depths occurring with decreased resolution when curve fitting probability distribution functions to data histograms. This may occur as the true ice gouge depth is not accurately known and wide class ranges can mask otherwise distinct occurrences or trends. Marcellus and Morrison (1986) studied this form of data bias through analysis of an analogue data set using both 0.5 and 1.0m gouge depth data intervals, with a resulting bias towards deeper predicted ice gouge depths for the decreased resolution (1.0m), as shown in Figure 16. The analysis

was conducted using an exponential distribution convolved with the Gaussian distribution for shallow ice gouge depths (see Marcellus & Morrison, 1986 for discussion of this process). As shown in the figure, the decreased resolution (1.0m) predicts ice gouge depths on the order of approximately 0.33 to 0.5m deeper than does the 0.5m resolution at any given probability level.

Marcellus and Morrison (1986) also compared ice gouge depth data distributions retrieved via linear surveys vs. areal (mosaic) surveying procedures for analysis of potential data bias. Linear survey data corresponded to the maximum ice gouge depths recorded per individual gouges, whereas mosaic data represented the distribution of all gouge depths observed per given seabed survey area containing grouped geophysical survey lines. In general, minimal differences were observed between exceedence probability curves fit to each data distribution (linear vs. mosaic). However, Marcellus and Morrison (1986) provided little discussion on the analysis conducted.

As summarized above in Table 6, each of the American Beaufort Sea ice gouge data collections investigated and compiled as part of this thesis work exhibited ice gouge depth resolutions on the order of 0.1 to 0.15m. Ice gouge width resolutions were found to range from 0.1 to 2m. Therefore, merger of this data will not produce any ice gouge depth or width data bias due to measurement resolution or associated cut-off limits. As shown in the table, each data collection contained ice gouge data ranging from shallow water depths (less than 5m) to some distance offshore. However, the maximum surveyed water depths ranged from 20 to 125m. It is therefore suggested that combination of the

American Beaufort Sea data collections may potentially bias the (combined) data set population towards measurements obtained in approximately 20 to 30m water depths or less, with decreased data representation available for deeper water depths. Refer to the analyzed gouge depth data populations provided per water depth range in Table 3.

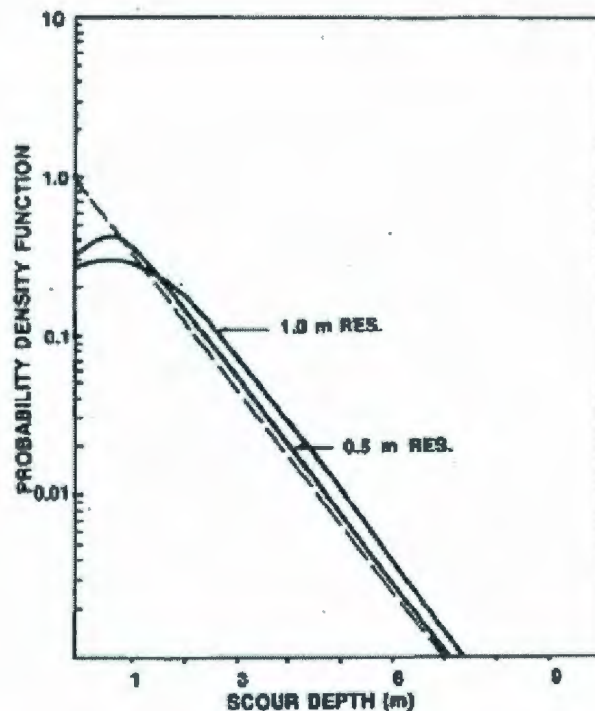


Figure 16: Effect of Poor Ice Gouge Depth Resolution/Wide Data Bins (Marcellus & Morrison, 1986)

Table 7 indicates that ice gouge depth resolutions ranged from 0.1 to 0.6m for the ice gouge depth data extracted from available Canadian Beaufort Sea data collection summaries (see Section 2.5). Limited ice gouge width data could be gathered, at a resolution of 5m. As shown in the table, each of the available data summaries covered water depths approximately ranging from 0 to 50m. Merger of this data for combined

analysis may potentially bias the distribution towards deeper gouge depths due to the 0.6m cut-off imposed by the 5,240 unknown age ECHOBASE data points extracted from the Comfort et al. (1990) study. Gilbert et al.'s (1987) updates to the SCOURBASE and ECHOBASE databases allowed gouge depth resolution to 0.1m, thus supporting Comfort et al.'s (1990) explanation that the 0.6m cut-off was due to (unspecified) data inconsistencies and not actual depth resolution. Similarly, Shearer et al. (1986) recorded 0.17m gouge depth resolution for additional data incorporated into the SCOURBASE database. The early data obtained from Wahlgren's (1979) study exhibited an apparent gouge depth resolution of 0.1m.

The summarized Chukchi Sea ice gouge data collections (Table 8) indicate that of the two available data collections, one exhibited a gouge depth resolution equal to 0.2m (USGS 88-25), whereas the other was 0.5m (USGS 78-693). Combination of these data sets may inadequately represent the number of shallow ice gouges, since the USGS 78-693 survey program did not resolve gouge depths shallower than 0.5m. Likewise, when analyzed alone, the USGS 78-693 data collection will exhibit bias towards deeper ice gouge depths due to the exclusion of gouge records less than 0.5m deep. Ice gouge width data was only recorded in one of the data collections, with a minimum measurement resolution of 2m.

3 PREVIOUS ENGINEERING ANALYSES

As presented above in Section 2, numerous American Beaufort, Canadian Beaufort, and Chukchi Seas ice gouge data collections have been researched and reviewed as part of this thesis work. The studies reviewed in this section represent previous engineering statistical analyses of ice gouge data parameters and correlations relevant to the present study.

Section 3.1 provides detailed discussion of statistical ice gouge analysis methods presented by previous researchers. Ice gouge infilling and sedimentation information is provided in Section 3.4, along with discussion of wave and current action, seabed soil conditions, and geographical influences upon gouge infilling rates. A significant amount of regional ice gouge recurrence rate data has been researched and reviewed as part of this thesis, with results provided in Section 3.5.

3.1 EXTRAPOLATION TO DESIGN EVENTS

The scraping of an ice keel along the seabed poses a significant threat to subsea pipelines, among other facilities, which may be damaged by the gouging ice keel. Subsea pipelines are generally trenched and buried beneath the seabed in areas prone to ice gouging and sediment reworking events caused by grounding ice keels. The required burial depth for the protection of pipelines from interaction(s) with ice keels during gouging is a function of the maximum gouge depth (the design ice gouge depth) that may be expected to occur in a specific area during the installation's designed lifetime for a specified level of acceptable risk (the design gouge depth return period). Consequently, analysis of ice

gouge statistics for design gouge depth prediction also commonly involves examination of maximum gouge depth distributions broken down according to water depth.

Exceedence probability plots may be generated for historical ice gouge depth data sets and subsequently utilized to estimate extreme gouge depths at fixed levels of risk (i.e., for a given probability of exceedence). However, exceedence probability analysis only considers numerical ice gouge depth data and fitted probability distribution functions, and neglects factors such as the methods used to obtain the data, gouge depth resolution cut-off, the effects of dynamic environmental activities (sedimentation, gouge infilling, reworking), pipeline and gouge orientations, pipeline length, etc. Therefore, design ice gouge depths should not be selected on the basis of exceedence probability assessments only.

Weeks et al. (1983) established one of the most well known methods of predicting extreme ice gouge depths on the basis of exponentially distributed historical data collected as part of USGS Open-File Reports 81-950 (Barnes et al., 1981) and 78-730 (Barnes et al., 1978). Lanan et al. (1986) added to the analytical ice gouge works by Weeks et al. (1983) by developing a more thorough equation for predicting extreme ice gouge depths and associated trenching requirements for arctic subsea pipeline design. The exponential distribution has been proposed to model American Beaufort Sea ice gouge depth data well, however, Wang (1990a) has recommended that the following procedure is only appropriate for pipelines orientated approximately perpendicular to the dominant ice gouge trend due to the randomness of gouge directions. As shown by

Weeks et al. (1983) and later refined by Lanan et al. (1986), the maximum ice keel incision depth can be calculated for different return periods (hence, a fixed level of acceptable risk of ice gouging to the design depth) using the following formula:

$$d = c + \frac{1}{\lambda} * \text{Ln}[g * T * L * \sin(\theta)] \quad (3.1)$$

where

d = design maximum ice gouge depth for specified return period and fixed level of risk to the pipeline (meters);

c = cut-off incision depth below which gouges become too small to identify and count (and the ice gouge incision depth which all of the observed gouges exceed) (meters);

g = the annual linear ice gouge recurrence rate (number of gouges/km/year);

T = extreme gouge average return period (years);

L = pipeline length (kilometres);

θ = the angle between the pipeline route and the trend of the ice gouges (degrees);

λ = the slope of the negative exponential gouge depth distribution curve (1/meter).

This equation is similar to other statistical methods used for predicting long return period extreme values based on a limited number of observation years. It assumes that ice gouges during future years will have a similar depth distribution as those observed during

the available survey years. The number of gouges (N) that is predicted to occur during the selected return period is computed as:

$$N = g * T * L * \sin(\theta) \quad (3.2)$$

The balance of the equation then predicts the depth of the deepest single gouge within that number of future ice gouges.

Two approaches, graphical and analytical, can be taken to solve for the two parameters λ and c . The graphical approach calculates the two parameters, λ and c , from the exponential best-fit function for plots of exceedence probability of gouge depth vs. ice gouge depth class limits (that is, the plots of the calculated probability that the calculated design ice gouge depth will exceed a specified upper depth class limit).

The analytical approach (see Section 4.1.1) consists of using the same straight line to determine the cut-off depth, c (which is the intersection between the interpolation straight line and the 100% exceedence mark). The parameter λ is then calculated as (Lanan et al., 1986; Weeks et al., 1983):

$$\lambda = \frac{1}{d_{bar} - c} \quad (3.3)$$

where d_{bar} = the mean gouge depth (meters).

Other researchers have presented alternate methods of statistical ice gouge depth analysis, which are reliant upon various statistical distributions and/or required input criterion for

design gouge depth prediction. Lewis (1977a; 1977b) has presented the exponential distribution as the simplest and most reliable method of Canadian Beaufort Sea ice gouge depth analysis, as follows:

$$n = n_o \exp(-k * d) \quad (3.4)$$

where

n = number of ice gouges per dm of gouge depth per km of seabed;

n_o = number of ice gouges per dm at zero gouge depth per km of seabed (physically interpreted as the number of ice gouges barely visible on sonar records and about to be completely infilled);

k = a parameter of the exponential distribution (1/dm); and,

d = ice gouge depth (dm).

However, the gamma and/or Weibull probability distributions generally provide a better fit to Canadian Beaufort Sea ice gouge depth data when compared to the exponential function, and are suggested to provide a particularly good fit to data records in the upper distribution tail (extreme events; see Section 4.2.3) (Nessim & Hong, 1992; Lever, 2000).

Lewis (1977a) also studied the Gumbel distribution of extreme value theory for analysis of extreme ice gouge depth prediction, which assumed large numbers of ice gouge statistics, and unlimited, independent variants with similar initial gouge depth

distributions. The Gumbel extreme value theory was developed in terms of an asymptotic relationship and thus exhibits increasing validity with increasing sample population. The cumulative distribution of the Gumbel extreme value analysis theory (briefly) studied by Lewis (1977a) is as follows:

$$\Phi(x) = \exp[-\exp(-y)] \quad (3.5)$$

where

y = linear function of the observed variant x (gouge depth), with coefficients estimated from a sample of maximum (ice gouge depth) values, as follows (Lewis, 1977a):

$$y = \frac{1}{\beta}(\mu - x) \quad (3.6)$$

where

μ = mode of the maximum ice gouge depth frequency curve; and,

β = measure of spread related to the standard deviation of the cumulative distribution.

Refer to the Lewis (1977a) study for further discussion and results of the Gumbel extreme value analyses.

Pilkington and Marcellus (1981) presented numerous statistical procedures for utilization in Canadian ice gouge data analysis. These methods included recurrence rate analysis procedures, scoring equilibrium analysis, ice keel draft and gouge depth correlations, and

traditional probabilistic analysis procedures, as discussed below. Simpler methods were also introduced, such as burial beneath the saturated scour zone or below the deepest observed ice gouge records.

Recurrence rate analysis procedures discussed by Pilkington and Marcellus (1981) relied on knowledge of ice gouge recurrence rates and statistical ice gouge depth data, to calculate predicted ice gouge depth as follows (after Weeks et al., 1980):

$$d = \frac{\text{Ln}(1/N * T * L)}{-k} \quad (3.7)$$

where

d = the predicted ice gouge depth (m);

L = length of the pipeline route (km);

T = design ice gouge return period (years);

N = average ice gouge recurrence rate (average number of gouges/km/year); and,

k = reciprocal of the mean ice gouge depth for a specified water depth range (1/m).

This method may potentially over- or under-predict ice gouge depths, depending on the amount of statistical ice gouge depth data available for averaging (k). Also, this method does not correct for the infilling of seabed ice gouges during the analyst-specified design ice gouge return period.

A second method of ice gouge depth prediction presented in Pilkington and Marcellus' (1981) study is 'scoring equilibrium analysis', which takes into account seabed sedimentation and ice gouge crossing rate statistics, as follows (after Lewis, 1977b):

$$d = \left[\text{Ln} \left\{ \frac{V}{\left(u * n_o + \frac{(V * u * n_o)}{k} \right)} \right\} \right] / -k \quad (3.8)$$

where

d = the predicted ice gouge depth over gouge return period (m);

$V = 1/(L * T)$;

L = total pipeline length subjected to ice gouging (km);

T = ice gouge return period (years);

u = sedimentation rate (mm/year);

n_o = ice gouge crossing rate or linear density in area subjected to sedimentation (gouges/km); and,

k = reciprocal of the mean ice gouge depth for a specified water depth range (1/m).

In the preceding design ice gouge depth estimation method, the sedimentation rate is calculated as the total sediment thickness divided by the total time available for deposition of sediment in the area (Pilkington & Marcellus, 1981). However, Pilkington

and Marcellus (1981) have indicated that this was an incorrect assumption based on knowledge of preferential ice gouge infilling and variation of seabed sedimentation rates with water depth. Therefore, this method predicts conservative ice gouge depths in deep water but may potentially estimate inadequate and/or non-conservative design gouge depths in shallow water areas (Pilkington & Marcellus, 1981).

A third method of ice gouge depth prediction studied by Pilkington and Marcellus (1981) involved analysis of spatial ice keel draft and gouge depth statistics, and estimated design ice gouge depths through correlation of measured ice keel draft and seabed gouge depth distributions. Methods of ice keel draft measurement include upward looking sonar, submarine or laser profilers, diver reconnaissance, etc. This procedure represents the number of ice feature keels passing over a specified seafloor area each year with draft greater than D (m) as:

$$N(> D) = N_o \exp\left(-D/D_o\right) \quad (3.9)$$

where

N_o = total number of keels passing over the seafloor area per year (spatial density);

D_o = is a constant; and,

D = ice keel depth (m).

The total number of ice feature keels passing overtop of a pipeline of length (L) with draft greater than D may be calculated as:

$$T_k = f * N(> D) \quad (3.10)$$

where

$$f = 2 * L / w \quad (3.11)$$

where

L = pipeline length (m); and,

w = width or length of the ice keel (m).

After Lewis (1977a; 1977b) (discussed above), the ice gouge distribution (gouges/km/year) on the seabed is exponentially distributed with the probability of an ice gouge of depth d (m) occurring at a water depth of D (m) defined by:

$$P(d) = N_o \left[\exp\left(-D/D_o\right) \right] * f * \exp(-k * d) \quad (3.12)$$

where

k = reciprocal of the mean ice gouge depth for a specified water depth range (1/m) and all other parameters are as defined above.

As discussed by Pilkington and Marcellus (1981), the preceding statistical analysis procedure assumes that the ice gouge depth distribution is constant with time, which may be conservative if shallow gouges infill faster than deep gouges, and non-conservative otherwise. Finally, extreme ice gouge/keel draft events of depth (d) could be modeled based on observed ice gouge/keel draft statistics. Following this exceedence probability method, the predicted ice gouge depth (m) is calculated as follows (Pilkington & Marcellus, 1981), where necessary parameters are as defined above:

$$d = \text{Ln} \left[L * T * N_o * f * \exp \left(-D/D_o \right) \right] / k \quad (3.13)$$

The preceding methods of extrapolating ice gouge data to design events have utilized linear extreme ice gouge depth prediction methods for subsea pipeline design. An areal method was developed by Wang (1990a) to allow probabilistic extreme ice gouge depth prediction for alternate subsea structure shapes (2-dimensional). Areal methods require knowledge of spatial ice gouge generation rates. Wang (1990a) has suggested restrictions on the applicability of extreme ice gouge depth prediction methods developed by Lewis (1977a; 1977b), Weeks et al. (1983), and Lanan et al. (1986), which include application to linear subsea structures only (i.e., pipelines) and the requirement for ice gouge data to be collected in the same orientation as the pipeline being analyzed.

Wang's (1990a) spatial extreme ice gouge depth prediction method was developed with great similarity to the linear extreme ice gouge prediction method introduced by Weeks et al. (1983) and later refined by Lanan et al. (1986). Wang (1990a) defined the average

number of new ice gouges to occur in a given survey area (R) per year (i.e., new gouges/year) as αA , where A is the area of the region to be analyzed (m^2) and α is the spatial ice gouge recurrence rate. Linear ice gouge recurrence rates (gouges/km/yr) can be converted to spatial recurrence rates (gouges/ km^2 /yr) as follows:

$$\alpha = G / [l * \cos(\theta)] \quad (3.14)$$

where

G = linear ice gouge recurrence rate (gouges/km/yr) measured in the north – south direction;

l = average length of gouges (km); and,

θ = orientation of ice gouges ($^\circ$), referenced to the east – west direction (θ cannot equal 90°).

Alternately, the spatial ice gouge recurrence rate can be estimated from gouge endpoint frequencies obtained from repetitive field data observations, and defined as one-half the number of gouge endpoints (or start-points) occurring in a specified area (km^2) per year (Wang, 1990a). This method takes into consideration that not all gouges will occur within the area of interest (i.e., the 0.5 multiplier). Therefore, Wang's (1990a) procedure has assumed that if a new ice gouge was observed to initiate inside the region of interest but terminate outside R , then only half of the gouge was generated in R (and vice versa). Alternately, spatial ice gouge recurrence rates may be determined using ice feature drift

rate data, as presented by McKenna et al. (2003) and King et al. (2003) (see Section 3.5.5.1). Upward looking sonar ice feature monitoring programs (see Section 3.5.5.3) may also be utilized. d'Apollonia and Lewis (1986) have presented a unidirectional deterministic method of determining spatial iceberg grounding rates (groundings/km²/yr, analogous to the gouge recurrence rate). The analysis method utilizes annual iceberg flux data, draft distributions, loss rates, water depth, and spatial location parameters.

Similar to methods developed by previous researchers (Weeks et al., 1983; Lanan et al., 1986; among others), Wang (1990a) has presumed an exponential ice gouge depth probability distribution as described in Section 4.1.1. The predicted maximum ice gouge depth (m) for the region (R) is thus calculated as follows:

$$d = c + \frac{1}{\lambda} * \text{Ln}[\alpha * A * T] \quad (3.15)$$

Where λ , c , and T are as defined at the beginning of this section in discussion of the Weeks et al. (1983) and Lanan et al. (1986) procedure. A potential setback with Wang's (1990a) spatial extreme ice gouge depth prediction method is that it is limited by the number of gouges located within region R , and is thus constrained by the selection of R . Also, the calculation of α requires knowledge of highly prescriptive values of G occurring along the north – south axis, which may not be readily available. Sample linear and spatial extreme ice gouge depth prediction simulations were provided in the Wang (1990a) report.

Gaskill and Lewis (1988) have also addressed ice gouge risks to 2-dimensional subsea structures; however, their emphasis was on calculating the probability that a gouge would occur in a specified area and assumed that the spatial ice gouge recurrence rate was known and constant. This assumption is oftentimes incorrect. Ice gouge occurrence was assumed to be a Poisson process. Discussions of Monte Carlo simulation and closed form solution methods were also provided, but extreme ice gouge depth prediction was not addressed.

The preceding has been provided as a thorough review of previous researchers' work regarding ice gouge depth statistical analyses. As discussed in Section 4, this study has investigated and assessed the suitability of the exponential, gamma, and Weibull distributions for recommendation of the most appropriate distribution for statistical ice gouge depth data analysis.

3.2 ICE GOUGE PARAMETER CORRELATIONS

Barnes and Reimnitz (1986) provided a summary and overview of USGS ice gouge survey programs conducted on the Alaskan shelf of the American Beaufort Sea, along with limited analysis of collected data. The study presented a general correlation between maximum ice gouge depths and water depth, which proposed maximum gouge depths to be approximately one tenth of the water depth, to a maximum water depth of 40m. Ice gouges were studied to 64m water depth, although deepwater gouges were suggested to be relic with 47m proposed as the limit of modern gouging.

Canadian Beaufort Sea ice gouge parameter analysis conducted by Hnatiuk and Brown (1977) exhibited positive relationships between gouge widths and depths, and gouge depths and water depths. Similar analyses conducted by Hunting Geology and Geophysics (1971; 1973) found that gouge depths increased with increasing water depths, and the deepest observed ice gouges were also found to be the widest. However, gouge widths were not necessarily shown to increase with increasing water depth. Rescouring rate and ice gouge recurrence rate analysis was conducted by Shearer (1979) during APOA Project 151, although the data was skewed by subjective ice gouge counting bias. Shearer (1979) contended that the majority of Canadian Beaufort Sea ice gouging occurs during the winter, with minimal gouging associated with initial ice feature grounding processes (i.e., the localized formation of ice feature grounding 'pock' marks).

Historically, frequent ice gouging has been observed between approximately 15 and 45m water depths in the Canadian Beaufort Sea, as reported by numerous researchers (Hunting Geology and Geophysics, 1971; 1973; Hnatiuk & Brown, 1977; Lewis 1977a; 1977b; Hnatiuk & Brown, 1983). The 15m bathymetric contour coincides with the shoreward boundary of the dynamic shear ice zone (Hnatiuk & Brown, 1977) and thus represents the nearshore boundary of frequent ice gouging, although significant ice gouge activity has been found close to shore in shallower water depths (Lewis et al., 1976; Shearer, 1979). The approximate 10 to 50m water depth range was found to be saturated by ice gouging activity (Shearer & Blasco, 1986), with the maximum new gouge occurrence frequency exhibited inshore of approximately 25m water depth (CSR, 2008). Multiple research studies (Lewis et al., 1976; 1977a; 1977b; Hunting Geology &

Geophysics, 1971; 1973) have commonly reported decreasing ice gouge frequencies with increasing water depth, particularly beyond approximately 45m in the Canadian Beaufort Sea, with essentially no gouging observed beyond 80m water depth. Hnatiuk and Wright (1983) reported that the deepest ice gouges were located approximately 80km north of Herschel Island.

The Alaskan Coastal Current has been found to strongly influence Chukchi Sea ice gouge processes, although maximum ice gouge water depths are shallower than those observed in the Beaufort Sea (Wilson et al., 1982). This is most likely due to ice feature and drift pattern relationships in the Chukchi Sea. Multiple researchers (Phillips & Reiss, 1984; 1985; among others) have found Chukchi Sea ice gouge orientation to generally parallel bathymetric contours, thus supporting the Alaskan Coastal Current's influence upon regional ice gouge processes.

In general, Chukchi Sea ice gouging studies have found ice gouge frequencies to increase with increasing latitude and seafloor slope, but decrease with increasing water depth, as reported by numerous researchers (Toimil, 1978; MMS, 1990; 2007; Wilson et al., 1982; Grantz et al., 1982a). Toimil (1978) found maximum ice gouge depths to be the greatest between 36 and 50m water depths in the Chukchi Sea, with no ice gouge depths greater than 1m observed beyond 56m water depth and all gouges observed in the 21 to 25m water depth range exhibiting depths of 2m or less. Toimil (1978) also observed that the widest Chukchi Sea ice occurred between 31 and 45m water depths.

Numerous Chukchi Sea researchers (Grantz et al., 1982b; Phillips et al., 1988; MMS, 1990) have reported shallower ice gouge depths for the northwest, northeast, and Herald Shoal regions which may be attributed to the presence of crustaceous bedrock at or near the seabed surface, and providing high resistance to ice gouge activity (see Section 3.3). Similarly, Grantz et al. (1982b) have suggested that decreasing ice gouge frequencies in southwesterly directions towards Herald Shoal may potentially be attributed to hard seabed sediments providing resistance to ice gouge mechanisms.

Refer to Section 5.1 for the results and analysis of ice gouge parameter correlations assessed as part of this study.

3.3 ICE GOUGE VARIATION WITH SEABED SEDIMENT TYPE

In general, seabed sediment properties are one of the most important parameters within the overall ice gouging process (Green et al., 1983). Deterministic ice gouge modeling conducted by Croasdale et al. (2005) predicted decreasing maximum ice gouge depths with increasing seabed soil strengths, and increasing maximum gouge depths with increasing ice keel attack angles. Dense seabed sediments may be expected to provide greater resistance to ice gouging than loose, unconfined sediments (Green et al., 1983). Numerical modeling by Sayed and Timco (2008) indicated increasing mean normal stresses on gouging iceberg keels with increasing ice gouge depth, thus signifying increasing seabed soil resistance to gouging with increasing depths below the seabed (as may be expected). However, parametric models developed by Liferov et al. (2007) indicated increasing ice gouge depths with position along the gouge track in soft, weak

soils, thus indicating the influence of seabed soil strengths upon gouge processes. A study by Clark and Zhu (2000) has shown ice-soil interaction failure modes to be dependent on the ice keel contact area that occurs during ice gouge processes. The probability of ice keel failure increases with increasing contact area, as the bearing capacity and thus resistance to ice gouging increases with increasing contact area (or footing) size. Therefore, a critical contact area may be defined according to seabed soil and ice keel strength characteristics for prediction of ice gouge failure mechanisms (soil vs. indenting ice keel).

Apparent qualitative correlations between Canadian Beaufort Sea sediment properties and ice gouge depths suggest that (extreme) gouge depths greater than 2m are mainly associated with thick, soft silty clays (Shearer & Blasco, 1986; Crooks et al., 1986). Silty sands have been found to generally exhibit shallower gouge depths. Similarly, Lewis and Blasco (1990) have reported deeper, narrower ice gouge occurrences in areas of dominantly clay seabed sediments, and wider, shallower gouges on the western Canadian Beaufort Shelf near Mackenzie Bay where, in general, seabed sediments are dominantly soft silty marine clay containing approximately 1% sand (Hnatiuk & Wright, 1983; Shearer et al., 1986; Shearer & Blasco, 1986; Gilbert & Pedersen, 1987; Comfort et al., 1990; Rogers, 1990; Rogers et al., 1993; Héquette et al., 1995). Hnatiuk and Brown (1977) have suggested that sand layers beneath marine mud (clay and silt) surficial seabed sediments would potentially provide greater resistance to ice gouging compared to a continuous layer of marine mud.

Ticken and Toimil (n.d.) analyzed ice gouge data collected at 10 survey sites located between Smith Bay and Flaxman Island in the Alaskan Beaufort Sea, and found that ice gouges in silty seabed soils commonly exhibited longer residence times than those in sandy seabed materials. Similarly, Wahlgren (1979) reported Canadian Beaufort Sea ice gouges to be better preserved in silt and clay seabed sediments than in sand. This is due to easier obliteration of ice gouges in coarser-grained sandy sediments as a result of wave and current action (see Section 3.4.1), compared to cohesive clay and/or stiff silt which tends to preserve gouge records (Ticken & Toimil, n.d.; Wahlgren, 1979). Stiff sandy silt (69% coverage) and silty fine sand (31%) dominated Ticken and Toimil's (n.d.) survey area, with 85% of the ice gouge records associated with the silty sediment locations.

Similar seabed sediments have been observed in the Canadian Beaufort Sea shelf, which dominantly exhibits soft silty marine clays with increasing sand fractions and a thinning veneer of silty clay towards the eastern shelf (Hnatiuk & Wright, 1983; Shearer et al., 1986; Shearer & Blasco, 1986; Gilbert & Pedersen, 1987; Comfort et al., 1990; Rogers, 1990; Rogers et al., 1993; Héquette et al., 1995). One exception is exhibited by a dominantly sandy seafloor found near Pullen Island (Shearer et al., 1986) and shoreward of the 10m bathymetric contour (Héquette et al., 1995). Crooks et al. (1986) have reported stiff silty clay basal units to the west of 135°W longitude, with dense sands and silts found to the east of 135°W. Rogers et al. (1993) have reported that thick sand beds covered by a thin silty clay veneer are located on the eastern Canadian Beaufort Sea shelf. Lewis and Blasco (1990) reported wider and shallower ice gouge depths with increasing seabed sand fractions, which was supported by Blasco et al. (1998) who found

greater populations of ice gouges 1m deep or greater on the western Canadian Beaufort shelf, in dominantly soft clay seabed sediments, than located to the east.

Hill et al. (1986) have studied nearshore sediment properties in the southern Canadian Beaufort Sea, based on borehole samplings obtained along three survey transects located north-northwest of Richard's Island in the nearshore zone. The samplings were obtained shoreward of approximately 10m water depths. Detailed description of borehole sediments were provided in terms of eight sediment facies in addition to undifferentiated non-marine silt and clay (refer to Hill et al., 1986 for detailed discussion). The eight sedimentological facies included (Hill et al., 1986):

- (1) Bioturbated clay;
- (2) Bioturbated silt with minor clay;
- (3) Laminated silt and clay;
- (4) Massive medium to thick-bedded silt;
- (5) Lenticular (lens-shaped) and thin-bedded sand;
- (6) Diamicton (poorly sorted coarse- and fine-grained sediments);
- (7) Medium to coarse-grained grey sand; and,
- (8) Medium-grained brown sand.

Physical geotechnical properties were reported for the fine-grained sediment facies, as follows (Hill et al., 1986):

- Facies 1: very soft marine clay with undrained shear strength ranging from 5 to 50 kPa and water content ranging from 35 to 55%. Shear strength increases linearly with depth below the seafloor, and water content decreases with depth. Hill et al. (1986) have indicated that this facies is typical of marine clay surficial sediments found across most of the Canadian Beaufort Sea shelf.
- Facies 2: bioturbated sediment exhibiting increasing undrained shear strength with depth below seabed, on the order of 5 to 35 kPa, with water content ranging from 21 to 38% and less than its liquid limit.
- Facies 3: reported to span the geotechnical ranges of Facies 1 and 2, with undrained shear strengths ranging from 4 to 85 kPa (very soft to stiff) and water contents on the order of 25 to 50%. However, unlike facies 1 and/or 2, the shear strength range was not found to increase linearly with depth below the seabed, but varied with sedimentary laminations.
- Facies 4: undrained shear strengths were reported to range from 4 to 75 kPa with water content ranging from 20 to 49%, although lower shear strengths (4 to 20 kPa) and higher water contents (40 to 49%) were found in shallow samples obtained less than 5m below the seabed.

In addition to the preceding geotechnical properties, Hill et al. (1986) recorded grain size distributions for the coarse-grained sediment facies, acoustic, and thermal properties, as well as radiocarbon dating for some of the sampled sediment cores. The thermal property measurements confirmed the presence of permafrost in very nearshore locations, as well as located at the seabed in the landfast ice zone and/or areas where sea ice is grounded (Hill et al., 1986).

Crooks et al. (1986) have reported that the surficial layer of recently deposited clayey soils in the Canadian Beaufort Sea are generally soft to very soft, and exhibit extensive evidence of ice gouge activity. These surficial sediments are located across the Canadian Beaufort continental shelf, and become finer with increasing distance from the Mackenzie Delta, due to littoral drift (Crooks et al., 1986). Undrained shear strengths have been found to increase linearly at a rate of 6 kPa per meter of depth below mudline from a projected zero shear strength at the mudline. In-situ effective and yield stress testing results were also provided for tests conducted at the Tarsiut site. As may be expected, effective horizontal and vertical stresses were observed to increase with increasing depth below the seabed.

Pressuremeter testing conducted in the surficial clay strata of the general Kringalik Plateau and Kugmallit Channel regions (see Figure 12) indicated similar, weak clay behaviour in the upper 3 to 4m depth below seabed (Rogers et al., 1993). Upper sediment weakness was attributed to continuous reworking of surficial clays by ice gouge activity.

To summarize, numerous researchers (Crooks et al., 1986; Hill et al., 1986; Shearer & Blasco, 1986; Lewis & Blasco, 1990; Rogers et al., 1993) have shown that dominantly soft marine clay surficial seabed sediments may be expected to provide low available shearing resistance to ice gouge activity, and have indicated that maximum gouge depths are correlated well with maximum low-strength sediment thicknesses. Shearer and Blasco (1986) and Rogers et al. (1993) have indicated that maximum observed ice gouge depths may be correlated well with the maximum thickness of weak surficial seabed sediments, thus signifying the limiting effects of seabed soil properties on ice gouge depths.

In addition to the Canadian Beaufort Sea information, a limited amount of American Beaufort shelf and Chukchi Sea soil strength data has been obtained from Dobson and Wickham (1985). Generally, competent sediments were found in the study areas, although weak surficial soils may be widespread in the Chukchi and locally present in the Beaufort Sea. The weak sediments exhibited undrained shear strengths on the order of 20 to 50 kPa, with low bearing capacity and lateral sliding resistance, and therefore low resistance to ice gouge processes (similar to the Canadian Beaufort). In some instances, the zones of weak shear strengths may be potentially attributed to the thawing of subsea permafrost. Due to noted similarities between American and Canadian Beaufort marine sediments, it is postulated that similar zones of weak soil (due to thawing permafrost) may be locally present in the Canadian Beaufort Sea as well. However, further literature research and review is required on this topic.

Dobson and Wickham (1985) reported very strong seabed soils or rock at or near the seafloor surface in the western American Beaufort Sea, with high resistance to seabed penetrations (i.e., ice gouging). Thus, shallower ice gouge depths may be expected to occur in the western Beaufort Sea compared to those occurring to the east. Similarly, numerous Chukchi sea researchers (Grantz et al., 1982b; Phillips et al., 1988; MMS, 1990) have reported shallower ice gouge depths for the northwest, northeast, and Herald Shoal regions due to the presence of bedrock at or near the seabed surface and thus providing high resistance to ice gouge activity.

3.4 ICE GOUGE INFILLING & SEDIMENTATION STUDIES

As discussed in Section 2.1, the weathering, infilling and subsequent obliteration of ice gouge deformations in the seafloor is a dynamic and time dependent process which is influenced by seabed sediment properties, general sediment deposition rates, waves, currents, water depth, gouge geometry, and local geography (Palmer & Niedoroda, 2005). Immediate and/or long-term sediment reworking processes may be observed upon arctic seabed areas subjected to ice gouging. Various terminologies have been found synonymous with ice gouge 'infilling' during this literature review, including ice gouge 'weathering' and 'obliteration.' 'Infilling' has been utilized within this thesis.

In general, ice gouge infilling predominantly occurs during the open-water summer months in arctic nearshore areas. This is due to peak river discharge into the Beaufort Sea occurring in late spring and early summer, which represents the principal introduction of sediment for deposition in nearshore areas (Weeks et al., 1985). Also, extensive ice cover

persisting from late fall to early spring dampens waves and limits the effective transfer of atmospheric momentum required to produce sediment transport by wave and current action. Sediment transport by wave and current action is believed to be the dominant mechanism which infills and obliterates ice gouge depressions in the seabed (Weeks et al., 1985).

Barnes and Reimnitz (1979) studied immediate ice gouge infilling rates which demonstrated the episodic influence of waves and currents upon seabed sediment reworking processes and ice gouge characteristics on the inner shelf of the American Beaufort Sea. The analyzed data was originally studied by Barnes et al. (1978) for ice gouge surveys conducted in eastern Harrison Bay, Alaska. Through the study, Barnes and Reimnitz (1979) postulated that measured depths of unknown age ice gouges may potentially underestimate the actual ice keel incision depth due to rapid sediment infilling that can occur immediately following gouge formation. This hypothesis is highly dependent upon the frequency of occurrence of wave and current-driven sediment reworking events following gouge formation, in addition to the age of the gouge at the time of survey.

Similarly, the MMS (1990) study reported that Chukchi Sea ice gouges may be quickly infilled or eliminated in the stamukhi zone (approximately 10 to 20m water depths) by sediment reworking due to current action. Phillips et al. (1988) indicated that low ice gouge densities observed along shoreward sections of outer gravel and coastal current sand lithofacies in the Barrow Sea Valley resulted from active infilling of shallow water

ice gouges due to current action. Phillips et al. (1988) also indicated that currents, waves, and biological processes were found to actively rework the seafloor and potentially mask the effects of ice gouging in deepwater areas of the southern Chukchi Sea. The Alaskan Coastal Current is also known to actively rework the seabed in specific Chukchi Sea nearshore areas inshore of 30m water depths (Phillips et al., 1988). The effect of storm generated waves on immediate ice gouge infilling rates was also indicated by Phillips et al. (1984) through analysis of Peard Bay, northeast Chukchi Sea ice gouges before and after a storm event. Phillips et al. (1984) reported numerous ice gouge observations in sandy seabed sediments in less than 11m water depth prior to a storm, but these gouges were rapidly erased by storm driven waves with no gouge deformations observed in the same area following the storm.

Following immediate ice gouge infilling events, long-term ice gouge infilling may occur due to sedimentation and sediment redistribution processes. Knowledge of local sedimentation rates and associated ice gouge infilling observations is one method of estimating the age of seabed ice gouges, as discussed above in Section 2.2.

In addition to immediate ice gouge infilling data, Barnes et al. (1978) have studied seabed sedimentation rates, ice gouge re-plow, and associated sedimentary structures occurring on the inner shelf of the American Beaufort Sea. Barnes et al. (1978) quote an estimated sedimentation rate of 10 cm per 100 years for nearshore areas of the American Beaufort Sea, which was originally estimated by Reimnitz and Barnes (1974). Weeks et al. (1985) have estimated Beaufort Shelf sedimentation rates to range from 0.05 to 0.2 cm/year,

based on observation of recent Holocene sediment thicknesses. In addition, Weeks et al. (1985) estimated maximum sedimentation rates of 0.6 cm/year for American Beaufort Sea areas near Prudhoe Bay.

Similar general sedimentation rates have been estimated for the Canadian Beaufort Sea, ranging from 0.03 cm/year in deepwater (50 to 80m water depth) to 0.2 cm/year in shallow water locations (0 to 10m water depth) (Weeks et al., 1985). Gilbert and Pedersen (1987) provided site-specific sedimentation rates for the Canadian Beaufort Sea shelf which ranged from less than 0.08 to 2.5 mm/yr, as shown in Figure 17. Wahlgren (1979) provided sedimentation rates ranging from 0.15 to 0.28 mm/yr for 17.5m water depth offshore Pullen Island, 0.18 to 0.29 mm/yr for 32m water depth north of the Tuktoyaktuk Peninsula, and 1.7 to 1.9 mm/yr occurring between 40 to 50m water depth in east Mackenzie Bay. Based on these sedimentation rate predictions, an observed seabed ice gouge depression could persist for a long period of time, assuming seabed sedimentation is the only infilling mechanism (which is not the case, as discussed below).

Barnes et al. (1978) estimated sediment reworking rates and generated a proportional seabed ice gouge re-plow curve which suggested 20% undisturbed seabed per 100 year ice gouge period. On this basis, any gouges present in the 20% undisturbed seabed area that are less than 10 cm deep were predicted to be filled-in during the long term (within 100 years). Other ice gouge infilling processes, such as preferential infilling and/or gouge superimposition, may potentially cause ice gouge infilling and total obliteration at rates greater than expected based on average seabed sedimentation rates (Pilkington &

Marcellus, 1981). Blasco et al. (n.d.) have estimated preferential gouge infilling to be five times the regional sedimentation rate in areas of the Canadian Beaufort Sea.

Shearer and Blasco (1986) have suggested that more recent ice gouge events may be biased towards shallow water depths, but exhibit significantly lower residence times than offshore locations due to increased sedimentation and gouge infilling nearshore. Therefore, increased ice gouge frequencies in offshore locations do not necessarily indicate greater gouging activity in these areas since longer residence times are exhibited in deeper water. More recent investigations have indicated that 75% of the Canadian Beaufort seafloor is reworked by ice gouge activity between 12 and 18m water depths, with the boundary between moderate, nearshore ice gouging and severe offshore activity occurring in the 10 to 12m bathymetric range (Héquette et al., 1995).

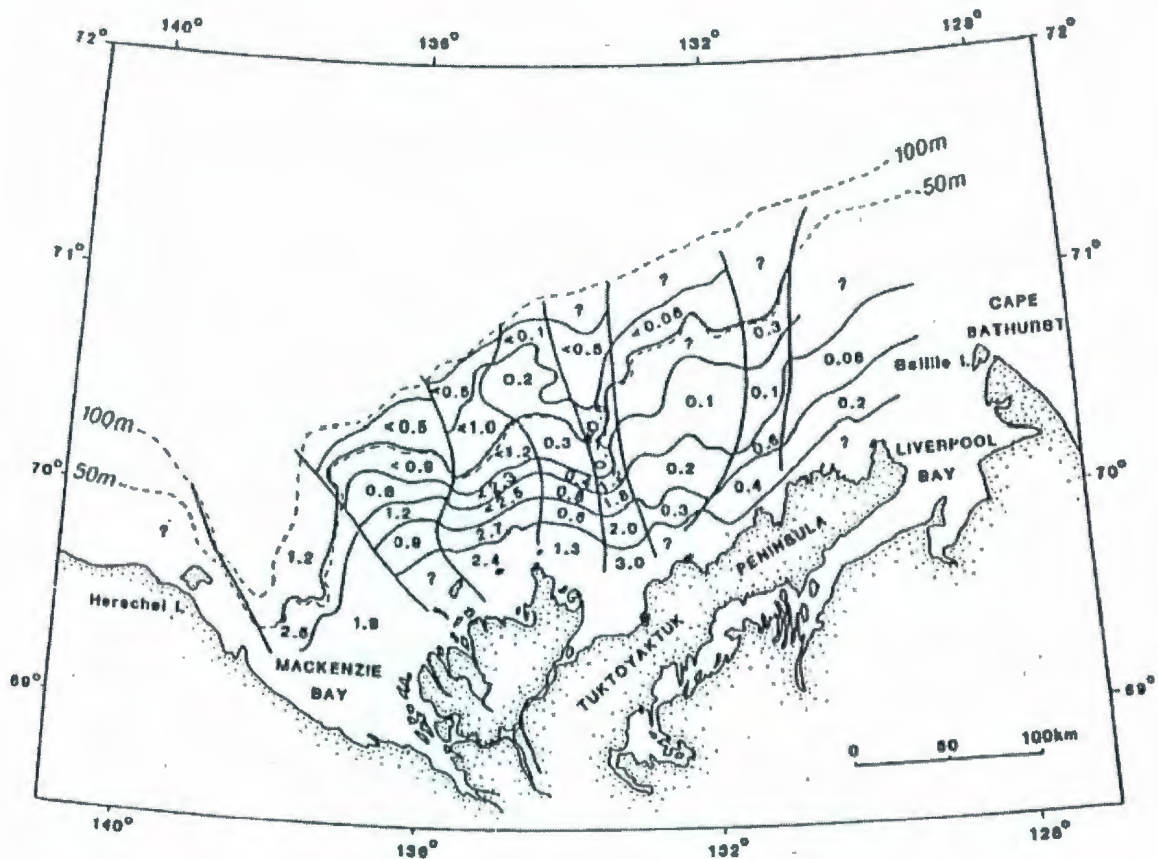


Figure 17: Canadian Beaufort Sea Shelf Sedimentation Rates (mm/yr) (Gilbert & Pedersen, 1987)

3.4.1 Wave & Current Action

Sediment reworking events driven by wave and current action redistribute seabed sediment materials from areas of high relief, such as ice gouge berms (or ridges), and deposit this sediment into areas of low relief, such as ice gouge deformation troughs. Palmer (1998) has stated that, in shallow water areas of the Beaufort Sea(s), seabed sediment transport is an effective method of ice gouge obliteration, with sedimentation rates approximately proportional to wave heights. Storm conditions therefore cause swift ice gouge obliteration, as large waves are much more effective in reworking ice gouged

seabed sediments than are smaller waves (Palmer, 1998). In addition, Palmer (1998) has discussed how modest sea states occurring in shallow water inshore of 5m water depth can produce sufficient sediment transport rates to completely erase ice gouges. Weeks et al. (1985) also found that hydrodynamic activity resulting from large waves and wind-driven currents associated with storms could rapidly obliterate ice gouges in shallow water depths of the Beaufort Sea shelf. Lewis (1977a) hypothesized that the Canadian Beaufort Sea nearshore zone could be extensively ice gouged inshore of 10m water depths, although the non-cohesive sandy seabed appeared to be seasonally smoothed by wave and current action, thus erasing any potential ice gouge deformations. This is potentially a reason why ice gouging appears to be more pronounced in intermediate water depths (20m) than in shallow water regions; shallow water ice gouges may be swiftly erased by wave and current action.

Weeks et al. (1985) developed a numerical simulation program to predict ice gouge infilling rates on the Beaufort Sea shelf due to bedload sediment transport resulting from waves and currents, as well as known regional sedimentation rates. The program utilized Monte Carlo simulation of exponentially distributed ice gouge depths and Poisson distributed gouge recurrence rates, and considered numerous seabed soil properties in calculation of design sediment transport rates under specified environmental conditions. The seabed soil properties utilized in the simulator included relative sediment densities, mean grain diameters, and critical seabed shear stress data for determination of scenarios that would produce movement of a particular sediment type. Using the simulator, Weeks et al. (1985) estimated the number of ice gouges that would be observed along a one-

kilometre survey line as a function of residence time and steady current velocity. The predicted time series results of current velocity on ice gouge populations are provided in Figure 18 and Figure 19 for sand and silt seabed sediments, respectively. As shown in the figures, predicted ice gouge populations were found to decrease significantly with increasing current velocity, thus indicating the relationship of increasing ice gouge infilling rates with increasing current velocities. For this analysis, the simulator assumed constant environmental and ice gouge occurrence parameters (refer to Weeks et al., 1985) and assumed that the constant current flow(s) existed for two months per year.

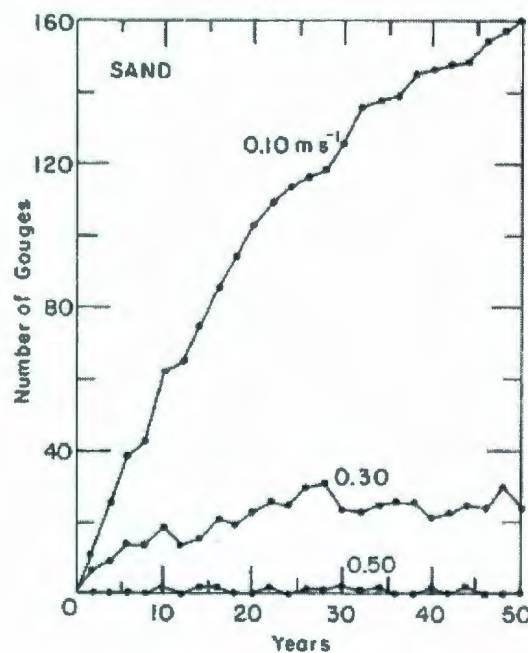


Figure 18: Simulated Ice Gouge Population as a Function of Time and Current Velocity:
Sand Seabed Sediment (Weeks et al., 1985)

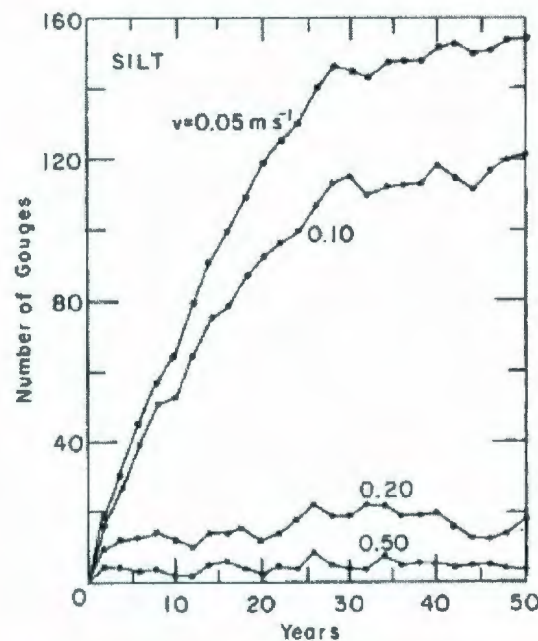


Figure 19: Simulated Ice Gouge Population as a Function of Time and Current Velocity:
Silt Seabed Sediment (Weeks et al., 1985; 1986)

Palmer (1998) suggested that a significant wave height (H_s) with a period of 5.3s could mobilize any seabed soil finer than coarse gravel (D_{20} mm) in 5m water depths. Offshore, in approximately 20m water depths, this wave could only mobilize soils finer than very fine gravel (D_{3} mm) (Palmer, 1998). Therefore, as water depths increase, the effects of wave-induced infilling are minimized and potentially become negligible.

Palmer and Niedoroda (2005) analyzed ice gouge infilling rates using a time-dependent coupled process-based hydrodynamic, sediment transport, and morphometric model. This model utilized a numerical solution to the Reynolds-Averaged Navier-Stokes equations with shallow water assumptions for hydrostatic pressure, the scalar transport equation, and the Exner equation for seabed evolution (Palmer & Niedoroda, 2005). Palmer and Niedoroda (2005) reported that the model represented turbulence generation and mixing,

and wave-current interactions, among other occurrences, and simulated seabed sediment erosion, transport, and deposition.

The Palmer and Niedoroda (2005) model analyzed an analogue seabed consisting of fine sand ($D_{50} = 12.5$ mm), with 1m wave heights with a period of 8s acting in conjunction with a 0.1 m/s constant current and superimposed 0.2 m/s oscillating tidal current. A simple, 'V' shaped ice gouge cross-sectional profile was assumed for analysis, however, the gouge shape has a major effect on (preferential) ice gouge infilling rates (discussed below) (Palmer & Niedoroda, 2005; Pilkington & Marcellus, 1981).

Based on these hydrodynamic conditions, Figure 20 presents the time-dependent evolution of Palmer and Niedoroda's (2005) analysis of an initially 2m deep and 12m wide 'V' shaped ice gouge profile as it infills due to wave and current action. It must be noted that inner ice gouge infilling rates (on the order of 33mm/day) should not be compared to the general seabed sedimentation rates discussed above (i.e., 0.03 cm/yr), as gouges may be subjected to greater infilling as a result of preferential infilling and increased hydrodynamic effects. Similar to other researchers, Palmer and Niedoroda (2005) also recognized decreasing ice gouge infilling rates with increasing water depths, as shown in Figure 21. Modeling of the 2m deep ice gouge was conducted using constant environmental conditions, with water depth being the only manipulated variable in the simulation program.

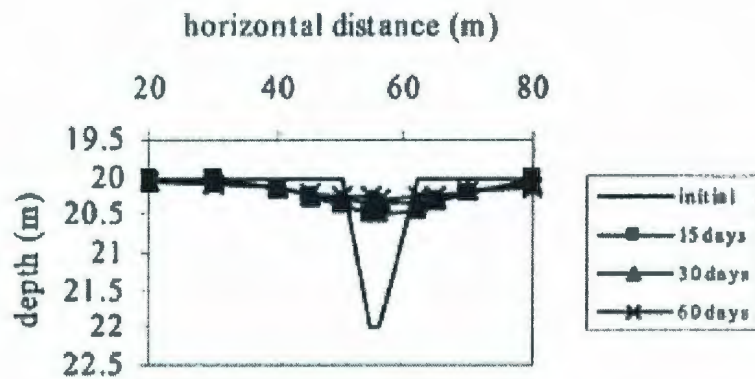


Figure 20: Time-Dependent Infilling of the Palmer & Niedoroda (2005) Ice Gouge

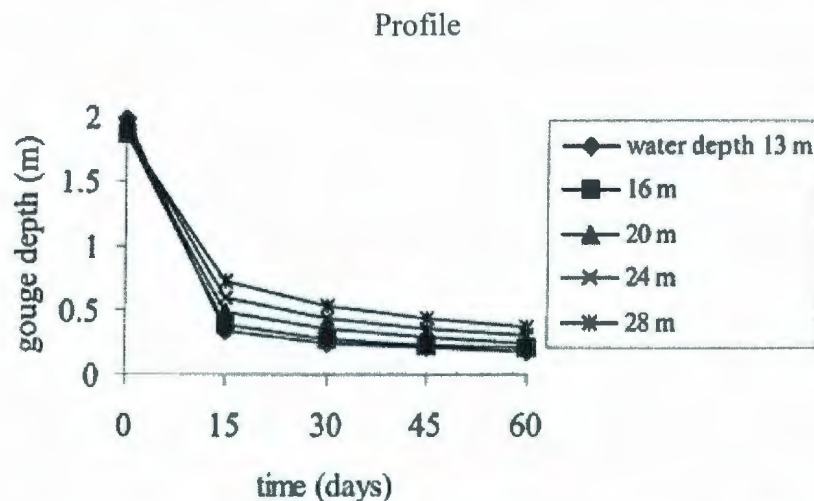


Figure 21: Infilling of a 2m Deep Ice Gouge as a Function of Water Depth (Palmer & Niedoroda, 2005)

The final environmental impact statement conducted for the *Liberty* pipeline project (MMS, 2002) located in Foggy Island Bay (of the American Beaufort Sea) included brief discussions and data presentation for applicable ice gouge infilling rates due to natural hydrodynamics and wind-induced waves. Observed ice gouge infilling rates ranged from 1 to 8 feet per year due to sedimentation resulting from suspended particles in the seawater, bottom currents, and/or waves redistributing sediments along the seafloor

(MMS, 2002). Yearly average ice gouge infilling rates measured in the Liberty pipeline vicinity are provided below in Table 9. Refer to MMS (2002) for listings of the references noted in the table.

Table 9: Liberty Pipeline Project Ice Gouge Infilling Rates due to Winds, Subsea Currents & Sedimentation (MMS, 2002)

Study	In-Filling Rate (ft/year) Yearly Average	Comments
Egg Island	4 - 7	Reimnitz and Kempema (1982, 1983)* Island sheltered from currents.
Sagavanirktok Delta	5 - 8	Reimnitz and Kempema (1982, 1983)* Exposed areas. From currents.
Depth of deposit immediately after an event	1.6	Reimnitz and Kempema (1982, 1983)* From suspended particle immediately after event. Initial in- filling will depend on the soil type, and could be nearly negligible for cohesive soil or flat-sided craters.
Endicott Strudel	0.3 - 1	Adjacent to the causeway; attributed to the settlement of suspended particles.
Duck Island/Sagavanirktok Delta	5	Harding Lawson (1981)* and McClelland (1982)*.
Liberty Pipeline Route	8.1 (maximum)	Coastal Frontiers Corporation (1999)*.
Off Resolution Island in the Sagavanirktok Delta	1.8	Coastal Frontiers Corporation (1999)*.
Northstar Test Trench	2 - 4	Coastal Frontiers Corporation (1999)*.
Liberty area (before 1997 survey)	0.2 - 0.7	Based on an analysis of winds ≥ 20 knots.

Source: *as cited in Blanchet et al. (2000)

Pilkington and Marcellus (1981) have investigated the process of preferential ice gouge infilling which results from physical environmental occurrences in various water depth ranges. Preferential infilling refers to preferential deposition of seabed sediments into ice gouge depressions based on in-situ seabed slopes, dominant wave and/or current patterns, and/or gouge orientation. Unlike uniform sedimentation, preferentially infilled gouges exhibit greater sedimentation against one berm or gouge sidewall compared to the other, and generally exhibit non-uniform sediment deposition thickness across the gouge profile (i.e., sediment deposition is concentrated in the gouge trough as opposed to being equally

distributed over the gouge sidewalls). In this manner, wide and deep ice gouges may be expected to exhibit the greatest rates of (non-uniform) gouge infilling (Weeks et al., 1985).

Preferential infilling may occur as the result of normal and tidal currents, wave-induced currents, ice keel-induced currents, or turbidity, which are all partially dependent upon the water depth in which they occur. Thus, ice gouge infilling may occur continuously in shallow water areas, whereas periodic infilling may be expected in deepwater locations during extreme environmental conditions (such as storms) (Pilkington & Marcellus, 1981).

The study conducted by Palmer and Niedoroda (2005) also modeled the effects of biased hydrodynamic effects, or preferential infilling, on a simulated 2m deep and 12m wide 'V' shaped ice gouge profile. The results of the model simulation are provided below in Figure 22 for a biased hydrodynamic current flowing from left to right across the figure. As shown in the figure, the deepest portion of the ice gouge (the *thalweg*) was found to move to the right, in the direction of the biased current, as the ice gouge filling process progressed (Palmer & Niedoroda, 2005). The infilling rate shown in the figure is the difference between the rate at which sediment is deposited into and carried away from the gouge trough, and decreases as the gouge deformation is progressively infilled and made smoother.

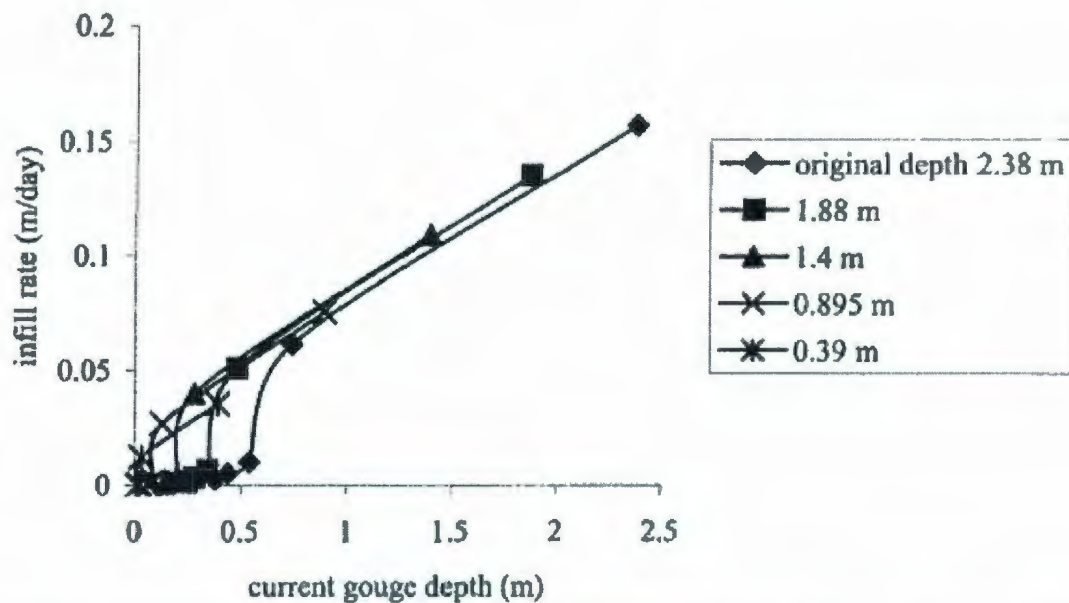


Figure 22: Relationship between Ice Gouge Infilling Rate and Gouge Depth for Biased Hydrodynamic Effects (Palmer & Niedoroda, 2005)

3.4.2 Influence of Local Seabed Soil Conditions

Pilkington and Marcellus (1981) studied immediate ice gouge infilling in the Canadian Beaufort Sea and found immediate infill rates to be dependent upon the characteristics of the seabed soil, as well as the probability of superimposition infilling caused by gouge recurrence. Seabed sediment roughness generally dictates the quantity of sediment available for transport and redistribution in specific areas and during specific time periods (Pilkington & Marcellus, 1981).

As discussed above in Section 3.4.1, Weeks et al. (1985) developed a simulator program to estimate the number of ice gouges that would be observed along a one-kilometre survey line as a function of residence time and relevant environmental parameters, including seabed sediment type. Figure 18 indicates the predicted number of ice gouges

observed per survey kilometre for sand seabed sediments ($D = 0.1$ mm), whereas Figure 19 indicates the predicted gouge population for silt ($D = 0.01$ mm). As discussed above, all other environmental input parameters were constant in the simulation program for each analyzed current velocity and seabed material. As shown in the figures, decreased ice gouge populations were predicted in silt seabed sediment when compared to sand (i.e., see the predicted number of gouges for a current of 0.10 m/s in each seabed sediment). This observation therefore suggests that greater ice gouge infilling rates occur in silt sediments than in sand, since the simulator assumed constant environmental and ice gouge occurrence parameters and considered infilling rates when predicting gouge formation.

The Weeks et al. (1985) simulator program also predicted annual ice gouge infilling rates as a function of water depth and seabed sediment grain size. As shown in Figure 23, the preliminary results of the Weeks et al. (1985) study found that medium sands with 0.4 mm mean grain size diameter ($D = 0.4$ mm) exhibited greater ice gouge infilling rates than did fine ($D = 0.16$ mm) and very fine ($D = 0.09$ mm) sands when subjected to the same set of representative Beaufort Sea shelf wave and current regimes. The simulator assumed representative Beaufort Sea wave and current conditions during the ice-free (summer) season and calculated infilling rates along the centerline of a sample 2m deep ice gouge (Weeks et al., 1985). Local seabed soil conditions were thus shown to strongly influence potential ice gouge infilling rates in the Beaufort Sea.

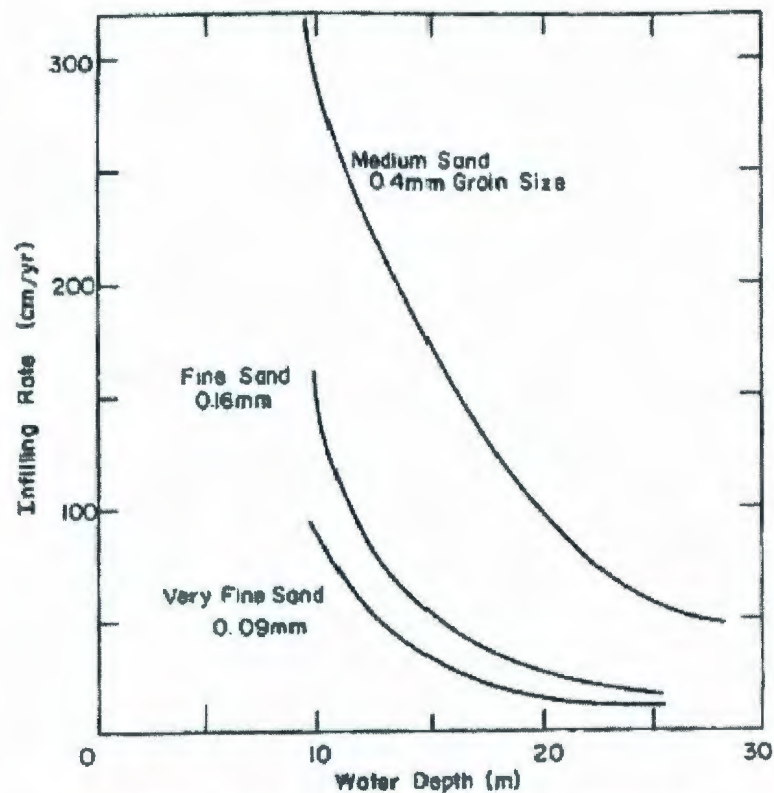


Figure 23: Ice Gouge Infilling Rates as Functions of Grain Size & Water Depth (Weeks et al., 1985)

3.4.3 Influence of Local Geography

Ice gouge infilling rates are significantly influenced by immediate infilling, gouge superimposition, and preferential infilling regimes (see Sections 3.4.1 and 3.4.2). Pilkington and Marcellus (1981) proposed that ice gouge infilling due to river sediment deposition presents minimal effects upon the overall infilling rate of Canadian Beaufort Sea ice gouges. However, Héquette et al. (1995) have hypothesized that Canadian Beaufort Sea ice gouge infilling is dominated by fine-grained sediment deposition in water depths greater than 10m due to suspended sediment transport by the Mackenzie River. In nearshore areas, Héquette et al. (1995) found ice gouges to be rapidly reworked

by wave and current action (see Section 3.4.1). Thus, the influence of local geography and proximity of the ice gouged seabed to areas of river discharge and/or overflow may be expected to be minimal when compared with other processes, such as reworking by wave and current action.

3.5 ICE GOUGE RECURRENCE RATE STUDIES

Knowledge of regional ice gouge recurrence rate information is oftentimes a necessary input parameter for probabilistic ice gouge analysis procedures and extrapolation to design events (see Section 3.1). Literature review and assessment was therefore conducted with respect to regional ice gouge recurrence rate studies for review and evaluation of historical design data, as provided below. Historical design recurrence rate data has been summarized in Section 3.5.4.

3.5.1 American Beaufort Sea

Weeks et al. (1981; 1983) analyzed ice gouge recurrence rate, or *temporal frequency*, data that was obtained along the inner shelf of the Alaskan Beaufort Sea between Smith Bay and Camden Bay, in water depths reaching 38m. This data was previously presented by Barnes et al. (1978) and Rearic et al. (1981). According to Weeks et al. (1983), American Beaufort Sea ice gouge recurrence rate data is rare, particularly in areas sheltered by barrier islands and in lagoons, and is limited to the data presented within Barnes et al. (1978) for the purposes of their study.

A plot of observed ice gouge recurrence rate values versus water depth is provided by Weeks et al. (1983), which exhibits a large data scatter and indicates no strong trend

pattern. Linear ice gouge densities (or *spatial frequencies*) were also studied by Weeks et al. (1983) by determining the number of gouges incised deeper than 0.2m below the seabed per linear kilometer of surveyed trackline. Ice gouge incisions less than 0.2m deep were neglected. Consequently, actual ice gouge densities were underestimated by neglecting the shallow gouge depth data. In keeping with USGS ice gouge analysis procedures (see Section 2.1), each individual gouge deformation on the seabed was counted as a single ice gouge, including those likely produced by (common) multiplet events. In addition, ice gouge density values were corrected by to account for the gouge orientation and direction of survey vessel travel so that the gouge density could be determined for a hypothetical survey route oriented perpendicular to the gouge trend (Weeks et al., 1983).

Weeks et al. (1981) reported that analysis of limited data produced an average recurrence rate of 5 gouges/km/year. Data analysis conducted in the Weeks et al. (1983) study indicated an average recurrence rate of 5.2 gouges/km/year with values for individual years varying from 2.4 (1975-76) to 3.5 (1976-77) to 7.9 (1977-78).

As presented above, Weeks et al. (1983) studied ice gouge recurrence rate data obtained during repetitive mapping programs conducted by Barnes et al. (1978). The Barnes et al. (1978) survey program indicated an average ice gouge recurrence rate of 50 gouges/km²/year for 1976, with minimum and maximum values of 20 and 80 gouges/km²/year, respectively. Surveyed water depths varied from 4m to 18m. Again, in 1977, Barnes et al. (1978) observed an average ice gouge recurrence rate of 50

gouges/km²/year, with minimum and maximum values of 25 and 75 gouges/km²/year, respectively. Surveyed water depths ranged from 1.5m to 20m during the 1977 program.

Based on this data, ice gouge recurrence rates may be calculated by simply dividing the observations of Barnes et al. (1978) by the observable width of the survey corridor. In example, if an analogue ice gouge survey swath width of 250m is utilized, then this corresponds to approximate ice gouge recurrence rates ranging from approximately 5 to 20 gouges/km/year, with an average of 12.5 gouges/km/year.

As presented by Weeks et al. (1983), Barnes et al. (1978) determined ice gouge densities by counting every observed linear ice gouge feature as a single ice gouge event and corrected the number of observed ice gouge features within the survey area for gouge orientation and the direction of survey. The echo sounder and side-scan sonar system used during repetitive ice gouge surveying allowed detection and resolution of gouge deformations and bottom relief to less than 0.1m. Ice gouge deformations which did not cross the survey trackline and were not recorded by the echo sounder were assigned an assumed gouge depth of 0.05m (Barnes et al., 1978). Similarly, gouge deformations which were crossed by the side-scan sonar trackline but indistinguishable on the echo sounder were assigned an assumed gouge depth of 0.1m (Barnes et al., 1978). Thus, the number of observed shallow ice gouges may be potentially overestimated due to these assumptions. Consequently, American Beaufort Sea ice gouge recurrence rates presented by Barnes et al. (1978) may also be overestimated.

Weber et al. (1989) also studied ice gouge recurrence and crossing rate data for 9 survey sites located on the inner shelf of the American Beaufort Sea. This data was originally presented by Barnes and Rearic (1985) but contains data from two additional 1985 surveys (corridors 4 and 9). Surveyed water depths ranged from 3.3m to 27.2m.

Weber et al. (1989) inferred undated ice gouge crossing rates (or linear densities) from the total number of gouges observed at known water depths per one-kilometer segments of survey corridor tracklines. Similarly, ice gouge recurrence rates were inferred from the number of gouges observed at known water depths during repetitive survey operations, per one-kilometer survey corridor trackline segments. Table 10 summarizes the ice gouge density and recurrence rate data presented in the Weber et al. (1989) study.

Table 10: Summary of USGS Open-file Report 89-151 Ice Gouge Density and
Recurrence Rate Data

Survey Corridor	Approximate Water Depth Range (m)	Average Ice Gouge Density (Gouges / km)	Average Ice Gouge Recurrence Rate (Gouges / km / year)
1	4.2 – 16.7	85.60	4.12
2	6.5 – 18.5	57.10	3.57
3	10.2 – 24.2	102.94	1.70
4	3.1 – 19.9	89.00	4.18
5	3.8 – 14.6	42.75	2.40
6	5.3 – 27.4	47.33	0.87
7	5.5 – 18.6	73.71	7.50
8	11.9 – 27.7	107.86	2.00
9	6 – 18.7	106.00	3.95

3.5.2 Canadian Beaufort Sea

Hunting Geology and Geophysics (1973) provided possible ice gouge depth range return periods for the Canadian Beaufort Sea, based on analysis of the APOA Projects 19 and 32 data. However, these estimates were formulated on the basis of highly arguable assumptions regarding ice gouge recurrence and infilling rates and were thus deemed too unreliable for use in this thesis.

Hnatiuk and Brown (1977) presented ice gouge recurrence rate densities for the Canadian Beaufort Sea which ranged from 0.6 to 1.2 new gouges/square mile/year, based on initial results from a limited amount of repetitive side-scan surveys. This is equivalent to approximately 0.23 to 0.46 gouges/km²/year. A preliminary recurrence rate estimate may be obtained by dividing this data by the survey trackline width. In example, if an ice gouge survey swath width of 250m is utilized, then this corresponds to approximate ice gouge recurrence rates ranging from 0.06 to 0.12 gouges/km/year.

In a later study, Hnatiuk and Wright (1983) presented recurrence rates ranging from approximately 1.1 to 2.7 gouges/km/year based on repetitive surveys conducted at the *Tingmiark* and *Pullen* sites in the Canadian Beaufort Sea. The greatest frequency of ice gouging was reported between 15 and 46m water depths for both the Hnatiuk and Brown (1977) and Hnatiuk and Wright (1983) studies. The Hnatiuk and Wright (1983) data included data previously analyzed by Hnatiuk and Brown (1977).

Lewis (1977a) presented areal ice gouge recurrence rates on the order of one new gouge per 3 km² of survey area per year for the southeastern Canadian Beaufort Sea, based on

analysis of side-scan sonar records obtained in 15 to 20m water depths during the early 1970s. It was subsequently estimated that $1.1 \pm 0.9\%$ of the Canadian Beaufort Sea shelf was annually disturbed by ice gouging and that the seabed would be completely reworked in 90 years (Lewis, 1977a). On a linear transect basis, Lewis (1977a) estimated these recurrence / reworking rates to be 0.19 ± 0.06 gouges/km/year (in the 15 to 20m water depth range). Slightly greater estimates were provided by Shearer (1979), who has reported ice gouge recurrence rates on the order of 1 ± 0.5 gouges/km/yr for 13 to 17m water depths in the southeastern Canadian Beaufort Sea. This analysis was conducted as part of APOA Project 151 for repetitive data collected offshore Pullen Island from 1971 to 1978.

Lewis (1977b) provided ice gouge impact (recurrence) rates as functions of burial depth below the seabed and water depth on the Canadian Beaufort Sea shelf. Impact rates calculated by Lewis (1977b) for 0m burial depth (i.e., the undisturbed seabed elevation) are summarized below in Table 11.

Table 11: Canadian Beaufort Sea Ice Gouge Impact Rates at Seabed Surface (Lewis, 1977b)

Water Depth (m)	Ice Gouge Impact (Recurrence) Rate (Gouges/nautical mile/year)	Ice Gouge Impact (Recurrence) Rate (Gouges/km/year)
15	0.31	0.17
21	0.25	0.13
27	0.082	0.044
33	0.044	0.024
39	0.044	0.024
45	0.013	0.007

Shearer et al. (1986) studied ice gouge recurrence rates obtained from analysis of repetitive ice gouge survey data. Their study recorded ice gouge recurrence rates as high as 4 gouges/km/year for water depths ranging from 20 to 25m in the western Canadian Beaufort Sea. Ice gouge recurrence rates were found to decrease towards eastern portions of Mackenzie Bay, with rates on the order of 1 gouge/km/year exhibited in 10 to 20m water depths. For the eastern Canadian Beaufort Sea, ice gouge recurrence rates of 0.2 to 0.4 gouges/km/year were found in approximately 30m water depths. In general, Shearer et al. (1986) observed ice gouge recurrence rates to decrease towards the east, with higher rates displayed in western Mackenzie Bay than in the eastern Beaufort Sea. Figure 24 presents Shearer et al.'s (1986) ice gouge recurrence rate data observations as a function of water depth. As shown in the figure, ice gouge recurrence rates were found to peak in the 20 to 25m water depth range and then decrease with increasing water depth. Shearer et al.'s (1986) ice gouge recurrence rate data and analysis was also recorded in a study paper by Shearer and Stirbys (1986). Shearer and Stirbys (1986) provided ice gouge recurrence rate data for two separate survey locations in the western Canadian Beaufort Sea (*Tarsiut/Nektoralik Corridor* and *Pullen*) and found gouge depth recurrence rates to decrease with increasing gouge depth, similar to other studies.

Comfort et al. (1990) presented summary data and analysis of the ESRF ECHOBASE Canadian Beaufort Sea ice gouge database, with observed ice gouge recurrence rate data provided in tables below. Table 12 presents recurrence rate data obtained via repetitive seabed mapping for specified water depth ranges in eastern Mackenzie Bay (western

Canadian Beaufort), whereas Table 13 presents recurrence rate data for eastern Canadian Beaufort Sea regions located northwest of the Tuktoyaktuk Peninsula.

Lewis and Blasco (1990) presented an analysis of ice gouge data obtained via repetitive geophysical mapping conducted on the inner shelf of the Canadian Beaufort Sea, although the source of the data was not provided. This study provided recommended ice gouge recurrence rates for the Canadian Beaufort Shelf as a function of water depth, as presented below in Figure 25.

In reporting 1990 updates to the NEWBASE data set, Myers et al. (1996) presented maximum ice gouge recurrence (impact) rates for a select few survey lines and bathymetric classes. Myers et al. (1996) found maximum ice gouge recurrence rates to range from 4.69 to 12.50 gouges/km/year in water depths ranging from 9 to 29m. The maximum recurrence rate was determined from analysis of a single ice gouge over a very short survey line segment length (0.08 km); therefore, it is suggested that this value be neglected in the current (thesis) analysis as it is deemed unrepresentative of the actual ice gouging regime. Similarly, the next highest ice gouge recurrence rate (7.14 gouges/km/year) was calculated for only 2 gouges observed along a 0.28 km survey line segment length; again, this value may be unrepresentative of the actual ice gouge recurrence as a result of the limited amount of analyzed data. Myers et al. (1996) also investigated 'extreme' ice gouge recurrence rates, which corresponded to analysis of gouges exhibiting depths of 2m or greater and exclusion of all shallower gouges. Calculated recurrence rates for 'extreme' ice gouge depth events were significantly lower

than maximum values calculated for the entire NEWBASE data set. 'Extreme' ice gouges represented only 2.3% of the total NEWBASE data set.

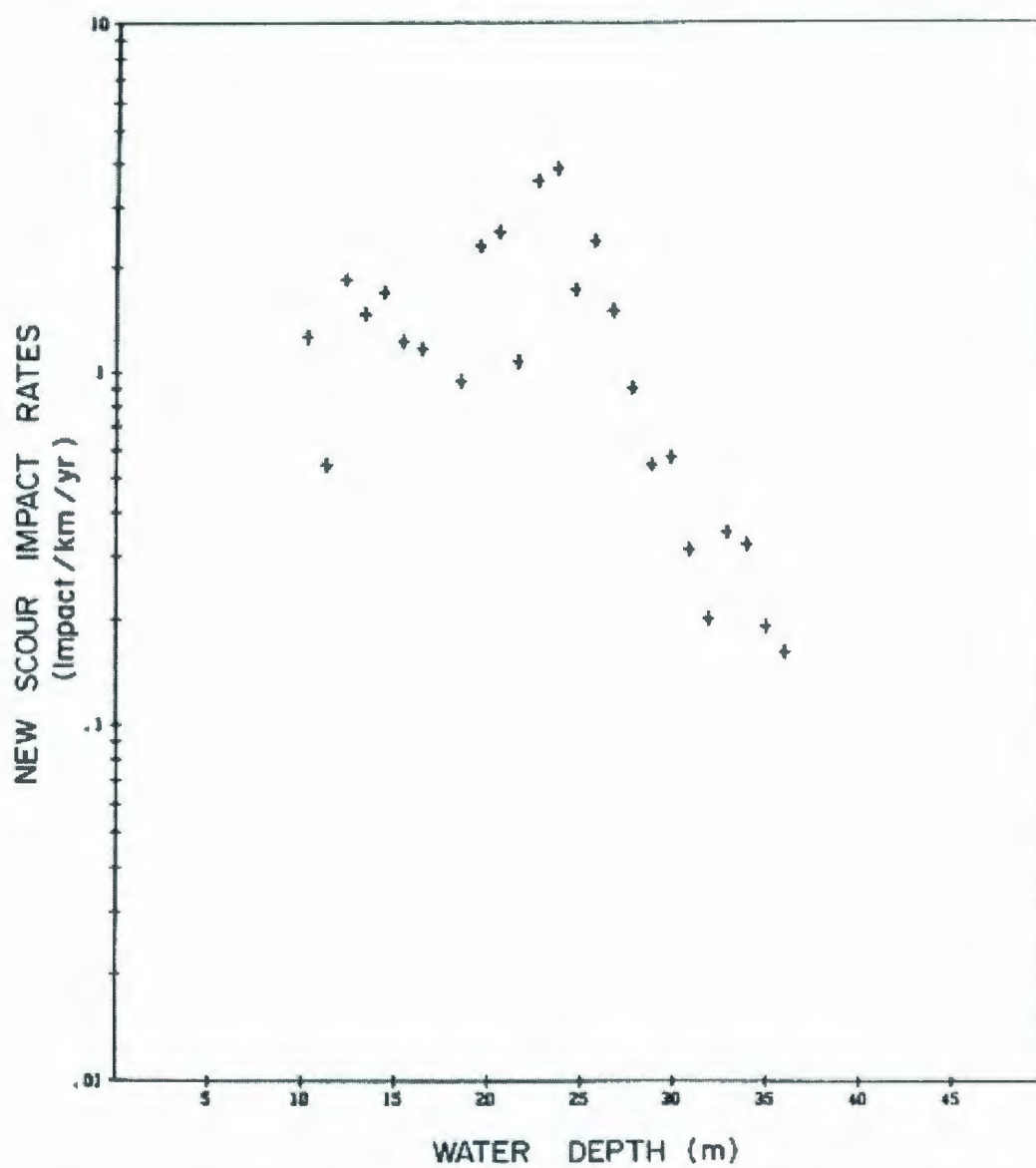


Figure 24: Canadian Beaufort Sea Ice Gouge Recurrence Rate Data from ESRF Report

No. 032 (Shearer et al., 1986)

Table 12: Ice Gouge Recurrence Rates for Eastern Mackenzie Bay, Canadian Beaufort Sea (Comfort et al., 1990)

Water Depth Range (m)	Predicted Ice Gouge Recurrence Rate (Gouges/km/year)
0 – 10	0.76
10 – 20	2.7 – 3.25
20 – 30	0.75 – 6.5
30 – 40	0 – 0.93
40 – 50	0

Table 13: Ice Gouge Recurrence Rates for Offshore Tuktoyaktuk Peninsula, Canadian Beaufort Sea (Comfort et al., 1990)

Water Depth Range (m)	Predicted Ice Gouge Recurrence Rate (Gouges/km/year)
0 – 10	0.76
10 – 20	1.92 – 2.0
20 – 30	0.7 – 6.5
30 – 40	0 – 0.93
40 – 50	0

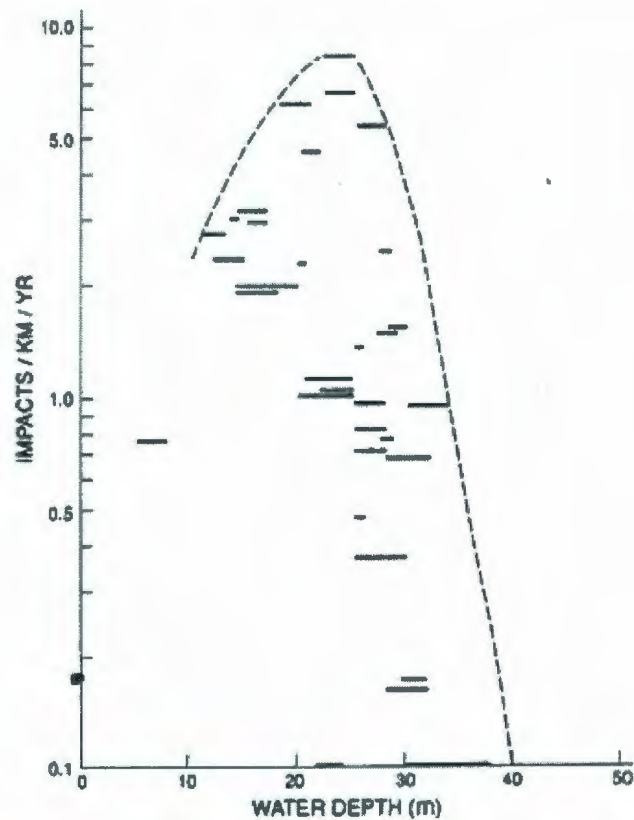


Figure 25: Recommended Ice Gouge Recurrence Rates for the Canadian Beaufort Shelf
(Lewis & Blasco, 1990)

Blasco et al. (1998) have provided Canadian Beaufort Sea ice gouge recurrence rate data for regions located offshore of the Tuktoyaktuk Peninsula. The analyzed data was obtained from Myers et al.'s (1996) updates to the NEWBASE ice gouge database. Blasco et al. (1998) observed a maximum recurrence rate in 20m water depth and found that recurrence rates decreased drastically in deeper water depths, with variation in recurrence rate data reported to be potentially attributable to the combination of single-keeled and multi-keeled ice gouge events during analyses. Yearly variations in the Canadian Beaufort Sea landfast ice extent may also be a factor. Blasco et al. (1998) have

predicted the amount of disturbed (or reworked) seabed per 100 years, based on ice gouge recurrence rate and gouged seabed density data (see Table 14). As indicated in the table, Blasco et al. (1998) have shown the 8 to 25m water depth range in the Canadian Beaufort Sea to be almost completely reworked in 100 years, with disturbance rates decreasing with increasing water depth. New ice gouges resulting from both first-year and multiyear ice keels were included in the analysis.

CSR (2008) provided 2005 updates and analysis of the NEWBASE Canadian Beaufort Sea new ice gouge database. CSR's (2008) study included analysis of ice gouge recurrence rate information using the exponential distribution, as provided in Figure 26. This figure was derived using weighted average ice gouge survey segment lengths and ages; see the CSR (2008) summary report for description of the analysis procedure and data utilized to generate Figure 26. CSR (2008) observed maximum ice gouge recurrence rates to range from 5.048 to 30.66 gouges/km/year based on analysis of the 2001, 2003, and 2004 NEWBASE survey data baselines located in 7 to 23m water depths. On a regional basis, ice gouge recurrence rates were related to water depths, with recurrence rates decreasing exponentially with increasing water depth.

Table 14: 100-year Seabed Disturbance (Blasco et al., 1998)

Water Depth Range (m)	Amount of Seabed Disturbed in 100 Years (%)
8 – 25	99
30	70
32.5	40
35	22
40	5
45	1

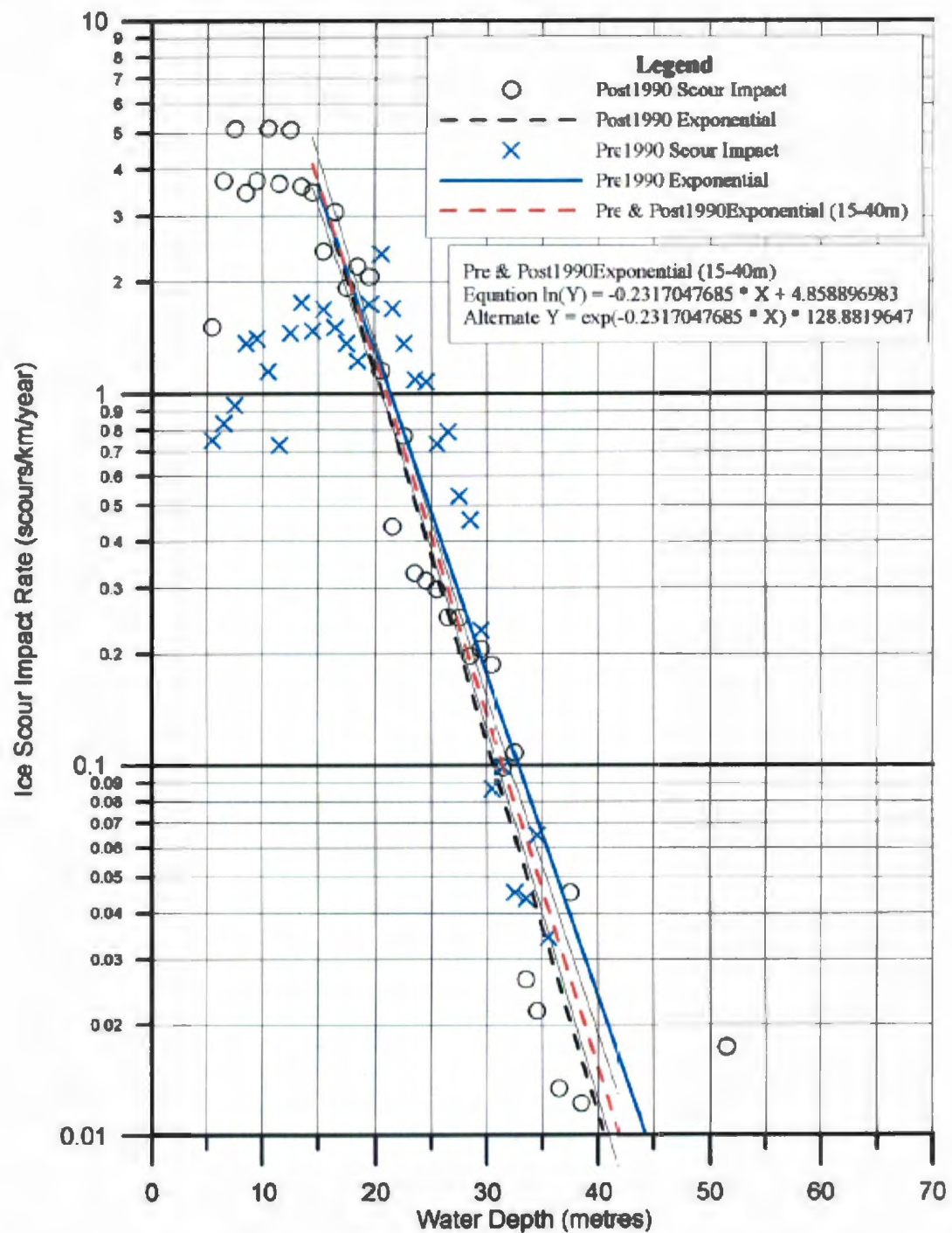


Figure 26: Exponentially Distributed Weighted Ice Gouge Recurrence Rates for the Canadian Beaufort Sea, Analysis of 2005 Updated NEWBASE Database (CSR, 2008)

3.5.3 Chukchi Sea

No ice gouge recurrence rate data has been found applicable to the Chukchi Sea. As discussed by MMS (2007), quantitative ice gouge data is rare to nonexistent for nearshore regions of the Chukchi Sea. No record has been found of repetitive ice gouge surveying programs conducted in the Chukchi Sea, which has thus lead to the paucity of applicable ice gouge recurrence rate information. However, a limited amount of general, linear ice gouge density data has been provided by numerous researchers (Toimil, 1978; Phillips et al., 1988; Wilson et al., 1982; Phillips & Reiss, 1984). Grantz et al. (1982a) reported that, although ice gouge recurrence rates are unknown for the Chukchi Sea, it is estimated that 1 to 2% of the seafloor is gouged annually. These estimated seafloor disturbance rates are similar to estimates for the Alaskan Beaufort Sea (Grantz et al., 1982). It is therefore suggested that American Beaufort Sea ice gouge recurrence rates may also be utilized in Chukchi Sea ice gouge analyses in light of the current paucity of regional or site-specific data.

3.5.4 Historical Data

Where possible, historical ice gouge recurrence rate data has been summarized in the following tables per applicable region and water depth range. The data has been obtained from previous ice gouge recurrence rate studies which were analyzed in the preceding thesis discussions, provided above. Available American Beaufort Sea ice gouge recurrence rate data is summarized in Table 15. Similarly, Table 16 summarizes the

Canadian Beaufort Sea ice gouge recurrence rate data found during the current thesis work.

Recent Canadian Beaufort Sea ice gouge recurrence rate investigations have shown an approximate 40% reduction in observed recurrence rates, based on comparison of 1976 to 1990 and 1990 to 2003 ice gouge data (Blasco, 2005). However, this trend is not explicit within available recurrence rate data summarized in Table 16, but should be considered in design ice gouge recurrence rate evaluations.

Table 15: American Beaufort Sea Ice Gouge Recurrence Rate Summary Data

Data Source	Water Depth Range (m)	Recurrence Rate (gouges / km / year)
Weeks et al. (1981)	N/A	Avg: 5
Weeks et al. (1983) ^a	0 – 10	~4
	10 – 20	5.6
	>20	1.4
USGS 78-730 (Barnes et al., 1978)	0 – 20	Min: 5; Max: 20; Avg: 12.5
USGS 89-151 (Weber et al., 1989) ^b	0 – 20	3.4
	>20	1.5

^a Obtained by averaging ice gouge recurrence rate data points presented in Table 5 of Weeks et al. (1983) for the appropriate water depth range.

^b Obtained by averaging ice gouge recurrence rate data presented in Table 10. Recurrence rate data points which bridged two water depth ranges were utilized in the averaging calculation for each range.

Table 16: Canadian Beaufort Sea Ice Gouge Recurrence Rate Summary Data

Data Source	Water Depth Range (m)	Recurrence Rate (gouges / km / year)
Hnatiuk & Brown (1977)	15 – 46	~0.06 – 0.12
Hnatiuk & Wright (1983)	15 – 46	1.1 – 2.7
Lewis (1977a)	15 – 20	0.13 – 0.25
Lewis (1977b)	15	0.17
	21	0.13
	27	0.044
	33	0.024
	39	0.024
	45	0.007
Shearer (1979)	13 – 17	0.5 – 1.5
Shearer et al. (1986) ^a	10 – 20	~1.4
	20 – 30	~2.3
	30 – 40	~0.3
Shearer & Stirbys (1986) (Analyzed data from Shearer et al., 1986)	10 – 20	1
	20 – 25	4
	~30	0.2 – 0.4
Comfort et al. (1990)	0 – 10	0.76
	10 – 20	1.92 – 3.25
	20 – 30	0.7 – 6.5
	30 – 40	0 – 0.93
	40 – 50	0
Lewis & Blasco (1990)	10	2.4
	20	7
	30	4
	40	0.1
Myers et al. (1996)	~10 – 20	~4.69 – 5.18
	~20 – 30	~4.74 – 7.14
Blasco et al. (1998)	<10	1.5
	20	1.2 – 4.5
	25	1.0
	30	0.24
	35	0.048
	40	0.01
	45	0.002
CSR (2008) ^b	15	~3.75
	20	~1.5
	25	0.4
	30	~0.15
	35	0.05
	45	~0.015

^a Obtained by averaging ice gouge recurrence rate data points presented in Figure 24 for the appropriate water depth range.

^b Obtained from Figure 26.

3.5.5 Alternate Methods

In the absence of reliable repetitive seabed surveying data, ice gouge recurrence rate estimates may be determined through application of alternate prediction mechanisms, including analysis of ice feature drift rates, knowledge of design ice feature keel draft to sail height ratios, and/or upward looking sonar (ULS) technology, as discussed below. Therefore, extrapolation to design ice gouge depths may be conducted for first-year ice gouge data sets, although analysis of multiple years of historical data derived from repetitive geophysical surveying procedures is preferred.

3.5.5.1 Ice Feature Drift Rates

In circumstances where repetitive ice gouge surveying data is limited or unavailable, ice gouge frequencies may be estimated through analysis of ice keel and bathymetric data. Ice feature drift rate data may be used as an input to numerical approximation methods to estimate gouge recurrence rates, although it is postulated that these procedures are likely less reliable than physical observations obtained via repetitive surveying techniques. As discussed below, McKenna et al. (2003) and King et al. (2003) have developed numerical models to predict annual ice gouge frequencies and iceberg grounding rates, respectively, on the basis of ice keel frequencies, drift rates, and bathymetry. Although these procedures represent good alternatives to repetitive seabed surveying techniques, Sonnichsen et al. (2005) have indicated that such models involve simplifications and assumptions which nonetheless require validation with reliable ice gouge recurrence rate data obtained via repetitive mapping.

McKenna et al. (2003) have presented a method to predict the annual frequency of ice gouging per unit area for a defined pipeline segment length through analysis of known ice feature drift velocities and ice keel incursion statistics. Following McKenna et al.'s (2003) procedure, the annual ice gouge frequency per unit area (n_g) is estimated as follows (units not specified):

$$n_g = q_b * n_k^* * \Delta F^*(z_1, z_2) * v^* * \frac{s}{(z_2 - z_1)} \quad (3.16)$$

where

q_b = unit-less bathymetric shielding factor;

n_k^* = average number of ice keels per unit area, based on ice keel observation statistics;

$\Delta F^*(z_1, z_2)$ = increment of ice keel draft cumulative distribution over the water depth range z_1 to z_2 ;

v^* = net upslope (incursion) ice drift velocity (the velocity of ice moving upslope towards decreasing bathymetry); and,

s = average seabed slope.

According to McKenna et al. (2003), the bathymetric shielding factor is a scaling factor which accounts for seabed areas that cannot be subjected to ice keel gouging due to the shape of the surrounding seabed, barrier islands, etc, which thus limits the possible amount of ice keel/seabed interaction. The upslope drift velocities may be estimated via

numerous methods, which include acoustic Doppler current profilers, marine radar tracking, drift beacons, and/or potentially estimated on the basis of known wave and current data.

Predicted ice gouge crossing frequencies (n) across a specified pipeline segment length (gouges/year) may be subsequently determined as follows (McKenna et al., 2003):

$$n = n_g * X * L^* \quad (3.17)$$

where

n_g = predicted annual ice gouge frequency per unit area;

X = pipeline segment length; and,

L^* = mean effective ice gouge length measured perpendicular to the pipeline segment for analysis.

The mean effective ice gouge length may be estimated from ice gouge length and dominant orientation data or ice gouge process models (McKenna et al., 2003). Therefore, as may be concluded from the preceding calculation procedure, the predicted ice gouge crossing frequency (n) is analogous to the ice gouge recurrence rate (g), as discussed in Sections 3.1 and 4.1.1, among others.

King et al. (2003) have presented an alternate method to predict approximate *iceberg* keel grounding frequencies based on mean iceberg keel drift velocities, as follows:

$$f_g = \rho_k * U * W * \cos(\theta) \quad (3.18)$$

where

f_g = iceberg keel grounding frequency;

ρ_k = areal (spatial) density of iceberg keels with sufficient draft to impact the seabed in a specific area (iceberg keels/km²/yr);

U = mean iceberg keel drift velocity towards a section of the seabed to be analyzed (m/s);

W = width of the seabed section subjected to iceberg keel grounding (m); and,

θ = orientation between the upslope seabed and dominant iceberg keel drift direction (°).

The King et al. (2003) method then utilizes a reduction factor (r_d) to account for the proportion of icebergs exhibiting keel drafts in the appropriate water depth range being analyzed, as follows:

$$f_g = n_o * r_d * U * W * \cos(\theta) \quad (3.19)$$

where

n_o = areal density of all icebergs (sails) observed on the water surface (icebergs/km²/yr);

and,

r_d = proportion of total icebergs with sufficient draft to impact the seabed in a specific water depth range (1/m).

Further development of this estimation procedure resulted in considerations for the proportion of time that an iceberg drifts in a particular direction, as well as the seabed slope and the proportion of an iceberg keel that may impact the seabed. The iceberg keel grounding frequency (ρ_g) was then expressed as a grounding rate per unit area (groundings/km²/yr), as follows (King et al., 2003):

$$\rho_g = n_o * r_d * \left(\frac{W}{A}\right) \int_{-\pi/2}^{\pi/2} r_\theta(\theta) * U * \cos(\theta) d\theta \quad (3.20)$$

where

A = seabed unit area (W²); and,

r_θ = proportion of time that an iceberg drifts in a particular (specified) direction; and all other terms are as defined previously.

The seabed slope (S) may be defined as $1/W$, or W/A . In the absence of directional ice drift velocity data, ρ_g may be calculated using a non-directional form of the preceding equation which assumes a uniform distribution of the drift direction, which, integrated over the specified limits and using $r_\theta = 1/2\pi$ reduces to (King et al., 2003):

$$\rho_g = n_o * r_d * S * U / \pi \quad (3.21)$$

Thus, as shown through the preceding method, ice keel grounding (or gouging) frequencies may be approximated using areal density data. Therefore, iceberg and/or ice feature sighting data may be utilized to estimate ice gouge *occurrence* rates for a given

observation year, which may preclude the requirement for ice gouge *recurrence* rate data for a specified area. That is, the recurrence rate aims to predict the rate of ice gouge occurrences in the seabed for any given year based on repetitive mapping and historical data, whereas the King et al. (2003) estimation procedure aims to calculate the number of ice gouges occurring in a given year, based on observations made during that same year.

3.5.5.2 Keel Draft to Sail Height Ratios

Kovacs and Mellor (1974) indicated that first-year pressure ridge ice keel draft to sail height (K/S) ratios range from 3 to 9 in the American Beaufort Sea, with an average value of 4.5 for most observations. Knowledge of average Beaufort Sea K/S ratios is useful in that sail elevations may be readily determined using conventional surveying techniques and the measured height then utilized to calculate predicted ice keel depths corresponding to the sail observations (using design K/S ratio values).

A study by Kovacs (1983) presented the results of geometric and structural analysis of 11 multiyear pressure ridges observed during 1982 between Reindeer Island and Harrison Bay of the American Beaufort Sea. Ridge keel measurements were obtained via sonar and directly through drill holes in the ice for analysis of ridge cross-sections. Ridge sail elevations were measured using conventional surveying techniques. The Kovacs (1983) study observed an overall average K/S ratio of 3.22 for multiyear pressure ridge sea ice.

Kovacs et al. (1973) and Wright et al. (1981) reported similar average K/S ratios for multiyear pressure ridges observed in the Canadian Beaufort Sea. Keel depth to sail height ratios as high as 4.5 have been reported for the general Arctic Basin by Kovacs

(1972). Kovacs and Holladay (1989) updated the K/S relationships originally presented by Kovacs (1983), as presented below in Figure 27 for a combined data set of 56 American Beaufort, Canadian Beaufort, and American Chukchi Sea pressure ridge profiles. As indicated in the figure, the average K/S ratio calculated from the 56 pressure ridge profiles was found to be 3.23. As shown in the figure, there is little difference exhibited by K/S data obtained in each of the three regions.

Kovacs and Gow (1976) studied two grounded floebergs in April 1975 which were located approximately 12km north of Long Island, west of Prudhoe Bay in the American Beaufort Sea. Analysis of the first floeberg's (floeberg A) cross-sectional profile yielded a K/S ratio of 3.38, which accounted for 1.85m of uplift associated with grounding (Kovacs & Gow, 1976). This K/S ratio is therefore in agreement with the results of other analysis programs, as presented in preceding discussions. Analysis of the second floeberg (annotated 'floeberg B') indicated a maximum sail elevation of 6.65m and an associated keel grounded in approximately 12.5m water depth, which corresponded to an approximate K/S ratio of 1.88. Evidence of seabed ice gouging was also observed immediately behind floeberg B (Kovacs & Gow, 1976).

A study by Kovacs et al. (1987) utilized an airborne electromagnetic sounding system to profile ice geometry in the Prudhoe Bay area of the American Beaufort Sea. Analysis of a second-year pressure ridge was conducted using this system and cross-sectional profiles determined for three separate survey lines. The ridge profiles indicated K/S ratios of 2.7, 3.3 and 3.3 for each of the three surveys, with an average observed K/S ratio of 3.2.

In general, Kovacs and Mellor (1974) presented an average K/S ratio of 3.0 for multiyear pressure ridge ice observed in the southern Beaufort Sea. Refer to studies by Robe (1975) for discussion of observed K/S ratios for various iceberg formations.

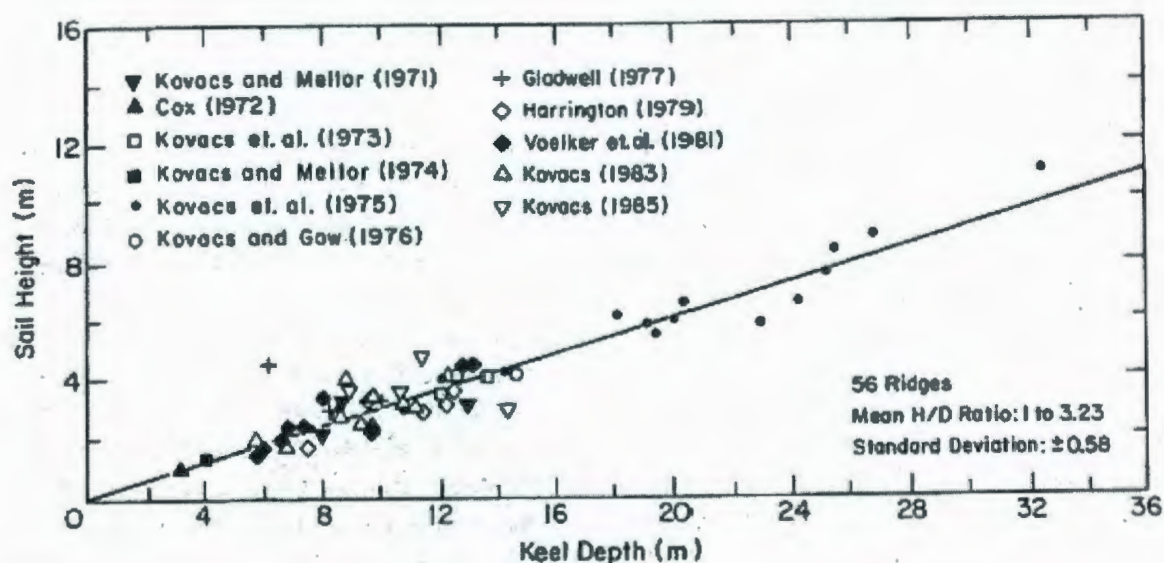


Figure 27: Multiyear Pressure Ridge K/S Relationship, Revised from Kovacs (1983)

(Kovacs & Holladay, 1989)

As discussed by Lewis (1977b) (see Section 3.1), ice keel draft statistics may be utilized to predict the total number of ice feature keels passing overtop of a pipeline with drafts greater than some threshold value. Pilkington and Marcellus (1981) indicated that ice keel draft statistics may be analyzed using an exponential distribution to predict the total number of keels passing over the seafloor area per year. The analysis procedure estimates design ice gouge depths through correlation of measured ice keel draft and seabed gouge depth distributions. Exponentially distributed ice gouge depth statistics are then utilized to calculate the probability of an ice gouge of depth d occurring at a water depth of D (i.e., $P(d)$), which is consequently the recurrence rate (gouges/km/year) of ice gouges of a

specified depth d . Refer to discussions of the Pilkington and Marcellus (1981) study (see Section 3.1) for further details on this method.

As shown through the preceding discussion, knowledge of design ice feature K/S ratios may be utilized to predict ice gouge recurrence rates based on sail height measurements obtained in areas lacking repetitively mapped ice gouge survey data.

3.5.5.3 Upward Looking Sonar

Wadhams (1983) has reported that upward looking sonar (ULS) is the best method of obtaining ice keel draft data for design depth prediction at a given location. Upward looking ice-profiling sonar (IPS) may be deployed and anchored subsea to monitor passing ice keel drafts and ice movement velocities as keel features pass overtop of the IPS system. In general, IPS systems are utilized to measure ice keel draft data, while acoustic Doppler current profilers obtain ice and current velocity measurements. An example IPS system emits an acoustic pulse in a narrow beam which is reflected off the underside of a passing ice feature, and corrects measurements for water level changes due to tides and surface winds (Birch et al., n.d.). Upward looking sonar systems have been operated offshore Sakhalin Island, Russia, by ASL Environmental Sciences Ltd to collect ice keel depth and ice velocity measurements over a two-year program (1996 to 1998) as part of a joint industry project for Sakhalin Energy Investment Company Ltd and Exxon Neftegas Ltd (Birch et al., n.d.).

The defining criteria for ice keel features influences the count and draft distribution of IPS keel measurements, as well as any subjective keel draft threshold and the

measurement reference datum. Ice keel definition criteria include independent events, Rayleigh criterion, minimum lengths exhibited between keel troughs, and/or fixed keel slope parameters, among others (Brooks, 1983). Refer to Birch et al. (n.d.) for further details on upward looking sonar and IPS system operational parameters.

Brooks (1983) and Wadhams (1983) have found that first order negative exponential distributions provide a good fit to ice keel draft data for statistical analysis and extrapolation to design events. Ice keel draft data observed via ULS may be utilized to determine recurrence rates for ice features with sufficient draft to contact the seabed over a specified time and/or spatial series. In this manner, ice gouge recurrence rates may be approximated on the basis of applicable keel recurrence rates in specific bathymetric settings. After Wadhams (1983), ULS ice keel draft statistics may be utilized to predict the number of ice keels passing a particular point with draft D (m) per year, as follows:

$$N_D = L * \mu * \exp \left[- \frac{(D - h_o)}{(h_{avg} - h_o)} \right] \quad (3.22)$$

where

D = water depth (m);

L = distance of annual ice cover drift (km);

h_o = ice keel low value limit (m);

h_{avg} = observed mean ice keel draft experimentally observed via ULS (m); and,

μ = mean number of ice keels observed per km of annual ice cover drift.

The annual ice gouge recurrence rate can then be estimated for a one-kilometre line oriented perpendicular to the mean direction of ice drift, as follows (Wadhams, 1983):

$$S_D = N_D * f \quad (3.23)$$

where

S_D = predicted ice gouge recurrence rate (gouge/km/year);

N_D = predicted number of ice keels passing a particular point with draft 'D'; and,

$$f = \frac{\pi}{(2 * l)} \quad (3.24)$$

where

l = mean ice keel length for a continuous keel with draft greater than 'D' (km).

Therefore, repetitive upward looking sonar ice profiling programs may be utilized to predict keel shapes, drafts, and recurrence distributions of analogue ice feature keels for use in engineering design applications. Refer to Wadhams (1983) for detailed description of additional ice keel draft analysis procedures, as well as applications to ice gouge depth prediction following methods presented by Pilkington and Marcellus (1981) and discussed in Section 3.1.

4 EXAMINATION & INTERPRETATION OF PHYSICAL ICE GOUGE DATA COLLECTIONS

4.1 STATISTICAL METHODS & APPLICATION TO ICE GOUGE DEPTH ANALYSIS

The following thesis sub-sections provide discussion of the exponential, gamma, and Weibull probability density functions (PDFs) and their application to ice gouge depth statistical analysis. Probability density functions ($f(x)$) are provided below for each of the analyzed data distributions. These distributions were selected for comparison of data fits provided by two-parameter (gamma, Weibull) versus single-parameter (exponential) distributions, as two-parameter distributions generally provide better fits to distribution tails (i.e., extreme ice gouge events). As discussed below, three-parameter versions of the gamma and Weibull distributions were used in this study to account for data thresholds. Similarly, the two-parameter version of the exponential distribution was utilized.

As part of the current project, statistical data analysis tools available in Minitab statistical software have been utilized. Probabilistic analysis of available ice gouge depth data has been conducted, as discussed in Section 5.2.

4.1.1 Exponential Distribution

The following parameters have been found by multiple researchers to be effective for calculating extreme ice gouge depths in nearshore areas of the Beaufort and Chukchi Seas (Wahlgren, 1979; Weeks et al., 1983; 1985; 1986; Lewis, 1977b; Barrie & Woodworth-Lynas, 1984):

λ = slope of the negative exponential gouge depth distribution curve (1/meter);

c = minimum cut-off gouge depth for measuring and recording small gouges from the survey data (meters); and,

g = annual ice gouge recurrence rate (new gouges / kilometer / year).

A number of researchers have used the single-parameter exponential probability density function to define the probability distribution of ice gouge depth based on physical survey data conducted in the Canadian and US Beaufort Sea (Weeks et al., 1983; 1985; 1986; Wheeler & Wang, 1985; Devore, 2004):

$$f(x) = \lambda e^{-\lambda x} \quad (4.1)$$

where

x = random variable in the data (gouge depth) distribution (m); and,

λ = exponential distribution rate parameter calculated as the inverse of the scale parameter, which in this case is the gouge depth distribution arithmetic mean (μ) (1/meter):

$$\lambda = \frac{1}{\mu} \quad (4.2)$$

The exponential distribution may be used to describe the average time between events, which occur continuously and independently, such as a Poisson process. Figure 28 illustrates the single-parameter exponential form and the influence of λ .

The exponential probability density function for ice gouge depth analysis can be transformed to account for the minimum gouge depth cut-off (c) and be rewritten as (Wang, 1990a; 1990b):

$$f(x) = \lambda e^{-\lambda(x-c)}; \quad x > c \quad (4.3)$$

The use of a minimum cut-off depth (parameter c) corrects the slope of the distribution curve for underestimation of shallow ice gouge depths, beneath the survey system's minimum resolution (Lever, 2000).

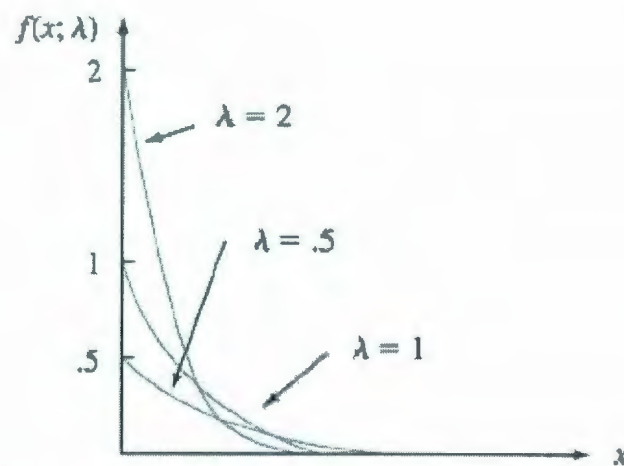


Figure 28: Sample Exponential Distribution Shape (Devore, 2004)

In general, the exponential distribution function has been found to provide a good fit to observed ice gouge depth data (Weeks et al., 1983; Lanan et al., 1986; Lever, 2000) and

often forms an effective basis for preliminary extreme ice gouge depth predictions. It has been found to represent shallow and moderate ice gouge depth data well, and has also been shown to characterize the depth distribution for ice keels as recorded by upward looking sonar on submarines (Weeks et al., 1983; Palmer et al., 2005). An attraction of the exponential distribution is that it may be characterized by the mean ice gouge depth (Palmer et al., 2005). However, extrapolation to design ice gouge events using the exponential distribution exhibits sensitivity to mean gouge depth data and tends to over-predict the number of deep gouges compared to historical survey observations (Wheeler & Wang, 1985; Lever, 2000; Liferov et al., 2007). The exponential distribution may therefore introduce unnecessary design conservatism when predicting design ice gouge depths, and has been found to be more conservative than gamma (Section 4.1.2) or Weibull (Section 4.1.3) extreme value distributions (Wheeler & Wang, 1985).

Nessim and Hong (1992) studied ice gouge depth data presented in the 1990 updated NEWBASE Canadian Beaufort Sea database and found the exponential distribution to fit low range (shallow gouge depth) data well, but provide a poor fit to the upper tail. Similarly, Palmer et al. (2005) have indicated a recurrent difficulty of extreme gouge depths being poorly modeled with the exponential distribution. Therefore, the exponential distribution may not be the best probabilistic distribution for accurate analysis of extreme ice gouge depths as recorded in the upper gouge depth distribution tail, although it has been successfully used in studies by other researchers (Lever, 2000).

This thesis has investigated the two-parameter exponential distribution in order to account for thresholds in the ice gouge depth data compiled for analysis (see Section 4.3).

The two-parameter exponential probability density function is defined as (Minitab, 2007):

$$f(x) = \left(\frac{1}{\beta} \right) e^{-(x-\theta)/\beta}; \quad x > \theta, \beta > 0 \quad (4.4)$$

where

θ = threshold parameter; and,

β = scale parameter = $1/\lambda$.

The scale and threshold parameters were estimated using the maximum likelihood method in Minitab. The threshold parameter shifts the probability distribution function away from zero (similar to a location parameter). The scale factor determines the statistical dispersion of the probability distribution; that is, it stretches or compresses the distribution along its measurement scale (Devore, 2004).

4.1.2 Gamma Distribution

The two-parameter gamma distribution represents a continuous random variable (x) in situations where the data is skewed and thus asymmetric across its range (Devore, 2004). Therefore, the gamma distribution may prove to be a suitable statistical function for analysis of ice gouge depth data which may be skewed towards deeper gouge depths in deeper water, or greater frequencies of occurrence dominantly exhibited in offshore locations.

The gamma distribution has been found to fit Canadian Beaufort Sea ice gouge depth data better than the exponential function, which tends to over-predict the number of deep ice gouges (Lever, 2000). Nessim & Hong (1992) observed the gamma distribution to provide a good fit to the 1990 updated NEWBASE ice gouge depth data, and exhibit an almost indistinguishable fit from the Weibull distribution form.

Analysis of chi-square test statistics calculated by Wheeler and Wang (1985) for an analogue American Beaufort Sea ice gouge data set indicated that the gamma distribution provided an unacceptable fit to the entire data set, but provided a good fit to ice gouge depth statistics obtained in shallow water depths ranging from 5 to 10m. However, this analysis was conducted using the midpoints of 0.2m ice gouge depth class range data obtained from Weeks et al. (1983), which was then 'shifted to the left' by 0.2m. This data shift was not explained further. The results of Wheeler and Wang's (1985) analysis are postulated (by the present author) to potentially be a result of the analyzed data set, rather than due to a poor fit provided by the gamma distribution. In addition, the chi-square test was utilized for analysis of the binned data, but this goodness-of-fit test can be negatively influenced by data bin class ranges, as discussed in Section 4.2.3 below.

The gamma distribution probability density function is defined as follows (Wheeler & Wang, 1985; Devore, 2004):

$$f(x) = \frac{1}{\beta^\alpha \Gamma(\alpha)} x^{\alpha-1} e^{-x/\beta}, \quad x > 0 \quad (4.5)$$

where

α = shape parameter;

β = scale parameter; and,

$\Gamma(\alpha)$ = the gamma function defined by:

$$\Gamma(\alpha) = \int_0^{\infty} x^{\alpha-1} e^{-x} dx \quad (4.6)$$

The shape parameter affects the shape of the probability distribution, as opposed to shifting (location parameter) or altering the dispersion (scale parameter). The gamma function shape and scale parameters may be estimated using the method of moments and rearrangement of the gamma distribution mean (μ) and variance (σ^2), as follows:

$$\alpha = \left(\frac{\mu}{\sigma} \right)^2$$
$$\beta = \frac{\sigma^2}{\mu} \quad (4.7) \text{ \& } (4.8)$$

Where μ and σ denote the mean and standard deviation of the distribution, respectively.

If $\alpha=1$, then the gamma distribution reduces to the single-parameter exponential distribution with $\lambda=1/\beta$. Figure 29 illustrates the two-parameter gamma distribution form and the influence of the shape and scale parameters.

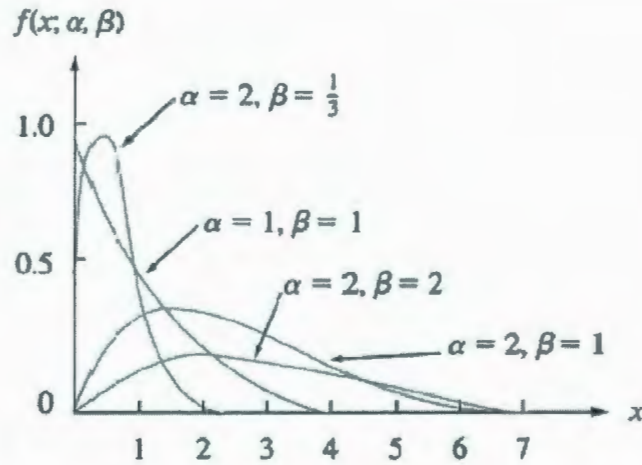


Figure 29: Sample Gamma Distribution Shape (Devore, 2004)

This thesis has investigated the three-parameter gamma distribution in order to account for thresholds in the ice gouge depth data (see Section 4.3). The three-parameter gamma probability density function is defined as (Minitab, 2007):

$$f(x) = \frac{1}{\beta^\alpha \Gamma(\alpha)} (x - \theta)^{\alpha-1} e^{-(x-\theta)/\beta}; \quad x > \theta, \alpha > 0, \beta > 0 \quad (4.9)$$

The shape, scale, and threshold parameters were estimated using the maximum likelihood method in Minitab.

4.1.3 Weibull Distribution

Wheeler and Wang (1985) also tested the suitability of the widely applicable two-parameter Weibull distribution for analysis of ice gouge depth statistics. Similar to the gamma distribution (Section 4.1.2), the Weibull distribution has been found to fit Canadian Beaufort Sea ice gouge depth data better than the exponential function (Lever, 2000). Nessim and Hong (1992) also found the Weibull distribution to provide the best fit

to Canadian Beaufort Sea ice gouge depth data, and to provide a superior fit to data records in the upper tail of the distribution (i.e., the extreme events which must be considered in design).

However, Devore (2004) has indicated that in many applications, the Weibull distribution simply provides a good fit to data observations for particular values of α and β , as opposed to fitting the full range of observed data well. Therefore, this distribution may not provide the most appropriate data fit to random/experimental data values. However, the current study has found that this is not the case for ice gouge depth data, as shown in Sections 4.3 and 5.2. Similar to the gamma distribution, Wheeler and Wang's (1985) chi-square analysis of the Weibull distribution fit to an analogue data set found that the Weibull distribution provided an unacceptable fit to the observed data (refer to discussions provided above).

The Weibull distribution probability density function is a two-parameter model and is defined as follows (Wheeler & Wang, 1985; Devore, 2004):

$$f(x) = \frac{\alpha}{\beta^\alpha} x^{\alpha-1} e^{-(x/\beta)^\alpha}; \quad x \geq 0 \quad (4.10)$$

Where α and β are the Weibull distribution shape and scale (i.e., degree of spreading) parameters, respectively. The shape and scale parameters are included in the mean (μ) and standard deviation (σ) equations; computation of these parameters necessitates use of the gamma function:

$$\mu = \beta \Gamma(1 + 1/\alpha) \quad (4.11)$$

$$\sigma^2 = \beta^2 \left\{ \Gamma(1 + 2/\alpha) - [\Gamma(1 + 1/\alpha)]^2 \right\} \quad (4.12)$$

Alternately, the Weibull parameters may be estimated using the method of median ranks and linear regression analysis procedures or using maximum likelihood estimation.

Refer to Devore (2004) or other probability and statistical texts for engineering and science applications for further discussions on calculating the Weibull parameters.

When $\alpha=1$, the Weibull distribution is reduced to the single-parameter exponential distribution with $\lambda=1/\beta$. Figure 30 illustrates the two-parameter Weibull distribution form and the influence of the shape and scale parameters.

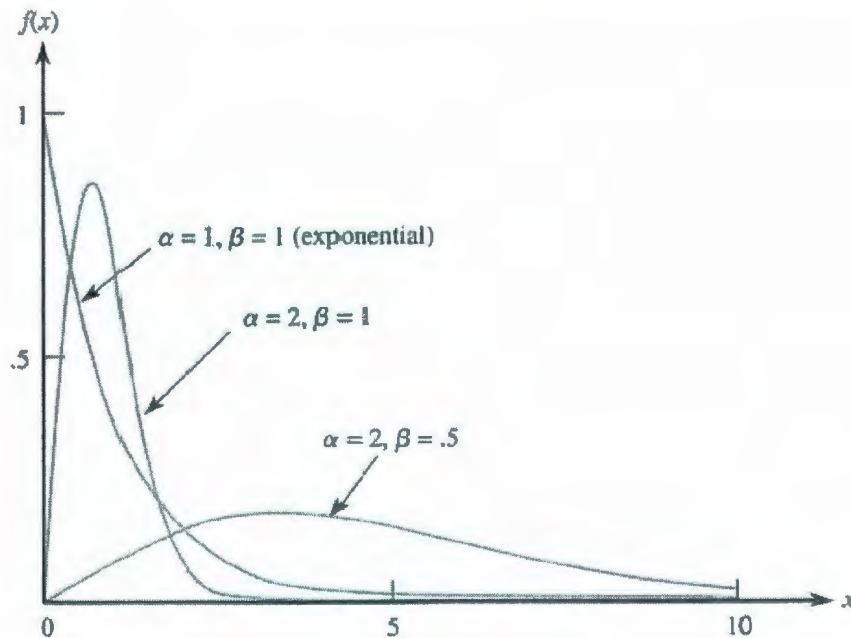


Figure 30: Sample Weibull Distribution Shape (Devore, 2004)

This thesis has investigated the three-parameter Weibull distribution in order to account for thresholds in the ice gouge depth data (see Section 4.3). The three-parameter Weibull probability density function is defined as (Minitab, 2007):

$$f(x) = \frac{\alpha}{\beta^\alpha} (x - \theta)^{\alpha-1} e^{-([x-\theta]/\beta)^\alpha}; \quad x > \theta, \alpha > 0, \beta > 0 \quad (4.13)$$

The shape, scale, and threshold parameters were estimated using the maximum likelihood method in Minitab.

4.2 STATISTICAL DISTRIBUTION CHARACTERISTICS

4.2.1 Correlation Analysis

Ice gouge parameter correlation was investigated in this thesis by generating matrix plots of gouge parameters using Minitab statistical software with a locally weighted scatter plot smoothing (LOWESS) of the relationships to limit the influence of outliers. LOWESS was conducted using a degree of smoothing equal to 0.5 and two smoothing iteration steps (Minitab defaults). From the LOWESS matrix plots, the gouge parameters were visually assessed for any relationship between the variables (linear or otherwise). The degree of smoothing corresponds to the fraction of the total number of data points used to calculate the fitted values at each independent variable (Minitab, 2007). The number of steps corresponds to the number of smoothing iterations used to limit the influence of outliers (Minitab, 2007).

4.2.2 Goodness-of-fit

The goodness-of-fit of each probabilistic distribution form (see Section 4.1) has been visually assessed through comparison of the ice gouge depth data distribution histograms and the fitted distributions (using Minitab statistical software). In addition, empirical cumulative distribution functions were superimposed on the ice gouge data cumulative distributions for visual assessment. This was conducted since the ice gouge depth data populations from each region were too large for use of probability plots and formal goodness-of-fit tests (i.e., Anderson-Darling, etc) (Personal Communication, 2009).

4.2.3 Distribution Tails

In statistical ice gouge depth distributions, the extreme gouge depth events which must be considered in design analysis are contained within the upper distribution tail. Therefore, a probability distribution function which fits upper distribution tails well is desired for design optimization and reliability.

A study by Wheeler and Wang (1985) has found that the chi-square statistical testing procedure is highly sensitive to differences that may exist in the tails of gouge depth distributions. However, limitations associated with the classical chi-square goodness-of-fit test arise from the influence of data bin class ranges (i.e., 0 to 0.2m gouge depth, 0.2 to 0.4m, and so on) and/or the test result dependence on the number of data bins defined for analysis (i.e., expected frequency calculations). Statistical texts (Walpole & Myers, 1985; Devore, 2004) recommend that the chi-square test should not be used for expected

frequencies less than five. In addition, Nessim and Hong (1992) have indicated that large sample populations often have difficulties passing the chi-square test.

A similar study by Nessim & Hong (1992) has concluded that the two-parameter Weibull distribution provides the best fit to extreme ice gouge depth data records in the upper distribution tail, whereas the single-parameter exponential distribution exhibits a rather poor fit. As discussed in Section 4.3, an independent assessment that concurs with the findings of Nessim & Hong's (1992) was conducted in this study.

4.3 ASSESSMENT OF STATISTICAL DISTRIBUTIONS

Exponential, gamma, and Weibull probability density functions have been fit to the American Beaufort, Canadian Beaufort, and Chukchi Sea ice gouge depth data sets obtained for use in the current study (see Sections 2.4 through 2.6, as well as Sections 4.1.1 through 4.1.3). As discussed in Section 4.2.2, visual assessment was conducted using Minitab to determine the most appropriate PDF for ice gouge depth analysis in each of the investigated regions.

Regional ice gouge depth distributions were analyzed for combined new and unknown age data collections, where available. The investigated statistical distributions were fit to ice gouge depth data observations across the full range of available water depths. Thresholds were used to shift the probability distribution functions away from zero to account for the large amount of shallow gouge depth data. Thus, the following analysis considered the gouge depth data distributions as mixed distributions with continuous PDFs fit to some portion of the data distribution tail. Extreme ice gouge events located in

distribution tails are of paramount interest to the present study as these records must be considered in ice gouge and pipeline design optimization procedures (see Section 4.2.3). Data discontinuities were visually assessed using histograms. These discontinuities do not imply any influence or importance of ice gouge driving forces/mechanisms, but are simply characteristics of the available data used for analysis. They may be influenced by available ice gouge driving forces, water depths, ice feature types, gouge infilling, seabed sediments, etc; however, any associated data trends could not be established in this study. Additional research and data analysis would be required.

4.3.1 American Beaufort Sea

Figure 31 provides a histogram of the combined new and unknown age American Beaufort Sea ice gouge depth data analyzed in this study. The gouge depth data was binned in 0.1m intervals (by midpoints). As shown by the histogram, approximately 45% of the gouge depth data is less than or equal to 0.1m. Therefore, the gouge depth data was analyzed as a mixed distribution and the investigated probability distributions fit to gouge depth data greater than 0.1m only. That is, the distribution was considered to exhibit a discrete probability below 0.1m gouge depth.

The histogram provided in Figure 32 indicates that the majority (approximately 60%) of available nearshore (0 to 15m water depth) ice gouge data for the American Beaufort Sea is in the 0.1m gouge depth bin. Approximately 82% of all available 0.1m or less gouge depth records (from the 0 to 65m water depth range) were found in 0 to 15m water depths. Compare Figure 31 and Figure 32. The 0 to 15m water depth range was selected

as this represents the zone of dynamic ice gouge infilling (see Section 3.4) and associated gouge depth measurement record uncertainty. The 15m bathymetric contour also represents the approximate limit of seabed gouging by multiyear ice features and the zone of grounded ridges/stamukhi (see MMS, 1996).

As shown by the distribution fits and empirical cumulative distribution functions (ECDFs) provided in Figure 33 through Figure 38, the three-parameter gamma and Weibull functions each fit the gouge depth data well (based on visual assessment). The two-parameter exponential underestimated the amount of shallow gouge depth data (i.e., less than approximately 0.25m), but provided a good fit to the upper end of the distribution. As shown, the tails of each distribution exhibited exponential decay.

To investigate the effect of the data discontinuity (the continuity limit) on continuous distribution fitting, probability distributions were also fit to gouge depth data greater than 0.9m only. Approximately 87% of the available gouge depth data is less than or equal to 0.9m. Gouge depths equal to or less than 0.9m represent approximately 98% of data in the 0 to 15m water depth range (see Figure 32). The distribution fits and ECDFs are provided in Appendix A. As shown in Appendix A, the two-parameter exponential distribution provided the better fit to all gouge depth data greater than 0.9m. The three-parameter gamma and Weibull distributions greatly over-predicted shallower gouge depth data in the approximate 0.91 to 1.1m gouge depth range. These results are contradictory to the results obtained using the 0.1m continuity limit.

Table 17 summarizes the parameters associated with each distribution for each investigated data discontinuity (0.1m and 0.9m gouge depth). Based on preceding analysis, this study recommends use of the three-parameter gamma or Weibull distributions with a continuity limit of 0.1m for American Beaufort Sea ice gouge depth modeling. Section 5.2 provides probabilistic analysis to support this recommendation.

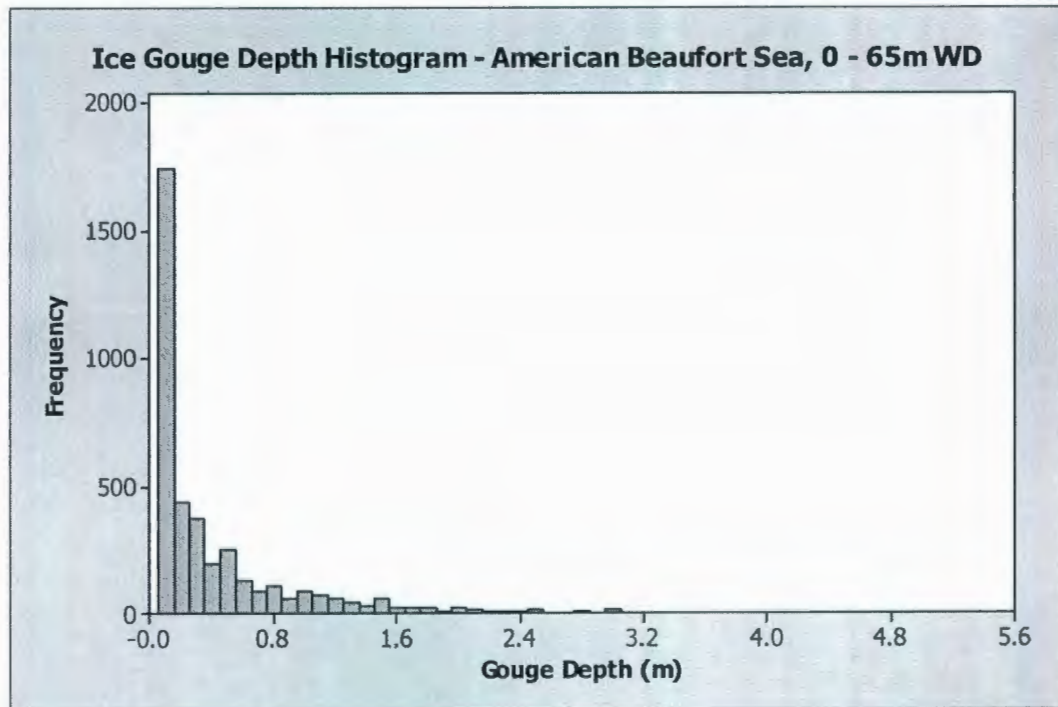


Figure 31: Histogram – American Beaufort Sea Ice Gouge Depth Data

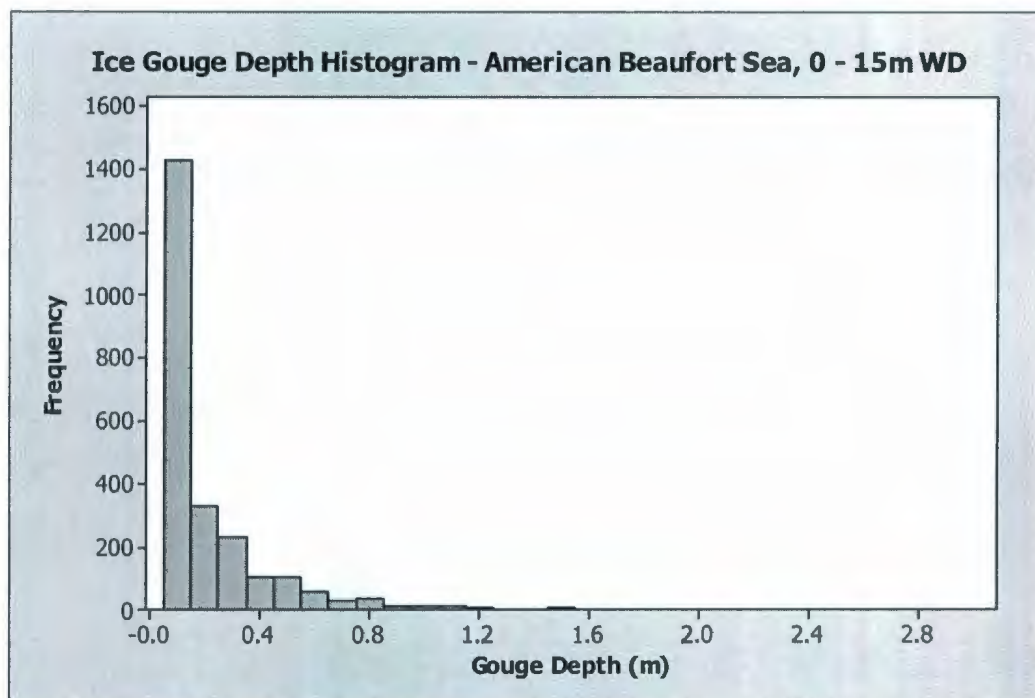


Figure 32: Histogram – American Beaufort Sea Ice Gouge Depth Data, 0 – 15m Water
Depths Only

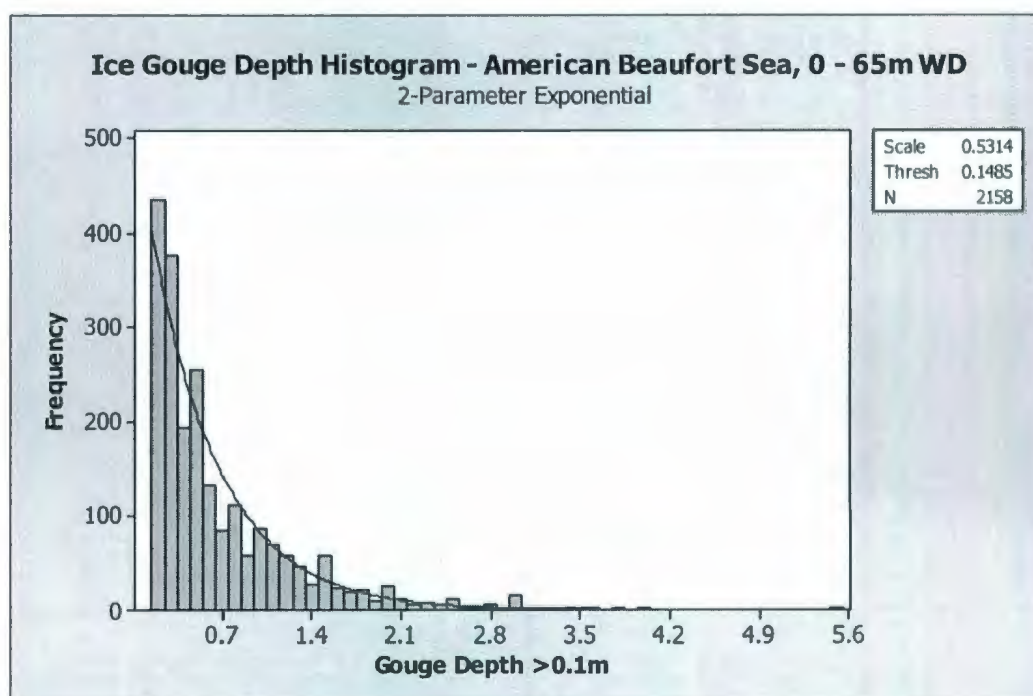


Figure 33: Exponential Fit – American Beaufort Sea Ice Gouge Depth Data >0.1m

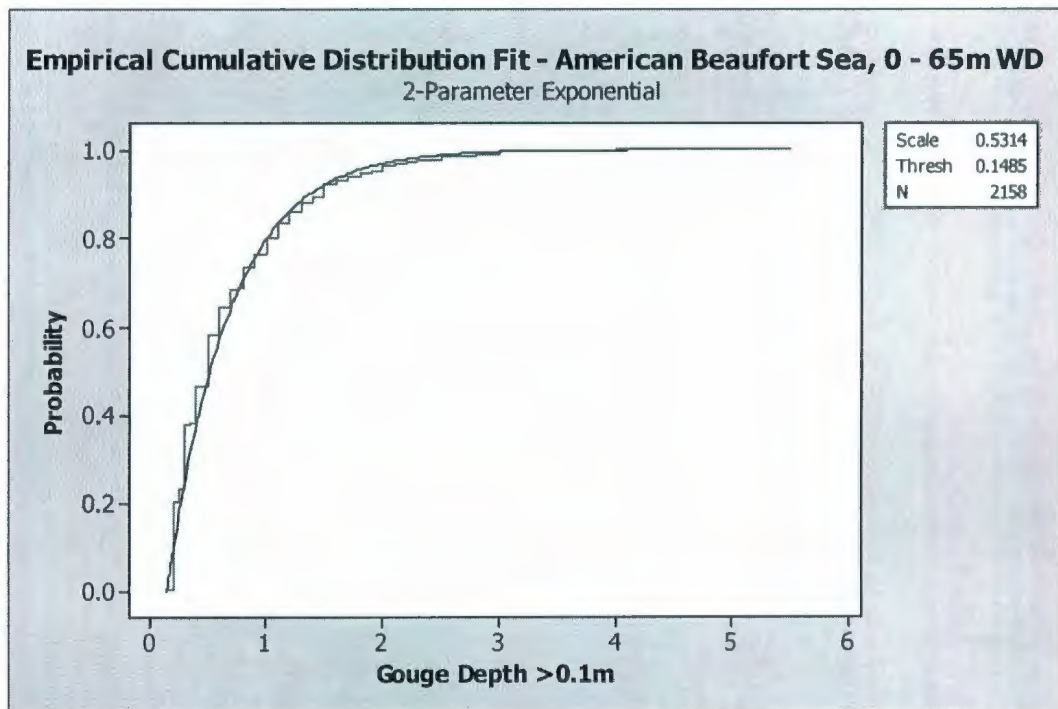


Figure 34: Exponential ECDF – American Beaufort Sea Ice Gouge Depth Data >0.1m

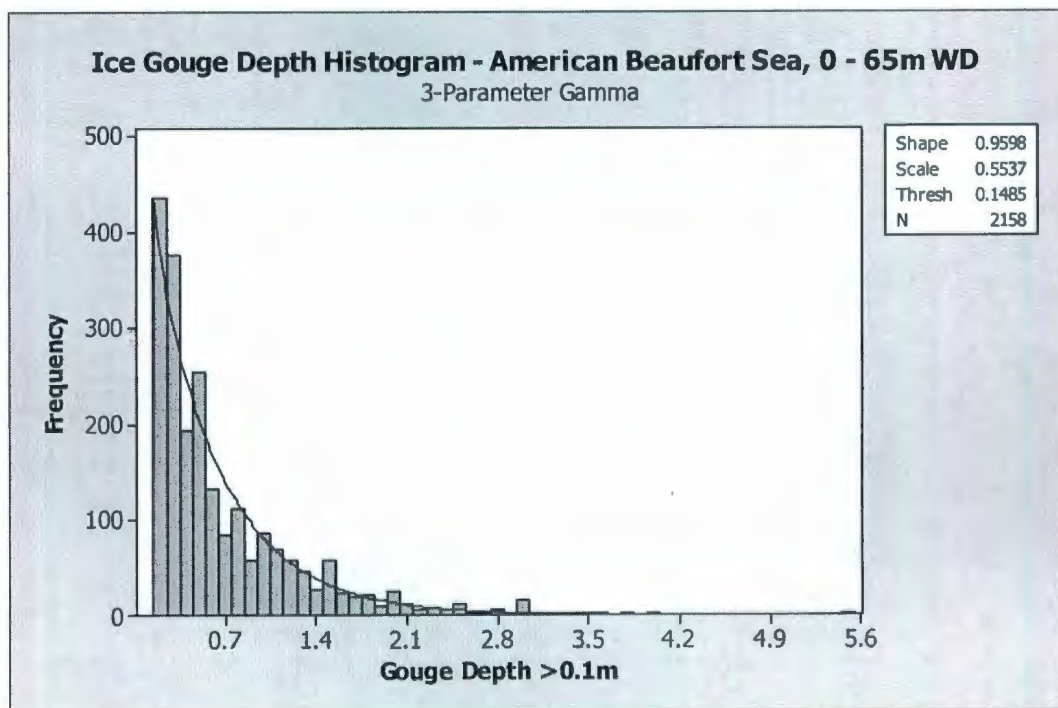


Figure 35: Gamma Fit – American Beaufort Sea Ice Gouge Depth Data >0.1m

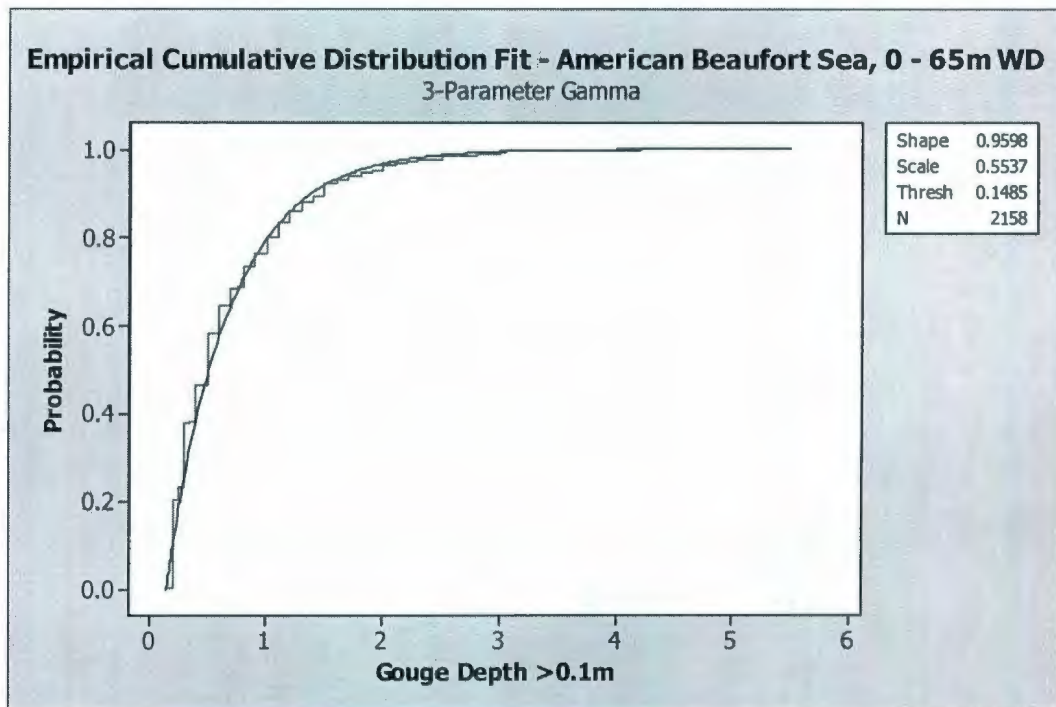


Figure 36: Gamma ECDF – American Beaufort Sea Ice Gouge Depth Data >0.1m

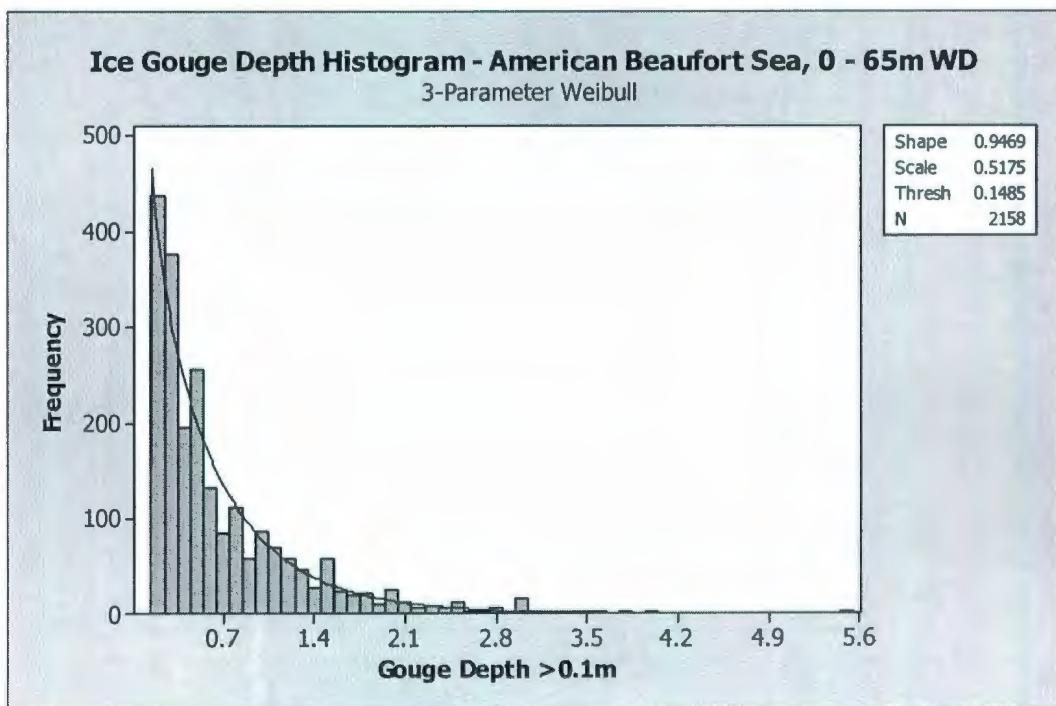


Figure 37: Weibull Fit – American Beaufort Sea Ice Gouge Depth Data >0.1m

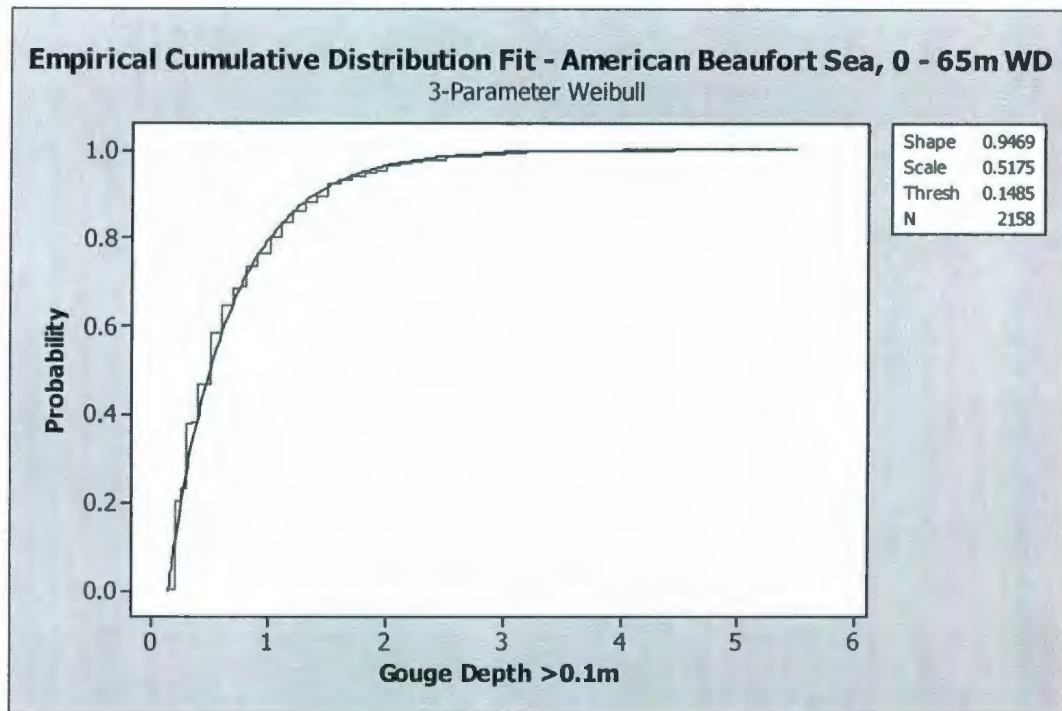


Figure 38: Weibull ECDF – American Beaufort Sea Ice Gouge Depth Data >0.1m

Table 17: Distribution Parameters – American Beaufort Sea Ice Gouge Depth Data

Continuity Limit (m)	0.1		0.9	
Threshold (m)	0.1485		0.99	
Sample Size	2158		513	
Distribution	Shape	Scale	Shape	Scale
Exponential	-	0.5314	-	0.5476
Gamma	0.9598	0.5537	0.7200	0.7606
Weibull	0.9469	0.5175	0.8212	0.4968

4.3.2 Canadian Beaufort Sea

As shown by Figure 39, approximately 69% of the combined new and unknown age Canadian Beaufort Sea ice gouge depth data analyzed in this study was less than or equal to 0.9m. Therefore, the gouge depth data was analyzed as a mixed distribution and the investigated probability distributions fit to gouge depth data greater than 0.9m only. The

distribution was considered to exhibit a discrete probability below 0.9m gouge depth. The distribution was considered to exhibit a discrete probability below 0.9m gouge depth. As shown in the histogram, the gouge depth data was binned in 0.15m intervals (by midpoints).

Figure 40 indicates that approximately 87% of available nearshore (0 to 15m water depth) ice gouge data for the Canadian Beaufort Sea is less than or equal to 0.9m. Approximately 50% of all available depth records less than or equal to 0.9m (from the 0 to 55.5m water depth range) were found in 0 to 15m water depths. Compare Figure 39 and Figure 40.

As shown by the distribution fits and empirical cumulative distribution functions (ECDFs) provided in Figure 41 through Figure 46, the three-parameter Weibull function provided the better fit to the gouge depth data (based on visual assessment); see Figure 45 and Figure 46. This result supports Nessim and Hong's (1992) findings (see Sections 4.1.3 and 4.4), which found that the Weibull distribution provides the better fit to Canadian Beaufort Sea ice gouge depth data across the full range of available water depths. The two-parameter exponential and three-parameter gamma distributions tended to under-predict the amount of shallow gouge depth data (i.e., gouge depths less than or equal to approximately 1.1m; see Figure 41 and Figure 43). Again, the tails of each distribution exhibited exponential decay.

To investigate the effect of a lower continuity limit on continuous distribution fitting, probability distributions were also fit to gouge depth data greater than 0.1m. However,

only 0.1% (approximately) of the available gouge depth data is less than or equal to 0.1m and no 0.1m or less gouge depths were recorded in the 0 to 15m water depth range. As shown by the distribution fits and ECDFs provided in Appendix A, the exponential, gamma, and Weibull distributions under-predicted shallow gouge depth data and provided poor fits to data less than approximately 1.1m. Each distribution did, however, provide a good fit to the distribution tail.

Table 18 summarizes the parameters associated with each distribution for each investigated data discontinuity (0.1m and 0.9m gouge depth). Based on preceding analysis, this study recommends use of the three-parameter Weibull distribution for Canadian Beaufort Sea ice gouge depth modeling using a continuity limit of 0.9m. Section 5.2 provides probabilistic analysis to support this recommendation.

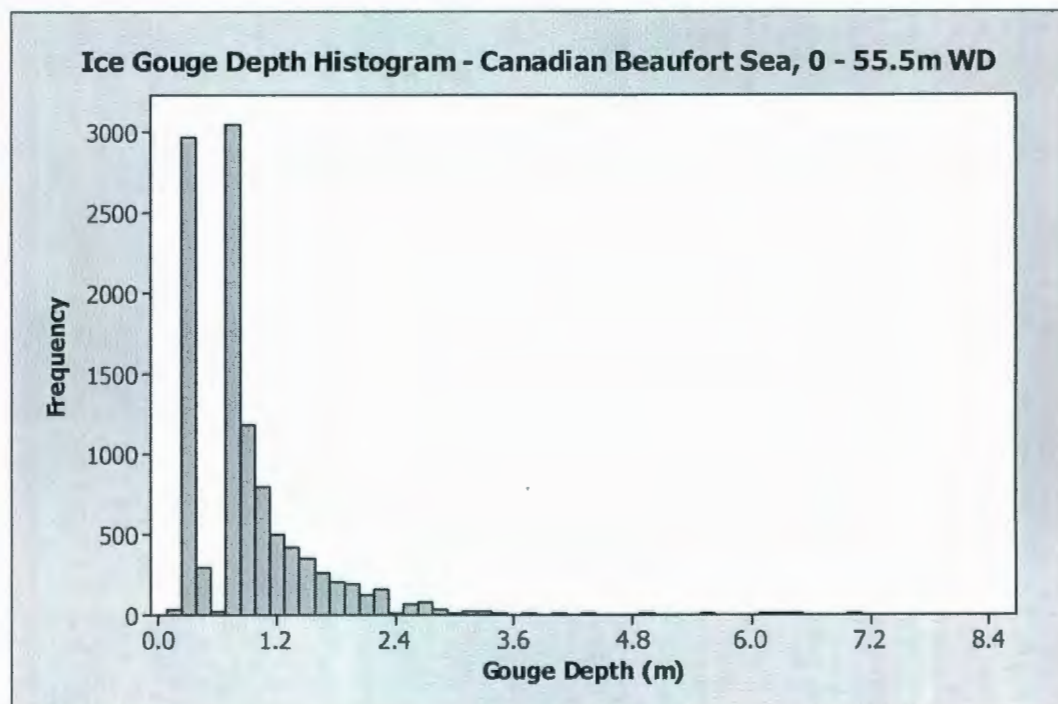


Figure 39: Histogram – Canadian Beaufort Sea Ice Gouge Depth Data

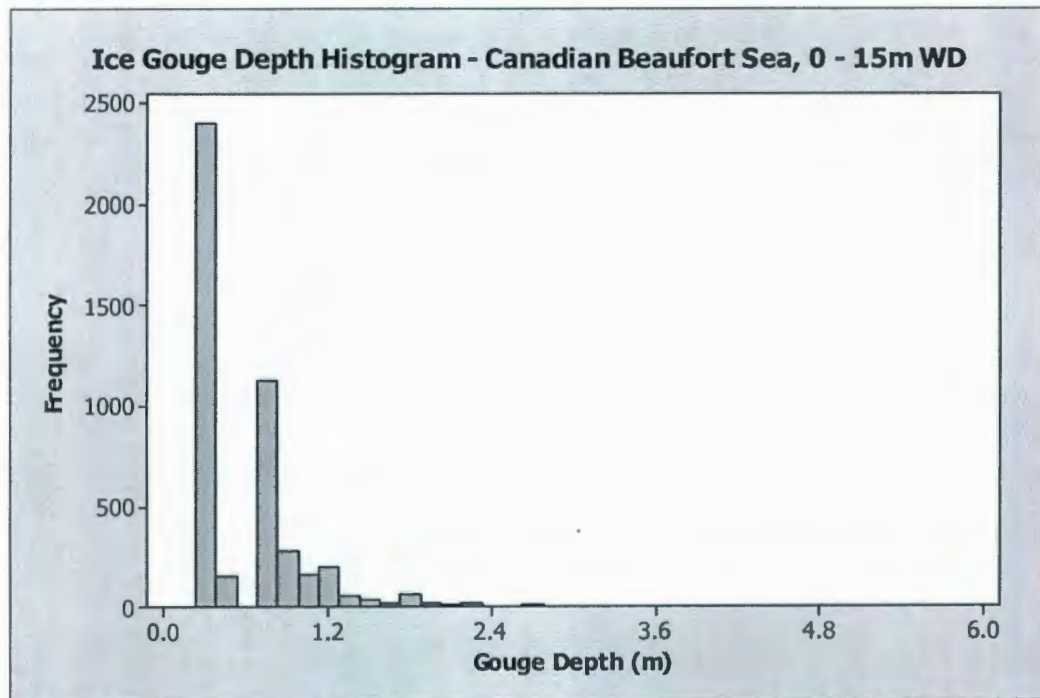


Figure 40: Histogram – Canadian Beaufort Sea Ice Gouge Depth Data, 0 – 15m Water
Depths Only

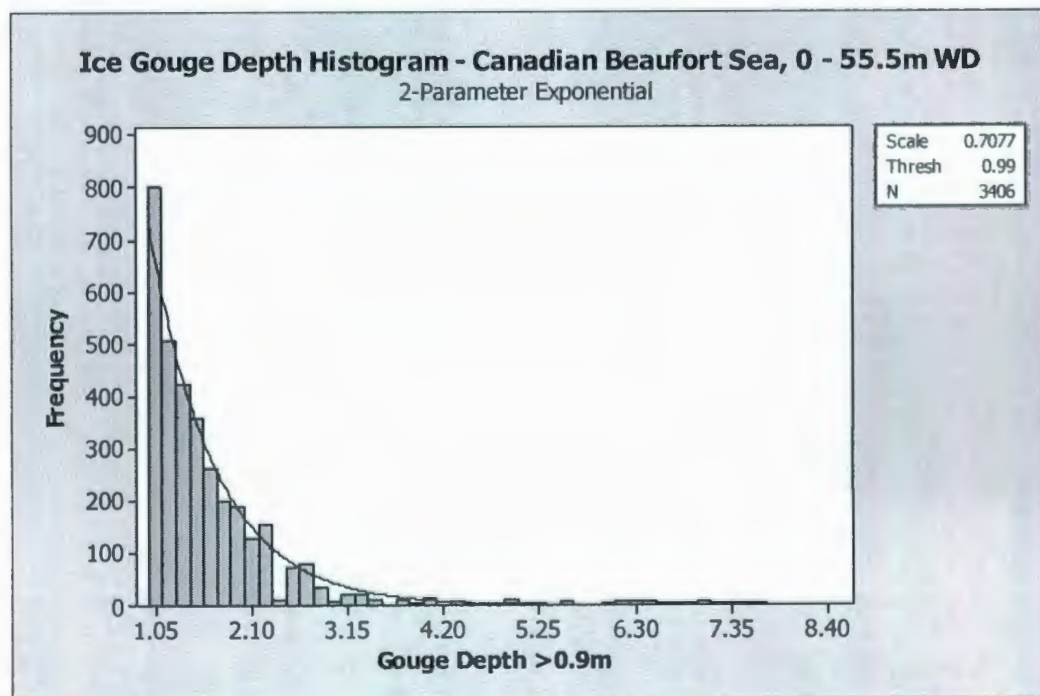


Figure 41: Exponential Fit – Canadian Beaufort Sea Ice Gouge Depth Data >0.9m

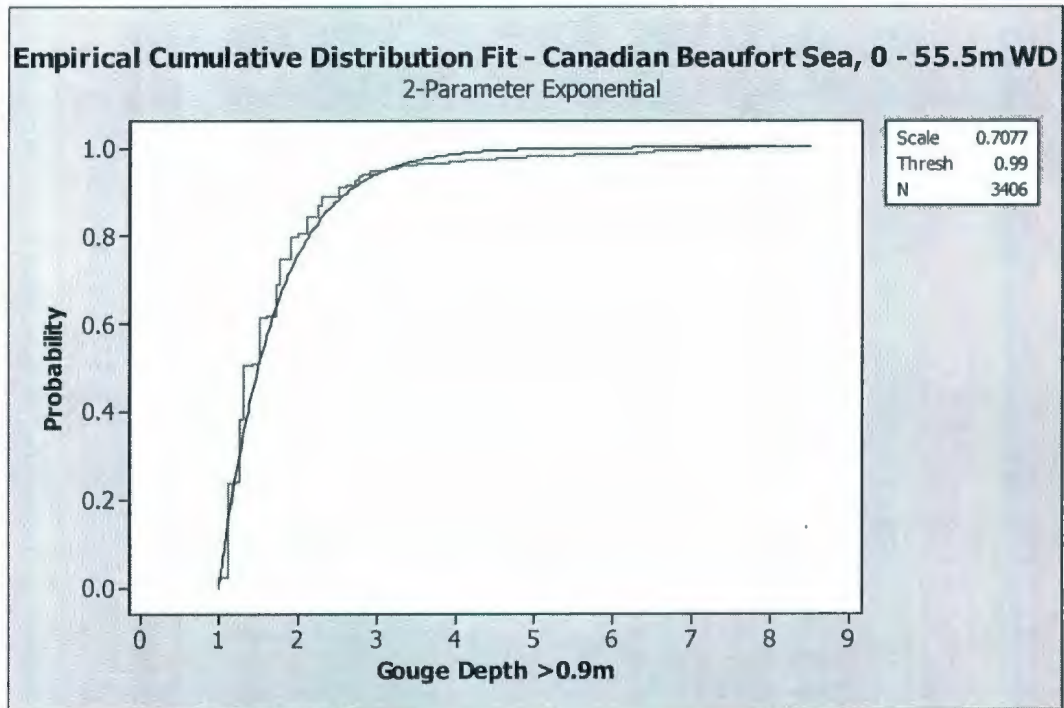


Figure 42: Exponential ECDF – Canadian Beaufort Sea Ice Gouge Depth Data >0.9m

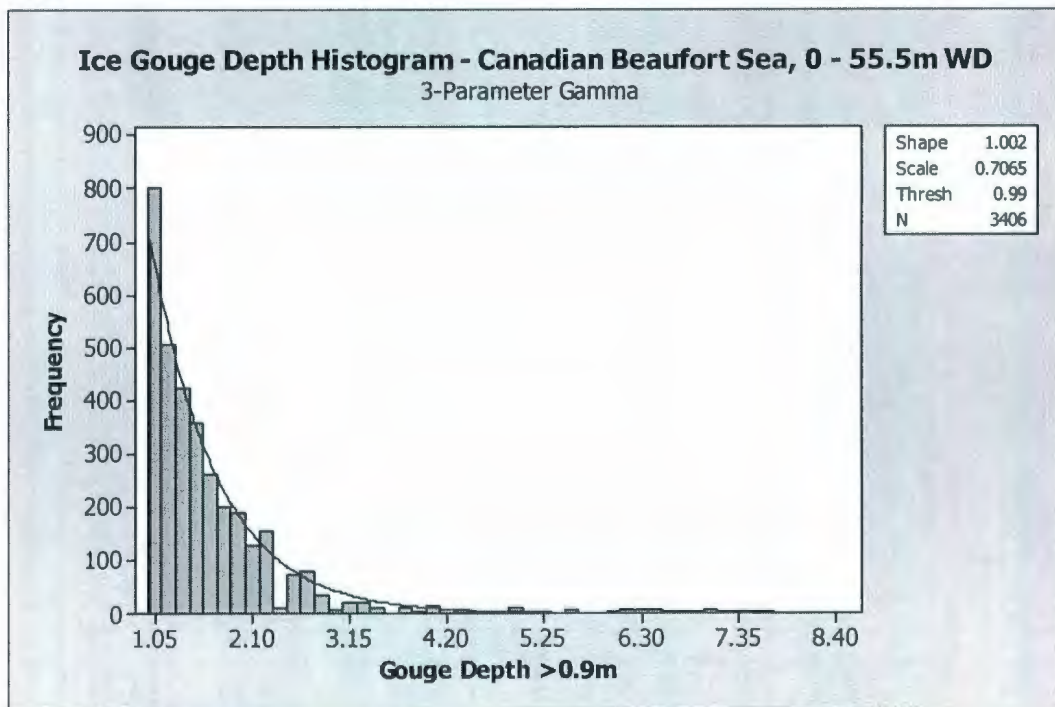


Figure 43: Gamma Fit – Canadian Beaufort Sea Ice Gouge Depth Data >0.9m

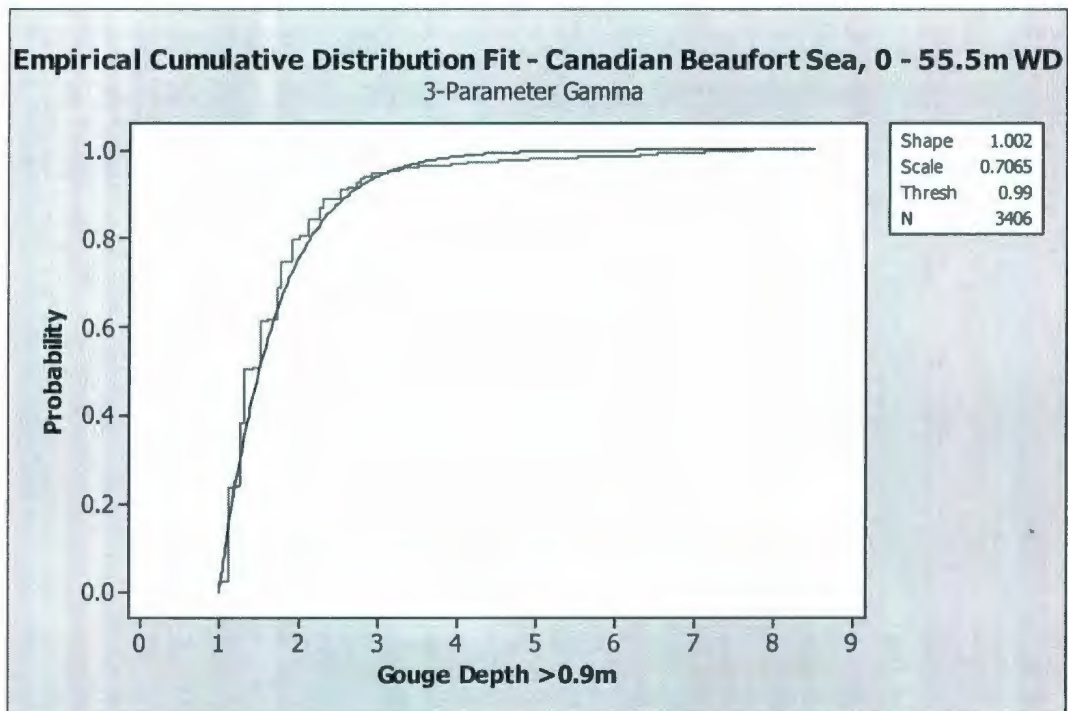


Figure 44: Gamma ECDF – Canadian Beaufort Sea Ice Gouge Depth Data >0.9m

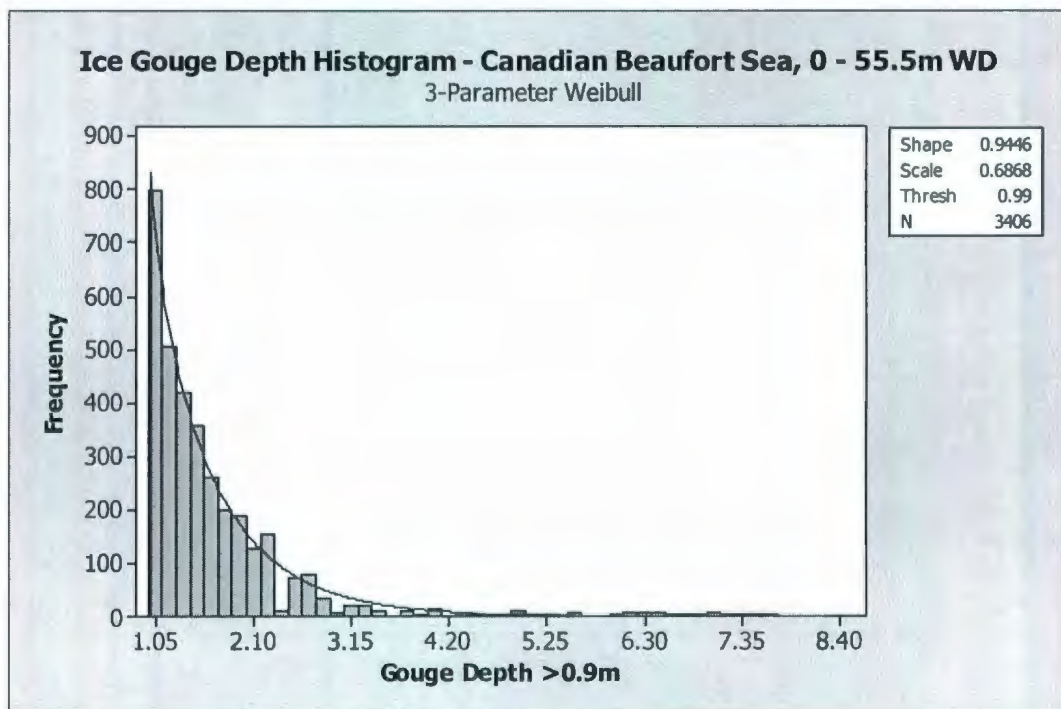


Figure 45: Weibull Fit – Canadian Beaufort Sea Ice Gouge Depth Data >0.9m

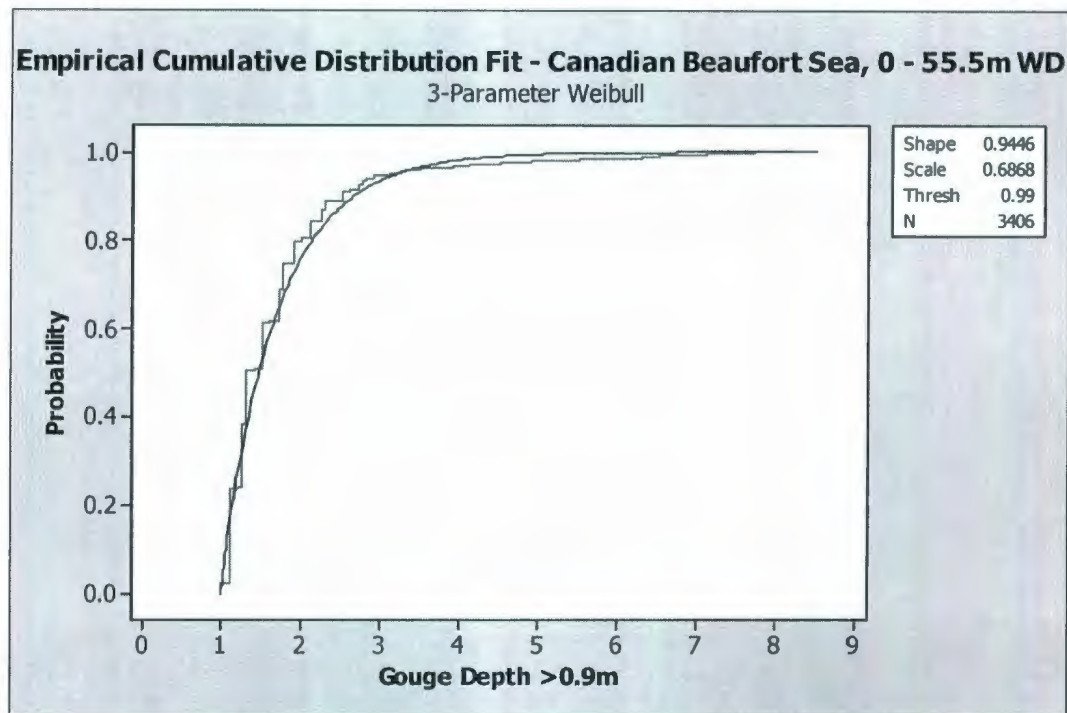


Figure 46: Weibull ECDF – Canadian Beaufort Sea Ice Gouge Depth Data >0.9m

Table 18: Distribution Parameters – Canadian Beaufort Sea Ice Gouge Depth Data

Continuity Limit (m)	0.1		0.9	
Threshold (m)	0.198		0.99	
Sample Size	10,946		3406	
Distribution	Shape	Scale	Shape	Scale
Exponential	-	0.7108	-	0.7077
Gamma	0.9182	0.7740	1.002	0.7065
Weibull	0.9506	0.6949	0.9446	0.6868

4.3.3 Chukchi Sea

Figure 47 provides a histogram of combined unknown age Chukchi Sea ice gouge depth data binned in 0.1m intervals (by midpoints). Approximately 76% of the ice gouge depth data analyzed in this study was less than or equal to 0.45m, and the data was therefore analyzed as a mixed distribution. Probability distributions were thus fit to gouge depth

data greater than 0.45m only, with data less than or equal to 0.45m considered to exhibit discrete probability.

Visual assessment of the probability distribution fits and associated empirical cumulative distribution functions (see Figure 48 through Figure 53) has indicated that the three-parameter gamma or Weibull distributions provide better fits to the data, compared to the two-parameter exponential. However, each over-predicts the number of gouge depth records occurring in the approximate 0.5m to 1m-gouge depth range.

Neither distribution fit the Chukchi Sea ice gouge depth data as well as the fits exhibited for the American or Canadian Beaufort Sea data (see Sections 4.3.1 and 4.3.2). This is potentially due to the lack of known age Chukchi Sea data available for analysis in this study. In addition, the Chukchi Sea data exhibited very distinct spikes in sample population within multiple gouge depth data bins (see figures below). An alternate gouge depth continuity limit was not investigated during this study due to uncertainty in the available Chukchi Sea data. The nearshore region could not be investigated as gouge depth data was only available for the 21 to 59m water depth range.

Table 19 summarizes the parameters corresponding to each distribution.

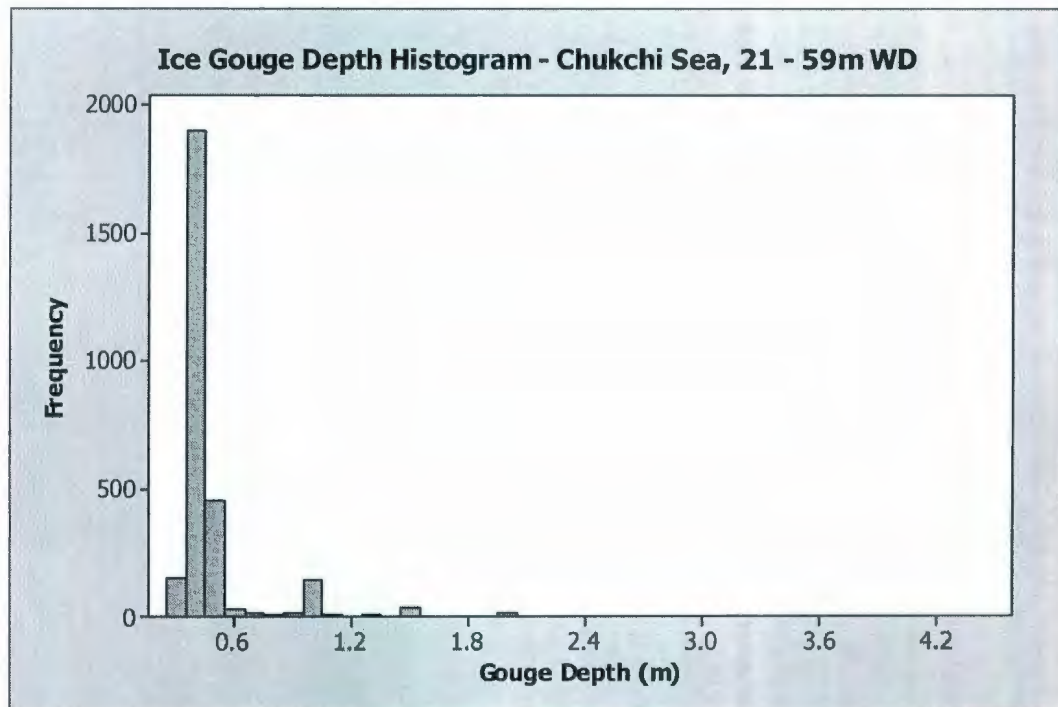


Figure 47: Histogram – Chukchi Sea Ice Gouge Depth Data

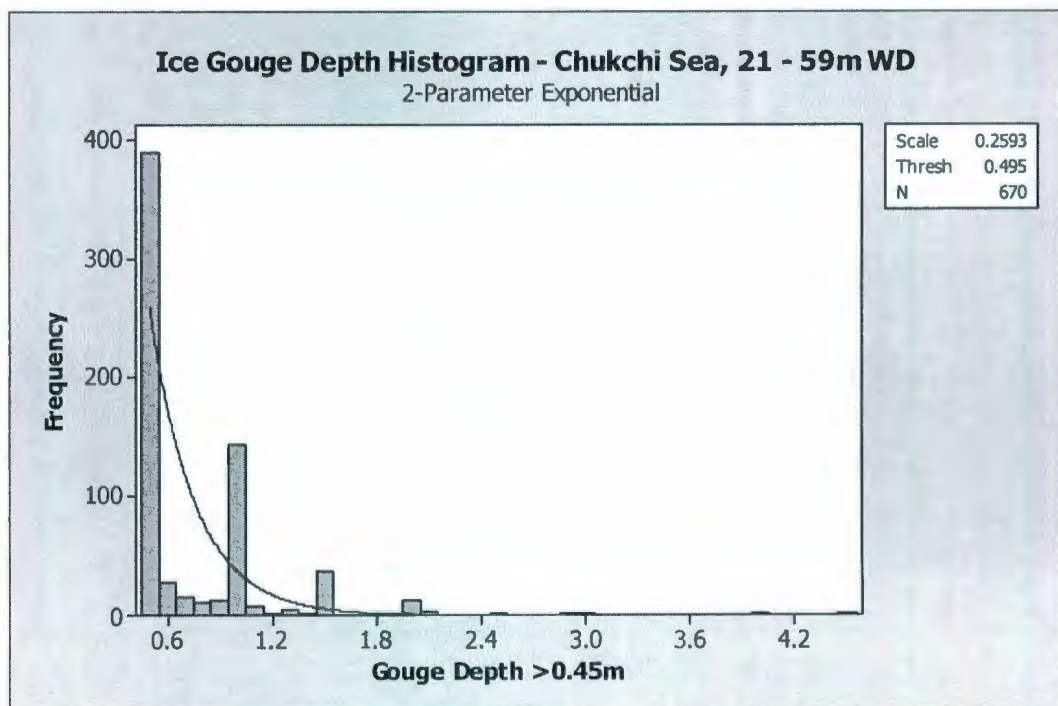


Figure 48: Exponential Fit – Chukchi Sea Ice Gouge Depth Data

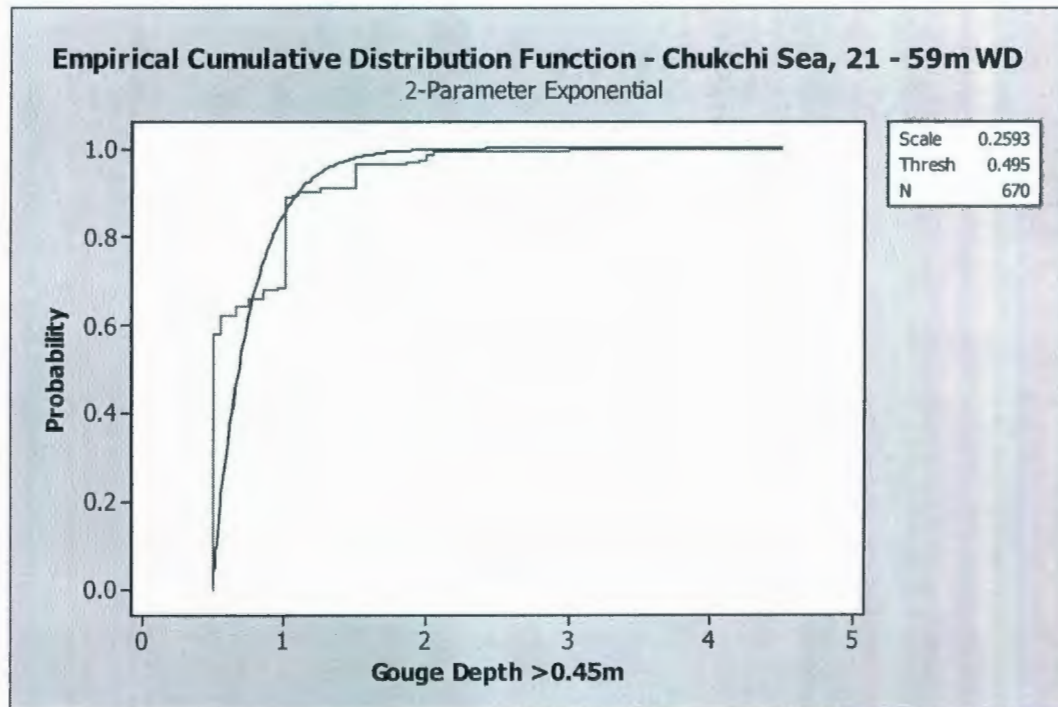


Figure 49: Exponential ECDF – Chukchi Sea Ice Gouge Depth Data

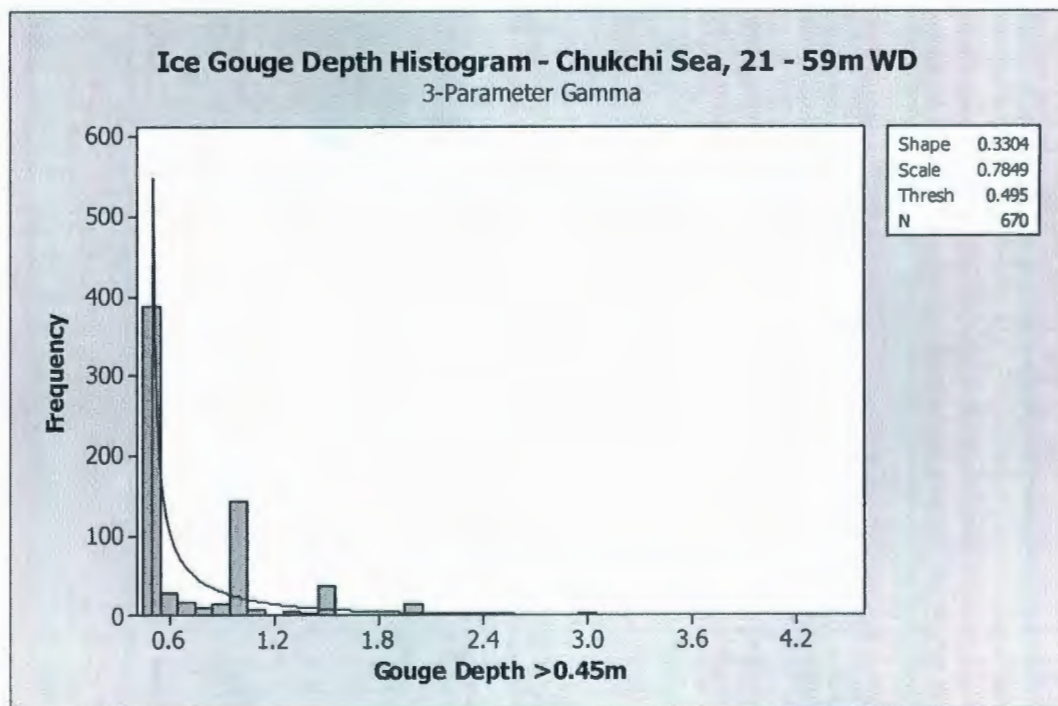


Figure 50: Gamma Fit – Chukchi Sea Ice Gouge Depth Data

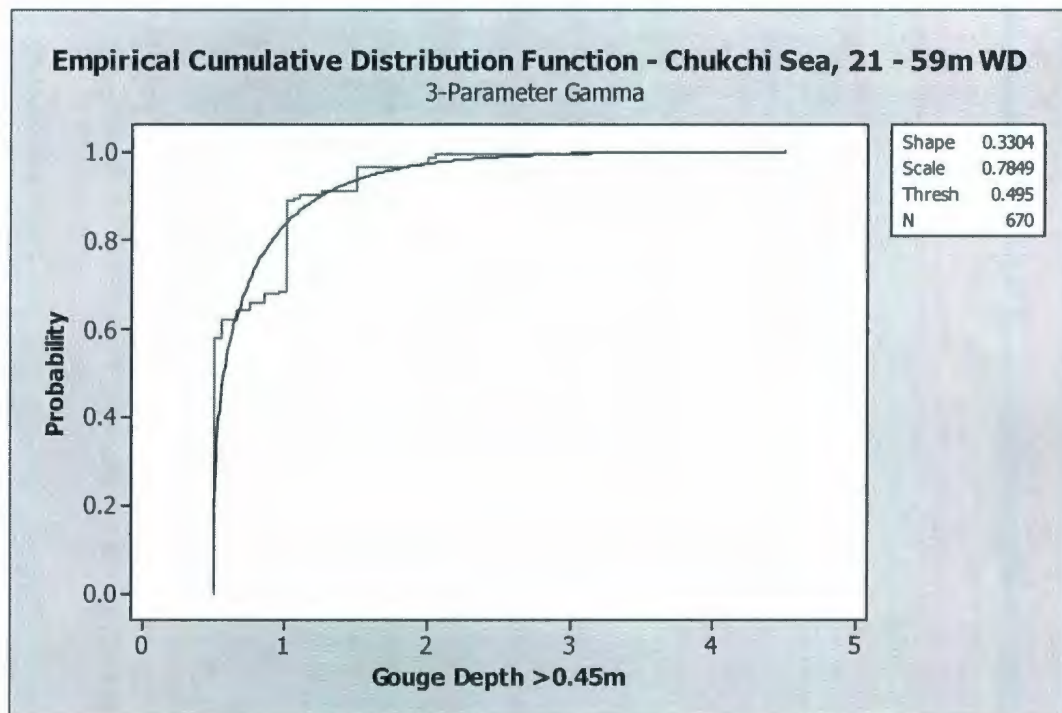


Figure 51: Gamma ECDF – Chukchi Sea Ice Gouge Depth Data

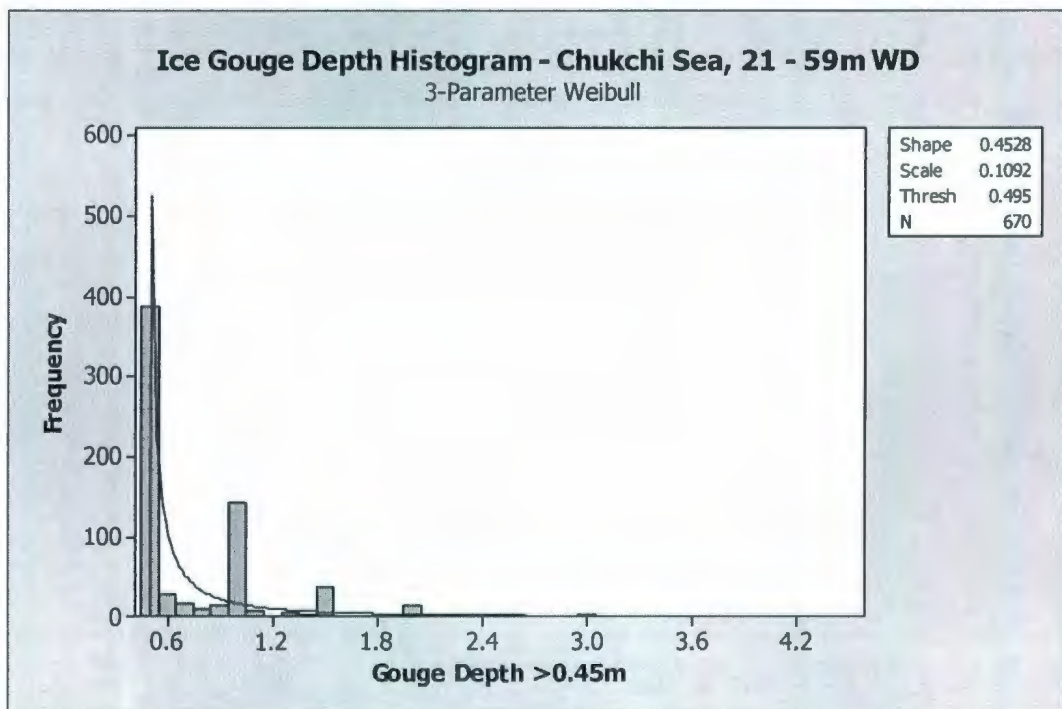


Figure 52: Weibull Fit – Chukchi Sea Ice Gouge Depth Data

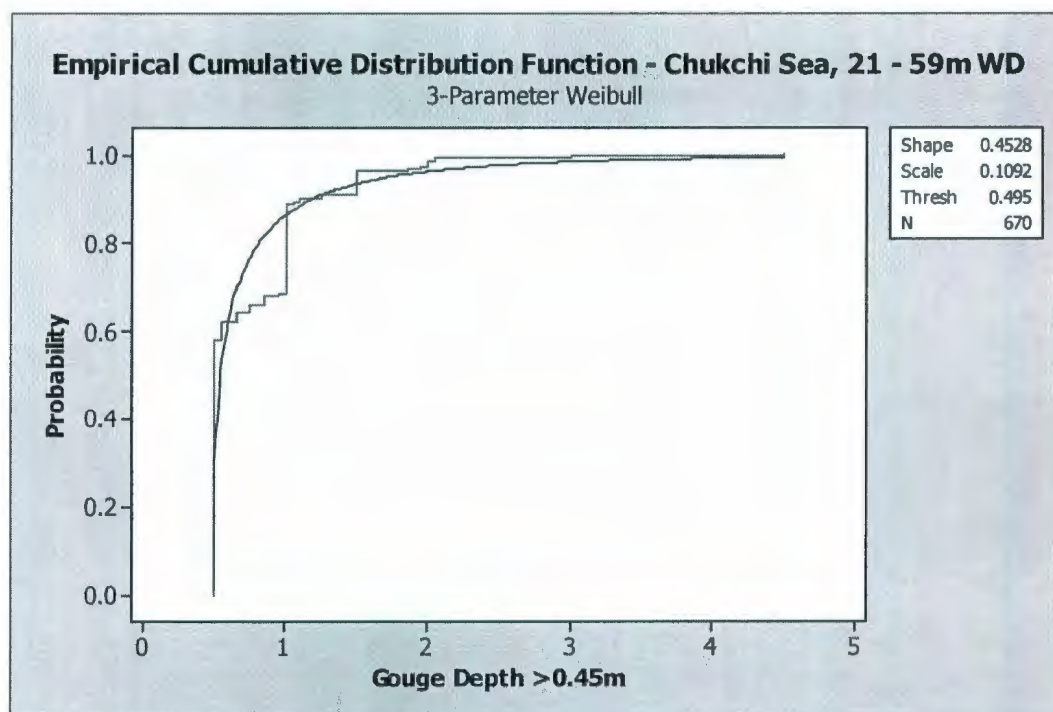


Figure 53: Weibull ECDF – Chukchi Sea Ice Gouge Depth Data

Table 19: Distribution Parameters – Chukchi Sea Ice Gouge Depth Data

Continuity Limit (m)	0.45	
Threshold (m)	0.495	
Sample Size	670	
Distribution	Shape	Scale
Exponential	-	0.2593
Gamma	0.3304	0.7849
Weibull	0.4528	0.1092

4.4 COMPARISON WITH PREVIOUS RESEARCH

As previously discussed (see Section 4.1), Nessim and Hong (1992) studied continuous distributions fit to known age Canadian Beaufort Sea ice gouge depth data from the approximate 5 to 40m water depth range. The analyzed probability distributions included the single-parameter exponential and the two-parameter gamma and Weibull forms. Data

thresholds were not utilized and analysis was conducted for continuous distributions fit to the full gouge depth and water depth range of available data. As discussed in Sections 4.2 and 4.3, the present study has analyzed available gouge depth data using mixed distribution methods.

Similar to the present study, Nessim and Hong's (1992) study visually assessed cumulative distributions fit to gouge depth data. Figure 54 provides a sample Weibull probability plot from their study. Nessim and Hong (1992) found the Weibull distribution to fit the upper distribution tail well, but fit lower gouge depth data poorly. Figure 54 indicates discontinuity in gouge depth natural logarithms ($\ln(D)$) less than approximately -1.60 , which corresponds to gouge depths less than approximately 0.2m . Figure 55 provides a Weibull distribution probability plot of all available new and unknown age Canadian Beaufort Sea gouge depth data compiled for use in the present study (from the 0 to 55.5m water depth range). When treated as a continuous distribution, data compiled for use in the present study exhibits discontinuities at lower gouge depths, similar to Nessim and Hong's (1992) analyses (compare Figure 54 and Figure 55).

Nessim and Hong (1992) concluded that Canadian Beaufort Sea ice gouge depths could be modeled using a Weibull distribution with shape and scale parameters of 1.107 and 0.5957 , respectively. This study has recommended that the three-parameter Weibull distribution be used with shape and scale parameters of 0.9446 and 0.6868 , respectively, and a threshold value of 0.99m ; refer to Section 4.3.2.

Refer to Nessim and Hong (1992) for further detail on their study.

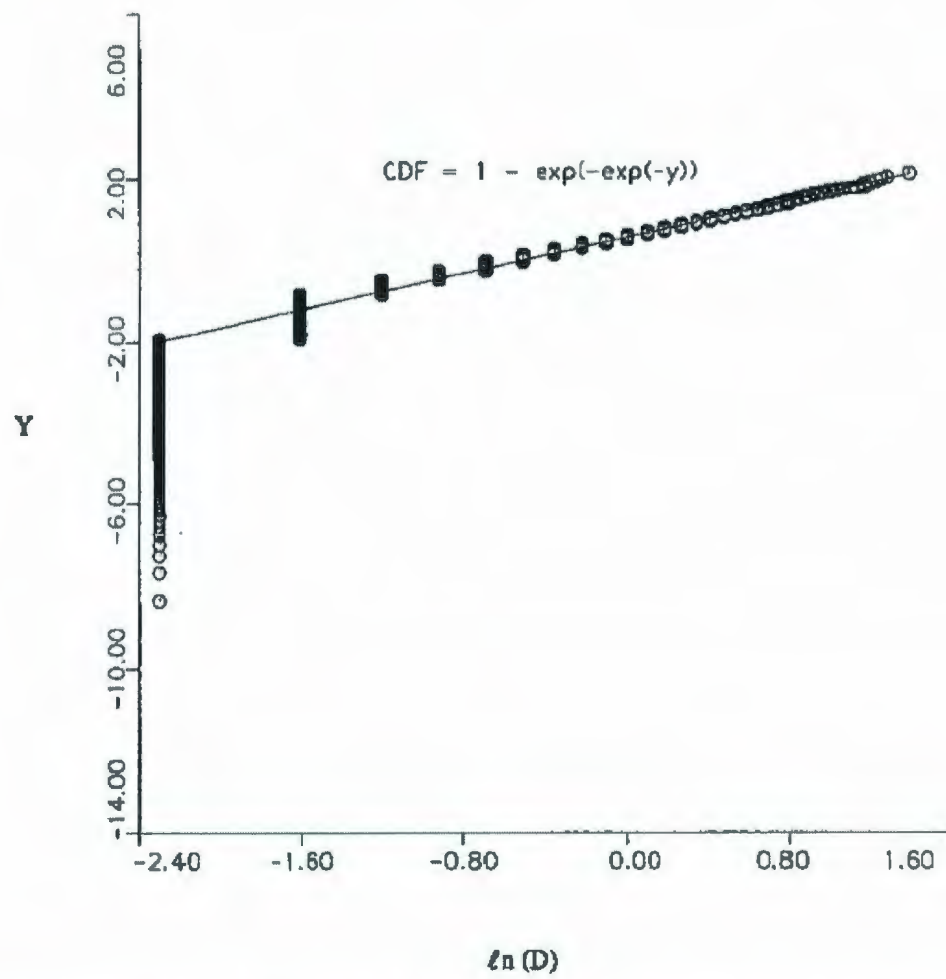


Figure 54: Probability Paper Plot for All Canadian Beaufort Sea New Gouge Data – Weibull Distribution (Nessim & Hong, 1992)

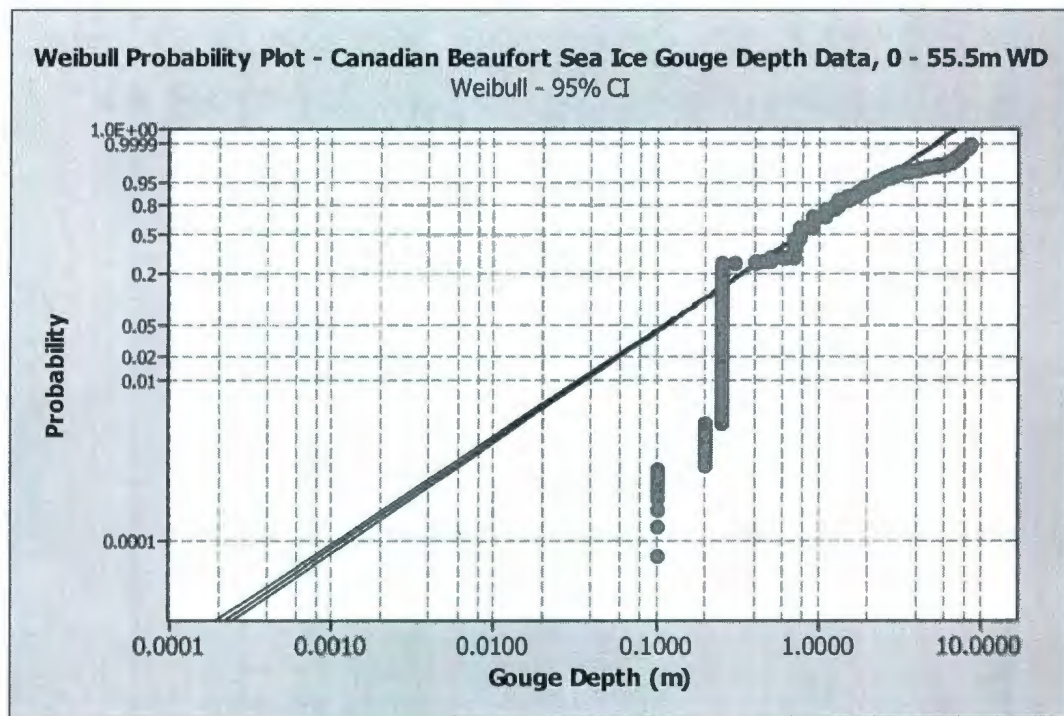


Figure 55: Probability Plot of All Available Canadian Beaufort Sea Ice Gouge Depth
Data – Weibull Distribution

5 STATISTICAL ICE GOUGE CHARACTERIZATION & MODELING

5.1 CORRELATION OF ICE GOUGE DISTRIBUTION CHARACTERISTICS

The following thesis subsections summarize correlation analyses of selected ice gouge parameters deemed relevant to design and analysis of the ice gouging processes. This was conducted to assess the existence of gouge parameter relationships, whether linear or nonlinear. Where possible, correlation was investigated for combined known and unknown age historical ice gouge data records across the full range of available water depths. For the Chukchi Sea, only unknown age data was available for analysis due to limited ice gouge surveys. The ice gouge width data corresponds to combined single-keeled and multiplet gouge width records, where specified in the available data collections. Refer to Section 2 for discussion of available public domain historical ice gouge data collections utilized in the present study. Section 2.8 discusses potential sources of regional ice gouge data bias. The analysis procedure utilized in correlation assessment is provided above in Section 4.2.1.

Two-parameter matrix plots were generated for investigation of correlation as available gouge parameter sample sizes differed per parameter. That is, corresponding gouge depth and water depth records did not necessarily possess corresponding width and length parameters, etc.

5.1.1 Gouge Depth vs. Water Depth

As shown in Figure 56 through Figure 58, Beaufort Sea ice gouge depth and water depth data generally exhibited a positive relationship, but no obvious linear or nonlinear

association was exhibited by the Chukchi Sea data. Refer to Table 20 for the sample size corresponding to each region. These results are potentially due to analysis of combined new and unknown age and/or relic ice gouge data. In addition, the Chukchi Sea results may be due to the lack of available shallow water records (i.e., less than 20m), and bedrock located at or near the seabed surface may limit possible ice gouge depths in Chukchi Sea locations (see Section 3.3). Previous studies by others (C-CORE, 2008) have found that Chukchi Sea ice gouge depths and water depths may be correlated lognormally; this was not examined in the current study.

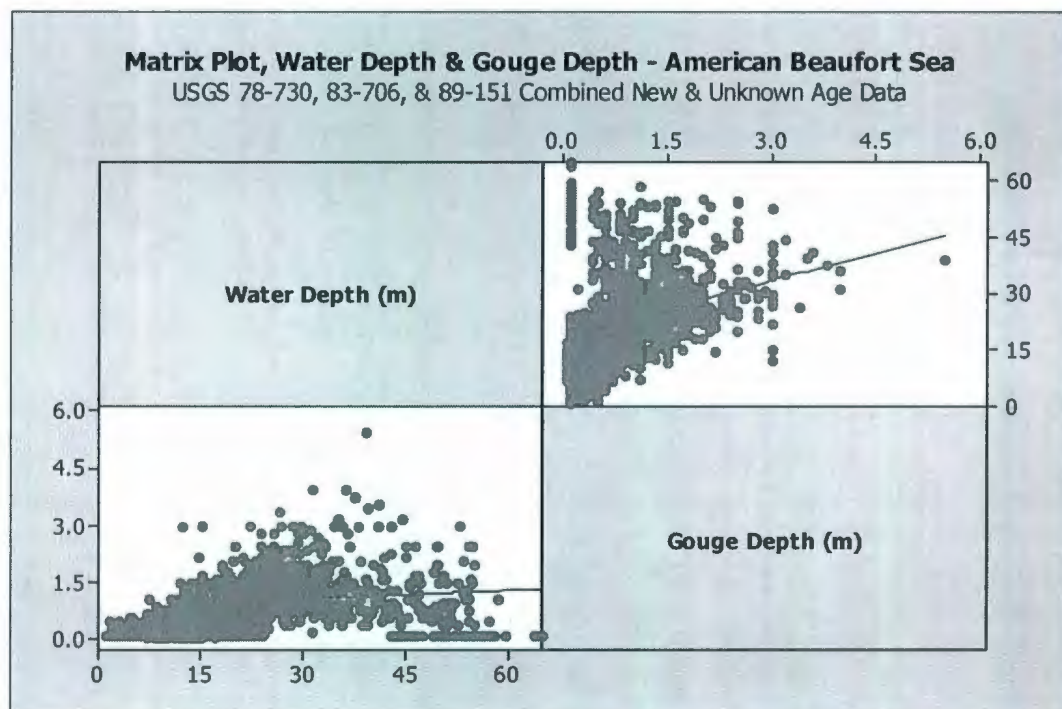


Figure 56: LOWESS Matrix Plot, Water Depth & Gouge Depth, American Beaufort Sea

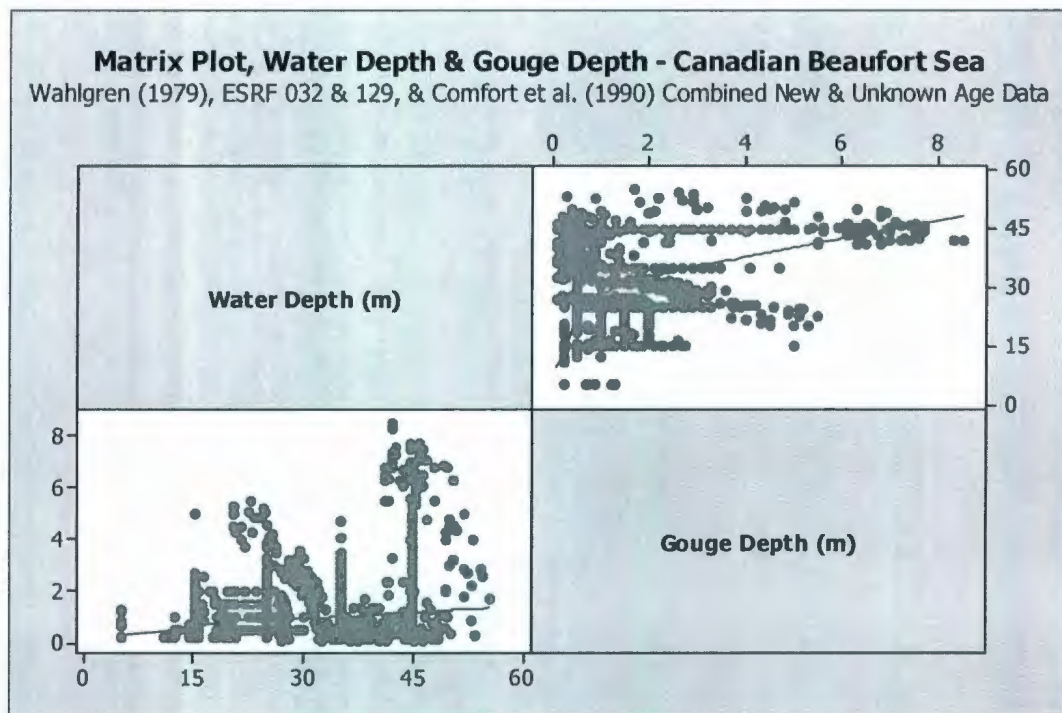


Figure 57: LOWESS Matrix Plot, Water Depth & Gouge Depth, Canadian Beaufort Sea

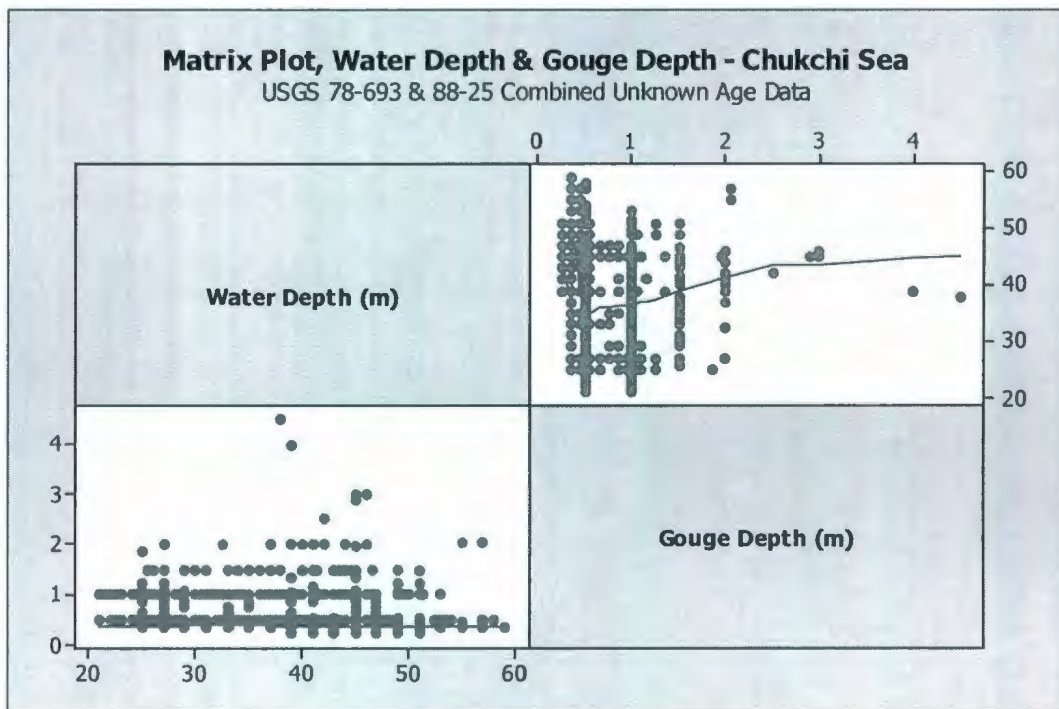


Figure 58: LOWESS Matrix Plot, Water Depth & Gouge Depth, Chukchi Sea

Table 20: Ice Gouge Depth vs. Water Depth Sample Populations

Region	Age of Data	Water Depth Range (m)	Sample Size
Canadian Beaufort	New & Old	5 – 55.5	10,990
American Beaufort	New & Old	1.2 – 65	3899
Chukchi	Old	21 – 59	2790

5.1.2 Gouge Width vs. Water Depth

Figure 59 through Figure 60 indicate no obvious linear or nonlinear association between ice gouge width and water depth data from the American Beaufort, Canadian Beaufort, and Chukchi Seas, respectively. It must be noted that no gouge width records were available for the Chukchi Sea for less than 21m water depth. Additional data is required for further analysis. C-CORE (2008) has suggested that Chukchi Sea ice gouge width and water depth data may be correlated lognormally; however, this was not examined in the current study. The Chukchi Sea ice gouge data available for this study was limited with high uncertainty. The available population of Canadian Beaufort Sea gouge width and water depth records was also limited. Table 21 provides the sample populations used in this analysis.

No obvious linear or nonlinear association has been found between gouge width and water depth data during this study; however, more ice gouge width data is required for this analysis. This could be obtained via discrete sampling (maximum measurements) and/or through continuous surveying along the ice gouge length. Also, ice gouge width analyses may be biased towards wider events by inclusion of multiplet ice gouge width data. This study has not differentiated between single and multiplet gouge width data;

therefore, these results should be considered approximate/preliminary. Ice gouge width measurement practices and reference datum may also bias available data sets.

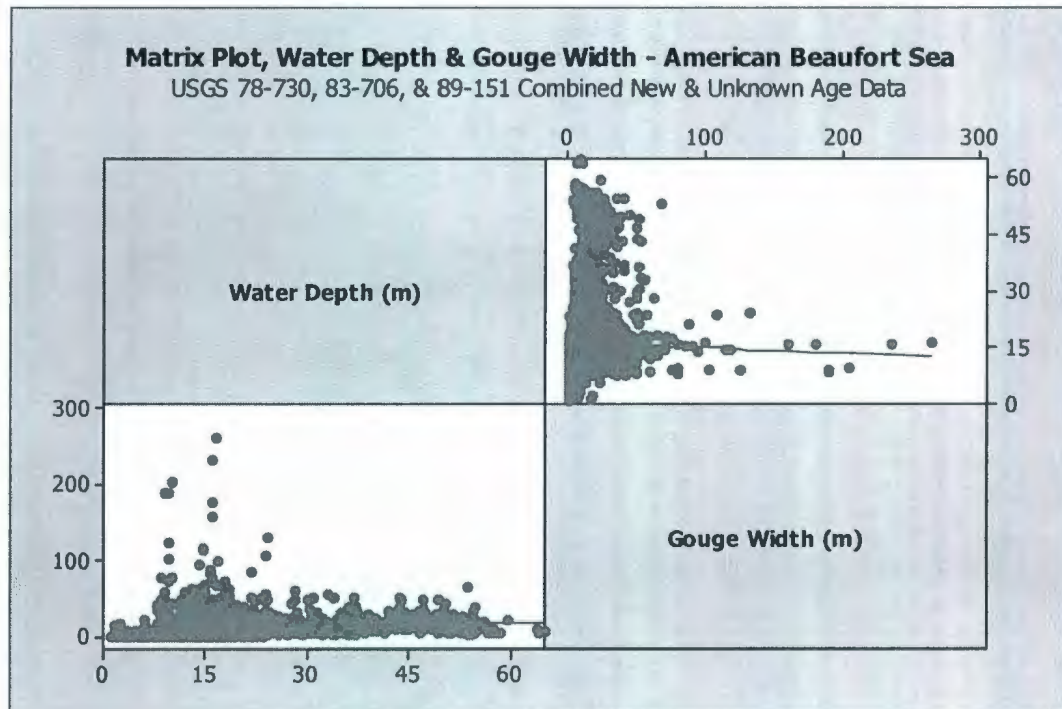


Figure 59: LOWESS Matrix Plot, Water Depth & Gouge Width, American Beaufort Sea

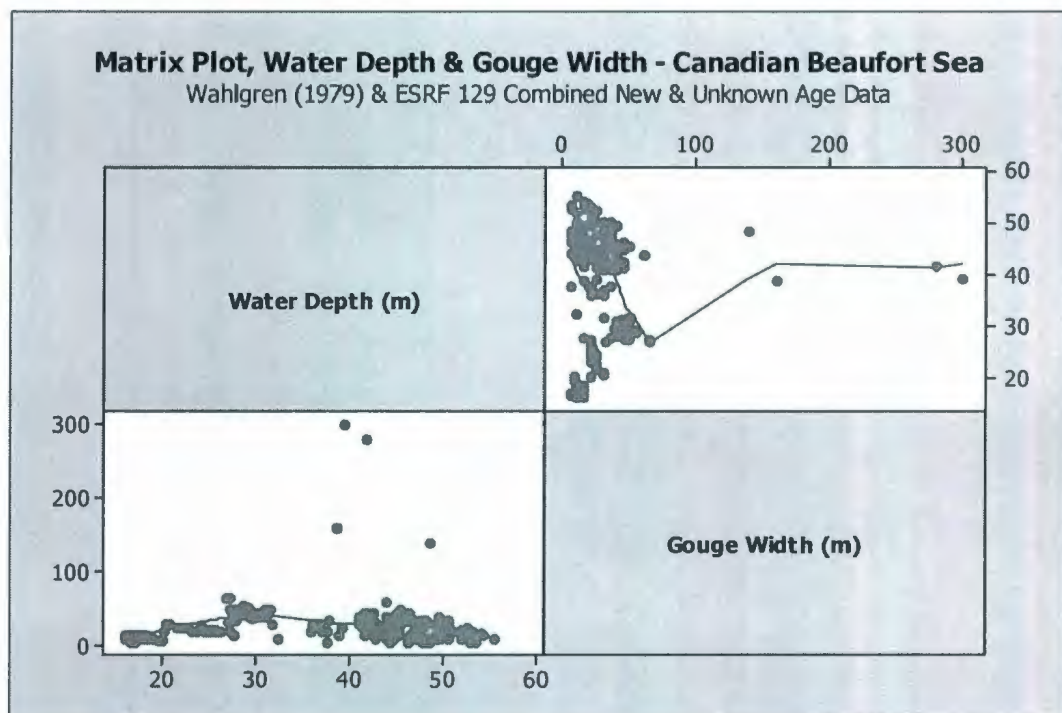


Figure 60: LOWESS Matrix Plot, Water Depth & Gouge Width, Canadian Beaufort Sea

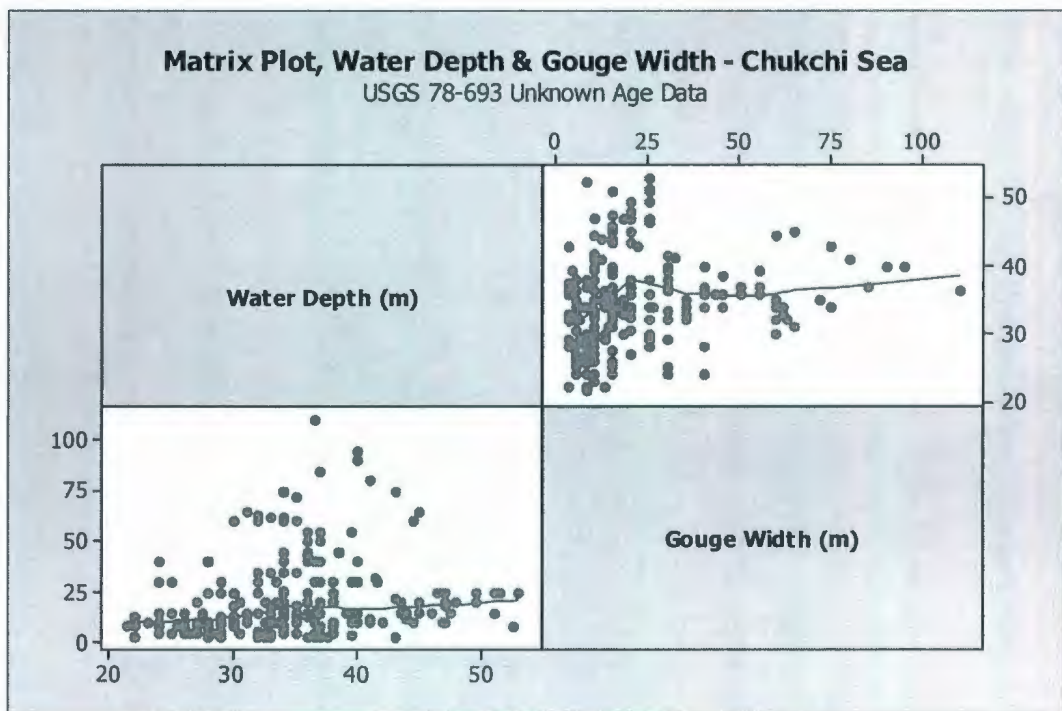


Figure 61: LOWESS Matrix Plot, Water Depth & Gouge Width, Chukchi Sea

Table 21: Ice Gouge Width vs. Water Depth Sample Populations

Region	Age of Data	Water Depth Range (m)	Sample Size
Canadian Beaufort	New & Old	16 – 55.5	291
American Beaufort	New & Old	1.2 – 65	4161
Chukchi	Old	21.5 – 53	245

5.1.3 Gouge Width vs. Gouge Depth

As shown in Figure 62 through Figure 64, correlation analysis has indicated no obvious linear or nonlinear association between ice gouge width and gouge depth data from the American Beaufort, Canadian Beaufort, or Chukchi Sea data collections. Table 22 provides the sample populations for each region. As discussed in Section 5.1.2, this study's ice gouge width analysis results should be considered preliminary and additional data is required for detailed analysis.

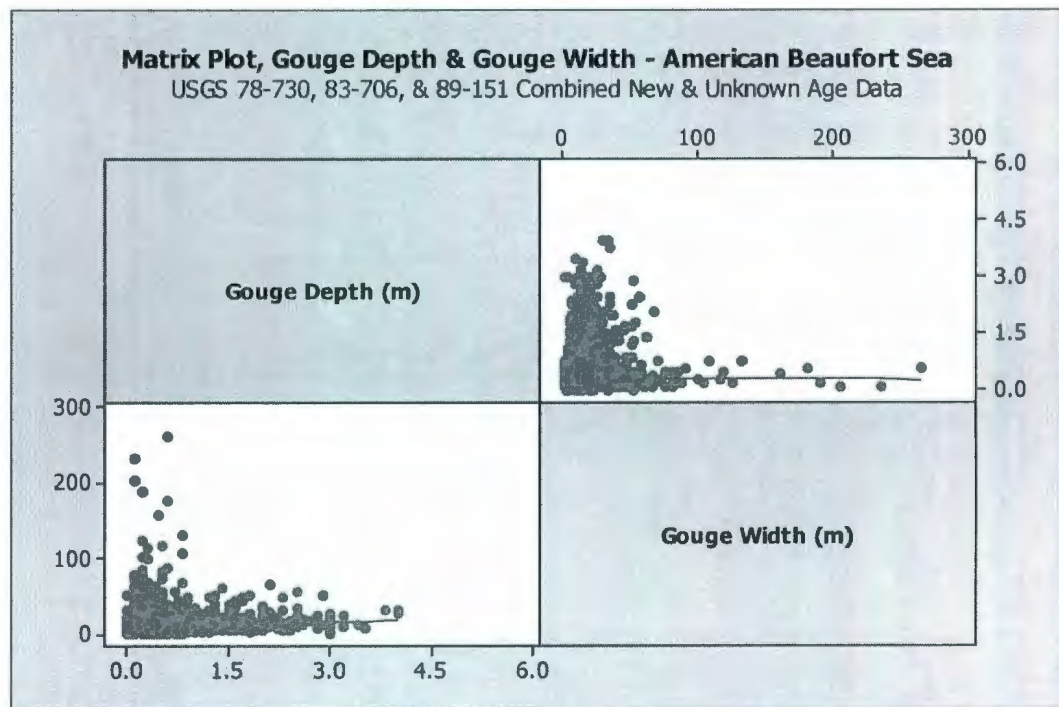


Figure 62: LOWESS Matrix Plot, Gouge Depth & Width, American Beaufort Sea

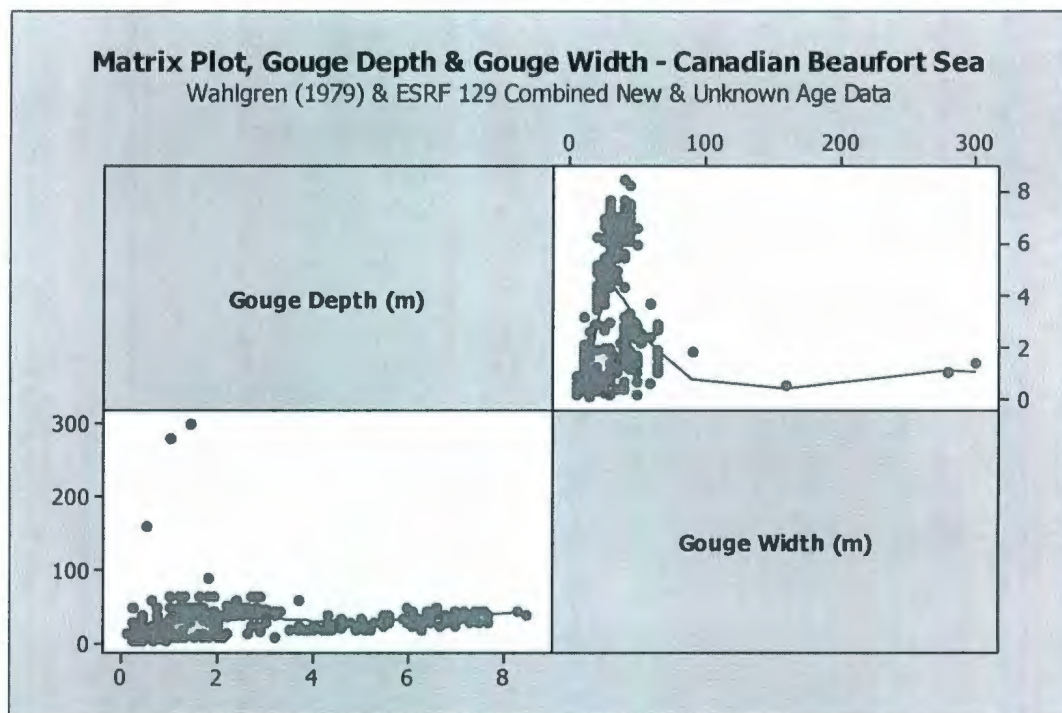


Figure 63: LOWESS Matrix Plot, Gouge Depth & Width, Canadian Beaufort Sea

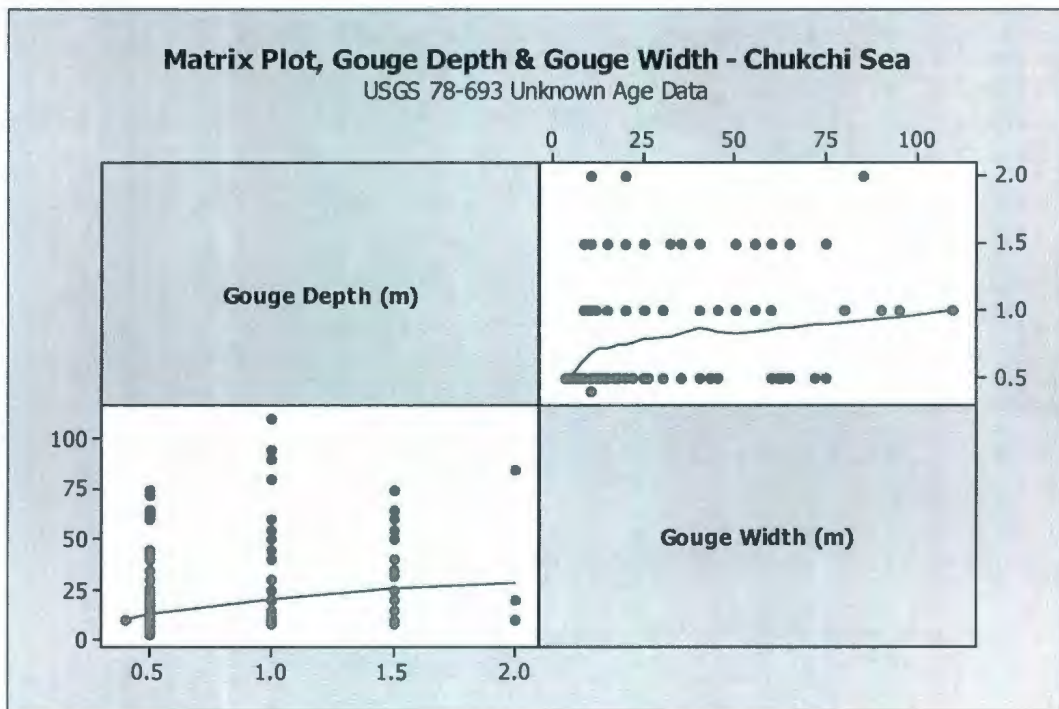


Figure 64: LOWESS Matrix Plot, Gouge Depth & Width, Chukchi Sea

Table 22: Ice Gouge Width vs. Gouge Depth Sample Populations

Region	Age of Data	Water Depth Range (m)	Sample Size
Canadian Beaufort	New & Old	16 – 55.5	265
American Beaufort	New & Old	1.2 – 65	3924
Chukchi	Old	21.5 – 53	244

5.1.4 Gouge Length vs. Water Depth

Figure 65 and Figure 66 indicate that there is no obvious linear or nonlinear association exhibited by ice gouge length and water depth data from the American or Canadian Beaufort Seas, respectively. However, additional data is required. The Canadian Beaufort Sea ice gouge length data was of unknown age only, corresponding to the Wahlgren (1979) study (see Table 23). As shown in the table, no Chukchi Sea ice gouge length data was available for analysis.

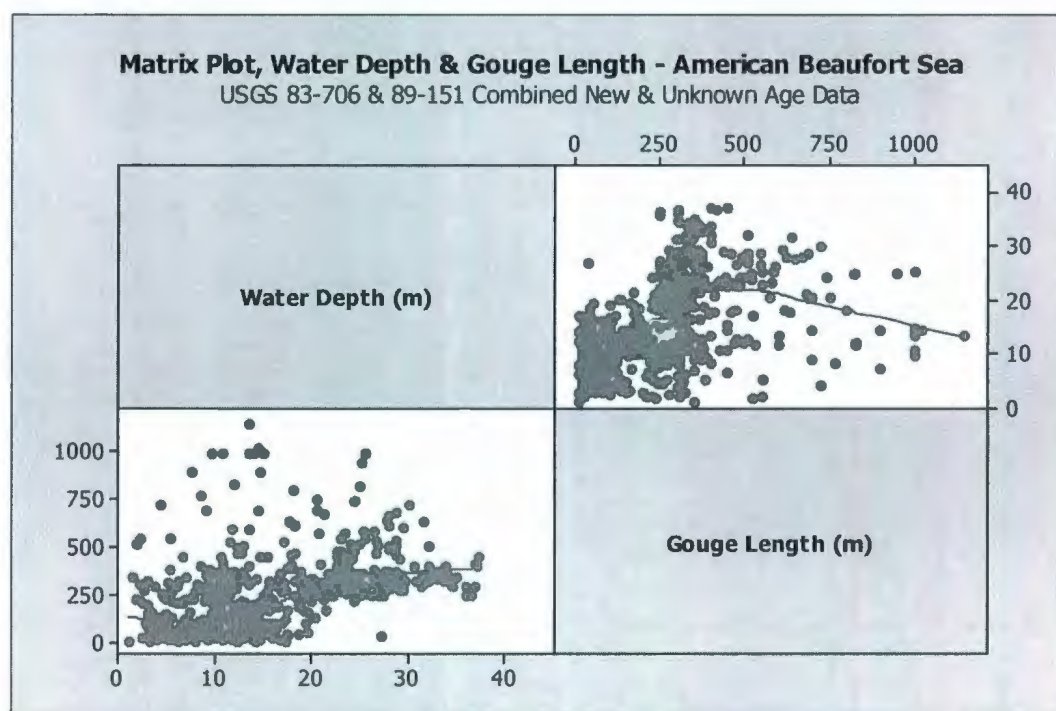


Figure 65: LOWESS Matrix Plot, Water Depth & Gouge Length, American Beaufort Sea

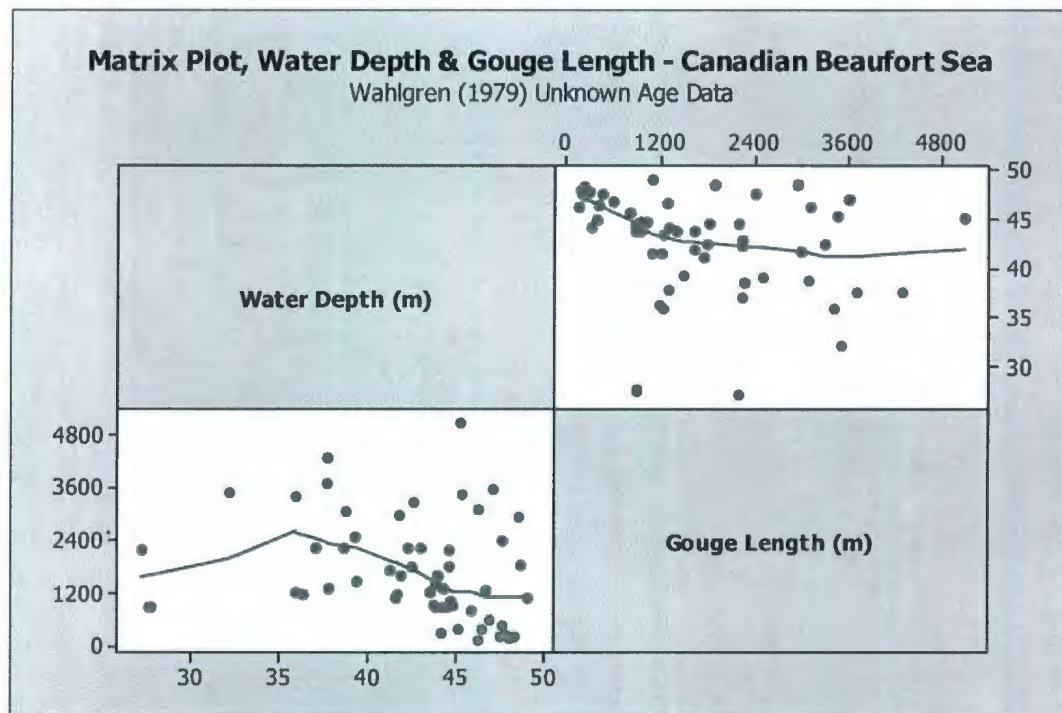


Figure 66: LOWESS Matrix Plot, Water Depth & Gouge Length, Canadian Beaufort Sea

Table 23: Ice Gouge Length vs. Water Depth Sample Populations

Region	Age of Data	Water Depth Range (m)	Sample Size
Canadian Beaufort	Old	~27 – 50	56
American Beaufort	New & Old	1.2 – 37.3	623
Chukchi	N/A		

5.1.5 Ice Gouge Orientation

American Beaufort Sea ice gouge orientation data was obtained from USGS Open-File Reports 83-706 and 89-151 by Rearic and McHendrie (1983) and Weber et al. (1989), respectively. Both data collections contained ice gouge orientation data which was corrected to account for the survey vessel's course, and measured relative to true north. However, unknown age gouge orientation measurements provided in USGS 83-706 ranged from 0 to 90°, whereas the new gouge orientation data provided in USGS 89-151

ranged from 0 to 180°. No rationale for these measurement ranges was found during data collection review. USGS 78-730 provided graphical, qualitative ice gouge orientations for new and unknown age gouge observations.

Canadian Beaufort Sea ice gouge orientation data collection was limited to unknown age measurements obtained from ice gouge tracking studies conducted by Myers et al. (1996) during 1990 updates the NEWBASE data set and early records presented by Wahlgren (1979). Myers et al. (1996) measured gouge orientations relative to true north and ranged from 0 to 360°. Wahlgren (1979) recorded orientation data in the 0 to 360° range, however the measurement reference is unknown (assumed to be true north for purposes of the current study). It is suggested that Myers et al. (1996) utilized the 0 to 360° range in order to fully describe gouge direction changes during their tracking studies.

Tabulated Chukchi Sea ice gouge orientation data was limited to the gouge data collection provided in USGS 78-693 by Toimil (1978). Similar to other USGS studies, Toimil's (1978) data was corrected to account for the survey vessel's course, although the measurement reference datum was not specified. For the purposes of the present study, it is assumed that the orientation data was measured relative to true north, similar to other USGS survey programs (see discussion of USGS 83-706 / 89-151 above).

Dominant ice gouge orientation frequency data is presented in Table 24 for each region analyzed as part of the current study. As shown in the table, dominant ice gouge orientation frequencies were observed to occur in the 71° to 80° or the 241° to 250° range (relative to true north), thus indicating a general northeast – southwest ice gouging

direction in the Canadian Beaufort, American Beaufort, and Chukchi Seas. As indicated in the table, all publicly available data was combined for analysis (where possible), for water depths inshore of approximately 55 to 65m.

Rosette (or ‘radar’) plots were created for 10° increment ranges during analysis of dominant ice gouge orientation frequencies, as provided in Figure 67 through Figure 69.

Table 24: Dominant Ice Gouge Orientation Analysis Summary Data

Region	Age of Data	Water Depth Range (m)	Sample Size	Dominant Orientation (°)
Canadian Beaufort	Old	27.1 – 53	219	241 – 250
American Beaufort	New & Old	1.2 – 65	3947	71 – 80
Chukchi ^a	Old	21 – 54	503	241 – 250

^a Chukchi Sea dominant ice gouge orientation data does not include information graphically presented in USGS 88-25 as radar plots; this information was deemed too uncertain for use in the present study.

New & Unknown Age Gouge Orientation Frequency - American Beaufort Sea
USGS 83-706 & 89-161 Data Set

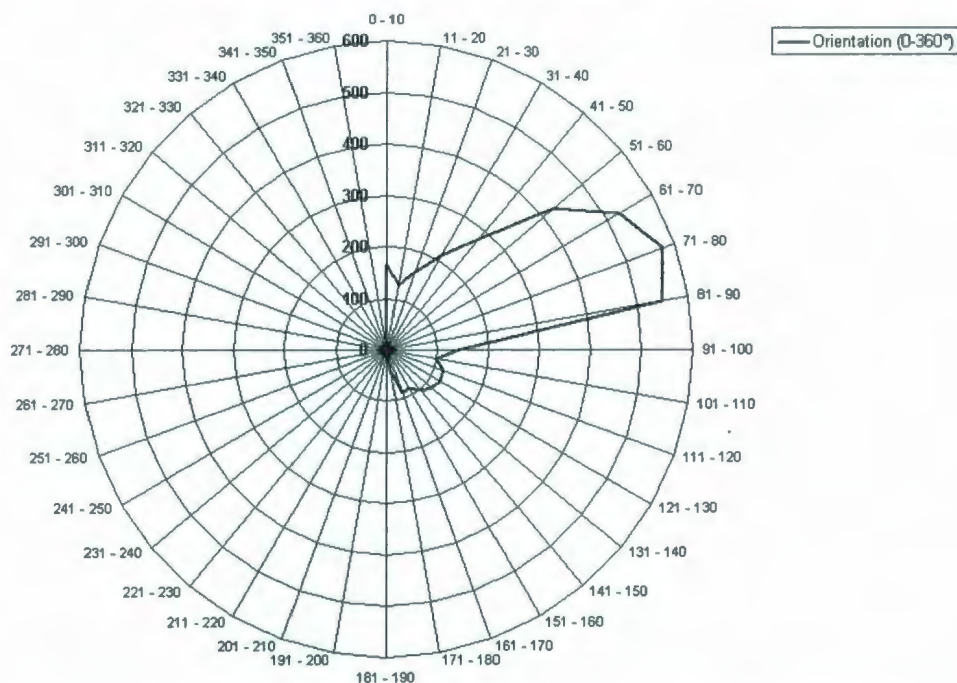


Figure 67: Ice Gouge Orientation Frequency – American Beaufort Sea

Unknown Age Gouge Orientation Frequency - Canadian Beaufort Sea
Wahlgren (1979) & ESRF 129 Data Set

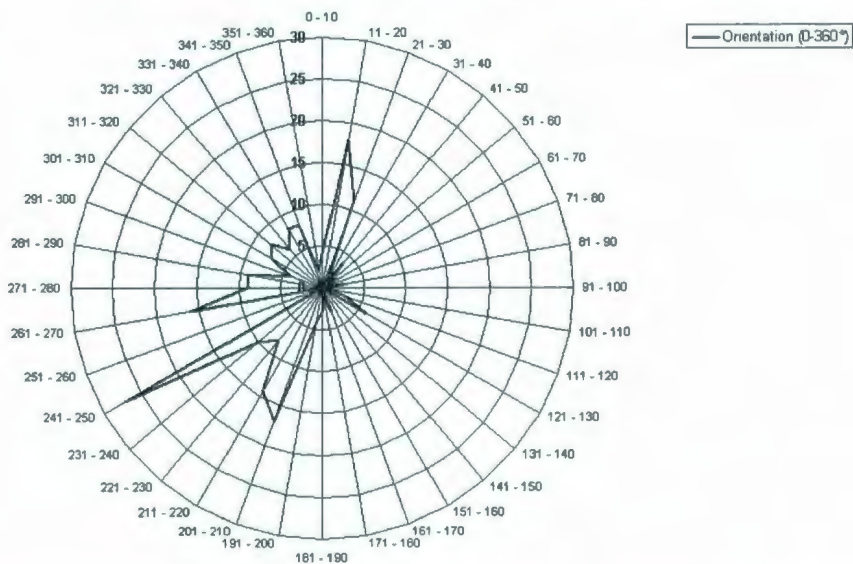


Figure 68: Ice Gouge Orientation Frequency – Canadian Beaufort Sea

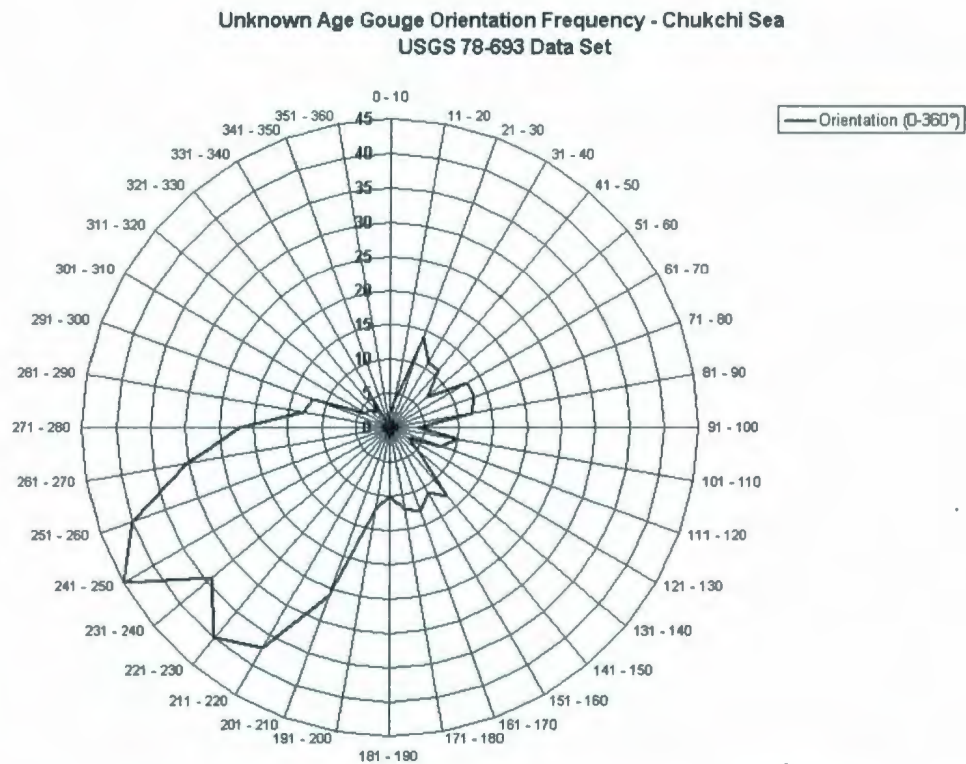


Figure 69: Ice Gouge Orientation Frequency – Chukchi Sea

5.2 PROBABILISTIC GOUGE DEPTH ANALYSIS

The current thesis work has focused on the application of probabilistic analysis of ice gouge depth statistics for prediction of design ice gouge depths. As discussed by Palmer (2000), early ice gouge design practices perceived that subsea arctic pipelines would be safe if trenched and buried below the maximum expected ice gouge depth. However, subsea pipeline design for ice gouge events is moving towards the joint consideration of subgouge soil deformations and pipeline limit state design implications for design optimization, in addition to probabilistic ice gouge parameter analysis. The advancement in pipeline design procedures for ice gouging has resulted from increased knowledge of

subgouge soil deformation and pipeline-soil-ice keel interactions, as well as increased application of limit state pipeline design practices.

Probabilistic ice gouge depth analysis has been conducted for each analyzed statistical distribution in order to assess the suitability and implications of each distribution to ice gouge and subsea pipeline design. Probabilistic analysis was conducted for each investigated region and available water depth and gouge depth ranges. The probability of exceedence for an ice gouge of depth (x) is defined as the complement of the cumulative distribution function (CDF):

$$P[X \geq x] = 1 - F(x) \quad (5.1)$$

Where $F(x)$ is the cumulative distribution function associated with the data distribution.

Exceedence probabilities generated from ice gouge depth distribution fitting were scaled according to the proportion of the data population modeled by the continuous distributions. Scaling was necessary as the gouge depth data were analyzed as mixed distributions and separated at a gouge depth continuity limit which was selected through visual assessment of the entire gouge depth distribution histogram (see Sections 4.3.1 to 4.3.3).

Table 25 provides approximate ice gouge depths corresponding to the 1% exceedence probability for each investigated region, statistical gouge depth distribution, and gouge depth continuity limit. Discrete exceedence probabilities for the selected continuity limits

are provided in Table 26. Exceedence probability plots are provided in Figure 70 through Figure 72 for the American Beaufort, Canadian Beaufort, and Chukchi Seas, respectively.

As discussed in Section 4.3.1, this study has found the three-parameter gamma and Weibull distributions to provide good fits to American Beaufort Sea ice gouge depth data greater than 0.1m. The two-parameter exponential distribution also provided a good fit to the upper end of the distribution but under-predicted shallow gouge records. Exceedence probabilities predicted using each distribution are similar, as shown in Table 25 and Figure 70. Continuous distributions fit to all gouge depth data greater than 0.9m predicted deeper gouge depths at 1% exceedence probability, compared to the recommended 0.1m continuity limit (see Table 25 and exceedence probability plots provided in Appendix A). Therefore, the 0.9m continuity limit produced poorer distribution fits (as discussed in Section 4.3.1) and also increased predicted gouge depths, hence supporting recommendation of the 0.1m limit for American Beaufort Sea gouge depth modeling.

The exponential, gamma, and Weibull distributions also predicted similar ice gouge depth exceedence probabilities in analysis of all available Canadian Beaufort Sea gouge depth data greater than 0.9m, as shown in Table 25 and Figure 71. However, the three-parameter Weibull distribution is recommended, based on discussions provided in Section 4.3.2. Continuous distributions fit using the lower continuity limit (0.1m) predicted deeper gouge depths at 1% exceedence probability, compared to the recommended 0.9m continuity limit (see Table 25 and Appendix A). These results support recommendation of the 0.9m continuity limit for Canadian Beaufort Sea gouge

depth modeling, as 0.1m produced poorer distribution fits (see Section 4.3.2) and increased gouge depth predictions.

As shown in Table 25 and Figure 72, the three-parameter Weibull distribution predicted the largest ice gouge depth exceedence probabilities in analysis of all available Chukchi Sea data greater than 0.45m. However, this distribution is recommended, based on assessment discussed in Section 4.3.3. It must be noted that the Chukchi Sea data set exhibited the most uncertainty as no repetitive mapping gouge data, recurrence rates, or shallow water records were available for use in this study. Thus, only one continuity limit (0.45m) was investigated. Additional Chukchi Sea gouge depth data would be required for further analysis.

As indicated through preceding discussions and analysis, the three-parameter Weibull distribution has consistently been shown to provide a good fit to ice gouge depth from each investigated arctic region (see Section 4.3). The dominant suitability of this distribution may potentially be a result of the shape and scale parameters allowing better fits to data distribution tails, compared to the exponential which is characterized by the mean gouge depth (scale parameter) only.

The Weibull distribution has, however, consistently predicted the deepest gouge depths at the 1% exceedence probability level. Gouge depth continuity limits and associated continuous distributions providing poorer data fits led to deeper gouge depth predictions, compared to the recommended continuity limits for gouge depth modeling.

Table 25: Predicted Ice Gouge Depths, 1% Probability of Exceedence per Statistical Distribution & Continuity Limit (Approximate)

Region	Gouge Depth Continuity Limit (m)	Predicted 1% Exceedence Probability Gouge Depth (m)		
		Exponential Distribution	Gamma Distribution	Weibull Distribution
American Beaufort Sea	0.1 ^a	2.3	2.3	2.4
	0.9	2.4	2.5	2.6
Canadian Beaufort Sea	0.1	3.5	3.6	3.7
	0.9 ^a	3.4	3.4	3.5
Chukchi Sea	0.45	1.3	1.7	1.9

Table 26: Gouge Depth Continuity Limit Discrete Exceedence Probability (Approximate)

Region	Gouge Depth Continuity Limit (m)	Probability of Exceedence
American Beaufort Sea	0.1 ^a	0.55
	0.9	0.13
Canadian Beaufort Sea	0.1	0.999
	0.9 ^a	0.31
Chukchi Sea	0.45	0.24

^a Recommended continuity limit for gouge depth modeling.

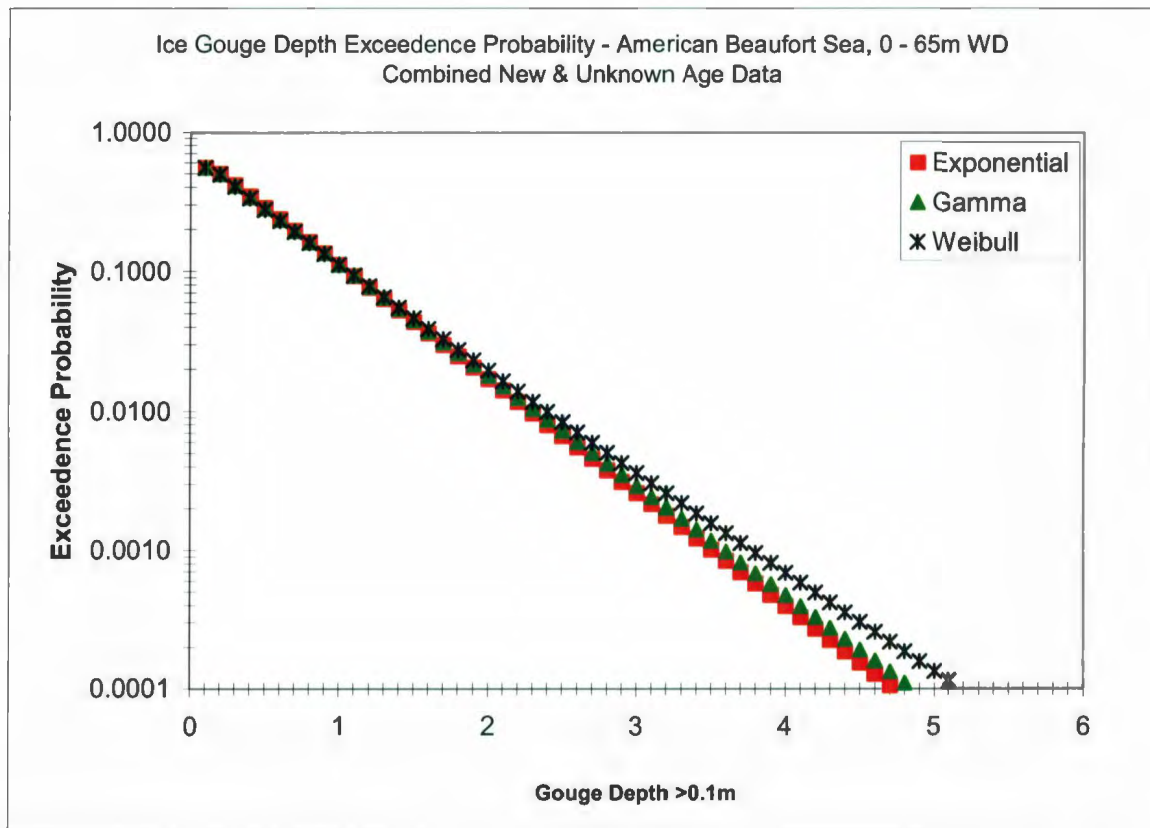


Figure 70: Ice Gouge Depth Exceedence Probability – American Beaufort Sea, 0 – 65m
WD, Gouge Depths >0.1m

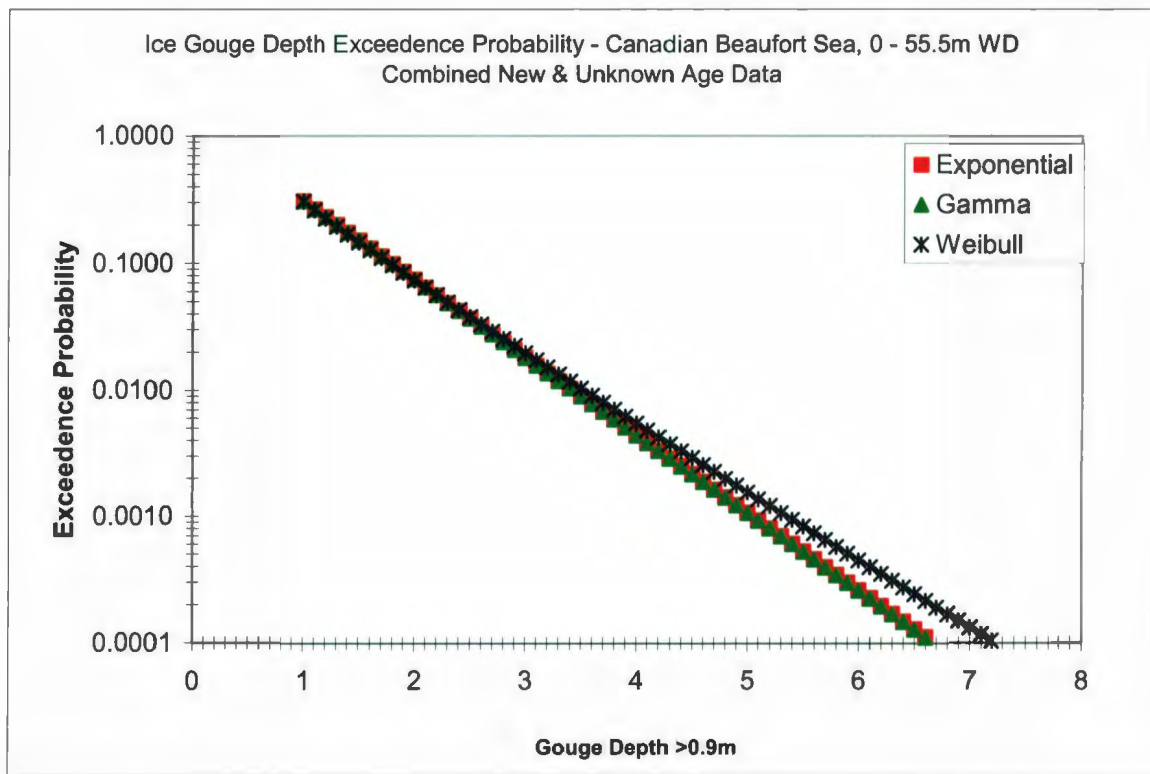


Figure 71: Ice Gouge Depth Exceedence Probability – Canadian Beaufort Sea, 0 – 55.5m
WD, Gouge Depths >0.9m

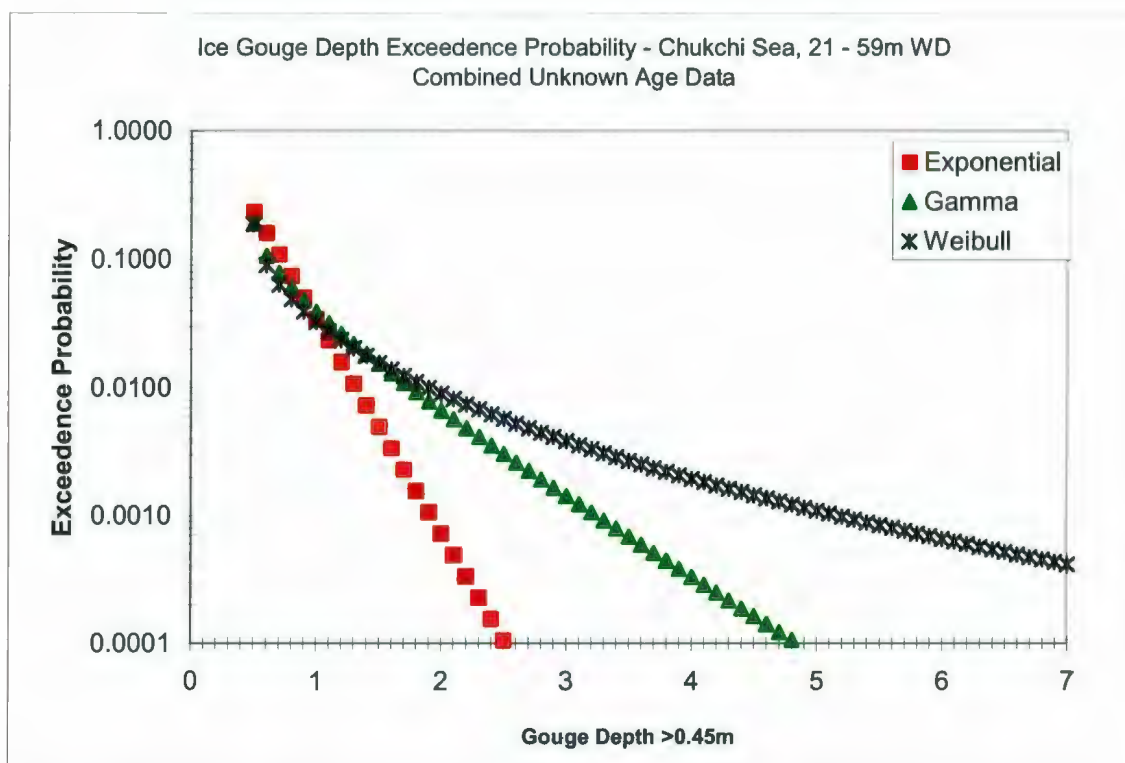


Figure 72: Ice Gouge Depth Exceedence Probability – Chukchi Sea, 21 – 59m WD,
Gouge Depths >0.45m

6 SUMMARY & CONCLUSIONS

The analysis presented in this thesis was conducted for assessment of the most applicable statistical distribution for probabilistic modeling of historical ice gouge depth data from the American Beaufort, Canadian Beaufort, and Chukchi Sea regions. Investigated statistical distributions included the three-parameter gamma and Weibull, and the two-parameter exponential forms. This study has analyzed ice gouge depth data distributions as being mixed with discrete probabilities for shallow gouge depth data, rather than assuming entire distributions to be continuous for the purposes of analysis.

The gamma and Weibull distributions were found to fit American Beaufort Sea ice gouge depth data greater than 0.1m well (see Figure 36 and Figure 38). The exponential distribution underestimated shallower data (see Figure 33). The three-parameter Weibull distribution was found to provide the best fit to available Canadian Beaufort Sea ice gouge depth data greater than 0.9m, based on visual assessment of the distribution fits and associated empirical cumulative distribution functions (see Figure 45 and Figure 46). The three-parameter gamma and Weibull distributions provided better fits to analyzed Chukchi Sea gouge depth data greater than 0.45m than did the exponential; however, neither appeared to fit the data distribution as well as fits provided for the Beaufort Sea data (see Figure 51 and Figure 53). This is due to uncertainty and limited availability of Chukchi Sea gouge depth data; additional data is required for further analysis.

In addition, various ice gouge parameters were analyzed for investigation of correlation exhibited between parameters from each region. Locally weighted scatter plot smoothing

was used to investigate all kinds of possible correlation, but exhibited no obvious relationship between water depth and gouge width, gouge depth and width, or water depth and gouge length data from each of the investigated regions. Available gouge depth data was found to generally increase with increasing water depth; however, this does not consider the effect of gouge infilling and is thus uncertain. Gouge parameter relationships are complex scenarios which involve bathymetry, seabed slope, soil type, and ice feature regime/shielding (i.e., barrier island) effects, among other factors. Potential data correlation may be masked or biased by underestimated gouge records in shallow water locations subject to rapid gouge infilling. Analysis of dominant ice gouge orientation data indicated a general northeast – southwest ice gouging direction in each analyzed region, although these findings were based on uncertain/assumed reference datum for some of the analyzed data collections.

Early investigators (i.e., Lewis, 1977a; 1977b; Weeks et al., 1983; Lanan et al., 1986) have proposed the exponential distribution to be effective, but conservative in modeling ice gouge depth statistics. The current study, as well as work by Nessim and Hong (1992), has found the Weibull distribution to more accurately model ice gouge depth data, and is suggested to provide particularly good fits to extreme gouge depth data which must be considered in design. Recommended probabilistic ice gouge model(s) resulting from assessments conducted as part of this thesis are provided below in Section 6.3.

6.1 ICE GOUGE PARAMETER INFLUENCES

Canadian Beaufort Sea ice gouge parameter interpretation techniques have been found to differ from that utilized in the US Geological Survey's analysis of American Beaufort and Chukchi Sea ice gouging; these subjective interpretation differences have been credited for perceived differences in regional ice gouge regimes. Interpretation subjectivity results from gouge parameter definition (i.e., single versus multiplet gouge definition, measurement datum, and gouge counting techniques) or bias introduced by minimum gouge depth resolution limits (cut-offs), dynamic gouge infilling processes, and large gouge depth reporting intervals/class ranges, among other factors.

Numerous seabed sediment studies and investigations of associated ice gouge effects have been reviewed, with deeper gouges observed in soft silty clay sediments which typically exhibit longer residence times. Wider, shallower ice gouges were reported to occur in sandy seabed sediments. Multiple researcher efforts (Hill et al., 1986; Crooks et al., 1986; Rogers et al., 1993) have shown that weak marine clay seabed sediments such as those found in the western Canadian Beaufort Sea provide low shearing resistance to ice gouge activity. Very strong seabed soils or rock at or near the seafloor surface in the western American Beaufort and Chukchi Seas provide high resistance to ice gouge activity and thus limit possible seabed penetration depths (i.e., due to ice gouging). Moreover, the work of previous researchers (Shearer & Blasco, 1986; Rogers et al., 1993) has found maximum ice gouge depths to exhibit good correlation with maximum low-strength seabed sediment thicknesses. Hence, comprehensive ice gouge analysis

programs must consider seabed sediment types during design gouge depth estimation, as seabed sediments can greatly influence and/or limit potential ice gouge processes.

Seabed sediment properties, general sediment deposition rates, waves, currents, water depth, gouge geometry, and local geography, among other factors, influence the dynamic ice gouge infilling process and thus ice gouge parameter records (see Palmer, 1998; Palmer & Niedoroda, 2005). Sediment transport by wave and current action is the dominant mechanism which infills and obliterates ice gouge depressions, although seabed sediment roughness generally dictates the quantity of sediment available for transport and redistribution in specific areas. Preferential ice gouge infilling may distort seabed ice gouges as a result of differing seabed slopes, dominant wave and/or current patterns, and/or ice gouge orientation. Preferentially infilled gouges generally exhibit non-uniform sediment deposition thickness across the gouge profile, and may consequently lead to inaccurate gouge parameter measurements during geophysical surveying.

6.2 PIPELINE BURIAL DEPTH CONSIDERATIONS

Probabilistic assessment of ice gouge depth statistics may be utilized for prediction of extreme ice gouge depths at specified levels of acceptable risk, based on historical gouge data from a given region and water depth location. However, probabilistic analysis (as investigated in this thesis) only considers numerical ice gouge depth statistical modeling, and neglects factors such as the methods used to obtain the data (Section 2.1), gouge depth resolution cut-offs (Section 2.8), the effects of dynamic environmental activities (sedimentation, gouge infilling, reworking; Section 3.4), pipeline and gouge orientations,

ice gouge recurrence rates (Section 3.5), and pipeline length, among other factors. Literature review has shown all of these factors to contribute to, and influence, ice gouge processes and/or ice gouge-pipeline interactions.

These effects were not integrated in probabilistic ice gouge depth analysis conducted as part of this thesis, but must be considered in regional ice gouge/burial depth analysis programs. Design ice gouge depths should not be selected on the basis of probabilistic assessments only.

Palmer (1998) has indicated that actual seabed ice gouges are irrelevant to the ice gouging problem, except as indicators of the ice gouging process and records of the depth to which ice has gouged the seabed. Therefore, Palmer (1998) has suggested that pipeline design engineers must focus on the pipeline's resistance to damage, as opposed to the physical ice gouge deformation in determination of pipeline burial depths required for ice gouge risk mitigation.

Research of ice-soil-pipeline interactions has shown that a buried subsea pipeline is not necessarily protected from ice gouge risks if it is simply buried sufficiently below the maximum possible gouge depth to avoid direct ice keel – pipeline contact. Subgouge deformations may occur to some depth below the gouging ice keel and impart significant structural loadings upon the buried pipeline. The principal objective of probabilistic analysis is to determine design ice gouge geometries and preliminary pipeline burial depth estimates for use in ice-soil-pipeline interaction analysis and design burial depth estimation.

6.3 RECOMMENDED ICE GOUGE MODEL

The three-parameter Weibull distribution was assessed to provide a good fit to ice gouge depth data in the upper distribution tails of Beaufort and Chukchi Sea data collections. Based on the findings of this study, a mixed distribution using the Weibull distribution is recommended for modeling of historic ice gouge depth data collected across the full range of regional water depth records. Applicable gouge depth continuity limits are summarized in Table 26; 0.1m is recommended for the American Beaufort Sea, whereas 0.9m is recommended for analysis of Canadian Beaufort Sea data. Only one continuity limit (0.45m) was investigated for the Chukchi Sea due to data uncertainty and a lack of shallow water depth records.

The data discontinuities were simply characteristics of the available data used for analysis and may be influenced by available ice gouge driving forces, water depths, ice feature types, gouge infilling, and seabed sediments. These values were assigned discrete probabilities of exceedence, with scaled exceedence probabilities predicted from continuous distributions fit to gouge depth data greater than the limits. As discussed above in Sections 4.2 and 4.3, this recommendation is based on visual assessment of gouge depth data histograms and cumulative distribution functions.

These recommendations are also supported by the results of a previous study by Nessim and Hong (1992) which found the gamma and/or Weibull distributions to provide the best fit to known age Canadian Beaufort Sea ice gouge depth data. However, Nessim and

Hong's (1992) study treated the analyzed data distribution as continuous (see Section 4.4); this study has provided modeling and assessment of mixed distributions.

Uncertainty in pipeline burial depth estimates may be reduced by probabilistic analysis of mixed ice gouge depth distributions; however, dynamic infilling processes significantly influence the amount of shallow gouge depth data. Consideration of ice gouge infilling effects may lead to selection of different gouge depth continuity limits than used in the present study.

It must be stated that the preceding statistical distribution and probabilistic assessments were based on analysis of combined new and unknown age ice gouge depth data collected in the American and Canadian Beaufort Seas. Only unknown age data records from the Chukchi Sea were found for use in this thesis. Design ice gouge depth assessment based on old ice gouge statistics may potentially over-predict deepwater gouge depths beyond the limits of modern ice keel drafts, as unknown age gouges may have been formed during periods of lower water depths. Assessment of separated new and unknown age ice gouge depth data distributions may lead to the recommendation of alternate statistical distributions for use in regional ice gouge and pipeline design procedures.

6.4 AREAS FOR FURTHER WORK

The following potential areas for further work have been derived from this thesis and are recommended for consideration in future investigations:

- The preceding analysis has provided statistical assessment of combined new and unknown age ice gouge data; future studies should investigate this data separately.
- This thesis work has identified a paucity of Canadian Beaufort Sea ice gouge data available in the public domain, although a significant amount of interpreted data is proprietary to Canadian Seabed Research Ltd. The preceding analysis should be updated and revised if this data becomes available for public use.
- Additional ice gouge data collection (repetitive mapping program) is required for the Chukchi Sea. Current assessments were conducted for a limited amount of unknown age data only. At present, no ice gouge recurrence rate information has been found publicly available for the Chukchi Sea. This information is pertinent to understanding ice gouge processes and will be required for future analyses.
- Sediment infilling data should be analyzed to counteract ice gouge parameter bias due to gouge infilling, and further work should be undertaken to investigate the effects of infilling on mixed gouge depth distribution modeling. Methods could include probabilistic derivation of typical sediment infilling thicknesses on a regional and/or water depth range basis, or adjustment of gouge depth records to account for applicable infill thickness data. This study should be updated if/when sediment infilling analysis is conducted.

- The preceding ice gouge depth analysis was conducted for water depth and gouge depth subdivisions only. Additional factors should be considered in future investigations, including:
 - Detailed analysis of continuous ice gouge profiling data (if available) to determine gouge depth and width correlations;
 - Analysis of ice gouge data to establish/evaluate correlations with geotechnical and environmental data;
 - Analysis of satellite imagery to link future ice gouge surveys with ice feature regimes and single-keeled versus multiplet zone estimates; and,
 - Analytical or numerical models to supplement gouge data records or confirm bounding envelope limits on gouge depth and width as a function of soil type and strength, and ice type and strength.

7 BIBLIOGRAPHY & REFERENCES

Abdelnour, R., Lapp, D., Haider, S., Shinde, S.B. & Wright, B. (1981). *Model Tests of Sea Bottom Scouring*. Proceedings, 6th International Conference on Port and Ocean Engineering Under Arctic Conditions.

APOA (1980). *Sea-bed Scouring by Ice*. Arctic Petroleum Operators Association, APOA Review, Vol. 3, No. 1, March, pgs. 17 – 18.

d'Apollonia, S.J. & Lewis, C.F.M. (1986). *Numerical Model for Calculating Spatial Distribution and Mean Frequency of Iceberg Grounding Events*. Proceedings, Ice Scour and Seabed Engineering, Proceedings of a Workshop on Ice Scour Research, Environmental Studies Revolving Funds Report No. 049, pgs. 221 – 232, December.

Barker, A. & Timco, G. (2002a). *Laboratory Experiments of Ice Scour Processes: Buoyant Ice Model*. Canadian Hydraulics Centre, National Research Council Canada. Technical Report CHC-TR-006, PERD/CHC Report 31-29, May.

Barker, A. & Timco, G. (2002b). *Laboratory Experiments of Ice Scour Processes: Rigid Ice Indentor*. Cold Regions Science and Technology, Vol. 35, pgs. 195 – 206.

Barker, A. & Timco, G. (2003). *Laboratory Experiments of Ice Scour Processes: Buoyant Ice Model*. Cold Regions Science and Technology, Vol. 36, pgs. 103 – 114.

Barnes, P.W. & Reimnitz, E. (1974). *Sedimentary Processes on Arctic Shelves Off the Northern Coast of Alaska*; in Reed, J.C. & Sater, J.E. (editors), *The Coast and Shelf of the Beaufort Sea*, The Arctic Institute of North America, Arlington, VA.

Barnes, P.W., Reimnitz, E., Drake, D. & Toimil, L. (1977). *Miscellaneous Hydrologic and Geologic Observations on the Inner Beaufort Sea Shelf, Alaska*. United States Geological Survey Open-File Report 77-477.

Barnes, P.W. & Hopkins, D.M. (editors) (1978). *Geological Sciences, in Environmental Assessment of the Alaskan Continental Shelf*. Interim Synthesis: Beaufort/Chukchi: US Department of Commerce, National Oceanic and Atmospheric Administration, Boulder, CO. Annual Report, pgs 101 – 133.

Barnes, P.W., McDowell, D., & Reimnitz, E. (1978). *Ice-Gouging Characteristics: Their Changing Patterns from 1975-1977, Beaufort Sea, Alaska*. United States Geological Survey Open-File Report 78-730.

Barnes, P.W. & Reimnitz, E. (1979). *Ice Gouge Obliteration and Sediment Redistribution Event; 1977-1978, Beaufort Sea, Alaska*. United States Geological Survey Open-File Report 79-848.

Barnes, P.W., Reimnitz, E. & Rearic, D. M. (1982). *Ice Gouge Characteristics Related to Sea-ice Zonation, Beaufort Sea, Alaska*. USGS, Pacific-Arctic Branch of Marine Geology, Menlo Park, CA. Prepared for Presentation at NRC Canada Ice Scour Workshop, Montebello, QC, April 1985.

Barnes, P. W. & Rearic, D. M. (1985). *Rates of Sediment Disruption by Sea Ice as Determined From Characteristics of Dated Ice Gouges Created Since 1975 on the Inner Shelf of the Beaufort Sea, Alaska*. United States Geological Survey Open-File Report 85-463.

Barnes, P.W. & Reimnitz, E. (1986). *Ice Gouge Studies, Alaskan Beaufort Sea*. Proceedings, Ice Scour and Seabed Engineering, Proceedings of a Workshop on Ice Scour Research. Environmental Studies Revolving Funds Report No. 049.

Barrie, J.V. & Woodworth-Lynas, C.M.T. (1984). *Ice Scour; Methods of Analysis*. Proceedings, *A Short Course on the Sediment Stability of the Canadian Shelves*, March 9 – 10th, 1982.

Been, K., Palmer, A. & Comfort, G. (1990a). *Analysis of Subscour Stresses and Probability of Ice Scour-Induced Damage for Buried Submarine Pipelines, Vol. II: Deterministic Model of Ice-Soil-Pipeline Interaction*. Panel for Energy Research and Development and Canada Oil and Gas Lands Administration – Energy, Mines and Resources, February.

Been, K., Kosar, K., Hachey, J., Rogers, B.T. & Palmer, A.C. (1990b). *Ice Scour Models*. Proceedings, 9th International Conference on Offshore Mechanics and Arctic Engineering, Vol. 5, pgs. 179 – 188.

Been, K. (1990c). *Mechanisms of Failure and Soil Deformation during Scouring*. Proceedings, Workshop on Ice Scouring and the Design of Offshore Pipelines, Calgary,

AB, April 18th – 19th, pgs. 179 – 191. Sponsored by Canada Oil & Gas Lands Administration and the Centre for Cold Ocean Resource Engineering, October.

Birch, R., Fissel, D., Melling, H., Vaudrey, K., Schaudt, K., Heideman, J. & Lamb, W. (n.d.). *Ice Profiling Sonar: Upward Looking Sonar Provides Over-Winter Records of Ice Thickness and Ice Keel Depths off Sakhalin Island, Russia.*

Blasco, S.M., Shearer, J.M., & Myers, R. (n.d.) *Seabed Scouring by Sea-Ice: Canadian Beaufort Shelf.*

Blasco, S.M. (1985). *Ice Scour Terminology.* Proceedings, Ice Scour and Seabed Engineering, Proceedings of a Workshop on Ice Scour Research, Environmental Studies Revolving Funds Report No. 049, December.

Blasco, S.M., Shearer, J.M., & Myers, R. (1998). *Seabed Scouring by Sea-Ice: Scouring Process and Impact Rates: Canadian Beaufort Shelf.* Proceedings of Ice Scour and Arctic Marine Pipelines Workshop. 13th International Symposium on Okhotsk Sea & Sea Ice, Mombetsu, Hokkaido, Japan, Feb. 1st – 4th.

Blasco, S. (2005). *PERD Pipeline POL, Ice Scour Research.* Proceedings, Program of Energy Research and Development Workshop, Oil & Gas Engineering Issues for the Beaufort Sea, October 18th – 19th, Calgary, AB. PERD/CHC Report 60-117.

Brooks, L.D. (1973). *Ice Scouring on the Northern Continental Shelf of Alaska.* Proceedings, Offshore Technology Conference, OTC 1813.

Brooks, L.D. (1983). *Statistical Analyses of Pressure Ridge Keel Definitions and Distributions*. Proceedings, 8th International Conference on Port and Ocean Engineering under Arctic Conditions.

C-CORE (1999). *Preliminary Report: Risk Assessment for Ice Damage to Subsea Pipelines*. Report submitted to the US Minerals Management Service by C-CORE, St. John's, NL, December 22nd. MMS TA&R Project No. 320.

C-CORE (2008). *Design Options for Offshore Pipelines in the US Beaufort and Chukchi Seas*. Prepared for US Minerals Management Service, C-CORE Report No. R-07-078-519, April.

Caulfield Engineering (1979). *Preliminary Field Report for 1979 Ice Scour Survey*. Prepared for Canadian Marine Drilling Limited (CANMAR), Calgary, AB. Project No. 1005, September.

Chari, T.R. (1979). *Geotechnical Aspects of Iceberg Scours on Ocean Floors*. Canadian Geotechnical Journal, Vol. 16, pgs. 379 – 390.

Chari, T.R., Green, H.P. & Reddy, A.S. (1982). *Some Geotechnical Aspects of Iceberg Furrows*. Proceedings, 2nd Canadian Conference on Marine Geotechnical Engineering, Halifax, NS, June.

Chari, T.R. (1986). *Iceberg-Scour Modelling at Memorial University of Newfoundland*. Proceedings, Ice Scour and Seabed Engineering, Proceedings of a Workshop on Ice

Scour Research, Environmental Studies Revolving Funds Report No. 049, pgs. 109 – 117, December.

Chouinard, L.E. (1995). *Estimation of Burial Depths for Pipelines in Arctic Regions*. Journal of Cold Regions Engineering, December, pgs. 167 – 182.

Clark, J.I. & Zhu, F. (2000). *Comparison of Ice Strength and Scour Resistance*. Proceedings, 2nd Ice Scour and Arctic Marine Pipelines Workshop, 15th International Symposium on Okhotsk Sea & Sea Ice, pgs. 141 – 149.

Comfort, G. & Graham, B. (1986). *Evaluation of Sea-bottom Ice Scour Models*. Environmental Studies Revolving Funds Report No. 037, Ottawa.

Comfort, G. (1990). *A Case Study Analysis of the Probability of Ice Scour-Induced Damage for Submarine Pipelines*. Proceedings, Workshop on Ice Scouring and the Design of Offshore Pipelines, Calgary, AB, April 18th – 19th, pgs. 145 – 162. Sponsored by Canada Oil & Gas Lands Administration and the Centre for Cold Ocean Resource Engineering, October.

Comfort, G., Gilbert, C., & Ferregut, C. (1990). *Analysis of Subscour Stresses and Probability of Ice Scour-Induced Damage for Buried Submarine Pipelines, Vol. I, Database of Key Ice Scour Parameters*. Panel for Energy Research & Development and Canada Oil and Gas Lands Administration – Energy Mines and Resources Indian and Northern Affairs, March.

Croasdale, K., Comfort, G. & Been, K. (2005). *Investigation of Ice Limits to Ice Gouging*. Proceedings, 18th International Conference on Port and Ocean Engineering Under Arctic Conditions, Vol.1, pgs. 23 – 32.

Crooks, J.H.A., Jefferies, M.G., Becker, D.E. & Been, K. (1986). *Geotechnical Properties of Beaufort Sea Clays*. Proceedings, 3rd Canadian Conference on Marine Geotechnical Engineering, Vol. 1, pgs. 329 – 343, St. John's, NL, June.

CSR (2008). *2005 Beaufort Sea Ice Scour Repetitive Mapping Program*. Draft report submitted to the Geological Survey of Canada, Atlantic, Bedford Institute of Oceanography, Dartmouth, NS. Prepared by Canadian Seabed Research Ltd, Project No. 0603, February 28th.

Davis, L., Ralph, T., Cumming, E., Sonnichsen, G.V. & King, T. (2005). *Morphometric Analysis of Iceberg Scours using Multibeam Sonar Bathymetry Data, Eastern Canadian Continental Shelf*. Proceedings, 18th International Conference on Port and Ocean Engineering under Arctic Conditions.

Devore, J.L. (2004). *Probability and Statistics for Engineering and the Sciences*. 6th Edition, Brooks / Cole – Thomson Learning, CA.

Dobson, B.M. & Wickham, J.T. (1985). *Overview of Soil and Engineering Geologic Conditions in the Beaufort, Chukchi, and Bering Seas*. Civil Engineering in the Arctic Offshore, Proceedings of the Conference Arctic '85, American Society of Civil Engineers.

Gaskill, H. & Lewis, C.F.M. (1988). *On the Spatial Frequency of Linear Ice Gouge Scours on the Seabed*. Cold Regions Science and Technology, Vol. 15, pgs. 107 – 130.

Gilbert, G.R., Blasco, S., Stirbys, A.F. & Lewis, C.F.M. (1985). *Beaufort Sea Ice Scour Analysis using a Computerized Data Base*. Proceedings, Offshore Technology Conference, OTC 4969.

Gilbert, G. & Pedersen, K. (1987). *Ice Scour Data Base for the Beaufort Sea*. Environmental Studies Revolving Funds Report No. 055, January.

Gilbert, G.R. (1989). *Ice Scour Morphology Study, Kringalik Pipeline Corridor Analysis, and New Scour Update, Beaufort Sea*. Report submitted to the Geological Survey of Canada.

Gilbert, G.R., DeLory, S.J. & Pederson, K. (1989). *Beaufort Sea Ice Scour Data Base (SCOURBASE) Update to 1986*. Environmental Studies Research Funds Report No. 097, March.

Gilbert, G.R. (1990). *Scour Shape and Sub-Scour Disturbance Studies from the Canadian Beaufort Sea*. Proceedings, Workshop on Ice Scouring and the Design of Offshore Pipelines, Calgary, AB, April 18th – 19th, pgs. 127 – 144. Sponsored by Canada Oil & Gas Lands Administration and the Centre for Cold Ocean Resource Engineering, October.

Goodwin, C.R., Finley, J.C. & Howard, L.M. (1985). *Ice Scour Bibliography*. Environmental Studies Revolving Funds Report No. 010, July.

Grantz, A., Dinter, D.A., Hill, E.R., May, S.D., McMullin, R.H., Phillips, R.L. & Reimnitz, E. (1982a). *Geologic Framework, Hydrocarbon Potential, and Environmental Conditions for Exploration and Development of Proposed Oil and Gas Lease Sale 87 in the Beaufort and Northeast Chukchi Seas*. USGS Open-File Report 82-482.

Grantz, A., Dinter, D.A., Hill, E.R., Hunter, R.E., May, S.D., McMullin, R.H. & Phillips, R.L. (1982b). *Geologic Framework, Hydrocarbon Potential, and Environmental Conditions for Exploration and Development of Proposed Oil and Gas Lease Sale 85 in the Central and Northern Chukchi Sea*. USGS Open-File Report 82-1053.

Green, H.P., Reddy, A.S. & Chari, T.R. (1983). *Iceberg Scouring and Pipeline Burial Depths*. Proceedings, 8th International Conference on Port and Ocean Engineering under Arctic Conditions.

Héquette, A., Desrosiers, M. & Barnes, P.W. (1995). *Sea Ice Scouring on the Inner Shelf of the Southeastern Canadian Beaufort Sea*. Marine Geology, Vol. 128, pgs. 201 – 219.

Hill, P.R., Moran, K., Kurfurst, P.J. & Pullan, S. (1986). *Physical and Sedimentological Properties of Nearshore Sediments in the Southern Beaufort Sea*. Proceedings, 3rd Canadian Conference on Marine Geotechnical Engineering, Vol. 1, pgs. 301 – 327, St. John's, NL, June.

Hnatiuk, J. & Brown, K.D. (1977). *Sea Bottom Scouring in the Canadian Beaufort Sea*. Proceedings, Offshore Technology Conference, OTC 2946.

Hnatiuk, J. & Wright, B.D. (1983). *Sea Bottom Scouring in the Canadian Beaufort Sea*. Proceedings, Offshore Technology Conference, OTC 4584.

Hunter, R.E. & Reiss, T.E. (1983). *Inner-Shelf Geology of Southeastern Chukchi Sea*. Attachment C of the U.S. Department of the Interior Minerals Management Service *Outer Continental Shelf Environmental Assessment Program (OCSEAP) 1985*, pgs. 97 – 124, August.

Hunting Geology & Geophysics Ltd (1971). *Investigation of Sea-Bed Scouring in the Beaufort Sea*. Arctic Petroleum Operators Association Project No. 19, November.

Hunting Geology & Geophysics Ltd (1973). *Investigation of Sea-Bed Scouring in the Beaufort Sea (Phase II)*. Arctic Petroleum Operators Association Project No. 32, February.

INTEC (1986). *Chukchi Sea Transportation Feasibility and Cost Comparison Joint Industry Study*, vol. 1. INTEC Job No. H-046.2, May. MMS TA&R Project No.105

INTEC (1991). *Chukchi Sea Transportation Feasibility and Cost Comparison: Joint Industry Study Update*. INTEC Job No. H-046.4, July. MMS TA&R Project 164.

Jukes, P., Eltaher, A., Abdalla, B. & Duron, B. (2008). *The Design and Simulation of Arctic Subsea Pipelines*. DNV Conference on Arctic activities; Høvik.

K.R. Croasdale & Associates Ltd. (2000). *Study of Iceberg Scour & Risk in the Grand Banks Region*. Submitted to National Research Council Canada, PERD/CHC Report 31-26, March.

Kempema, E.D. (1985). *Ice Gouge Infilling and Shallow Shelf Deposits in Eastern Harrison Bay, Beaufort Sea, Alaska*. Proceedings, Outer Continental Shelf Environmental Assessment Program, Final Reports of Principal Investigators, Vol. 34, August.

Kenny, S., McKenna, R.F., Phillips, R. & Clark, J.I. (2000). *Response of Buried Marine Arctic Pipelines to Ice Gouge Events*. Proceedings, ETCE/OMAE2000 Joint Conference, Energy for the New Millennium.

Kenny, S., McKenna, R., Bruce, J., Nobahar, A., King, T. & Phillips, R. (2004). *Probabilistic Design Methodology to Mitigate Ice Gouge Hazards for Offshore Pipelines*. Proceedings, International Pipeline Conference, IPC04-0527.

Kenny, S., Phillips, R., Clark, J., & Nobahar, A. (2005). *PRISE Numerical Studies on Subgouge Deformations and Pipeline/Soil Interaction Analysis*.

Kenny, S., Palmer, A. & Been, K. (2007a). *Design Challenges for Offshore Pipelines in Arctic Environments*. IBC Energy, 15 pgs.

Kenny, S., Barrett, J., Phillips, R. & Popescu, R. (2007b). *Integrating Geohazard Demand and Structural Capacity Modelling within a Probabilistic Design Framework*

for Offshore Arctic Pipelines. Proceedings, 7th International Offshore and Polar Engineering Conference.

King, A.D., McKenna, R.F., Jordaan, I.J. & Sonnichsen, G.V. (2003). *A Model for Predicting Iceberg Grounding Rates on the Seabed*. Proceedings, 17th International Conference on Port and Ocean Engineering under Arctic Conditions.

King, E.L., Gillespie, R.T., Carter, W.J. & Cumming, E.H. (1989). *Regional Ice Scour Database Update Studies*. Environmental Studies Research Funds Report No. 105, October.

Kioka, S. & Saeki, H. (1995). *Mechanisms of Ice Gouging*. Proceedings, 5th International Offshore and Polar Engineering Conference, Vol. II, pgs. 398 – 402. Reference not found – provided here for information only.

Kioka, S., Terai, Y., Otsuka, N., Honda, H., & Saeki, H. (1998). *Mechanical Model of Ice Gouging on Sloping Sandy Beach*. Proceedings, Ice Scour and Arctic Marine Pipelines Workshop, 13th International Symposium on Okhotsk Sea & Sea Ice, pgs. 71 – 76.

Konuk, I. & Gracie, R. (2004). *A 3-Dimensional Eulerian Finite Element Model for Ice Scour*. Proceedings, International Pipeline Conference. IPC04-0075.

Konuk, I., Yu, S. & Gracie, R. (2005). *A 3-Dimensional Continuum ALE Model for Ice Scour – Study of Trench Effects*. Proceedings, 24th International on Offshore Mechanics and Arctic Engineering. OMAE2005-67547.

Konuk, I., Liferov, P. & Løset, S. (2007). *Challenges in Modelling Ice Gouge and Pipeline Response*. Proceedings, 19th International Conference on Port and Ocean Engineering Under Arctic Conditions.

Kovacs, A. (1972). *Ice Scoring Marks Floor of the Arctic Shelf*. The Oil and Gas Journal, October 23rd, 1972.

Kovacs, A., Weeks, W.F., Ackley, S. & Hibler, W.D. (1973). *Structure of a Multi-year Pressure Ridge*. Reprinted from ARCTIC, Journal of the Arctic Institute of North America, Vol.26, No.1.

Kovacs, A. & Mellor, M. (1974). *Sea Ice Morphology and Ice as a Geologic Agent in the Southern Beaufort Sea*. US Army Corps of Engineers Cold Regions Research and Engineering Laboratory, Hanover, NH. Reprinted from The Coast and Shelf of the Beaufort Sea, The Arctic Institute of North America, Arlington, VA.

Kovacs, A. & Gow, A.J. (1976). *Some Characteristics of Grounded Floebergs Near Prudhoe Bay, Alaska*. Prepared by the US Army Corps of Engineers Cold Regions Research and Engineering Laboratory, Hanover, NH, for the National Oceanic and Atmospheric Administration. CRREL Report 76-34. September 1976.

Kovacs, A. (1983). *Characteristics of Multi-year Pressure Ridges*. US Army Corps of Engineers, Cold Regions Research & Engineering Laboratory. Reprinted from VTT Symposium 37, Proceedings, 7th International Conference on Port and Ocean Engineering, Vol.3.

Kovacs, A., Valleau, N. & Holladay, J.S. (1987). *Airborne Electromagnetic Sounding of Sea Ice Thickness and Sub-Ice Bathymetry*. Prepared by the US Army Corps of Engineers Cold Regions Research and Engineering Laboratory, Hanover, NH, for Naval Ocean Research and Development Activity. CRREL Report 87-23. December 1987.

Kovacs, A. & Holladay, J.S. (1989). *Development of an Airborne Sea Ice Thickness Measurement System and Field Test Results*. Prepared by the US Army Corps of Engineers Cold Regions Research and Engineering Laboratory, Hanover, NH, for US Department of Navy, Naval Oceanographic and Atmospheric Research Laboratory. CRREL Report 89-19. December 1989.

Lanan, G.A., Niedoroda, A.W. & Weeks, W.F. (1986). *Ice Gouge Hazard Analysis*. Proceedings, Offshore Technology Conference, OTC 5298.

Lever, J.H., editor (2000). *Assessment of Millennium Pipeline Project Lake Erie Crossing, Ice Scour, Sediment Sampling, and Turbidity Modeling*. US Army Corps of Engineers, Engineer Research and Development Center & Cold Regions Research and Engineering Laboratory, ERDC/CRREL TR-00-13.

Lewis, C.F.M., Blasco, S.M., McLaren, P. & Pelletier, B.R. (1976). *Ice Scour on the Canadian Beaufort Sea Continental Shelf*. Program, Geological Association of Canada, Vol. 1, pg. 83. Abstract Only.

Lewis, C.F.M. (1977a). *The Frequency and Magnitude of Drift-Ice Groundings from Ice-Scour Tracks in the Canadian Beaufort Sea*. Proceedings, 4th International Conference on Port and Ocean Engineering under Arctic Conditions.

Lewis, C.F.M. (1977b). *Bottom Scour by Sea Ice in the Southern Beaufort Sea*. Beaufort Sea Project, Department of Fisheries and the Environment. Technical Report No. 23, APOA Project No. 72.

Lewis, C.F.M. (1977c). *Scouring of the Beaufort Shelf by Sea Ice*. Program, Geological Association of Canada, Vol. 2, pg.32. Abstract Only.

Lewis, C.F.M., Parrott, D.R., Simpkin, P.G. & Buckley, J.T., editors (1986). *Proceedings of a Workshop on Ice Scour and Seabed Engineering*. Environmental Studies Revolving Funds Report No. 049.

Lewis, C.F.M. & Blasco, S.M. (1990). *Character and Distribution of Sea-Ice and Iceberg Scours*. Proceedings, Workshop on Ice Scouring and the Design of Offshore Pipelines, Calgary, AB, April 18th – 19th, pgs. 57 – 102. Sponsored by Canada Oil & Gas Lands Administration and the Centre for Cold Ocean Resource Engineering, October.

Liferov, P., Shkhinek, K.N., Vitali, L. & Serre, N. (2007). *Ice Gouging Study – Actions and Action Effects*. Proceedings, 19th International Conference on Port and Ocean Engineering Under Arctic Conditions.

Marcellus, R.W. & Morrison, T.B. (1986). *Some Recent Studies Relating to the Determination of Pipeline Depths*. Proceedings, Ice Scour and Seabed Engineering,

Proceedings of a Workshop on Ice Scour Research, Environmental Studies Revolving Funds Report No. 049, pgs. 295 – 303, December.

Marcellus, R.W. & Roth, D.R. (1991). *Comparison of Canadian and Alaskan Beaufort Sea Ice Scour Depth Data and Analysis Procedures*. Proceedings, 11th International Conference on Port and Ocean Engineering Under Arctic Conditions.

Marchenko, A. (2005). *Forming of Seabed Scours by Tidal Drift of a Floe Joined to a Grounded Ice Ridge*. Proceedings, 18th International Conference on Port and Ocean Engineering Under Arctic Conditions.

McKenna, R., King, T., Brown, R., Bruce., J. & Phillips, R. (2003). *Ice Gouge Risk to Offshore Pipelines – Making the Most of Available Data*. Proceedings, 17th International Conference on Port and Ocean Engineering under Arctic Conditions.

Miley, J.M, & Barnes, P.W., editors. (1986). *1985 Field Studies, Beaufort and Chukchi Seas, Conducted from the NOAA Ship Discoverer*. USGS Open-File Report 86-202.

Minitab (2007). *Minitab Version 15 Help Files*.

Minitab (2008). *What is the Anderson-Darling Goodness-of-fit Test Statistic?* Available Online (<http://www.minitab.com/support/answers/answer.aspx?id=731>).

Morrison, T.B. & Marcellus, R.W. (1985). *Comparison of Alaskan and Canadian Beaufort Sea Ice Scour Data and Methodologies*. Proceedings, 8th International Conference on Port and Ocean Engineering Under Arctic Conditions.

MMS (1987). *Chukchi Sea Oil & Gas Lease Sale 109, Final Environmental Impact Statement*. OCS EIS/EA MMS 87-0110.

MMS (1990). *Chukchi Sea Oil and Gas Lease Sale 126, Final Environmental Impact Statement*. OCS EIS/EA MMS 90-0095.

MMS (1996). *Final Environmental Impact Statement: Beaufort Sea Planning Area Oil and Gas Lease Sale 144*. Minerals Management Service, Alaska OCS Region, OCS EIS/EA MMS 1996-0012.

MMS (2006). *Final Programmatic Environmental Assessment: Arctic Ocean Outer Continental Shelf Seismic Surveys – 2006 (Oooguruk Project)*. Minerals Management Service, Alaska OCS Region, OCS EIS/EA MMS 2006-038.

MMS (2002). *Liberty Development & Production Plan, Final Environmental Impact Statement*. US Department of the Interior, Minerals Management Service, report no. OCS EIS/EA MMS 2002-020.

MMS (2003). *Beaufort Sea Planning Area Oil and Gas Lease Sales 186, 195, and 202, Final Environmental Impact Statement*. OCS EIS/EA MMS 2003-001.

MMS (2007). *Chukchi Sea Oil & Gas Lease Sale 193 and Seismic Surveying Activities in the Chukchi Sea, Final Environmental Impact Statement*. OCS EIS/EA MMS 2007-026.

Mudie, P.J. (1986). *Palynology as a Method for Dating Iceberg Scours*. Proceedings, Ice Scour and Seabed Engineering, Proceedings of a Workshop on Ice Scour Research, Environmental Studies Revolving Funds Report No. 049, December.

Myers, R., Blasco, S., Gilbert, G., & Shearer, J. (1996). *1990 Beaufort Sea Ice Scour Repetitive Mapping Program*. Environmental Studies Research Funds Report No. 129.

Nessim, M. & Hong, H. (1992). *Statistical Data Analysis of New Scour Characteristics in the Beaufort Sea*. C-FER Technologies Draft Report Submitted to Energy, Mines & Resources, Bedford Institute of Oceanography, May, Project 92-03.

NIST/SEMATECH (2008). *e-Handbook of Statistical Methods*. Available Online (<http://www.itl.nist.gov/div898/handbook>).

Nobahar, A., Kenny, S., King, T., McKenna, R. & Phillips, R. (2007). *Analysis and Design of Buried Pipelines for Ice Gouging Hazard: A Probabilistic Approach*. Journal of Offshore Mechanics and Arctic Engineering, ASME, Vol. 129, pgs. 219 – 228.

Palmer, A.C., Konuk, I., Comfort, G., and Been, K. (1990). *Ice Gouging and the Safety of Marine Pipelines*. Proceedings, Offshore Technology Conference, OTC 6371.

Palmer, A.C. (1998). *Alternative Paths for Determination of Minimum Burial Depth to Safeguard Pipelines Against Ice Gouging*. Proceedings, Ice Scour and Arctic Marine Pipelines Workshop, 13th International Symposium on Okhotsk Sea & Sea Ice, Mombetsu, Hokkaido, Japan, February 1st–4th, pgs. 9 – 16.

Palmer, A.C. (2000). *Are we Ready to Construct Submarine Pipelines in the Arctic?* Proceedings, Offshore Technology Conference, OTC 12183.

Palmer, A. & Niedoroda, A. (2005). *Ice Gouging and Pipelines: Unresolved Questions.* Proceedings, 18th International Conference on Port and Ocean Engineering under Arctic Conditions, vol 1, pgs. 11 – 22.

Palmer, A.C., Konuk, I., Niedoroda, A.W., Been, K. & Croasdale, K.R. (2005). *Arctic Seabed Ice Gouging and Large Sub-gouge Deformations.* Proceedings, International Symposium on Frontiers in Offshore Geotechnics, 19 – 21 September, Perth, AU.

Paulin, M.J., Clark, J.I., Poorooshab, F. & Yin, J-H. (1993). *Physical Model Analysis of Iceberg Scour in Dry and Submerged Sand.* C-CORE, St. John's, NL.

Pearson, E.S. & Hartley, H.O. (editors) (1958). *Biometrika Tables for Statisticians*, Vol. 1, 2nd edition. Cambridge, New York.

Pelletier, B.R. & Shearer, J.M. (1972). *Sea Bottom Scouring in the Beaufort Sea of the Arctic Ocean.* 24th International Geological Conference, Section 8.

Pelletier, B.R. (1973). *Bottom Studies of the Beaufort Sea.* Geological Survey of Canada, Vol. 73-1A, pgs. 115-116.

Pereira, C.P.G., Woodworth-Lynas, C.M.T., & Barrie, J.V. (1988). *Iceberg Scour Investigations and Sedimentology of the Southeast Baffin Island Continental Shelf.* ARCTIC, Vol. 41, No. 3, Pg. 221 – 230, September.

Personal Communication (2009). *Email Correspondence & Discussions between J. Caines & Dr. L. Lye, Memorial University Faculty of Engineering & Applied Science.*

Phillips, R.L. & Reiss, T.E. (1984). *Nearshore Marine Geologic Investigations, Icy Cape to Wainwright, Northeast Chukchi Sea.* USGS Open-File Report 84-828.

Phillips, R.L., Reiss, T.E., Kempema, E. & Reimnitz, E. (1984). *Nearshore Marine Geologic Investigations, Wainwright to Skull Cliff, Northeast Chukchi Sea.* USGS Open-File Report 84-108.

Phillips, R.L. & Reiss, T.E. (1985). *Nearshore Marine Geologic Investigations, Point Barrow to Skull Cliff, Northeast Chukchi Sea.* USGS Open-File Report 85-50.

Phillips, R.L., Barnes, P., Hunter, R.E., Reiss, T.E. & Rearic, D.M. (1988). *Geologic Investigations in the Chukchi Sea, 1984, NOAA Ship Surveyor Cruise.* USGS Open-File Report 88-25.

Phillips, R., Clark, J.I. & Kenny, S. (2005). *PRISE Studies on Ice Gouge Forces and Subgouge Deformations.* Proceedings, 18th International Conference on Port and Ocean Engineering under Arctic Conditions.

Pilkington, G.R. & Marcellus, R.W. (1981). *Methods of Determining Pipeline Trench Depths in the Canadian Beaufort Sea.* Proceedings, 6th International Conference on Port and Ocean Engineering Under Arctic Conditions.

Pilkington, G.R. (1986). *Estimating Ice-Scour Frequency and Risk to Buried Pipelines*. Proceedings, Ice Scour and Seabed Engineering, Proceedings of a Workshop on Ice Scour Research, Environmental Studies Revolving Funds Report No. 049, December.

Rearic, D.M., Barnes, P.W. & Reimnitz, E. (1981). *Ice-Gouge Data, Beaufort Sea, Alaska, 1972-1980*. United States Geological Survey Open-File Report 81-950.

Rearic, D.M. & McHendrie, A. G. (1983). *Ice Gouge Data Sets from the Alaskan Beaufort Sea; Magnetic Tape and Documentation for Computer Assisted Analyses and Correlation*. United States Geological Survey Open-File Report 83-706.

Rearic, D.M. (1986). *Temporal and Spatial Character of Newly Formed Ice Gouges in Eastern Harrison Bay, Alaska, 1977-1982*. United States Geological Survey Open-File Report 86-391.

Rearic, D.M. & Ticken, E.J. (1988). *Ice Gouge Processes in the Alaskan Beaufort Sea*. Reprinted from *Arctic Coastal Processes and Slope Protection Design, TCCR Practice Report, American Society of Civil Engineers (ASCE), May 1988*.

Reimnitz, E., Barnes, P., Forgatsch, T. & Rodeick, C. (1972). *Influence of Grounding Ice on the Arctic Shelf of Alaska*. Marine Geology, Vol. 13, pgs. 323 – 334.

Reimnitz, E., Barnes, P.W., Rearic, D.M., Minkler, P.W., Kempema, E.W. & Reiss, T.E. (1982). *Marine Geological Investigations in the Beaufort Sea in 1981 and Preliminary Interpretations for Regions From the Canning River to the Canadian Border*. United States Geological Survey Open-File Report 82-974.

Reiss, T.E., Hunter, R.E. & Phillips, R.L. (1984). *A Summary of U.S. Geological Survey Marine Geologic Studies on the Inner Shelf of the Chukchi Sea, Alaska, Summer, 1982*. United States Geological Survey Open-File Report 84-116.

Rex, R.W. (1955). *Microrelief Produced by Sea Ice Grounding in the Chukchi Sea near Barrow, Alaska*. Arctic, vol. 8, pgs. 177 – 186.

Robe, R.Q. (1975). *Height to Draft Ratios of Icebergs*. Proceedings, 3rd International Conference on Port and Ocean Engineering Under Arctic Conditions.

Rogers, B.T. (1990). *Influence of the Burial Trench and Subsurface Soil Conditions on the Stability of the Proposed Offshore Pipeline for Amauligak Development*. Proceedings, Workshop on Ice Scouring and the Design of Offshore Pipelines, Calgary, AB, April 18th – 19th, pgs. 303 – 318. Sponsored by Canada Oil & Gas Lands Administration and the Centre for Cold Ocean Resource Engineering, October.

Rogers, B.T., Blasco, S.M. & Jefferies, M.G. (1993). *Pressuremeter Testing in Beaufort Shelf Surficial Sediments*. Proceedings, 4th Canadian Conference on Marine Geotechnical Engineering, Vol. 1, pgs. 209 – 228, St. John's, NL, June.

Sayed, M. & Timco, G.W. (2008). *A Numerical Model of Iceberg Scour*. Cold Regions Science & Technology (in press).

Shearer, J. (1979). *Analysis of Side-scan Sonar Sea Bed Imagery from Repeated Surveys Off Pullen Island – Beaufort Sea*. Prepared for Gulf Oil Canada Ltd, Ottawa, May. APOA Project No. 151.

Shearer, J. & Blasco, S.M. (1986). *Regional Correlation of Beaufort Sea Ice Scour Extreme Depth and Relative Age with Environmental Factors*. Proceedings, Ice Scour and Seabed Engineering, Proceedings of a Workshop on Ice Scour Research, Environmental Studies Revolving Funds Report No. 049, pgs. 167 – 169, December.

Shearer, J., Laroche, B. & Fortin, G. (1986). *Canadian Beaufort Sea 1984 Repetitive Mapping of Ice Scour*. Environmental Studies Revolving Funds Report No. 032, Ottawa.

Shearer, J.M. & Stirbys, A.F. (1986). *Towards Repetitive Mapping of Ice Scours in the Beaufort Sea*. Proceedings, Ice Scour and Seabed Engineering, Proceedings of a Workshop on Ice Scour Research, Environmental Studies Revolving Funds Report No. 049, pgs. 284 – 287, December.

Sonnichsen, G.V., King, T., Jordaan, I. & Li, C. (2005). *Probabilistic Analysis of Iceberg Scouring Frequency based on Repetitive Seabed Mapping, Offshore Newfoundland and Labrador*. Proceedings, 18th International Conference on Port and Ocean Engineering under Arctic Conditions.

Stepanov, I. (2000). *Can Seabed Gouge Survey Data be Applied to Prediction of Maximum Depths of Ice Keel Penetration?* Proceedings, 2nd Ice Scour and Arctic Marine Pipelines Workshop, 15th International Symposium on Okhotsk Sea & Sea Ice, pgs. 93 – 100.

Stephens, M.A. (1974). *EDF Statistics for Goodness of Fit and Some Comparisons*. Journal of the American Statistical Association, Vol. 69, No. 347, pgs. 730 – 737.

Stephens, M.A. (1977). *Goodness of Fit for the Extreme Value Distribution*. Biometrika, Vol. 64, No. 3, pgs. 583 – 588.

Surkov, G.A. (1995). *Method for Determining the Optimum Burial Profile for Subsea Pipeline Facilities in Freezing Seas*. Sakhalin Research and Design Institute. Reference not found – provided here for information only.

Toimil, L.J. (1978). *Ice-gouged Microrelief on the Floor of the Eastern Chukchi Sea, Alaska: A Reconnaissance Survey*. United States Geological Survey Open-File Report 78-693.

Toimil, L.J. (1979). *Ice Gouge Characteristics in the Alaskan Chukchi Sea*. Proceeding of the Specialty Conference, Civil Engineering in the Oceans IV., Vol.II, American Society of Civil Engineers.

Thurston, D.K. and Theiss, L.A. (1987). *Geologic Report for the Chukchi Sea Planning Area, Alaska; Regional Geology, Petroleum Geology, and Environmental Geology*. MMS 87-0046.

Ticken, E.J. & Toimil, L.J. (n.d.). *Variations in Ice Gouge Parameters Related to Different Seabed Soil Types*. Harding Lawson Associates.

Ticken, E.J. & Toimil, L.J. (1992). *Characteristics of Newly Formed Ice Gouges in the Beaufort Sea, Alaska*. American Society of Mechanical Engineers (ASME), Offshore Mechanics & Arctic Engineering (OMAE) – Volume IV, Arctic / Polar Technology.

Wadhams, P. (1983). *The Prediction of Extreme Keel Depths from Sea Ice Profiles*. Cold Regions Science and Technology, vol. 6, pgs. 257 – 266.

Wahlgren, R.V. (1979). *Ice-Scour Tracks on the Beaufort Sea Continental Shelf: their form and an interpretation of the processes creating them*, vol. 1, 2, and 3. M.A. Thesis, Carlton University, Department of Geography, Ottawa.

Walpole, R.E. & Myers, R.H. (1985). *Probability and Statistics for Engineers and Scientists*, 3rd edition. Macmillan Publishing Company, NY.

Wang, A.T. (1990a). *Numerical Simulations for Rare Ice Gouge Depths*. Cold Regions Science & Technology, Vol. 19, pgs. 19 – 32.

Wang, A.T. (1990b). *Design Ice Gouge Depth Computation through Computer Simulations*. Proceedings, Workshop on Ice Scouring and the Design of Offshore Pipelines, Calgary, AB, April 18th – 19th, pgs. 237 – 246. Sponsored by Canada Oil & Gas Lands Administration and the Centre for Cold Ocean Resource Engineering, October.

Weber, W.S., Barnes, P.W. & Reimnitz, E. (1989). *Data on the Characteristics of Dated Gouges on the Inner Shelf of the Beaufort Sea, Alaska; 1977-1985*. United States Geological Survey Open-File Report 89-151.

Weeks, W.F., Barnes, P.W., Rearic, D. & Reimnitz, E. (1980). *Statistical Aspects of Ice Gouging on the Alaskan Shelf of the Beaufort Sea (DRAFT)*. United States Army Corps

of Engineers Cold Regions Research & Engineering Laboratory (CRREL) DRAFT Report. Reference not found – provided here for information only.

Weeks, W.F., Barnes, P.E., Rearic, D.M. & Reimnitz, E. (1981). *Statistics of Ice Gouging on the Alaskan Shelf of the Beaufort Sea*. EOS, Vol. 62, No. 45, pg. 902, November 10th.

Weeks, W.F., Barnes, P.W., Rearic, D.M. & Reimnitz, E. (1983). *Statistical Aspects of Ice Gouging on the Alaskan Shelf of the Beaufort Sea*. United States Army Corps of Engineers Cold Regions Research & Engineering Laboratory (CRREL) Report 83-21.

Weeks, W.F., Tucker, W.B. & Niedoroda, A.W. (1985). *A Numerical Simulation of Ice Gouge Formation and Infilling on the Shelf of the Beaufort Sea*. Proceedings, 8th International Conference on Port and Ocean Engineering Under Arctic Conditions, Narssarssuaq, Greenland. September 7th – 14th.

Weeks, W.F., Tucker, W.B. & Niedoroda, A.W. (1986). *Preliminary Simulation of the Formation and Infilling of Sea Ice Gouges*. Proceedings, Ice Scour and Seabed Engineering, Proceedings of a Workshop on Ice Scour Research, Environmental Studies Revolving Funds Report No. 049, pgs. 259 – 268, December.

Wilson, J.C., Wade, W.W., Feldman, M.L., and Younger, D.R. (1982). *Alaska OCS Socioeconomic Studies Program Barrow Arch Planning Area (Chukchi Sea) Petroleum Technology Assessment OCS Lease Sale No. 85*. Prepared for Minerals Management Service, Alaska Outer Continental Shelf Office by Dames & Moore et al., December. MMS Technical Report No. 79.

Wheeler, J.D. & Wang, A.T. (1985). *Sea Ice Gouge Statistics*, Proceedings, 8th International Conference on Port and Ocean Engineering Under Arctic Conditions, Narssarssuaq, Greenland. September 7th – 14th.

Wright, B., Hnatiuk, J. & Kovacs, A. (1981). *Multi-year Pressure Ridges in the Canadian Beaufort Sea*. Coastal Engineering, 5: pgs 125 - 145, January 1981.

Yoon, K., Choi, K. & Park, H. (1997). *A Numerical Simulation to Determine Ice Scour and Pipeline Burial Depth*. Proceedings, 7th International Offshore and Polar Engineering Conference, Vol. II, pgs. 212 – 219.

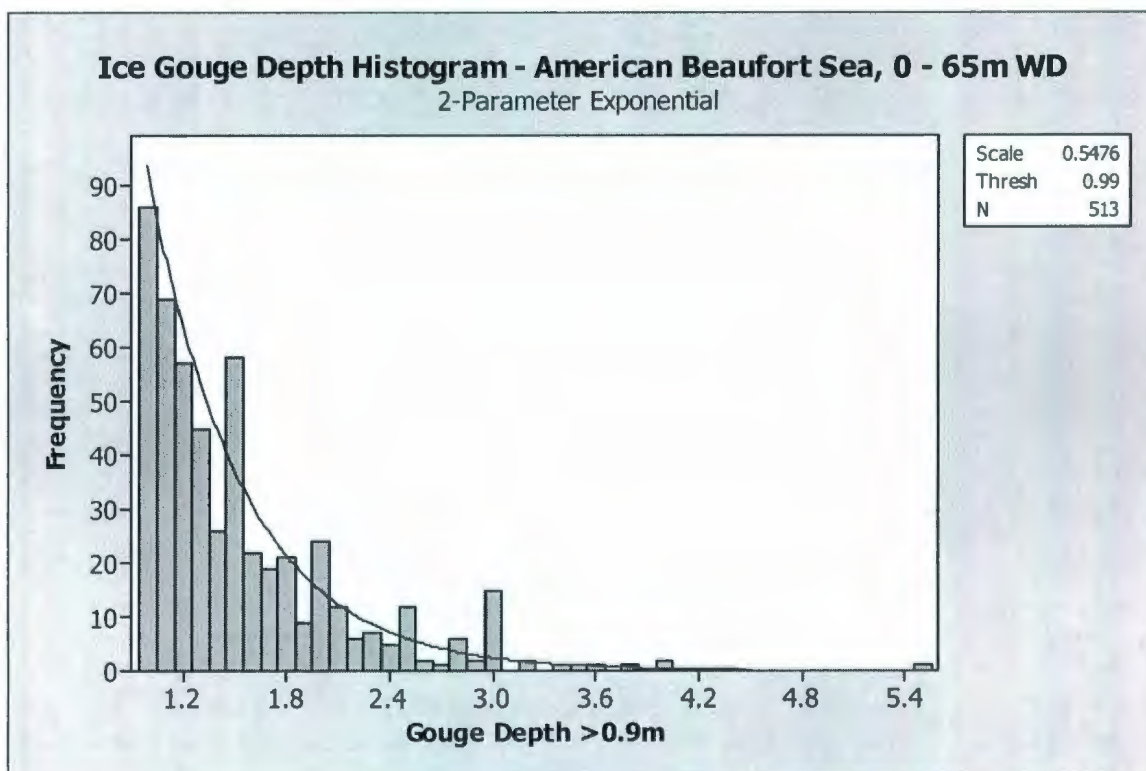
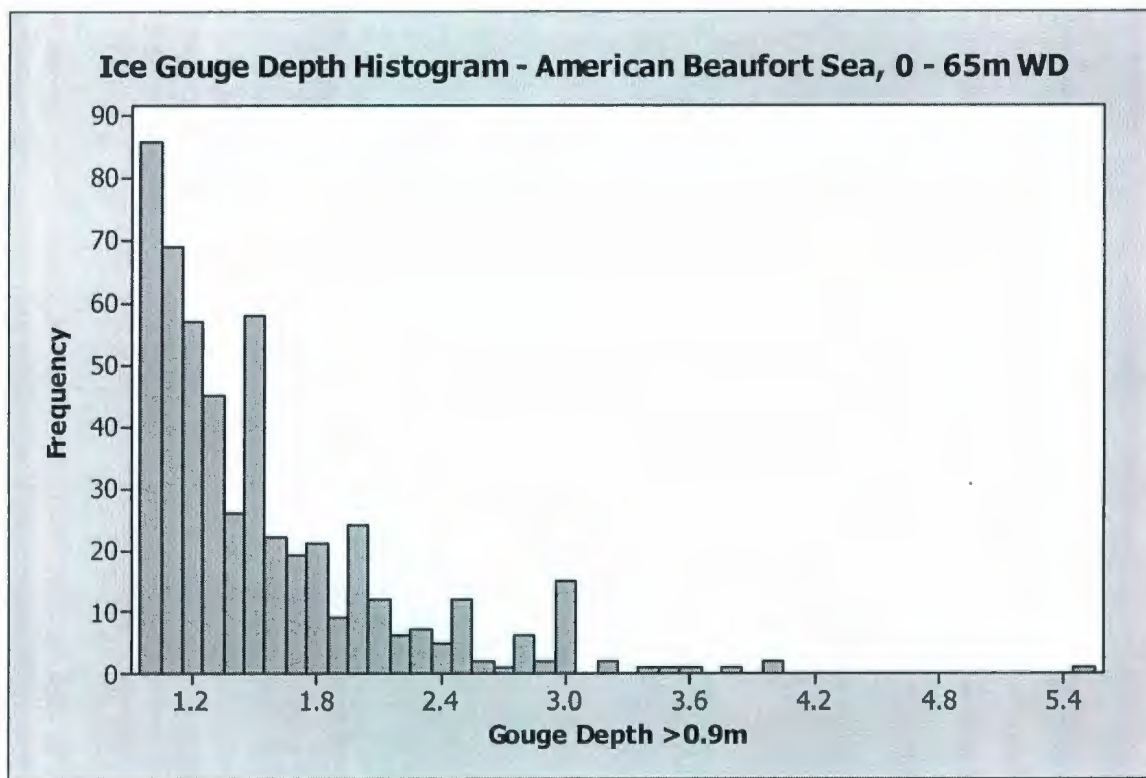
Younan, A.H., Hamilton, J.M. & Weaver, J. (2007). *Ice Gouge Reliability of Offshore Arctic Pipelines*. Proceedings, 26th International Conference on Offshore Mechanics and Arctic Engineering, OMAE2007-29071.

APPENDIX A

STATISTICAL DISTRIBUTIONS & PROBABILITY PLOTS USING

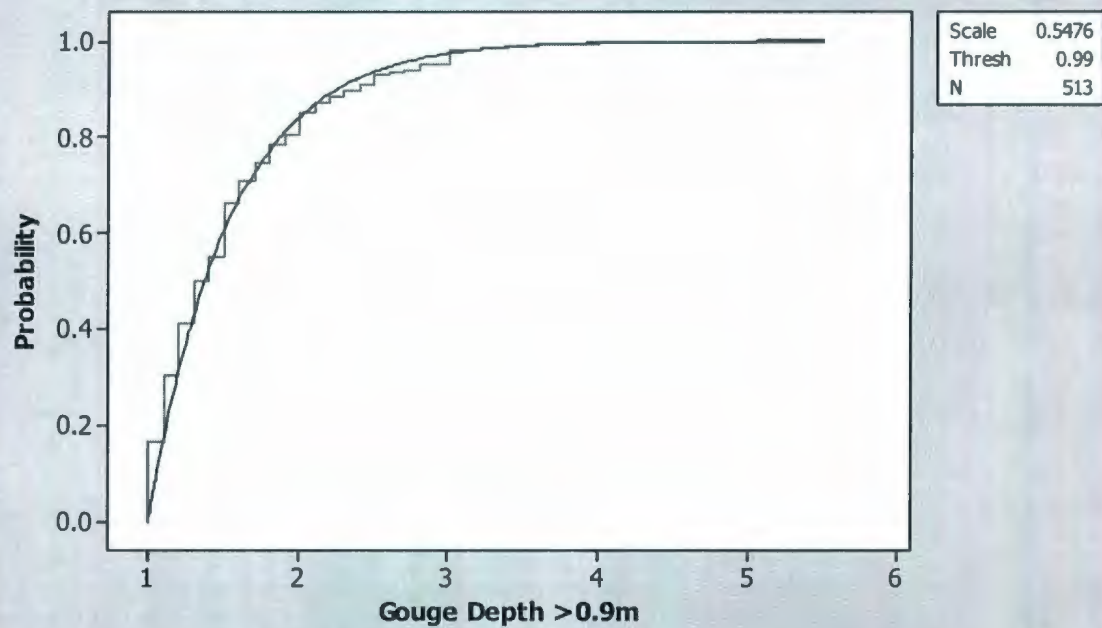
ALTERNATE MIXED DISTRIBUTION LIMITS

AMERICAN BEAUFORT SEA



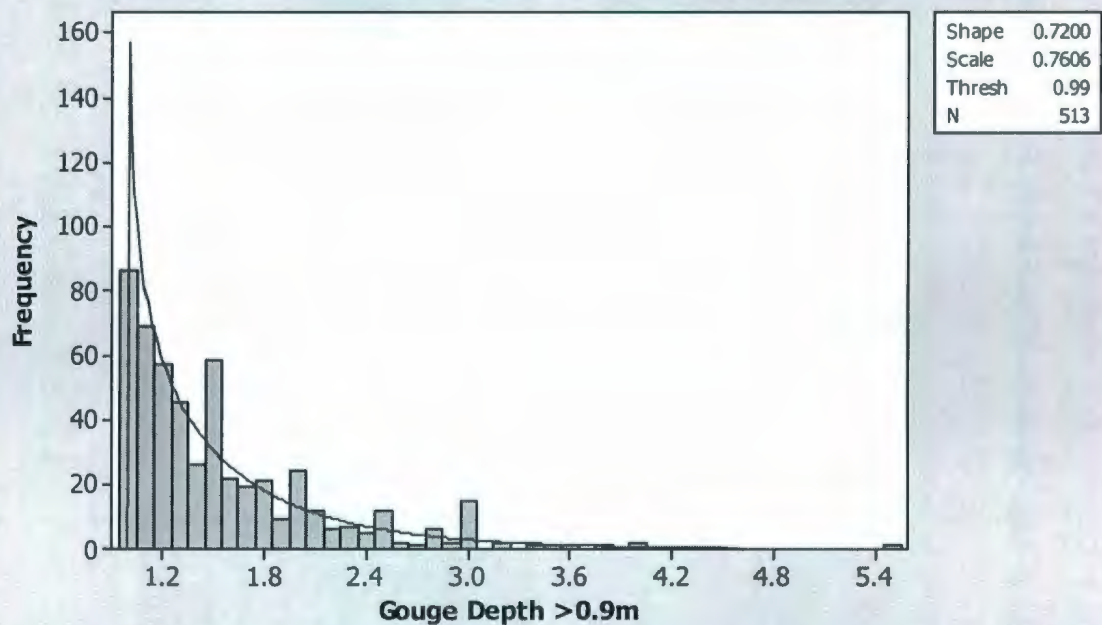
Empirical Cumulative Distribution Fit - American Beaufort Sea, 0 - 65m WD

2-Parameter Exponential



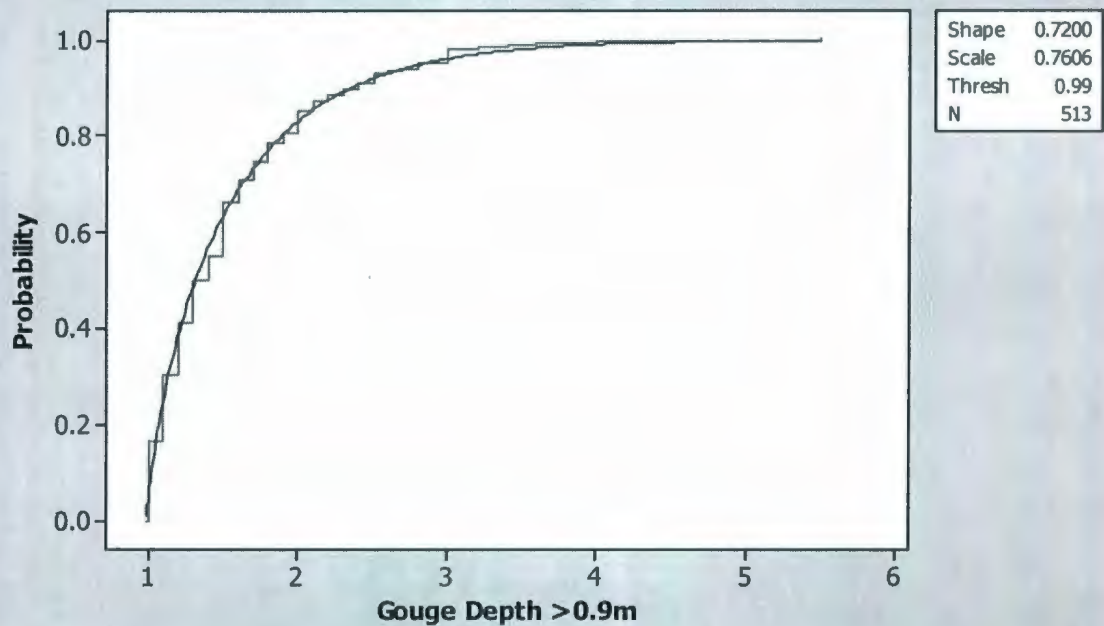
Ice Gouge Depth Histogram - American Beaufort Sea, 0 - 65m WD

3-Parameter Gamma



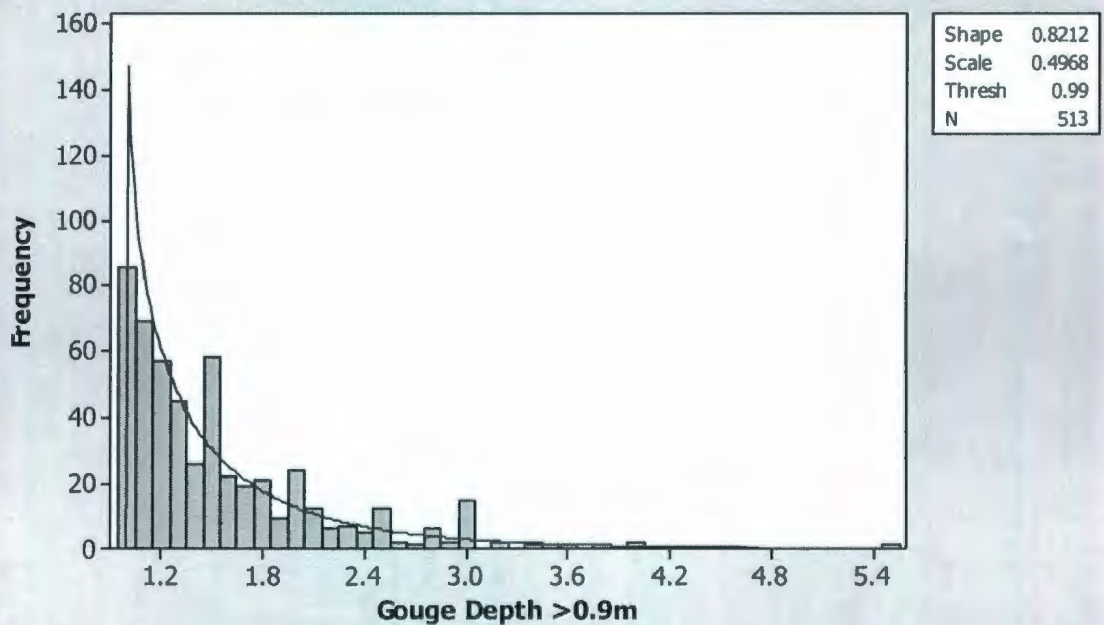
Empirical Cumulative Distribution Fit - American Beaufort Sea, 0 - 65m WD

3-Parameter Gamma



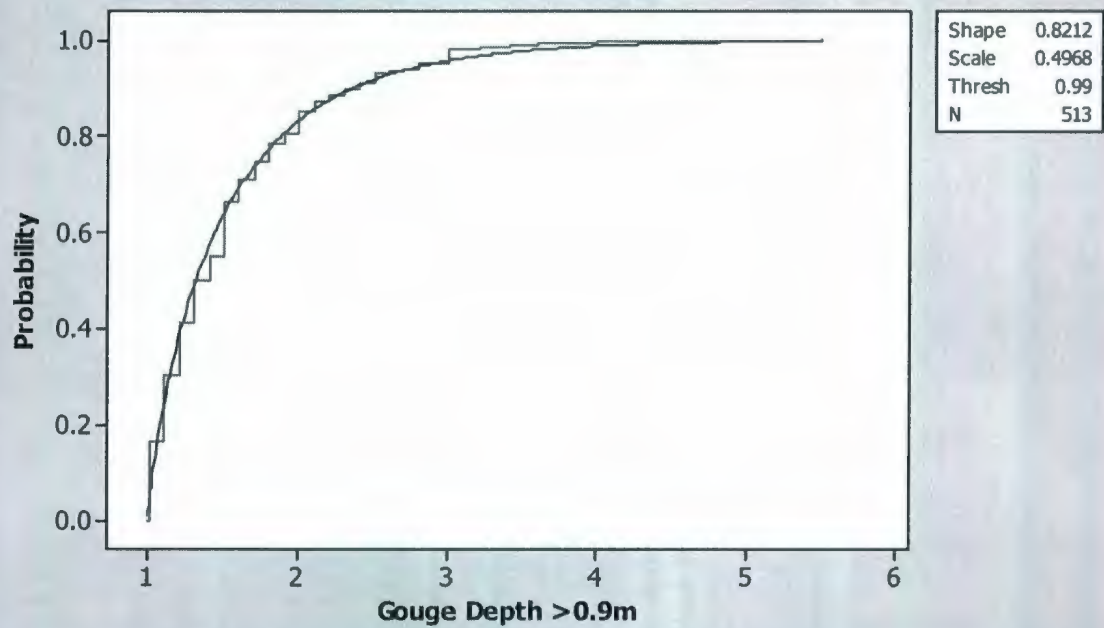
Ice Gouge Depth Histogram - American Beaufort Sea, 0 - 65m WD

3-Parameter Weibull

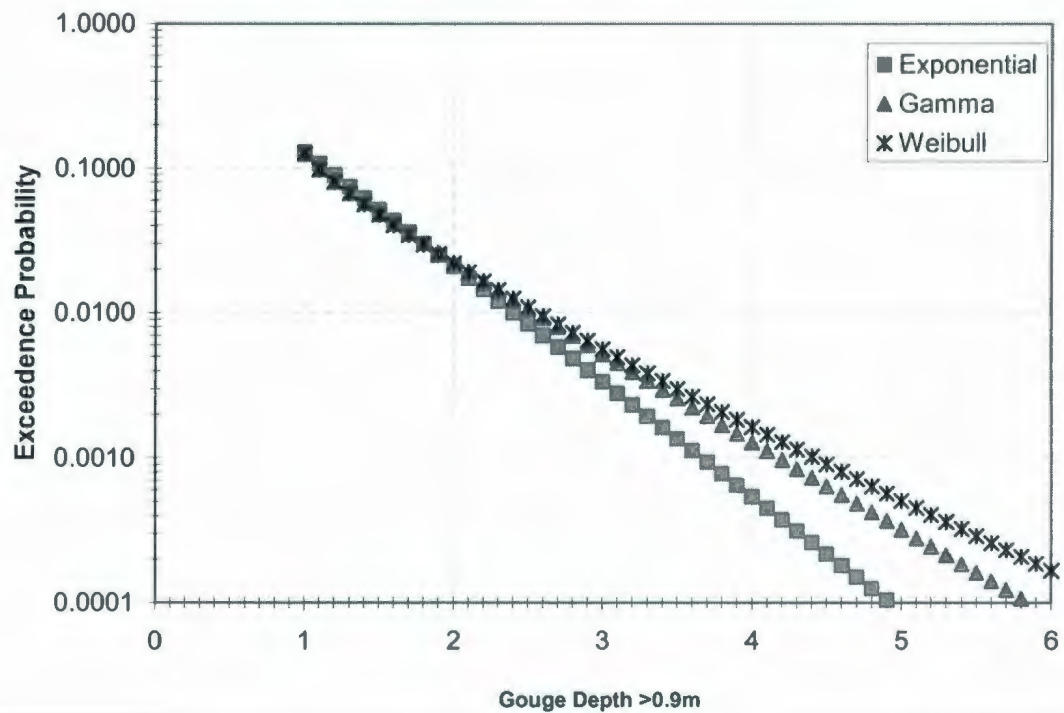


Empirical Cumulative Distribution Fit - American Beaufort Sea, 0 - 65m WD

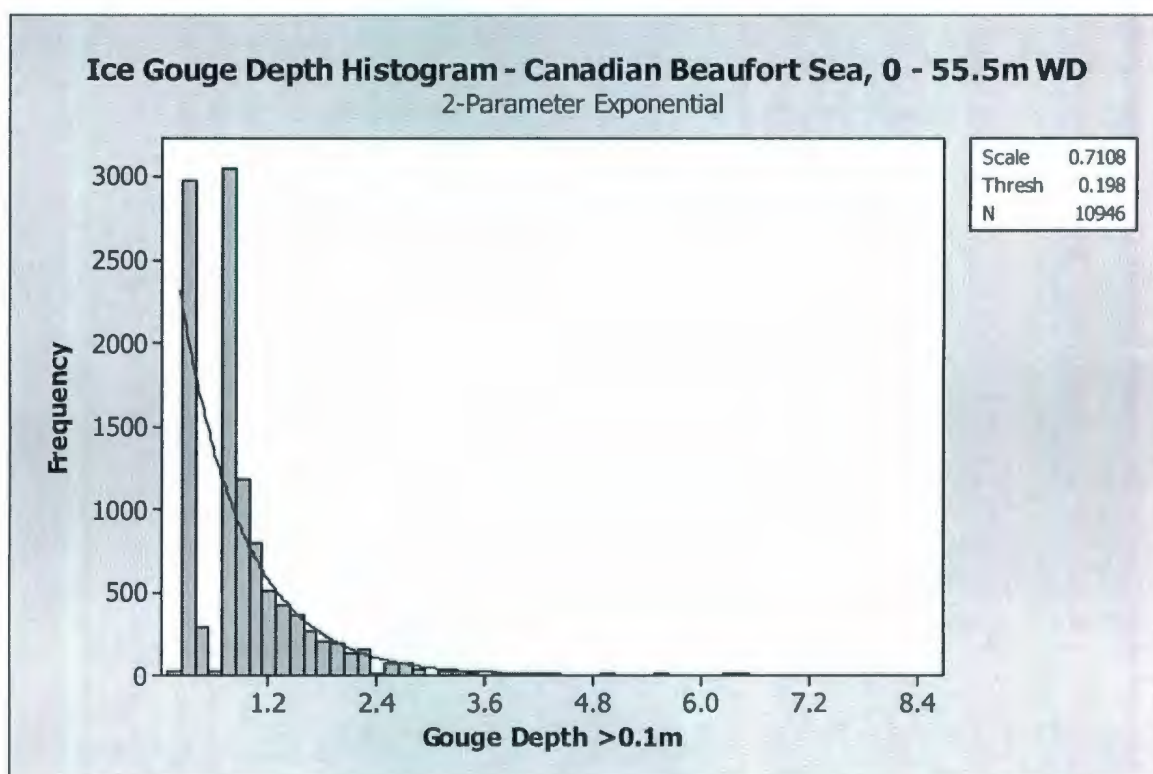
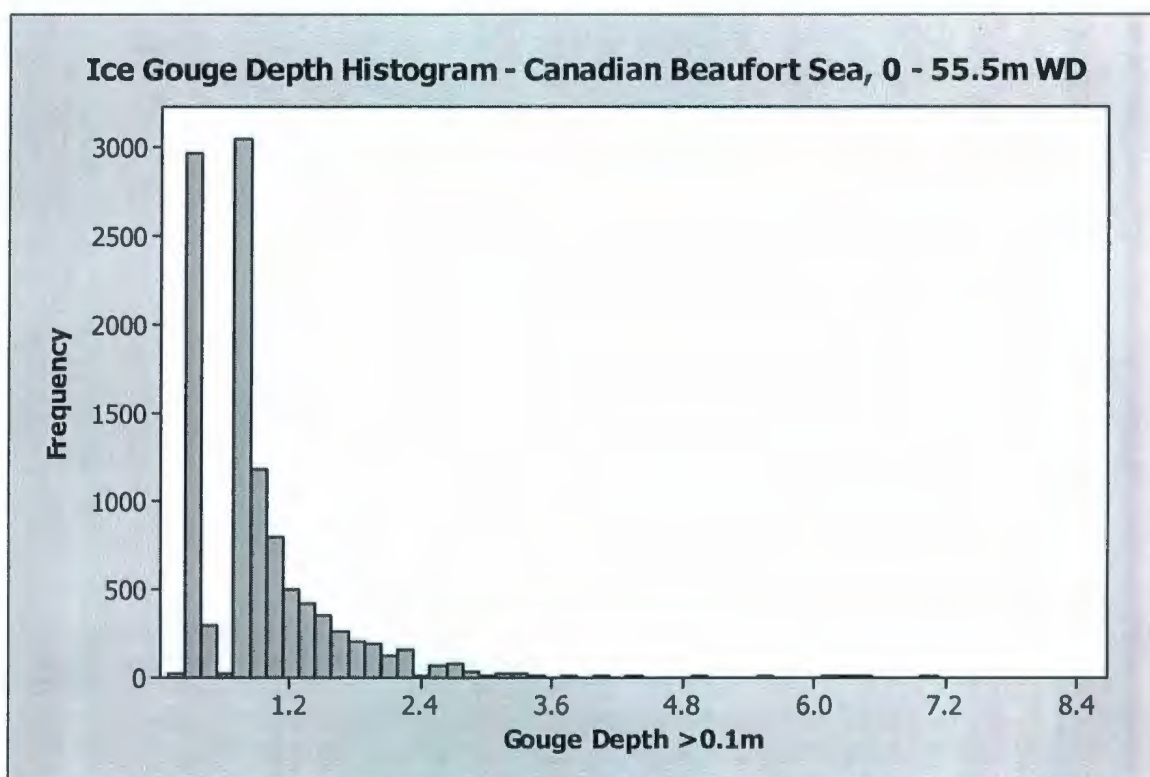
3-Parameter Weibull



Ice Gouge Depth Exceedence Probability - American Beaufort Sea, 0 - 65m WD Combined New & Unknown Age Data

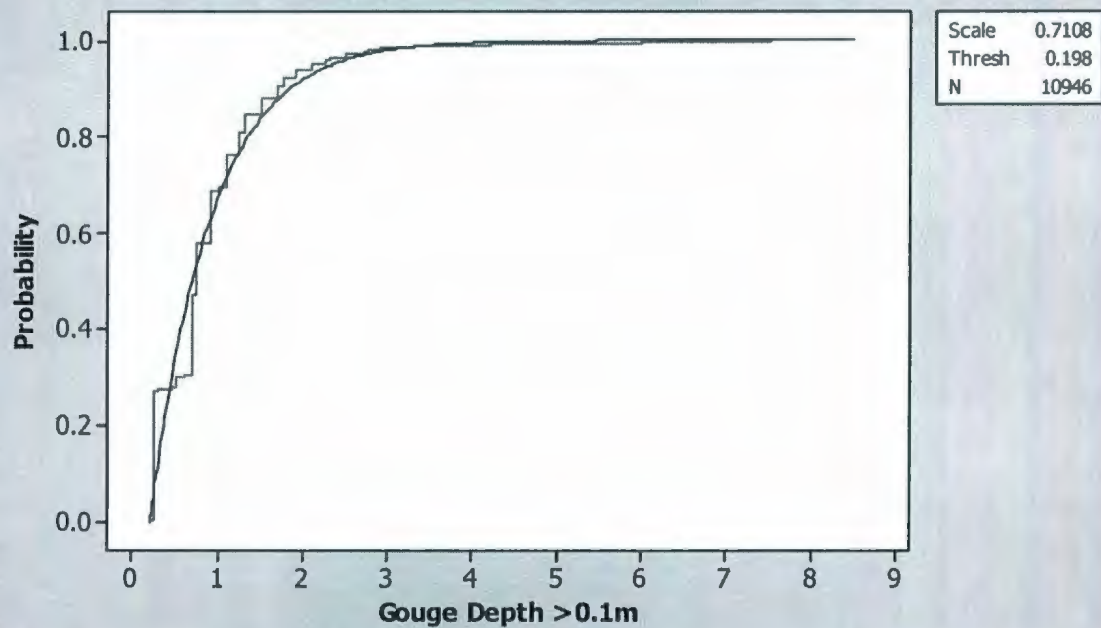


CANADIAN BEAUFORT SEA



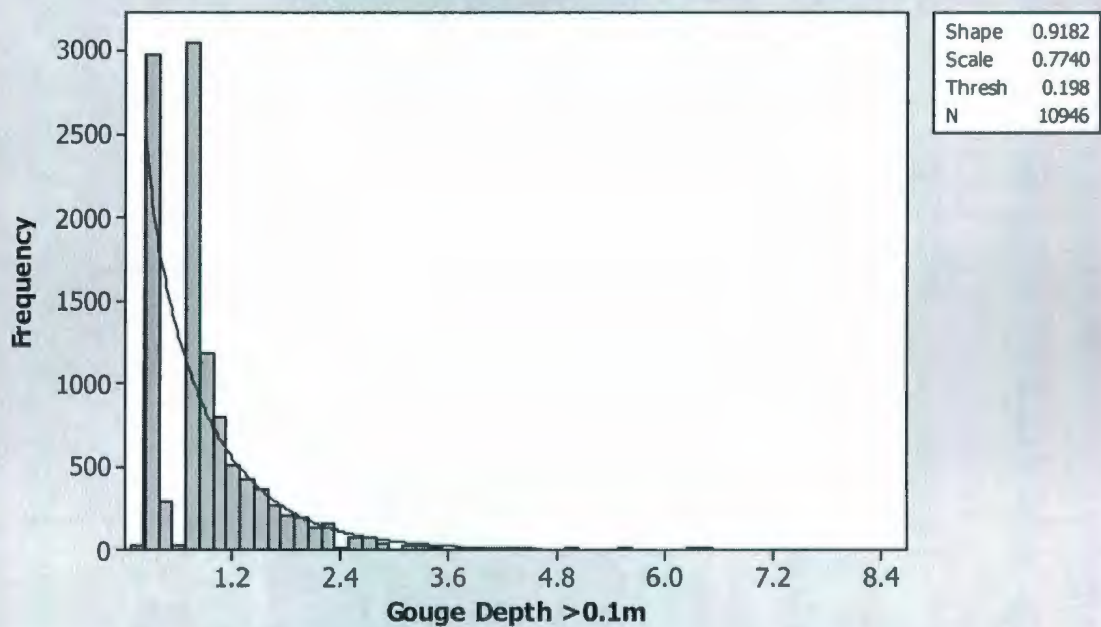
Empirical Cumulative Distribution Fit - Canadian Beaufort Sea, 0 - 55.5m WD

2-Parameter Exponential

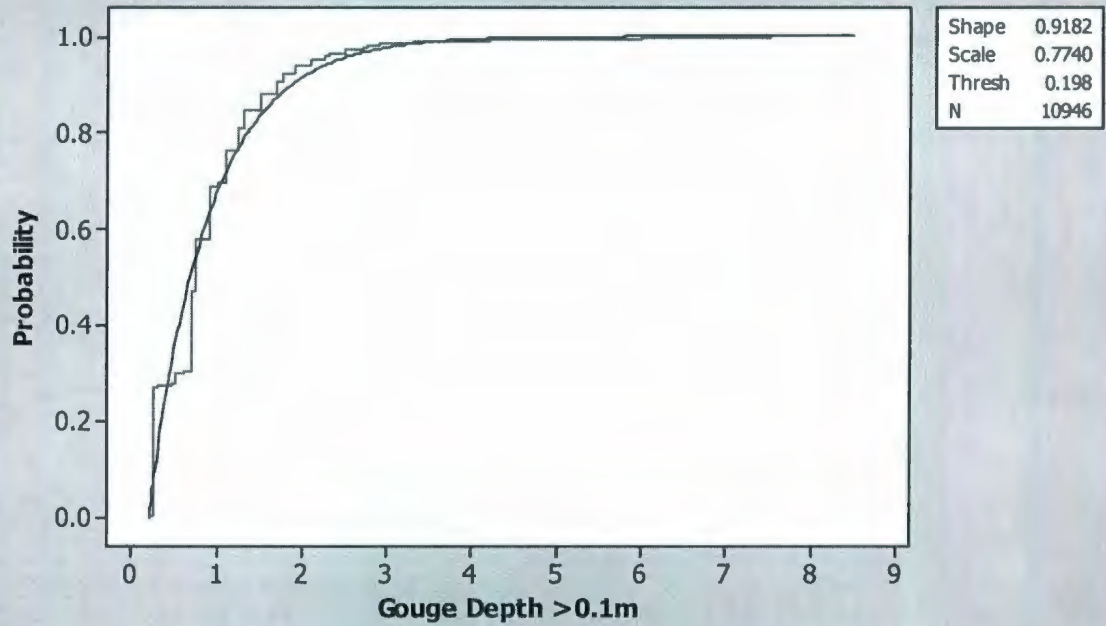


Ice Gouge Depth Histogram - Canadian Beaufort Sea, 0 - 55.5m WD

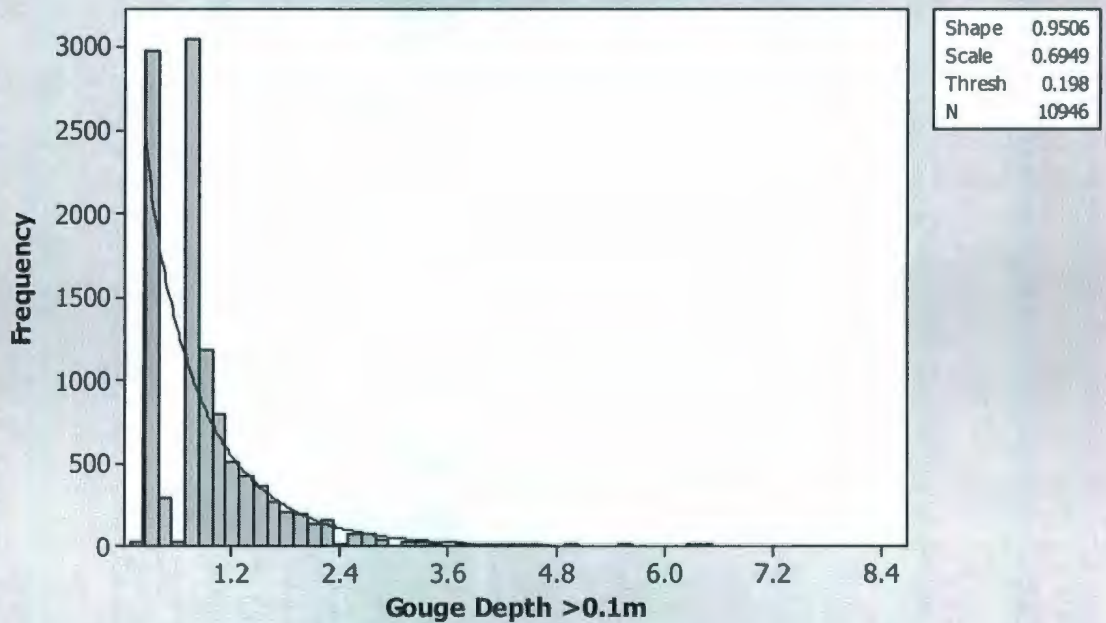
3-Parameter Gamma



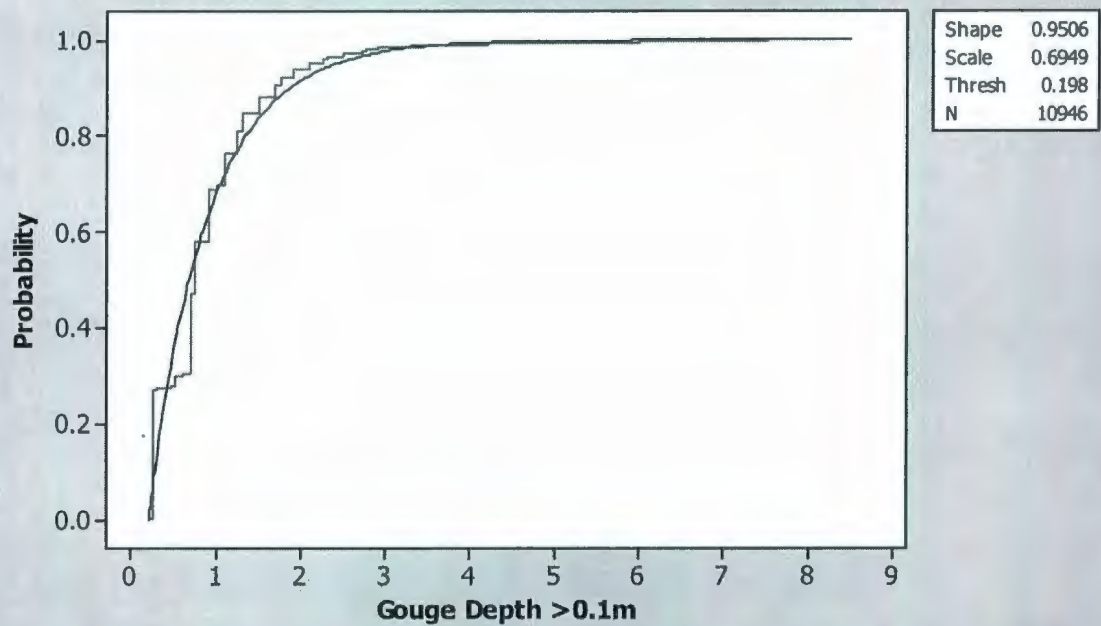
Empirical Cumulative Distribution Fit - Canadian Beaufort Sea, 0 - 55.5m WD
3-Parameter Gamma



Ice Gouge Depth Histogram - Canadian Beaufort Sea, 0 - 55.5m WD
3-Parameter Weibull



Empirical Cumulative Distribution Fit - Canadian Beaufort Sea, 0 - 55.5m WD
3-Parameter Weibull



Ice Gauge Depth Exceedence Probability - Canadian Beaufort Sea, 0 - 55.5m WD

Combined New & Unknown Age Data

